The NSF-Simons National Institute for Theory and Mathematics in Biology

MathBio Convergence Conference

NITMB MathBio Convergence Conference

National Institute for Theory and Mathematics in Biology

Funded by the U.S. National Science Foundation and the Simons Foundation

Chicago, Illinois

11-14 August 2025

National Institute for Theory and Mathematics in Biology

Funded by the U.S. National Science Foundation and the Simons Foundation

SIMONS FOUNDATION

Contents

1 Abstracts of Plenary Talks

Cycles upon cycles - collective rhythms during embryonic development

Alexander Aulehla
Head of Developmental Biology Unit
The European Molecular Biology Laboratory (EMBL)

Abstract

We study the origin and function of collective signaling oscillations in embryonic development. Oscillatory signaling is linked to the sequential segmentation of the vertebrate embryo body axis and the formation of pre-vertebrae, somites. Most strikingly, signaling oscillations are coordinated between neighboring cells and result in spatio-temporal wave patterns that traverse the embryo periodically. I will discuss how we employ general synchronisation principles and experimental entrainment to reveal the hidden dynamical properties of this embryonic coupled oscillator network.

Graphical domination and inhibitory control in recurrent networks

Carina Curto
Pablo J. Salame Goldman Sachs Professor of Computational Neuroscience
Brown University

Abstract

Recurrent neural networks can be modeled as dynamical systems on directed graphs. What graph features are important for shaping the emergent dynamics? In this talk we will introduce the concept graphical domination and present key theorems about domination that help us understand the associated nonlinear dynamics. In particular, domination can be used to reduce graphs to smaller equivalent networks. We also show how reducible graph modules can be chained together to produce larger networks with predictable dynamics. These networks are amenable to control via inhibitory pulses. While these results were originally developed for a special class of effectively inhibitory threshold-linear networks, we will show how they apply equally well to E-I networks with global inhibition.

Statistical opportunities in defining, modeling, and targeting cell state in cancer

Lorin Crawford
Principal Researcher & Distinguished Senior Fellow in Biostatistics
Microsoft Research & Brown University

Abstract

Project Ex Vivo is a joint cancer research collaboration between Microsoft and the Broad Institute of MIT and Harvard. Our group views cancers as complex (eco)systems, beyond just mutational variation, that necessitate systems-level understanding and intervention. In this talk, I will discuss a series of multimodal statistical and deep learning approaches to understand accurate representations of tumors by integrating genetic markers, expression state, and microenvironmental interactions. These representations help us precisely define and quantify the trajectory of each tumor in each patient. Our ultimate objective is to more effectively model cancer ex vivo – outside the body – in a patient-specific manner. In doing so, we aim to unlock the ability to better stratify patient populations and identify therapies that target diverse aspects of human cancers.

Discrete Morse graph construction for high-dimensional transcriptomic data

Michael Hawrylycz
Senior Investigator
The Allen Institute

Abstract

Discrete Morse theory, a combinatorial adaptation of classical Morse theory, is instrumental in analyzing topological features of discrete spaces like cell complexes. When combined with persistent homology in topological data analysis, it is particularly effective in simplifying complex data structures and extracting meaningful features from high-dimensional or noisy datasets. Single-cell transcriptomic data such as RNA-seq provides an interesting application of discrete Morse theory, where measurements of thousands of genes reflecting differential expression patterns are used to determine cell type and cell state. We introduce a novel algorithm, scDMGC, for discrete Morse graph reconstruction and demonstrate its efficacy in validating brain cell type taxonomies and gradients. Additionally, discrete Morse graph construction is employed to distinguish cell loss and altered transcription in early to late Alzheimer's disease transcriptomic data.

Uncovering the determinants of disease risk and within host-pathogen diversity in natural systems

Anna-Liisa Laine
Professor of Plant Biodiversity
University of Helsinki, Finland

Abstract

Disease risk in natural plant populations emerges from complex interactions between host diversity, community structure, and environmental variation. We integrate field experiments, long-term datasets, and molecular tools to explore how both ecological and evolutionary dynamics shape pathogen prevalence and community composition. We show that genetic and species-level host diversity can modulate pathogen spread — sometimes buffering, other times amplifying infection risk-depending on landscape structure and host traits. Our findings emphasize the need to bridge scales of biological organization-from genes to ecosystems-to predict when and where outbreaks will occur. Understanding these dynamics is increasingly important as ecosystems are reshaped by land-use change and climate variability.

Viruses under the mathematical microscope: viral geometry as a key to understanding viral infections

Reidun Twarock
Professor, Department of Mathematics
University of York

Abstract

Most viruses have protein shells, called viral capsids, that surround, and thus protect, their genetic material. Due to the highly symmetric nature of these capsids, mathematical techniques from group, graph and tiling theory can be used to model and classify virus architecture. By combining these geometric, and related topological, descriptors of virus architecture with stochastic simulations, I will demonstrate how viral geometry provides insights into viral life cycles that pave the way to innovation in antiviral therapy and virus nanotechnology.

2 Abstracts of Oral Talks

A Biological Oscillator Controls Mineralization of the Zebrafish Spine

Priyom Adhyapok, James Norman, Jennifer Bagwell, Michel Bagnat, Stefano Di Talia
Duke University

Many biological phenomena generate periodic patterns. While multiple processes can build periodicity through mechanical or bio-chemical inputs, one motif is the presence of intrinsic cellular clocks, which can coordinate to generate tissue-wide periodic structures. Clocks have been used in the generation of repeated and segmented units along the body axis, using temporal information to create spatial patterns across vertebrate and invertebrate species. The zebrafish notochord, which has recently been reported to segment into molecular domains to form the vertebral column of the spine, presents an excellent system to address the emergence of periodicity. In this work, I will present the first known evidence that the notochord uses a molecular clock with a periodicity of 10 hours to build the spine through a process of molecular segmentation. Reported by the MAPK/ERK pathway, this oscillator modulates periodic differentiation of cells to form segments. This work highlights dynamical features of the notochord oscillatory system. Most notably, this oscillator achieves synchrony across several millimeters of the fish length. Tracing the system through development shows the emergence of synchronization and periodicity in the tissue, with a larger first cycle of oscillation of 24 hours, suggesting a change in frequency as the system transitions through a bifurcation. Overall, this work provides a new *in vivo* system to study biological oscillations and identify paradigms in which molecular clocks can coordinate segmentation.

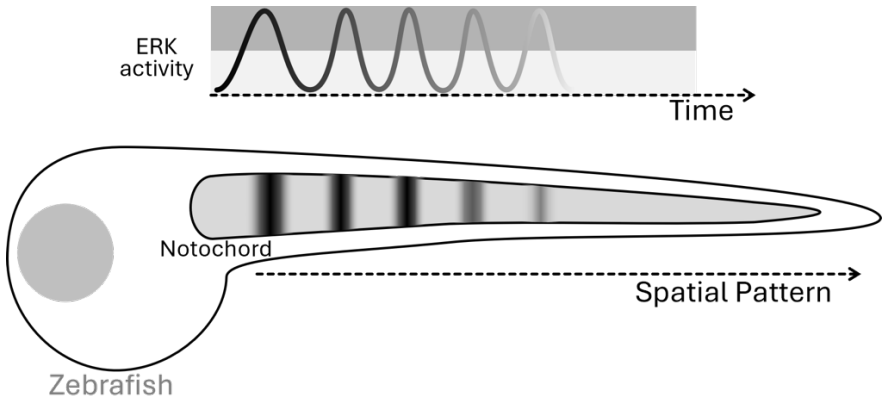

References:

1. Wopat S., Adhyapok P., Daga B., Crawford JM., Norman J., Bagwell J., Peskin B., Magre I., Fogerson SM., Levic DS., Di Talia S., Kiehart DP., Charbonneau P., Bagnat M. (2024). Notochord segmentation in zebrafish controlled by iterative mechanical signaling. *Developmental Cell*. DOI:10.1016/j.devcel.2024.04.013.
2. Peskin, B., Norman, J., Bagwell, J., Lin, A., Adhyapok, P., di Talia, S., & Bagnat, M. (2023). Dynamic BMP signaling mediates notochord segmentation in zebrafish. *Current Biology*, *33*(12). DOI:10.1016/j.cub.2023.05.039.

Biomolecular network discovery through GenAI-driven time series analysis in living cells

Orlando Arguello-Miranda[1], Jackson McClintock[1], Surya Sukumar[1], Arsalan Taassob[1], Kevin Flores[2]

Abstract

Biological processes are driven by networks of proteins coordinated in time and space that define cell behavior in health and disease. Although protein networks can be inferred from sequencing-based techniques and fluorescence microscopy, these methods often destroy cells to recover information or use biochemical sensors that alter cell physiology. These limitations prevent the direct visualization of complex protein networks in single living cells. For instance, under optimal conditions, up to six fluorescent markers can be reliably tracked in living cells; however, even small molecular networks, such as signaling cascades, can surpass dozens of proteins. Therefore, new methods are required to visualize large protein networks in single living cells and produce more accurate models of cellular behavior.

Most methods to increase the number of proteins measured in cells focus on improving microscopy hardware or optimizing biochemical sensors. Here, we propose an alternative approach based on generative AI (GenAI) to produce bio-realistic visualizations using customized algorithms for image-to-image translation. We created generative models that take simple microscopy images, such as phase contrast micrographs, as input and produce a multidimensional array of synthetic images depicting multiple proteins in living cells over time (Fig. 1). To achieve this, we produced a unique ground truth dataset of multidimensional fluorescent images with dozens of proteins encompassing signaling networks in the model organism *Saccharomyces cerevisiae*.

To test whether the time series derived from synthetic images could be used for biological inference, we compared ordinary differential equation models for networks based on time series measurements from real or synthetic images. Our results showed that time series derived from synthetic images resembled real time series, enabling the discovery of protein correlations, cross-correlations, hypothetical network motifs, and protein-protein interactions in single living cells.

We envision that biomolecular network discovery through GenAI-driven time series analysis will accelerate research by expanding the information obtained from single images and allowing faster parameter optimizations for network models of complex biological systems.

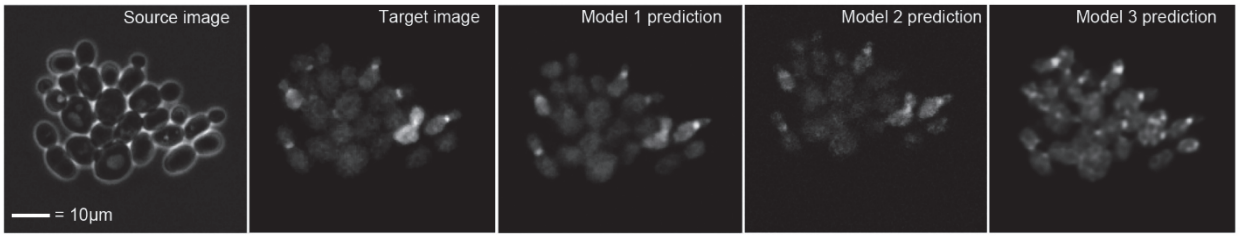

Figure 1. Cross-modality predictions for different types of microscopy using custom GenAI models. Source image, *S. cerevisiae* phase contrast micrograph; target image, a fluorescent image; Model prediction 1-3, different image predictions for the target image obtained from the source image.

References:

[1] Swaraj Kaondal, Arsalan Taassob, Sara Jeon, Su Hyun Lee, Henrique L. Nuñez, Bukola A. Akindipe, Hyunsook Lee, So Young Joo, Samuel M.D. Oliveira, Orlando Argüello-Miranda. (2025). Generative frame interpolation enhances tracking of biological objects in time-lapse microscopy. bioRxiv 2025.03.23.644838; doi: https://doi.org/10.1101/2025.03.23.644838

[2] Taylor Kennedy, Berk Yalcinkaya, Shreya Ramakanth, Sandhya Neupane, Nika Tadic, Nicolas E. Buchler, Orlando Argüello-Miranda. (2024). Deep learning-driven imaging of cell division and cell growth across an entire eukaryotic life cycle, bioRxiv 2024.04.25.591211; doi: https://doi.org/10.1101/2024.04.25.591211

[1] Plant and Microbial Biology, North Carolina State University

[2] Mathematics, North Carolina State University

The dynamical system landscape underlying chirality bias in rotational doublets

Egun Im* Andreas Buttenschoen† Calina Copos‡

Abstract

Left-right asymmetry is a vital part of embryonic development in vertebrates that positions internal organs asymmetrically across the left-right axis. Asymmetric organ morphogenesis follows asymmetric signaling cascades, which in turn follow asymmetric events on the cellular scale. Recent experiments report cell-scale movement asymmetries by spontaneously rotating Madin-Darby canine kidney (MDCK) epithelial cells confined to a circular adherent island. Importantly, the actin cytoskeleton contractility appears to modulate the chirality bias. Here, we build a minimal particle-based model to demonstrate that confinement forces together with cell-cell adhesion and cell polarization can give rise not only to coherent angular rotation of a confined pair of cells but also to the observed chirality bias. Using simulations, linear stability analysis and bifurcation analysis we identify the underlying mechanism leading to the observed bias in rotational movement.

*Northeastern University
†University of Massachusetts Amherst
‡Northeastern University

An ensemble modeling framework to predict synapses from optokinetic stimuli in larval zebrafish

Selimzhan Chalyshkan[1,2], Tirthabir Biswas[2], Fumi Kubo[3], Herwig Baier[4], James Fitzgerald[2,5,6,7]

Abstract

Studying the link between neural network structure and function is crucial in understanding the principles underlying brain activity. With the growing use of large-scale activity recordings and advances in anatomical circuit-level reconstructions, researchers can now posit numerous neural network models that tie neural recordings with synaptic connectivity. However, understanding how well various neural network model classes relate to and predict observed neural activity with structural connections remains a significant challenge in systems and computational neuroscience. Here, rather than fitting a single model to find structural parameters matching a network's observed functional profile, we examined an ensemble modeling approach that finds consistent structure across models (Biswas et al., 2024). We applied ensemble modeling in a threshold-linear network to predict connectivity in larval zebrafish pretectum from the most common neuronal response types to optokinetic stimuli. In line with the previously hypothesized model, the strongest predictions included excitatory connections from the retina to monocular response types and connections from the monocular response types to binocular response types. We also tested the ensemble modeling framework by predicting neuronal activity for a given stimulus condition from the ensemble of models that account for the other stimulus conditions. We found that ensemble modeling produced up to five correct predictions for each response type before making an error. In contrast, the fit model that finds the solution that minimizes the weight norm predicted only one or two correct activity responses. Together, we have shown that ensemble modeling is a robust approach that makes accurate activity predictions and compelling structural predictions from threshold-linear recurrent neural network models. Forthcoming comparisons with the anatomically reconstructed circuit will further evaluate accuracy of the theoretical framework predictions.

The circuit responsible for gaze stabilization in larval zebrafish, also known as optokinetic response, is hypothesized to involve the pretectum, a retinorecipient brain area that integrates behaviorally relevant motion signals (Kubo et al., 2014; Naumann et al., 2016). We choose to test the ensemble modeling framework in this biological setting because a functional connectomics dataset is already available (Svara et al., 2022). In particular, the synaptic connections between pretectal neurons were measured with electron microscopy after the complete pretectum circuit was functionally characterized with Ca2+ imaging. The Ca2+ recording was obtained from the pretectum of a larval zebrafish stimulated by several visual motion stimuli on LED screens (Kubo et al., 2014) (Fig. A). These responses were used to describe pretectum neurons as one of eleven previously identified functional response types (Kubo et al., 2014). To apply the formalism, we constructed a response matrix (Fig. B), consisting of averaged fluorescence responses for each pretectal response type, modeled retinal activity, and a stimulus-independent bias. We modeled the retina-pretectum circuit as a recurrent network receiving feedforward connections from the retina (Fig. C). Using previously described methods (Biswas et al., 2024), we then computed the feedforward and recurrent weight matrices that accounted for the responses and minimized the L^2 norm, W_{min}. We similarly found the smallest weight norm required to make each individual synapse equal to zero, a quantity called W_{cr}. The larger the W_{cr}, the more consistent the sign of a synapse across the ensemble of solutions (Biswas et al., 2024). We thus ranked the strength of predictions by W_{cr} values (Fig. D). Future work will test these anatomical predictions.

[1] Northwestern University Interdepartmental Neuroscience PhD Program (NUIN), Evanston IL, USA

[2] Department of Neurobiology, Northwestern University, Evanston, IL, USA

[3] Riken Center for Brain Science, Saitama, Japan

[4] Genes - Circuits - Behavior, Max Planck Institute for Biological Intelligence, Martinsried, Germany

[5] Department of Physics and Astronomy, Northwestern University, Evanston, IL, USA

[6] Department of Engineering Sciences and Applied Mathematics, Northwestern University, Evanston, IL, USA

[7] NSF-Simons National Institute for Theory and Mathematics in Biology, Chicago, IL, USA

We also assessed the predictive power of the framework by making and testing activity predictions. We hid one of the stimulus conditions and recomputed W_{min} (Fig. E) and W_{cr} (Fig. F) from the other stimulus conditions to predict how neurons would respond to the hidden condition. We evaluated the accuracy of our W_{cr}-ranked predictions for each response type across all the stimulus conditions and found that the first three to five highly ranked predictions were correct across all response types (Fig. G). In contrast, when we ranked our W_{min}-based predictions according to their absolute input drive, we found only one or two correct predictions (Fig. H).

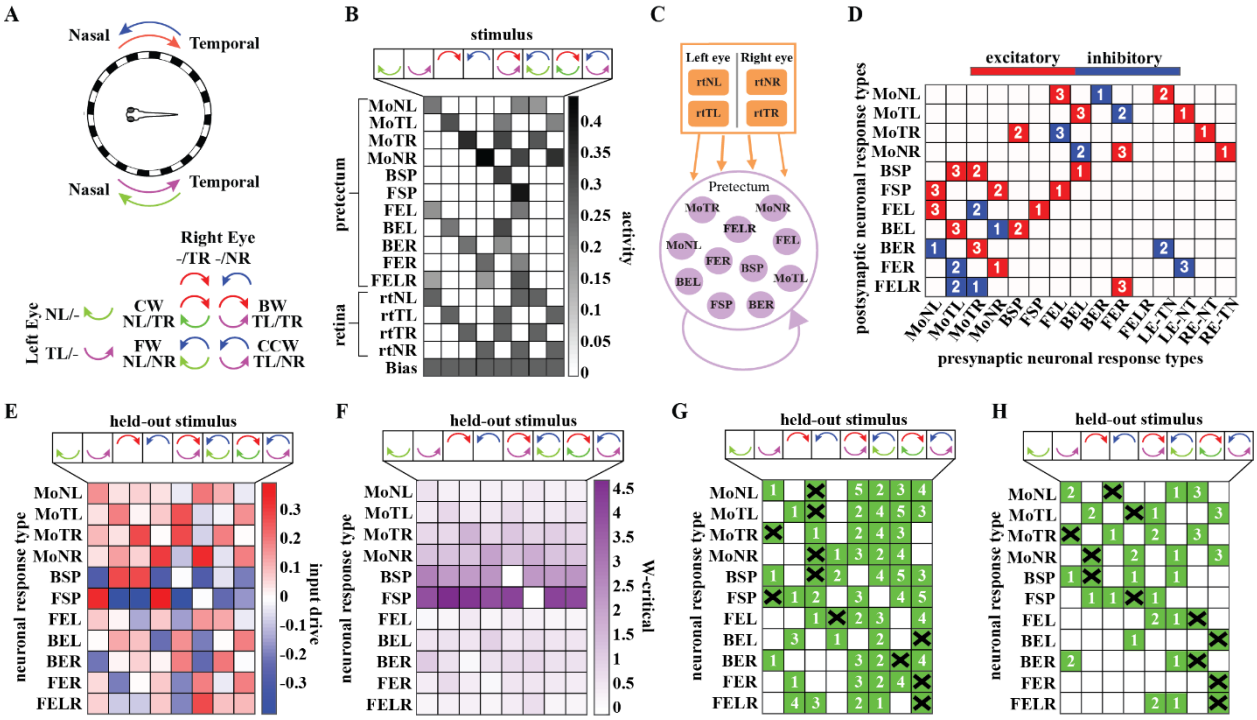

A. The experimental setup that generates a neural dataset to test the formalism (Kubo et al., 2014; Svara et al., 2022). NL/LE-TN—nasalward left eye, TL/LE-NT—temporalward left eye, NR/RE-TN—nasalward right eye, TR/RE-NT—temporalward right eye, CW—clockwise, CCW—counterclockwise, FW—forward, and BW—backward. B. Response matrix. The top eleven rows represent the activity patterns of major response types. Four monocular response types: MoNL, MoTL, MoTR, and MoNR. Seven binocular response types: FEL, FER, FSP, FELR, BEL, BER, BSP. See previous papers for explanation of response type names. The subsequent four rows represent the input activity from retinal neurons. The bottom row represents the bias term. (C) Neural network architecture. (D) Strongest structural predictions from W_{cr}. (E) Input drive predictions for a held-out stimulus condition for each response type. (F) W_{cr} matrix. (G) We ranked activity predictions based on W_{cr} magnitude across all stimuli for each response type in ascending order until the first incorrect prediction. The green boxes with the values on top indicate the correct prediction and ranking. The green boxes with the cross show the first incorrect prediction. No predictions were assessed after the first incorrect one, indicated by white boxes. (H) We similarly ranked activity predictions based on the input drives (e.g., panel E).

References:

[1] Biswas, T., Li, T. L., & Fitzgerald, J. E. (2024). Tensor formalism for predicting synaptic connections with ensemble modeling or optimization (No. arXiv:2310.20309). arXiv. https://doi.org/10.48550/arXiv.2310.20309

[2] Kubo, F., Hablitzel, B., Dal Maschio, M., Driever, W., Baier, H., & Arrenberg, A. B. (2014). Functional Architecture of an Optic Flow-Responsive Area that Drives Horizontal Eye Movements in Zebrafish. Neuron, 81(6), 1344–1359.

[3] Naumann, E. A., Fitzgerald, J. E., Dunn, T. W., Rihel, J., Sompolinsky, H., & Engert, F. (2016). From Whole-Brain Data to Functional Circuit Models: The Zebrafish Optomotor Response. Cell, 167(4), 947-960.e20.

[4] Svara, F., Förster, D., Kubo, F., Januszewski, M., Dal Maschio, M., Schubert, P. J., Kornfeld, J., Wanner, A. A., Laurell, E., Denk, W., & Baier, H. (2022). Automated synapse-level reconstruction of neural circuits in the larval zebrafish brain. Nature Methods, 19(11), 1357–1366.

Personalizing Agent-Based Models to Construct Medical Digital Twins*

Adam C. Knapp† Daniel A. Cruz† Borna Mehrad† Reinhard C. Laubenbacher†

Abstract

Digital twin technology, originally developed for engineering, is being adapted to biomedicine and healthcare. A key challenge in this process is dynamically calibrating computational models to individual patients using data collected over time. This calibration is vital for improving model-based predictions and enabling personalized medicine. Biomedical models are often complex, incorporating multiple scales of biology and both stochastic and spatially heterogeneous elements. Agent-based models (ABMs), which simulate autonomous agents such as cells, are commonly used to capture how local interactions affect system-level behavior. However, no standard personalization methods exist for these models. The main challenge is bridging the gap between clinically measurable macrostates (e.g., blood pressure, heart rate) and the detailed microstate data (e.g., cellular processes) needed to run the model. In this work, we propose an algorithm that applies the ensemble Kalman filter (EnKF), a classic data assimilation technique, at the macrostate level. We then link the Kalman update at the macrostate to corresponding updates at the microstate level, ensuring that the resulting microstates are compatible with the desired macrostates and consistent with the model's dynamics. This approach improves the personalization of complex biomedical models and enhances model-based forecasts for individual patients.

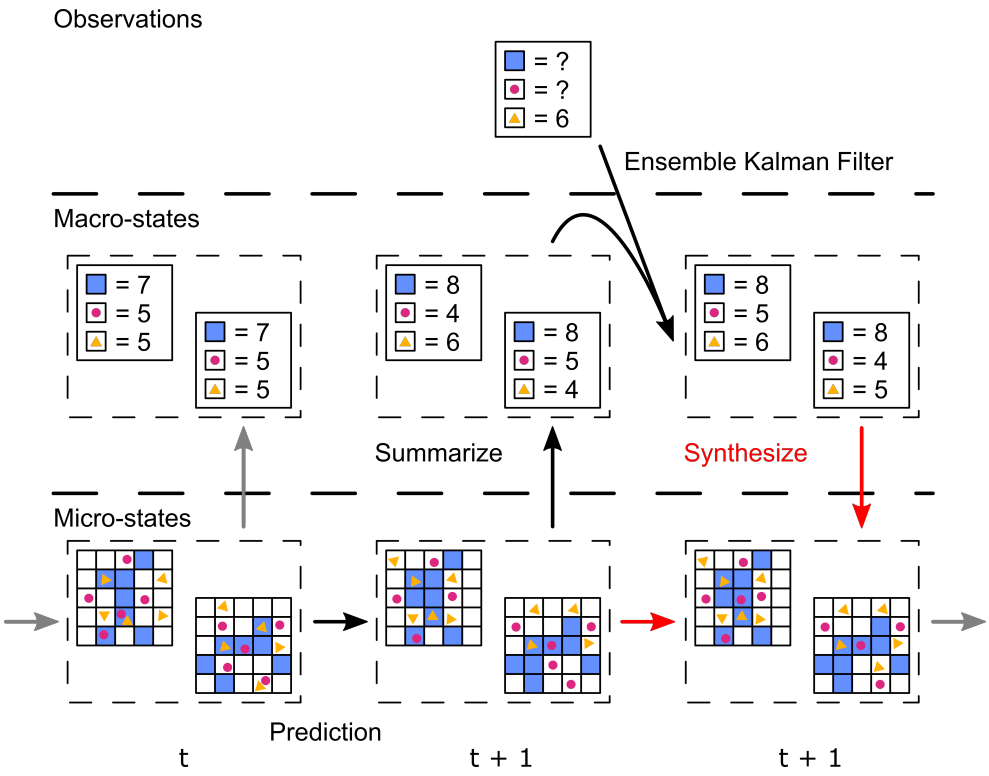

Figure 1: Overview of our algorithm. An ensemble of microstates at time t is advanced to $t + 1$ using the ABM to generate predictions. The updated microstates are then summarized into macrostates. The EnKF resamples the updated ensemble of macrostates. The previous microstates are used as seeds for the synthesis of new macrostate-compatible microstates (in red).

*Associated preprint can be accessed at `https://www.biorxiv.org/lookup/doi/10.1101/2024.05.31.596692`

†Division of Pulmonary, Critical Care and Sleep Medicine, Department of Medicine, University of Florida

Bicoid-nucleosome competition sets a concentration threshold for transcription constrained by genome replication

Eleanor A. Degen[1,2], Corinne Croslyn[1,2], Niall M. Mangan[3,4], and Shelby A. Blythe[2,4]

1: Interdisciplinary Biological Sciences Graduate Program, Northwestern University, Evanston Illinois 60208, USA
2: Department of Molecular Biosciences, Northwestern University, Evanston, Illinois 60208, USA
3: Department of Engineering Sciences and Applied Mathematics, Northwestern University, Evanston, Illinois 60208, USA
4: National Institute for Theory and Mathematics in Biology, Northwestern University and The University of Chicago, Chicago, IL, USA

Concentration gradients of transcription factors establish patterns of gene expression during a time in early embryonic development characterized by frequent mitotic divisions, rounds of genome replication, and chromatin reorganization. In the *Drosophila* embryo, an exponential gradient of the transcription factor Bicoid (Bcd) activates the earliest expressed patterning genes across the anterior-posterior axis. Bcd successfully navigates the chromatin of the replicating genome to bind its sites and facilitate transcription. However, we do not fully understand how genomic context leads to differential transcriptional outputs across Bcd concentrations. We aim to model how enhancer sequence, chromatin, and DNA replication together determine the Bcd concentration-sensitivity of the transcriptional process. By live-imaging an MS2-MCP transcriptional reporter for the *hunchback* P2 (hbP2) enhancer, we have found that the length of the delay between mitosis and the initiation of transcription uniquely reflects Bcd concentration-sensitive regulation. We have defined a stochastic model of transcriptional regulation that accurately predicts transcriptional onset times using mathematical descriptions of Bcd-nucleosome competition for occupancy and the probability of DNA replication at hbP2. Our work suggests that Bcd's ability to outcompete nucleosomes dictates a Bcd concentration threshold for expression, while DNA replication limits the rate of transcriptional activation at high concentrations where Bcd readily outcompetes nucleosomes. Disrupting nucleosome stability by promoting pioneer factor binding to hbP2 both expands the MS2 expression domain and preserves onset time variance at high concentrations, supporting the model's predictions. We provide a theoretical framework for understanding how the critical parameters of nucleosome positioning, stability, and replication dynamics can govern the sensitivity of gene expression to transcription factor concentration.

A continuum limit for dense spatial networks

Sidney Holden – Flatiron Institute

Abstract

Many physical systems–such as dense neuronal or vascular networks and optical waveguide lattices–can be modeled by spatial networks, where slender "wires" (edges) support wave or diffusion equations subject to conservation conditions at nodes. We propose a continuum-limit framework which replaces edgewise differential equations with a coarse-grained partial differential equation (PDE) defined on the continuous space occupied by the network. The derivation naturally introduces an *edge-conductivity tensor*, an *edge-capacity function*, and a *vertex number density* to encode how each microscopic patch of the graph contributes to the macroscopic phenomena. We calculate all macroscopic parameters from first principles via a systematic discrete-to-continuous local homogenization, finding an anomalous effective embedding dimension resulting from a homogenized diffusivity. These high-density networks encode emergent material and functional properties. They reflect the ability of many real-world, space-filling networks to operate simultaneously at multiple scales–both at the system-wide and local levels–using the continuum as a feature. Numerical examples—including periodic lattices and random graphs (figure left, center)—demonstrate that each finite model converges to its corresponding PDE (posed on different manifolds like tori, disks, and spheres) in the limit of increasing vertex density. We expect our results to be useful in modelling biological network growth and function (e.g. quail embryo vasculature–figure right).

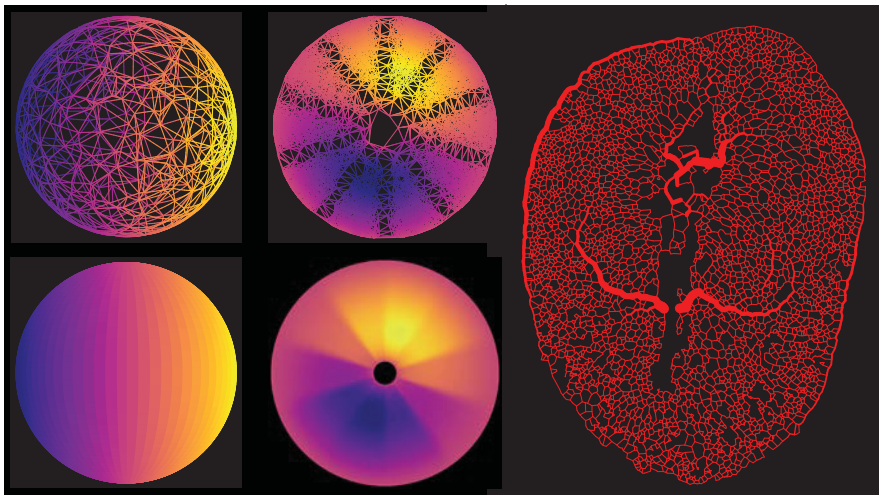

Network RNA Velocity

Boya Hou[1], Maxim Raginsky[1], Abhishek Pandey[2], and Olgica Milenkovic[1]

[1]Carl R. Woese Institute for Genomic Biology, University of Illinois Urbana-Champaign
[2]AbbVie

Abstract

RNA velocity is a powerful model for cellular RNA splicing events which can be used to infer dynamical properties of various regulatory functions. Despite its wide applicability, the model has not been adequately adjusted to account for multiway gene regulatory or intercellular interactions. Here, we propose to revise the RNA velocity approach by incorporating two new network components: an intracellular gene regulatory network (GRN) that regulates gene expression, and an intercellular interaction network that captures interactions between (neighboring) cells. By combining GRN and intercellular communication models, we aim to provide a more holistic understanding of single-cell gene expression dynamics through the lens of systems and control theory. In particular, we investigate network steady states, stability and targeted drug intervention.

RNA velocity is a useful tool for inferring differentiation trajectories from bulk and single-cell RNA sequencing data. By measuring the number of unspliced and spliced mRNA, RNA velocity serves as an indicator of the future state of mature mRNA and can therefore be used to infer cell cycle dynamics. Specifically, given a single cell and a single gene, the evolution of unspliced RNA $u(t)$ and spliced RNA $s(t)$ is captured by ordinary differential equations (ODEs) of the form $\frac{du}{dt} = \alpha(t) - \beta u(t)$, $\frac{ds}{dt} = \beta u(t) - \gamma s(t)$, per [3], where α stands for the transcription rate, β represents the splicing rate, while γ equals the degradation rate. RNA velocity is defined as $v(t) = \frac{ds}{dt}$ [3]. A positive RNA velocity suggests that the expression of the underlying gene is increasing, while a negative RNA velocity indicates an opposite trend; in addition, $v(t) = 0$ implies that the system reaches the steady state. The above equations only model the transcriptional dynamics of a single gene within a single cell, and abstracts various network controls through the rate parameters, which are allowed to change with time. However, to enable modeling of interventions, one needs to explicitly account for the regulatory relationships between genes that control the transcription process. Furthermore, to describe communications between cells, it is desirable to introduce consensus constraints that can be explained via spatial transcriptomics data (due to space limitations, we postpone the discussion of spatial networks to the full manuscript). Towards this end, we assume that each gene expression is controlled by a GRN comprising n_g regulatory genes[1]. Since gene expression can be either positively (promotion) or negatively (inhibition) regulated [2], we use two nonnegative matrices W^+ and W^- to represent weighted directed GRNs in which W^+ captures positive and W^- negative regulations. The evolution of unspliced RNA $u^g(t)$ and spliced RNA $s^g(t)$ can be described as

$$\frac{du^g}{dt} = \alpha^g \frac{\kappa + \sum_{q=1}^{n_g} W^+_{gq} s^q(t)}{\kappa + \sum_{q=1}^{n_g} W^-_{gq} s^q(t)} - \beta^g u^g(t), \quad \frac{ds^g}{dt} = \beta^g u^g(t) - \gamma^g s^g(t), \tag{1}$$

where $\kappa \geq 0$ is a constant. We further assume for simplicity that there are no self-loops, i.e., $W^+_{gg} = W^-_{gg} = 0$. Here the rates represent the *expression, splicing and degradation capacities* of individual genes, but how much of that capacity is utilized is controlled by the network of transcription factors indexed by g. This allows for direct accounting for individual transcription factor influences, as well as intervention efficiency. Next, let $u := [u^1, \cdots, u^{n_g}]^\top$, $s := [s^1, \cdots, s^{n_g}]^\top$, $\alpha = \text{diag}\left(\alpha^1, \cdots, \alpha^{n_g}\right)$, $\beta = \text{diag}\left(\beta^1, \cdots, \beta^{n_g}\right)$, and $\gamma = \text{diag}\left(\gamma^1, \cdots, \gamma^{n_g}\right)$. Define the nonlinear function

$$R_g(s) := \frac{\kappa + \sum_{q=1}^{n_g} W^+_{gq} s^q(t)}{\kappa + \sum_{q=1}^{n_g} W^-_{gq} s^q(t)}, \quad g = 1, \cdots, n_g. \tag{2}$$

[1]For simplicity, the proposed model is mostly tailored towards transcription factor regulatory networks.

Let $R(s) := [R_1(s), \cdots, R_{n_g}(s)]^\top$. Equation (1) can be compactly rewritten as

$$\frac{du}{dt} = \alpha R(s) - \beta u, \quad \frac{ds}{dt} = \beta u - \gamma s. \tag{3}$$

Our main analytical results for the networked dynamics (1) are listed below. The following theorem provides a sufficient condition for the existence of steady states.

THEOREM 0.1. *Suppose that $\beta^g > 0$ and $\gamma^g > 0$ for all genes $g = 1, \cdots, n_g$. Let $C = \max_g \sum_{q=1}^{n_g} W^+_{gq}$ and $\xi = \max_g \frac{\alpha^g}{\gamma^g}$. The networked dynamics admits a steady state (u^*, s^*) if $\kappa \geq C\xi$.*

We next study the stability of the networked dynamics. Notice that when W^- is a zero matrix, i.e., no gene acts as an inhibitor of any other gene, we have a linear system $\frac{du^g}{dt} = \alpha^g \left(\kappa + \sum_{q=1}^{n_g} W^+_{gq} s^q(t)\right) - \beta^g u^g(t)$, $\frac{ds^g}{dt} = \beta^g u^g(t) - \gamma^g s^g(t)$, which may be unstable.

LEMMA 0.1. *Suppose the condition of Theorem 0.1 holds. When there is no inhibitor, i.e., $W^-_{gq} = 0$, $\forall g, q = 1, \cdots, n_g$, the networked dynamics is stable if for all g, $\gamma_g > \beta_g > \alpha_g \sum_h W^+_{gh}$.*

When W^- is not the zero matrix, the system is nonlinear and may or may not be stable depending on how strong the negative feedback is (i.e., how large the incremental gains are). The following theorem characterizes the stability via the Lyapunov direct method [1].

THEOREM 0.2. *Suppose the conditions of Theorem 0.1 hold. Consider a positive semi-definite function $V(u, s) := \frac{1}{2}\|u - u^*\|^2 + \frac{1}{2}\|s - s^*\|^2$. Let $\|s\|_1 = \sum_{q=1}^{n_g} s^q(t)$, and suppose that there exists a $\delta > 0$ s.t. $\min_g [W^- s]_g \geq \delta \|s\|_1$. Denote $c_1 := \max_{g,q} \left(W^+_{gq}, W^-_{gq}\right)$, and $\omega := n_g \max\left(\frac{c_1}{\kappa}, \frac{c_1^3}{4\delta\kappa(c_1 - \delta)}\right)$. If $\gamma - \frac{\omega\|\alpha\|}{2} I \succ 0$, and $\beta - \frac{\omega\|\alpha\|}{2} I - \frac{1}{4}\beta\left(\gamma - \frac{\omega\|\alpha\|}{2} I\right)^{-1} \beta \succeq 0$, then, $\dot{V}(u, s) < 0$ for all $(u, s) \neq (u^*, s^*)$. That is, $V(u, s)$ is a valid Lyapunov function, and (u^*, s^*) is asymptotically stable.*

We also simulate the network dynamics (1), and present results for a GRN comprising five genes. In the simulation, W^+ (promotor) encodes positive regulations from gene 2 to 1 ($W^+_{21} = 0.6$), gene 4 to 1 ($W^+_{41} = 0.4$), and gene 5 to 4 ($W^+_{54} = 0.2$); and W^- (inhibitor) encodes negative regulation from gene 1 to 5 (weight $W^-_{15} = 0.1$), gene 3 to 1 ($W^-_{31} = 0.2$), and gene 3 to 4 ($W^-_{34} = 0.1$). At time $t = 3$, the transcription rate α^1 of gene $g = 1$ is set to 0, while the rates α^g for $g = 2, 3, 4, 5$ remain the same. Figure 1 shows that after intervention forces α^1 to 0, fewer unspliced RNAs u^1 are produced, and as a consequence of the regulatory effect of the GRN, u^2, u^3 and s^2, s^3 also decrease.

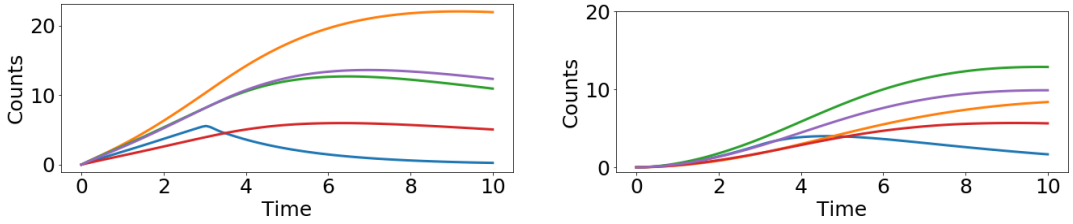

(a) Unspliced RNA concentration $u^g(t)$ (b) Spliced RNA concentration $s^g(t)$

Figure 1: Plots of u^g and s^g for gene 1 (—), gene 2 (—), gene 3 (—), gene 4 (—), gene 5 (—).

References

[1] Hassan K Khalil and Jessy W Grizzle. *Nonlinear systems*, volume 3. Prentice hall Upper Saddle River, NJ, 2002.

[2] Mustafa H Khammash. Cybergenetics: Theory and applications of genetic control systems. *Proceedings of the IEEE*, 110(5):631–658, 2022.

[3] Gioele La Manno, Ruslan Soldatov, Amit Zeisel, Emelie Braun, Hannah Hochgerner, Viktor Petukhov, Katja Lidschreiber, Maria E Kastriti, Peter Lönnerberg, Alessandro Furlan, et al. Rna velocity of single cells. *Nature*, 560(7719):494–498, 2018.

Geometric model manifold of space, time, and belief in hippocampal cognitive maps

Jason Z. Kim[1], James P. Sethna[1], Itai Cohen[1,2], Weinan Sun[3]

Abstract:

Cognitive maps are mental representations of spatial and conceptual relationships in an environment. The hippocampus, a key brain region for these maps, exhibits neural population activity that often evolves along nonlinear, low-dimensional manifolds. While cognitive maps have been characterized at the level of cell tunings to spatial location and decorrelations over time, a precise, unsupervised, and quantitative model of how this map forms and morphs at the population level remains elusive due to the large dimensionality and nonlinearity of neural activity. Current dimensionality reduction techniques have difficulty capturing this manifold in an interpretable way due to two shortcomings: they do not model regions of neural activity where there are no data, and the map from the embedding back to neural activity is too nonlinear. We solve these problems in a novel unsupervised technique using differential geometry to model the low-dimensional space in which the data reside as a gently curved manifold. We apply this method to activity from thousands of neurons across several days in the CA1 region of the hippocampus of mice learning to collect rewards under two task conditions on a linear maze. We show that the 3 relevant variables of position (space), trial (time), and task belief emerge as local directions on the population-level manifold that captures track topology, a consistent direction of representational drift within and between days, and task learning that evolves orthogonally to baseline drift (resulting in tuning decorrelation). Further, the manifold quantifies neuron-level features—such as changes in positional tuning across trials—at the population level, and we discover neurons tuned for generalized states including space, time and belief. We provide a novel technique and a unifying theory for how population-level neural manifolds encode generalized state-time information along gently curved manifolds, which we hypothesize is for efficient recall and co-localization in downstream regions.

VR task: We trained transgenic mice expressing GCaMP6f in CA1 neurons in the hippocampus to navigate in a virtual reality environment while head-fixed (Fig. 1a) to image neural activity as they learned the relationship between visual cues and the future location of water reward delivery in two linear tracks (Fig. 1b). On each trial, water was delivered at one of two reward zones, either near or far from the beginning of the track, which we call R1 and R2, respectively. Prior to these rewarded locations, a visually distinct indicator cue (Ind) perfectly predicted the rewarded location (Fig. 1b).

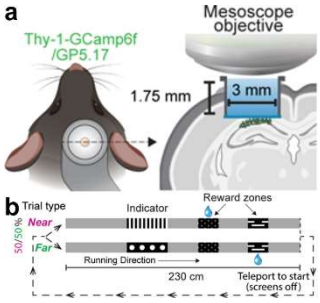

Figure 1: VR setup

Key Results:

Our first result is a method to build low-dimensional nonlinear manifolds from the neural activity across all days (Fig. 1a), directly in the high-dimensional space of neurons (Fig. 1b). Current dimensionality reduction techniques such as UMAP and VAEs have two shortcomings that make them difficult to interpret. First, they only model the regions where there are data, but not the geometry of the space between data (Fig. 1b). Second, the mapping from the low-dimensional embedding back to the space of neurons is too nonlinear to be interpretable. We render our manifolds interpretable by modeling the low-dimensional space in which the data reside as a k-dimensional manifold, and by regularizing its bending and stretching nonlinearities (Fig. 1c). Hence, points, lines, and angles in our embedding correspond to points, curves, and angles in the space of neurons. While the schematic manifold is a 2-dimensional surface, our results are in 3-dimensional volumes, and generalize to k dimensions.

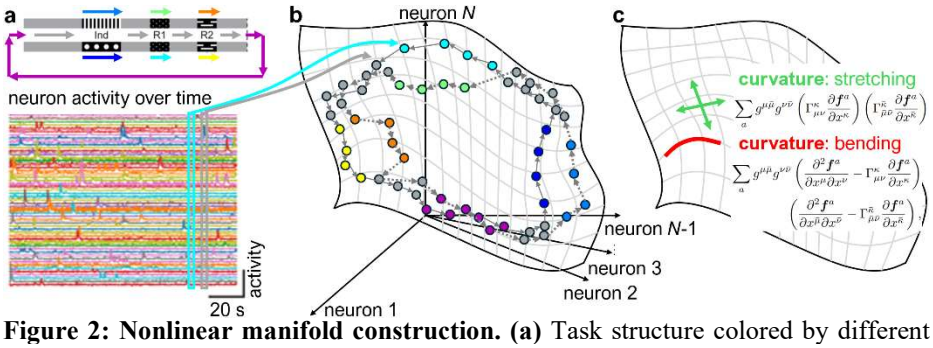

Figure 2: Nonlinear manifold construction. (a) Task structure colored by different segments and conditions (top) and example activity (bottom). **(b)** Each frame is a point in the high-dimensional space of N neurons, from which we construct **(c)** a low-dimensional geometric manifold with regularized nonlinearity to enable interpretability.

Our second key result is that, notably, the three relevant task variables of position (space) trial (time), and task condition (belief) emerge on a gently curved, 3-dimensional geometric manifold in high-dimensional neural activity space (Fig. 3ab).

[1]Department of Physics, Cornell University [2]Kavli Institute at Cornell for Nanoscale Science [3]Department of Neurobiology and Behavior, Cornell University

Specifically, the spatial topology of the track representation matches the topology of the maze (Fig. 3a), which evolves in an independent direction across trials (Fig. 3bc). By regularizing the stretching and bending curvatures (Fig. 2c), we preserve local distances and angles in neural coordinates (Fig. 3d): a flat plane in manifold coordinates (Fig. 3c) maps to a gently curving surface in neural coordinates (Fig. 3d). Hence, not only are the relevant task variables decodable from hippocampal activity, but they are decodable as the three most salient, gently curving projections directly in neuron space. We hypothesize that this geometrically smooth decodability plays a functional role in efficiently coding population activity to other regions.

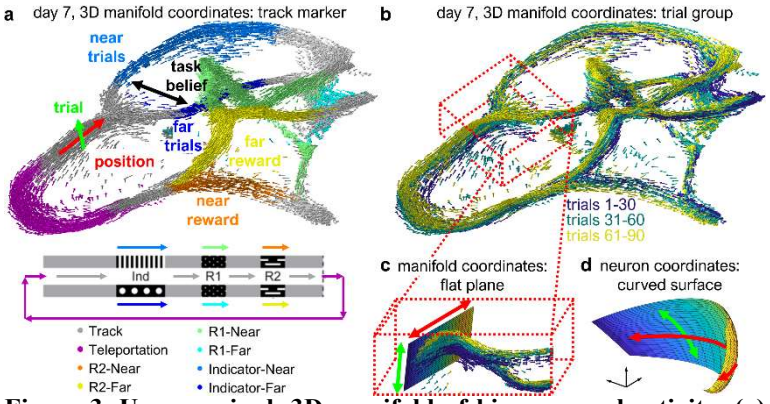

Figure 3. Unsupervised, 3D manifold of hippocampal activity. (a) Day 7 projection of mouse hippocampal activity onto a nonlinear 3D manifold colored by track marker and **(b)** trial number. **(c)** A flat plane in manifold coordinates is **(d)** a curved surface in neural coordinates.

Our third key result is that the evolution of the task representation varies smoothly, continuously, and consistently within the trials of one day (Fig. 3b), between the trials across many days (Fig. 4ab), and is independent from the directions of track position and task belief while preserving the geometry of the track (Fig. 4a). Additionally, we discover that task learning evolves orthogonally to the baseline representational drift toward the corresponding indicator activity (Fig. 4c), which manifests in the neuron-level activity as decorrelation, and tracks changes in licking behavior. We hypothesize that representational drift is an ongoing process that is consistent during (although perhaps more salient and requiring more volume in neuron space) and between behavior, and is a timekeeping mechanism to geometrically co-locate task and time.

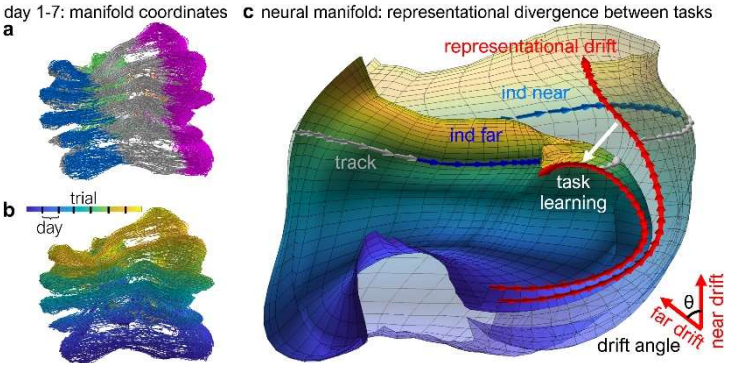

Figure 4. Geometry of representational drift. (a) Day 1-7 projection of neural activity onto a nonlinear 3D manifold colored by task marker and **(b)** trial. **(c)** 2D surfaces in manifold coordinates of track position and trial, with divergence after the indicator region.

Our final set of key results is that the manifold quantitatively models population-level coding observed in single cells. The manifold exhibits an acute angle between the track and trial directions (Fig. 4a), capturing the firing of some neurons at progressively earlier track positions over time (Fig. 3b) at a population rate of ~0.05 cm/trial (Fig. 3c). We discover cells are not only tuned for position, but also time (Fig. 4d) and task belief (Fig. 4e).

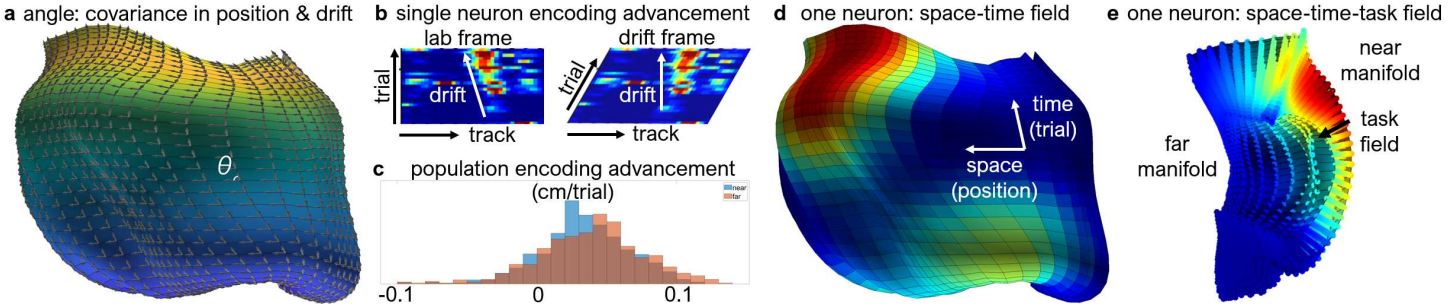

Figure 4. Population measures of neuron-level drift, and space-time-belief fields. (a) Neural manifold of "near" tasks with an acute angle between the directions along "track" position and "trial" time. **(b)** Same acute angle in the single neuron activity. **(c)** distribution of population-level advancement of ~0.05 cm/trial. **(d)** Decoded activity of one neuron on the manifold showing tuning for space and time. **(e)** Single neuron tuning for task belief, demonstrating activity gemoetrically codes for space (position), time (trial), and task belief.

Summary: We present a novel method using differential geometry to directly model the nonlinear geometry of neural representations. In hippocampus, we discover that representations of space, time, and belief live on gently curving manifolds in neuron space, flow skew along a consistent timekeeping axis, and code for generalized states.

References: Sun, Weinan, et al. *Nature* (2025). Kim, Jason Z. et al. arXiv:2403.01078

[1]Department of Physics, Cornell University [2]Kavli Institute at Cornell for Nanoscale Science [3]Department of Neurobiology and Behavior, Cornell University

Attractor-based models for sequences and pattern generation in neural circuits

Juliana Londono Alvarez* Katie Morrison† Carina Curto*

Abstract

Brain rhythms that generate walking, breathing, or swimming are traditionally modeled using coupled oscillators—intrinsically oscillating ("pacemaker") neurons. Alternatively, attractor networks—a framework in which cognitive processes are modeled as attractors of a dynamical system, typically implemented by a recurrent network—have been a central tool in theoretical neuroscience for modeling memory and pattern completion [1]. In this work, we show that attractor networks can also support rhythmic pattern generation. We present a single attractor network that can robustly encode five distinct quadruped gaits (bound, pace, trot, walk, and pronk) as coexisting attractors, without requiring parameter changes. Transitions between gaits can be triggered by simple external pulses. This contrasts with most existing locomotion models, which rely on finely tuned coupled oscillators whose parameters must be adjusted to switch between gaits. In addition, we introduce a novel method for encoding ordered sequences of gaits using *fusion* attractors, allowing the network to flexibly reuse existing patterns in different combinations (as in a sequence of dance moves).

Using theoretical results from a special family of threshold-linear networks (TLNs) [2, 3], we designed a single TLN with attractors corresponding to five distinct quadruped gaits (Figure 1A). In this network, each gait is represented by a distinct limit cycle. All of these attractors coexist for the same network parameters. Despite overlapping nodes between gaits, each attractor can be accessed through different initial conditions, without changing the network parameters. Moreover, external *targeted* pulses can be sent to the network to reliably trigger transitions between gaits (Figure 1B,C).

Next, to develop a network capable of stepping through a sequence of gaits (Figure 1D), we connect the 5-gait network to a discrete neural integrator TLN (not shown). This integrator TLN has multiple stable fixed points and can transition to "adjacent" ones in response to identical input pulses. When connected to the 5-gait network, attractors from both networks *fuse* together, resulting in an internally encoded sequence of gaits [4].

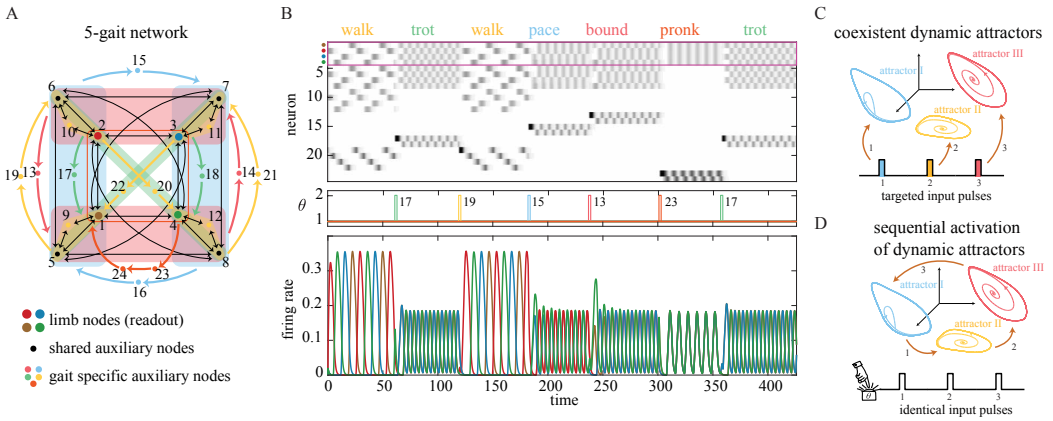

Figure 1: (A) Schematic of a 23-node network supporting 5 different quadruped gait patterns. (B) Attractors of the network in panel A, each accessed via targeted input pulses to gait-specific auxiliary nodes. Pink box highlights limb nodes. (C) Coexisting dynamic attractors, each accessible via distinct inputs, as in B. (D) Internally encoded sequence of dynamic attractors, with transitions triggered by identical inputs.

The construction that uses fusion attractors to step through gaits can also be applied to other CPG models [5], and suggests a possible mechanism for encoding ordered sequences of rhythmic patterns. All of this was done in the attractor network framework, combining stable fixed point attractors with dynamic ones, and was made possible, and analytically tractable, by the rich body of theoretical results available for TLNs.

*Brown University
†University of Northern Colorado

References

[1] M. Khona and I. R. Fiete, *Attractor and integrator networks in the brain*, Nature Reviews Neuroscience, 23 (2022), pp. 744–766.

[2] C. Curto and K. Morrison, *Graph rules for recurrent neural network dynamics*, Notices of the American Mathematical Society, 70 (2023), pp. 536–551.

[3] C. Parmelee, J. Londono Alvarez, C. Curto, and others, *Sequential attractors in combinatorial threshold-linear networks*, SIAM J. Appl. Dyn. Syst., 21 (2022), pp. 1597–1630.

[4] J. Londono Alvarez, K. Morrison, and C. Curto, *Attractor-based models for sequences and pattern generation in neural circuits*, bioRxiv preprint (2025).

[5] J. Londono Alvarez, *Attractor-based models for sequences and pattern generation in neural circuits*, Ph.D. thesis, The Pennsylvania State University, 2024.

Unraveling Prey Evasion Mechanisms in Zebrafish

Amlan Nayak* Andrew M. Hein†

Abstract

We developed an interactive platform using computer vision and feedback control to study zebrafish (Danio rerio) escape behavior in response to virtual predators and support the development of predictive models grounded in experimental data. Our results show that zebrafish adapt escape strategies based on neural impairments and social context, highlighting the role of internal models and predictive control. Embedding theory within our closed-loop experiments provides a testable framework for understanding the neural and computational basis of survival behavior.

Understanding predator–prey interactions requires more than ecological observation; it demands mechanistic, computational models that explain not only what behaviors occur, but why they emerge and persist. Traditional methods, such as open-loop laboratory experiments, often fail to capture the inherently closed-loop dynamics of pursuit and evasion interactions in which predator and prey continually adjust their movements in response to each other in real time. To overcome this limitation, we developed an interactive real-time experimental platform that integrates computer vision with feedback control algorithms to study escape behavior in Danio rerio (zebrafish). This system creates a true feedback loop, where virtual, algorithmically controlled predators pursue live prey, and the prey respond with naturalistic escape behavior. Unlike traditional assays that isolate individual escape responses, our approach allows us to examine the full temporal sequence of a pursuit and evasion maneuver.

Our central aim is not merely to describe observed behavior but to build predictive computational models, continually refined through experiment, that explain how prey and predators compute their actions under time constraints and uncertainty. This approach is directly inspired by and extends theoretical work in prior studies. Martin et al. (2021)[1] showed that escape outcomes cannot be explained by biomechanical traits alone. Instead, they depend critically on a prey's ability to estimate the predator's sensorimotor delay and precisely time its escape maneuver. Similarly, Martin et al. (2024)[2] demonstrated that predators cannot rely solely on delay-uncompensated feedback control; rather, predictive pursuit models which forecast both prey and self-motion better reproduce real-world chase trajectories. These findings suggest that effective pursuit relies on an internal forward model that anticipates the consequences of delayed perception and movement.

Our own experiments reinforce these insights. In trials with neurally manipulated zebrafish whose fast-start reflexes were impaired, we observed that prey adjust their decision thresholds to compensate for prolonged sensory-motor delays. Moreover, in group contexts, our system reveals that prey dynamically assess predation risk: only individuals directly in a predator's strike zone initiate escape, while others remain unaffected. This selective responsiveness indicates that prey use a combination of sensory input and internal risk estimation to gauge threat level.

By embedding computational models directly into our experimental loop, we not only test existing theories of pursuit and evasion but also develop biologically grounded models that capture the real-time constraints of neural processing, motion forecasting, and decision-making under uncertainty. Ultimately, what emerges from this recursive methodology is not just a description of behavior, but a dynamic, testable framework for understanding real-time decision-making in predator–prey systems. By fusing experimental data, neuroscience, and computational modeling, we aim to uncover the fundamental control algorithms that underlie survival strategies in nature.

References

[1] Martin, Benjamin T., Michael A. Gil, Ashkaan K. Fahimipour, and Andrew M. Hein. "Informational constraints on predator–prey interactions." Oikos 2022, no. 10 (2022): e08143.

*Department of Computational Biology, Cornell University. Email: an526@cornell.edu
†Department of Computational Biology, Cornell University. Email: amh433@cornell.edu

[2] Martin, Benjamin T., David Sparks, Andrew M. Hein, and James C. Liao. "Fish couple forecasting with feedback control to chase and capture moving prey." Proceedings of the Royal Society B 291, no. 2031 (2024): 20241463.

Division asymmetries and their effects on cell cycles promote *Drosophila melanogaster* pole cell heterogeneity

Hayden Nunley[*] Liu Yang[†] Alexandre O. Jacinto[*] Celia M. Smits[†‡] Niles Huang[†]
Brian Knight[*] Elizabeth R. Gavis[‡] Stanislav Y. Shvartsman[*†‡]

Development of a multicellular organism depends on the regulation of the relative timings and number of cell divisions. The core process for regulating divisions is the mitotic cell cycle, arising from a network of biochemical interactions. One can view each cell as an oscillatory dynamical system that divides after each completed oscillation. In such a growing population of oscillators, the number of cell divisions is often controlled by the build-up of inhibitors in each oscillator and/or by oscillator-oscillator interactions. Despite the relevance of these phenomena in development, experimental quantifications and corresponding mathematical models for them have been lacking. By live-imaging, segmentation and tracking, we quantify proliferation in a population of cells — the *Drosophila melanogaster* germ cell precursors, called pole cells — from their formation to cell cycle arrest. Then, we propose and analyze a mathematical model in which each cell is a non-linear phase oscillator whose phase progression is inhibited by translation of inherited mRNAs. Unequal partitioning of mRNAs at divisions promotes asynchrony until the population arrests. This model provides insights into inter-embryo variability in final cell number and intra-embryo variability in 'germ cell quality'. Rather than synchronizing and homogenizing the cells, cell cycle regulation counterintuitively acts to generate variability.

Our experimental model, *Drosophila melanogaster* pole cells, is a convenient system to study the regulation of cell proliferation. Relative to the development of the rest of the embryo — with stereotyped and coordinated cell cycles — pole cells exhibit significant intra- and inter-embryonic differences in the relative timings and extent of proliferation [1]. Their cell cycles arrest primarily due to the translation of inherited mRNAs into proteins that inhibit cell cycle progression [2]. Based on our live-imaging data, we construct lineage trees that then motivate a mathematical model for a growing population of oscillators. The initial condition is a small number of oscillators that unequally partition a pool of inherited mRNAs. Because of this partitioning, the cell-cycle-inhibitory concentrations slowly diverge from each other in this population. Once an oscillator completes a cycle, it divides and unequally splits its mRNAs — an assumption motivated by our data. For the observed sign of coupling between mRNA content and the non-linear phase oscillator, initial differences between pole cells are exacerbated by this process. We expect that our mathematical approach for growing dynamical systems will prove useful in other developmental contexts, including cases where cell-cell interactions couple cell cycles.

References

[1] T. T. Su, S. D. Campbell, and P. H. O'Farrell, *The Cell Cycle Program in Germ Cells of the Drosophila Embryo*, Dev. Biol., 196 (1998), pp. 160–170.

[2] M. Asaoka-Taguchi, M. Yamada, A. Nakamura, K. Hanyu, and S. Kobayashi, *Maternal Pumilio acts together with Nanos in germline development in Drosophila embryos*, Nat. Cell. Biol., 1 (1999), pp. 431–437.

[*]Center for Computational Biology, Flatiron Institute
[†]Lewis Sigler Institute for Integrative Genomics, Princeton University
[‡]Department of Molecular Biology, Princeton University

Structural Causes of Pattern Formation and Loss Through Model-Independent Bifurcation Theory*

Liam D. O'Brien † Adriana T. Dawes ‡

Abstract

During development, precise cellular patterning is essential for the formation of functional tissues and organs. These patterns arise from conserved signaling networks that regulate communication both within and between cells. In this talk, we will develop and present a model-independent ordinary differential equation (ODE) framework for analyzing pattern formation in a homogeneous cell array. In contrast to traditional approaches that focus on specific equations, our method relies solely on general assumptions about global intercellular communication (between cells) and qualitative properties of local intracellular biochemical signaling (within cells). Prior work has shown that global intercellular communication networks alone determine the possible emergent patterns in a generic system. We build on these results by demonstrating that additional constraints on the local intracellular signaling network lead to a single stable pattern which depends on the qualitative features of the network. Our framework enables the prediction of cell fate patterns with minimal modeling assumptions, and provides a powerful tool for inferring unknown interactions within signaling networks by analyzing tissue-level patterns.

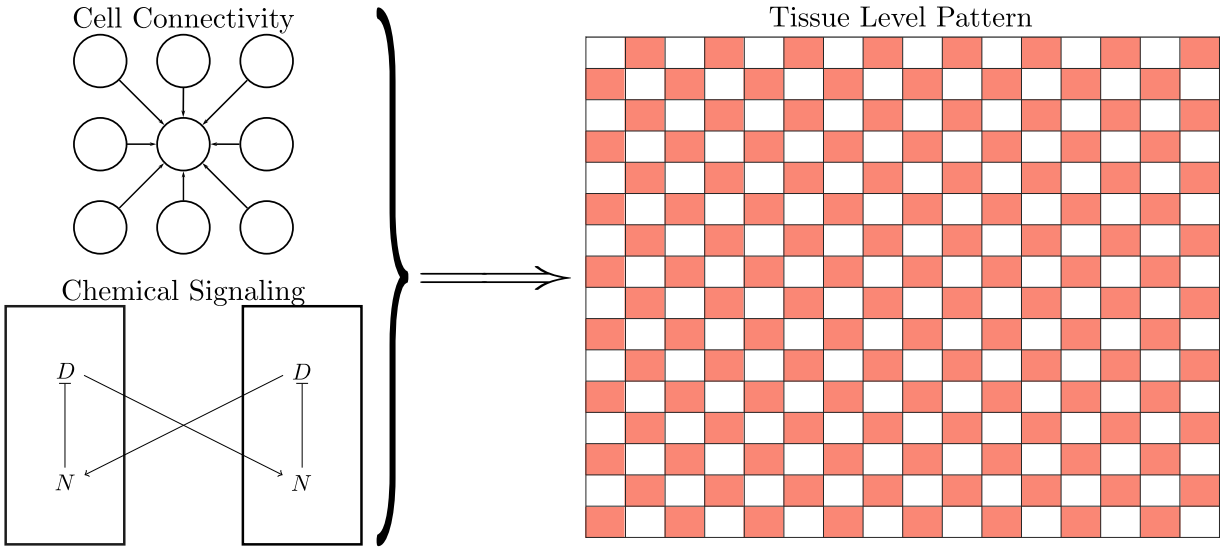

Figure 1: This schematic represents the results of our main theorem. Given qualitative information about the cell-communication network (e.g. top left) and chemical signaling network (e.g. bottom left), we are able to predict the tissue level pattern (e.g. right).

*The preprint of the article can be accessed at `https://www.researchsquare.com/article/rs-6098751/latest`

†The Ohio State University, Department of Mathematics

‡The Ohio State University, Department of Mathematics and Department of Molecular Genetrics

ABSTRACT

Modeling Mitotic Wave Origins in *Drosophila Melanogaster*

Harrison Oatman[1], Liu Yang[1], Hayden Nunley[2], Daniel Alber[1], Jared Toettcher[1], Stas Shvartsman[1, 2]

In the first few hours of embryonic development in *Drosophila melanogaster*, 13 rounds of rapid nuclear divisions bring the count of nuclei from one to nearly six thousand. Such quick advancement offers a selective advantage, but synchronizing cell cycle timing across the ~500 μm embryo with a precision better than five minutes presents a significant organizational challenge. The embryo's solution—studied for over four decades—is a series of mitotic waves originating from the poles of the egg and cascading towards the equator. Biologists and physicists, inspired by this feat of large-scale organization, have modeled these waves as a reaction-diffusion system based on careful observation of cell cycle kinase activity. Still, the precise reasoning for mitotic wave slowdown and the factors influencing mitotic wave origin are unclear.

Using high-resolution in toto lightsheet live imaging combined with newly developed machine learning methods for nuclear segmentation and lineage tracking, I provide a single-cell perspective on this phenomenon. By tracking cell lineages and monitoring cell cycle progression through the classification of nuclear morphology, I have determined that mitotic wave slowdown can be explained through small but persistent delays in interphase. Comparing healthy embryos with embryos lacking terminal signalling pattern, I have shown that Erk patterning speeds interphase progression and pushes the wave origins towards the anterior and posterior poles. This work highlights how advances in high-throughput imaging and modern machine learning can yield new insights into developmental dynamics and enable data-driven modeling of complex biological systems.

---

1 Princeton University

2. Flatiron Institute Center for Computational Biology

A Cell-Based Mechanical Model Captures Stress Relaxation and Flow in Proliferating Tissues with Subcellular Elasticity

Nonthakorn Olaranont Yifan Gu Min Wu
Assistant Research Professor

Department of Mathematical Sciences, Worcester Polytechnic Institute, MA 01609, USA

Abstract

Many developmental shape changes, such as brain convolution and gut folding, are governed by nonlinear mechanics under tissue growth. Yet living tissues also exhibit fluid-like behavior, dynamically rearranging to relieve stress and form complex shapes. It remains unclear how proliferating tissues simultaneously generate elastic forces, relax them, and exhibit fluidity at the intercellular level.

We present a vertex-based computational model that captures these multiscale behaviors by embedding subcellular shear elasticity via triangulated reference states and evolving deformation gradients. Cell pressure is tracked through deviations from reference cell size, with proliferation modeled as both a change in cell number and reference configuration. This framework enables simulation of tissue-scale flows with built-in growth and mechanical heterogeneity.

Our model reproduces buckling behavior consistent with continuum nonlinear growth-elasticity theory and further reveals how local intra- and intercellular rearrangements mediate stress relaxation and shape change. We also demonstrate how microscopic cellular architecture impacts macroscopic growth-driven flow and morphogenesis. Mathematically, the model leverages smooth optimization techniques, incorporating gradients and Hessians to improve computational performance and allow local linear stability analysis of solutions.

We apply the framework to simulate large-scale tissue flows during Drosophila wing disc and dorsal thorax morphogenesis, as well as in vitro circular wound closure in partial EMT monolayers. This predictive tool bridges cellular mechanics with emergent tissue-scale dynamics, with applications to development, regeneration, and cancer.

Acknowledgment. This work is partially supported by NSF-CAREER DMS 2144372 and NIH-NIGMS R01GM157590.

The space-time dynamics of sleep oscillations and its implications for cognition and health.

submitter and prospective speaker: Paola Malerba

Overview: Sleep is a state of highly rhythmic brain dynamics that is crucial for health and cognition. Current studies typically examine sleep brain oscillations measured by electroencephalography (EEG). Studies show that these sleep oscillations serve to organize information processing and communication in relation to a specific behavior, and are related to health functions of sleep such as homeostatic maintenance of synaptic architecture and clearance of the glymphatic system. Yet, the fundamental properties of brain oscillations that mediate these relations to function are not understood. This underscores the need for generalizable analytical methods that can support development of mechanistic knowledge linking sleep EEG to functional cognitive and health outcomes. This needs to be paired with understanding of within-subjects (i.e., personalized) factors influencing how changes in space-time organization of the sleep EEG can act as markers of functional differentiation, for example in translational studies.

In this talk, I will show that that space-time patterns of sleep brain oscillations can be identified in a data-driven way, and that they can differentiate brain dynamics beyond its topology (over which they are built) to reveal biophysical differentiation relevant to information processing and brain function. I will also show how we leverage machine learning to reveal a refined picture of space-time dynamics of NREM sleep oscillations, articulated across light and deep sleep stages, and in differentially organized space-time profiles that in turn recruit different functional networks. I will then introduce our feature-based approach to classification of sleep slow oscillations, which allows for study of space-time organization in clinical sleep EEG montages (with traditionally sparse head electrode density), and briefly mention our recent effort on modeling the emergence of slow oscillations across the night as a point process. I will conclude with example of preliminary results in translational applications of the space-time organization techniques in hypersomnolence and depression.

Detailed Description: We introduce a data-driven approach to the algorithmic discovery of space-time profiles of events on the EEG manifold that is clearly interpretable and widely applicable. We deployed this approach to slow oscillations (SOs, .5-1Hz) and spindles (10-16 Hz), where SOs are generally understood as large travelling waves, thought to reflect sleep homeostasis, as well as support memory formation, and spindles are understood as highly variable locally organized events that promote activity-dependent synaptic plasticity. We use co-detection of events at a small delay to generate a binary non-sparse matrix that is analyzed with k-means clustering with Hamming distance[1]. This allows the identification of structurally different space-time profiles, which can then be compared at a biophysical and functional level. For SOs, we found a Global, Local and Frontal differentiation. The clusters had different biophysical properties, such as amplitude and coordination with sleep spindles. In spindles[2], we also found a differentiation in biophysical properties across space-time profiles, spanning amplitude, frequency and coupling with SOs. Further analysis[3] with directional information flow (Generalized Partial Directed Coherence) showed that Global SOs create short-lived windows of opportunity in which information processing among distal regions is enhanced, a property not shared by other SO types. The patterning of SOs in Global/Local/Frontal was replicated in another study, where a machine learning analysis showed that the cortical-subcortical estimated profiles of Global SOs are differentiated from non-Global SOs within individuals[4]. Furthermore, pilot results suggest that SO types contribute differently to synergistic cognitive process, with long-term memory improvement associated with an increase in Global SOs and a decrease in Local SOs. We have prepared an open-source version of our analysis code that could be leveraged by other laboratories to study the space-time activity of events of their interest[5]. We have also developed a feature-based approach to classification of SOs that allows for study of SO space-time profiles in clinical sleep study EEG montages (traditionally sparse on the scalp). In a translational collaborative effort, this method was applied to sleep recordings from people with hypersomnolence (excessive sleepiness during the day), the most common sleep complaint, associated to emergence of depression and numerous comorbidities. We showed a specific excess in the amount of Frontal SOs in individuals related to hypersomnolence[6].

References: [1] Malerba et al. Sleep 2019, https://doi.org:10.1093/sleep/zsy197; [2] Malerba et al., Sleep 2022 https://doi.org:10.1093/sleep/zsac132; [3] Niknazar et al., PNAS, 2022 https://doi.org:10.1073/pnas.2122515119 ; [4] Seok et al. Fr. Net. Phys. 2022 https://doi.org/10.3389/fnetp.2022.947618; [5] Snedden et al. In Prep.; [6] Alipour et al. Under revision.

Novel quantification of morphological variation in D. melanogaster wings using the Wasserstein-Fisher-Rao metric

Ryan Robinett[1*], Evan Gibbs[2], Richard W. Carthew[3], Samantha J. Riesenfeld[1], Lorenzo Orecchia[1], Shmuel Weinberger[1]

April 16, 2025

[1] University of Chicago
[2] York College of Pennsylvania
[3] Northwestern University
* robinett@uchicago.edu

Living systems exhibit remarkable fidelity in form (morphology) when comparing individual organisms from the same species or closely related species. To understand the constraints underlying morphological variation requires geometric analysis of form. However, historical study of morphological geometry has relied on a sparse number of handpicked anatomical landmarks within the given structures. In this talk, we present methods for quantifying morphological differences between anatomical structures of two individuals, as well as for quantifying modes of variation in morphology for a large number of specimens. These methods leverage the Riemannian manifold structure of the Wasserstein-Fisher-Rao metric introduced by Chizat, Peyré, Schmitzer, and Vialard[1]. We demonstrate the power of these methods by applying them to wing morphology in Drosophila melanogaster, capturing modes of intra- and inter-strain morphological variation

[1]Chizat, L., Peyré, G. Schmitzer, B, and Vialard, F.-X. "An Interpolating Distance Between Optimal Transport and Fisher-Rao Metrics." *Found Comput Math* **18**, 1-44 (2018).

Inferring Cell Lineage Trees and Differentiation Maps from Lineage Tracing Data

Palash Sashittal*

Organismal development is a complex process that involves repeated cell divisions and gradual differentiation of cells through a hierarchy of progenitor cell types, each with progressively restricted differentiation potential. A central goal in developmental biology is to reconstruct the cell lineage tree – which describes the complete history of cell divisions – and the cell differentiation map – which describes the hierarchy of progenitor cell types and cell type transitions that occur during development. Even for simple organisms such as *Caenorhabditis elegans*, uncovering the cell lineage tree and the differentiation map of has led to key insights, including the critical role of programmed cell death during development [23]. Creating comparable cell lineage trees and differentiation maps for mammalian development will have far-reaching implications in regenerative medicine and advancement of therapies for developmental disorders.

Recent advances in genome editing and single-cell sequencing have enabled high-throughput lineage tracing of cells in complex developmental systems [1, 16, 17, 21]. In these technologies, heritable barcodes are induced in cells, either at specific stages of development [4, 7, 13, 14] or dynamically as cells divide and differentiate [8, 11, 18–20, 22], using genome editing tools such as CRISPR-Cas9. Single-cell RNA sequencing is subsequently used to simultaneously measure barcodes (revealing the lineage of cells) and gene expression (revealing cell types) for thousands of individual cells [2, 5, 6, 9, 10, 12, 15]. While these technologies offer the scalability to investigate development in complex organisms, they do not observe every cell division and the differentiation decisions made by each dividing cell during development. As such, we require computational methods to infer cell lineage trees and differentiation maps from single-cell lineage tracing data.

In this talk, we will present two algorithms to infer cell lineage trees and differentiation maps from lineage tracing data. First, we will present STARTLE [6], an algorithm to infer cell lineage trees from CRISPR-Cas9-based lineage tracing. STARTLE introduces the *star homoplasy* evolutionary model that constrains a phylogenetic character to mutate at most once along a lineage, capturing the *non-modifiability* property of CRISPR-Cas9 mutations. We derive a combinatorial characterization of star homoplasy phylogenies and use this characterization in STARTLE to compute a maximum parsimony star homoplasy phylogeny from lineage tracing data. The second algorithm, CARTA [3], infers cell differentiation maps from lineage tracing data in which observed and unobserved progenitor cell types are represented by their *potency*. CARTA introduces a novel mathematical framework that balances the trade-off between the complexity of the differentiation map and the fit of the map with the cell lineage trees derived from lineage tracing data. We also introduce a formal quantitative framework to systematically assess different models of cell differentiation maps with varying numbers of progenitors. Throughout the talk, we will demonstrate that STARTLE and CARTA outperform existing methods on both simulated and real data. Overall, my talk will underscore the crucial role of specialized models and algorithms to effectively analyze lineage tracing data and uncover the dynamics of developmental biological systems.

*Department of Computer Science, Virginia Tech

References

[1] Adriano Bolondi, Benjamin K Law, Helene Kretzmer, Seher Ipek Gassaloglu, René Buschow, Christina Riemenschneider, Dian Yang, Maria Walther, Jesse V Veenvliet, Alexander Meissner, et al. Reconstructing axial progenitor field dynamics in mouse stem cell-derived embryoids. *Developmental cell*, 2024.

[2] Uyen Mai, Gillian Chu, and Benjamin J Raphael. Maximum likelihood inference of time-scaled cell lineage trees with mixed-type missing data. In *International Conference on Research in Computational Molecular Biology*, pages 360–363. Springer, 2024.

[3] Palash Sashittal, Richard Zhang, Benjamin Law, Alexander Strzalkowski, Henri Schmidt, Adriano Bolondi, Michelle Chan, and Benjamin Raphael. Inferring cell differentiation maps from lineage tracing data. *Nature Methods (in print)*, 2024.

[4] Kunal Jindal et al. Single-cell lineage capture across genomic modalities with celltag-multi reveals fate-specific gene regulatory changes. *Nature Biotechnology*, pages 1–14, 2023.

[5] Xinhai Pan, Hechen Li, Pranav Putta, and Xiuwei Zhang. Linrace: cell division history reconstruction of single cells using paired lineage barcode and gene expression data. *Nature Communications*, 14(1):8388, 2023.

[6] Palash Sashittal*, Henri Schmidt*, Michelle Chan, and Benjamin J. Raphael. Startle: A star homoplasy approach for CRISPR-Cas9 lineage tracing. *Cell Systems*, 14(12):1113–1121.e9, 2023.

[7] Zhisong He, Ashley Maynard, Akanksha Jain, Tobias Gerber, Rebecca Petri, Hsiu-Chuan Lin, Malgorzata Santel, Kevin Ly, Jean-Samuel Dupré, Leila Sidow, et al. Lineage recording in human cerebral organoids. *Nature methods*, 19(1):90–99, 2022.

[8] Dian Yang, Matthew G Jones, Santiago Naranjo, William M Rideout, Kyung Hoi Joseph Min, Raymond Ho, Wei Wu, Joseph M Replogle, Jennifer L Page, Jeffrey J Quinn, et al. Lineage tracing reveals the phylodynamics, plasticity, and paths of tumor evolution. *Cell*, 185(11):1905–1923, 2022.

[9] Jean Feng, William S Dewitt III, Aaron McKenna, Noah Simon, Amy D Willis, and Fredrick A Matsen IV. Estimation of cell lineage trees by maximum-likelihood phylogenetics. *The annals of applied statistics*, 15(1):343, 2021.

[10] Wuming Gong, Alejandro A Granados, Jingyuan Hu, Matthew G Jones, Ofir Raz, Irepan Salvador-Martínez, Hanrui Zhang, Ke-Huan K Chow, Il-Youp Kwak, Renata Retkute, et al. Benchmarked approaches for reconstruction of in vitro cell lineages and in silico models of c. elegans and m. musculus developmental trees. *Cell systems*, 12(8):810–826, 2021.

[11] Jeffrey J Quinn, Matthew G Jones, Ross A Okimoto, Shigeki Nanjo, Michelle M Chan, Nir Yosef, Trever G Bivona, and Jonathan S Weissman. Single-cell lineages reveal the rates, routes, and drivers of metastasis in cancer xenografts. *Science*, 371(6532):eabc1944, 2021.

[12] Matthew G Jones, Alex Khodaverdian, Jeffrey J Quinn, Michelle M Chan, Jeffrey A Hussmann, Robert Wang, Chenling Xu, Jonathan S Weissman, and Nir Yosef. Inference of single-cell phylogenies from lineage tracing data using cassiopeia. *Genome biology*, 21(1):1–27, 2020.

[13] Wenjun Kong, Brent A Biddy, Kenji Kamimoto, Junedh M Amrute, Emily G Butka, and Samantha A Morris. Celltagging: combinatorial indexing to simultaneously map lineage and identity at single-cell resolution. *Nature protocols*, 15(3):750–772, 2020.

[14] Caleb Weinreb, Alejo Rodriguez-Fraticelli, Fernando D Camargo, and Allon M Klein. Lineage tracing on transcriptional landscapes links state to fate during differentiation. *Science*, 367(6479):eaaw3381, 2020.

[15] Hamim Zafar, Chieh Lin, and Ziv Bar-Joseph. Single-cell lineage tracing by integrating crispr-cas9 mutations with transcriptomic data. *Nature communications*, 11(1):3055, 2020.

[16] Michelle M Chan, Zachary D Smith, Stefanie Grosswendt, Helene Kretzmer, Thomas M Norman, Britt Adamson, Marco Jost, Jeffrey J Quinn, Dian Yang, Matthew G Jones, et al. Molecular recording of mammalian embryogenesis. *Nature*, 570(7759):77–82, 2019.

[17] Macy W Veling, Ye Li, Mike T Veling, Christopher Litts, Nigel Michki, Hao Liu, Bing Ye, and Dawen Cai. Identification of neuronal lineages in the drosophila peripheral nervous system with a "digital" multi-spectral lineage tracing system. *Cell reports*, 29(10):3303–3312, 2019.

[18] Anna Alemany, Maria Florescu, Chloé S Baron, Josi Peterson-Maduro, and Alexander Van Oudenaarden. Whole-organism clone tracing using single-cell sequencing. *Nature*, 556(7699):108–112, 2018.

[19] Bushra Raj, James A Gagnon, and Alexander F Schier. Large-scale reconstruction of cell lineages using single-cell readout of transcriptomes and crispr–cas9 barcodes by scgestalt. *Nature protocols*, 13(11):2685–2713, 2018.

[20] Bastiaan Spanjaard, Bo Hu, Nina Mitic, Pedro Olivares-Chauvet, Sharan Janjuha, Nikolay Ninov, and Jan Philipp Junker. Simultaneous lineage tracing and cell-type identification using crispr–cas9-induced genetic scars. *Nature biotechnology*, 36(5):469–473, 2018.

[21] Daniel E Wagner, Caleb Weinreb, Zach M Collins, James A Briggs, Sean G Megason, and Allon M Klein. Single-cell mapping of gene expression landscapes and lineage in the zebrafish embryo. *Science*, 360(6392):981–987, 2018.

[22] Aaron McKenna, Gregory M Findlay, James A Gagnon, Marshall S Horwitz, Alexander F Schier, and Jay Shendure. Whole-organism lineage tracing by combinatorial and cumulative genome editing. *Science*, 353(6298):aaf7907, 2016.

[23] John E Sulston, Einhard Schierenberg, John G White, and J Nichol Thomson. The embryonic cell lineage of the nematode caenorhabditis elegans. *Developmental biology*, 100(1):64–119, 1983.

Modeling genetic drift and selection in spermatogonial stem cell dynamics

Frederick R. Adler[1,2], James A. Gagnon[2], **Connor R. Shrader[1]**, Andrea L Sposato[2], Jenna M Weber[2]

Stem cells maintain and repair our tissues, but not all stem cells are identical. As organisms age, distinct stem cell "clones" can begin to dominate the cell population. While this behavior has been observed across multiple species and organs, the mechanisms and consequences of stem cell clonality are still poorly understood. We have developed a novel experimental approach using a CRISPR-Cas9 system to permanently “barcode” the spermatogonial stem cell clones in the zebrafish testis. Once these fish reach sexual maturity, we sample sperm each month to determine the contribution of each uniquely labeled stem cell clone to the sperm pool. To better understand the factors that drive clonal dynamics, we have also designed stochastic models of stem cell population dynamics. These models are formulated as hidden Markov models that describe rules for the division and differentiation of stem cells within the testis. We then use these models to quantify evidence of genetic drift and selection in our experimental data. Our models provide insight into how individual stem cell behavior can lead to population-level mosaicism and inform experimental efforts to verify our hypotheses.

[1] University of Utah, Department of Mathematics
[2] University of Utah, Department of Biology

Rigidity Homeostasis of the Actin Cortex via Tension-Sensitive Filament and Crosslinker Dynamics

Haina Wang* Marco A. Galvani Cunha† John C. Crocker‡ Andrea J. Liu§

Abstract

The actin cortex is a biopolymer network that maintains mechanical rigidity despite constant structural changes through assembly and disassembly of filaments and crosslinkers. The biological advantage of this energy-intensive remodeling, as well as the microscopic mechanisms underlying rigidity homeostasis, remains unclear. To address these questions, we have developed two independent elastic network models that achieve rigidity homeostasis while undergoing complete architectural turnover, capturing filament and crosslinkers dynamics, respectively. We find that both models require the following minimal ingredients: (1) preferential disassembly of edges or nodes that are under small tension or force, (2) a small fraction of random disassembly, and (3) energy injection upon assembly. The trajectories toward steady states are analyzed with graph-theoretical metrics to reveal the relationship between rigidity and network topology. Remarkably, we find that the edges in our networks undergo diffusion, whereas the elastic moduli and structural correlations remain statistically invariant, analogous to the representational drift found in learning systems in which the architecture self-adjust via local rules. We hypothesize that the cortex functions as a tunable matter, where remodeling dynamics enables the cell to balance robustness and flexibility in fluctuating mechanical environments, creating survival advantages that justify the energy consumption. Our models provide platforms to design and study bio-inspired tunable metamaterials.

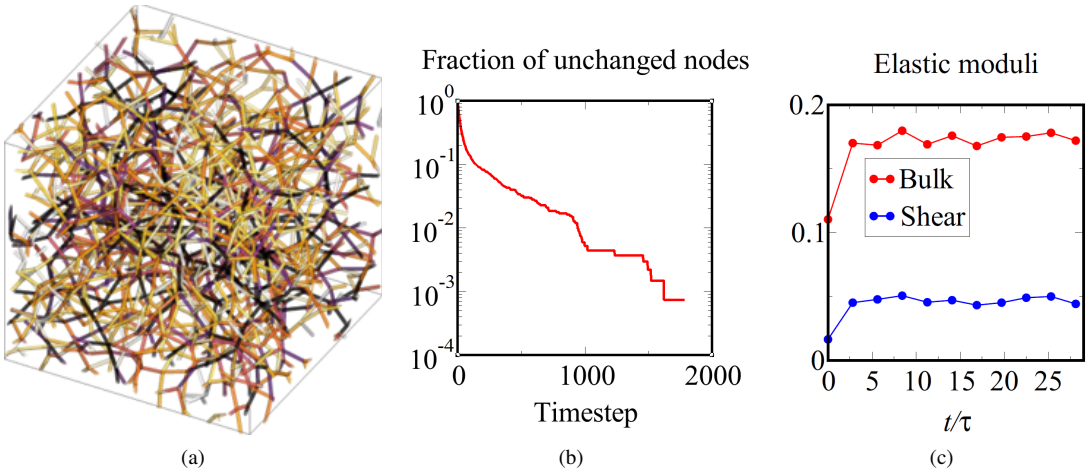

(a) (b) (c)

Figure 1: (a) Snapshot of our cortex model at the steady state, obtained via crosslinker binding and unbinding dynamics. The colors of edges represent tension on the filaments, with darker color corresponding to higher tension. (b) The fraction of nodes that have not changed coordination number shows an exponential decay with simulation time. Turnover time scale $\tau = 273$ timesteps. (c) The bulk and shear moduli clearly show that a rigid steady state is reached.

*Presenter, Department of Physics and Astronomy, University of Pennsylvania
†Department of Physics and Astronomy, University of Pennsylvania
‡Department of Chemical and Biomolecular Engineering, University of Pennsylvania
§Department of Physics and Astronomy, University of Pennsylvania

The impact of ephaptic coupling and ionic electrodiffusion on arrhythmogenesis in the heart

Ning Wei[1], Alena Talkachova[2], Joyce Lin[3], Yoichiro Mori[4]

Abstract

The synchronized contraction of the heart relies on the ordered propagation of the cardiac action potential, which occurs through gap junctions (GJs)-rich intercalated disc (ID). GJs are low-resistance pathways that directly connect the cytoplasm of adjacent cardiac cells for the exchange of ions and small molecules. However, ongoing theoretical and experimental studies have suggested the potential incompatibilities in applying GJ-mediated microscale coupling to explain macroscopic propagation. Notably, GJ knockout mice are still able to maintain heart structure and function, albeit GJs are undetectable at IDs. Ephaptic coupling (EpC) is an electric field effect developed at the ID, which is a narrow and torturous cleft connecting the individual cardiac cells to form a functional syncytium. Recent research has substantiated EpC as an alternative mechanism for cellular communication when GJs are impaired. Given the current absence of *direct* experimental evidence for the *existence* of EpC, modeling studies play a vital role in elucidating its physiological and pathological functions in the heart. We developed a two-dimensional (2D) model of EpC that incorporates multidomain electrodiffusion of multiple ions, providing the *first physiologically detailed* framework for studying ephaptic conduction in both healthy and ischemic heart. Our results showed that strong EpC, combined with ionic electrodiffusion, significantly decreases the occurrence of conduction failure into ischemic region, indicating the *potential benefits* of EpC. In addition, strong EpC can markedly influence ionic concentrations within the cleft, notably elevating K^+ levels and nearly depleting Ca^{2+}, while changes in Na^+ remain moderate. These findings shed light on the underlying mechanism of EpC. Moreover, our findings indicate that sufficiently strong EpC tends to *suppress the initiation of reentry*, leading to absent or nonsustained reentrant activity, while could also introduce instability and heterogeneity into the cardiac dynamics. In contrast, relatively weak EpC supports sustained reentry with a stable rotor. Furthermore, we demonstrated that strong EpC can *terminate reentrant arrhythmias* in ischemic hearts with complex anatomical structures. Our findings revealed two distinct *termination mechanisms*: (1) sufficiently strong EpC leads to rapid self-attenuation of reentry, and (2) moderate EpC results in termination via self-collision over a longer period, driven by increased conduction velocity and anisotropy. In summary, our research is *the first* to demonstrate that EpC exerts *anti-arrhythmic effects* by both preventing the initiation of reentry and terminating established reentrant circuits, *fundamentally shaping our understanding of EpC*.

Affiliations of all authors associated with this presentation:

1. Department of Mathematics, Purdue University.
2. Department of Biomedical Engineering, University of Minnesota.
3. Department of Mathematics, Cal Poly.
4. Department of Mathematics, Department of Biology, University of Pennsylvania.

3 Abstracts of Posters

Stability Analysis of Markov Models of Voltage-gated Ion Channels Mediated Action Potential Generation

Youssof Abdullah[1], Violet Hart[2], Moumita Das[1,2]

[1] School of Mathematics and Statistics Rochester Institute of Technology
[2] School of Physics and Astronomy Rochester Institute of Technology

Abstract

We perform non-linear dynamical stability analysis on a system of differential equations governing neuron ion channel dynamics to determine regions of stable action potential generation.

Action potentials are the mechanism by which chemical energy is converted into electrical energy in neurons. Voltage gated ion channels (VGIC), such as sodium and potassium ion channels, play an important role in the generation of these signals. The Hodgkin-Huxley model, which consists of coupled nonlinear equations for the electrophysiological properties of neurons, has been used to computationally simulate this phenomenon over the years. More recently Markov Models are being used to model VGIC allowing for a more accurate representation of their multiple states and transitions [1]. We perform a stability analysis on Markov models of voltage gated sodium ion channels to predict regions in the parameter space where action potential spikes are feasible. We study the stability of the system by examining the eigenvalues of the Jacobian at the fixed points of the system for a broad range of parameters that include physiologically relevant domains. We find regions of spontaneous and stimulated spikes for a combination of nine sodium channel isoforms and two potassium channels isoforms. Our results may provide insights into the generation of action potential not only in biological neurons but also in other excitable cells as well as in bottom-up synthetic constructs of neurons.

References:

[1] P. Balbi, P. Massobrio, and J. Hellgren Kotaleski, “A single markov-type kinetic model accounting for the macroscopic currents of all human voltage-gated sodium channel isoforms,” *PLOS Computational Biology*, vol. 13, no. 9, Sep. 2017. doi:10.1371/journal.pcbi.1005737

This work was supported by the NSF Emerging Frontiers (EF) Award 1935277

Gentlest Ascent Dynamics for Rapid Exploration of Energy Landscapes

Siddarth Achar[1] Armin Shayesteh Zadeh[21]
Andrew L. Ferguson[1,2]

Abstract

The exploration of molecular configuration space is often hindered by thermally activated barriers on complex, high-dimensional potential energy surfaces. These barriers make conventional molecular dynamics (MD) simulations inefficient for accessing rare but important transitions. Enhanced sampling techniques based on collective variables (CVs) are commonly used to overcome this limitation. However, they typically require prior knowledge of the system's slow modes, which can be difficult to determine for large or disordered systems. In this work, we present a method based upon gentlest ascent dynamics (GAD) [1], a technique originally developed to locate index-1 saddle points. GAD computes the Hessian matrix to identify the eigenvector corresponding to the lowest eigenvalue—the direction of minimum curvature. It then projects this direction out of the force vector, effectively steering the system away from local minima and toward saddle points. We repurpose this idea to create a finite-temperature framework called gentlest ascent dynamics for enhanced sampling (GADES). Instead of searching for saddle points, GADES flattens the energy landscape along the minimum curvature eigenfunctions to eliminate energy barriers and promote efficient diffusive dynamics between system critical points (i.e., minima and saddles). Importantly, GADES does not require predefined CVs or prior knowledge of the energy surface. The first phase of GADES promotes rapid sampling of the important metastable states of the system, but, since the dynamics do not evolve according to a gradient potential, they do not admit reweighting to the Boltzmann distribution (i.e., Gibbs measure). In the second phase of GADES, the trajectories are used to uncover high-variance or slow CVs via data-driven nonlinear dimensionality reduction methods such as diffusion maps (dMaps) [2], autoencoders, or deep time-lagged independent component analysis (Deep-tICA) [3], and learned CVs are then implemented within efficient off-the-shelf CV-biasing enhanced sampling techniques such as metadynamics [4] to recover a low-dimensional, system-specific embedding of the molecular system and the Boltzmann distribution over this projection. We validate GADES in molecular dynamics simulations of a number of biomolecular systems of varying size and complexity to demonstrate its capacity to efficiently navigate and sample molecular energy without requiring any *a priori* knowledge of CVs or critical points.

References:

[1] Weinan, E., & Zhou, X. (2011). The gentlest ascent dynamics. *Nonlinearity*, *24*(6), 1831.
[2] Ferguson, A. L., Panagiotopoulos, A. Z., Debenedetti, P. G., & Kevrekidis, I. G. (2010). Systematic determination of order parameters for chain dynamics using diffusion maps. Proceedings of the National Academy of Sciences, 107(31), 13597-13602.
[3] Bonati, L., Piccini, G., & Parrinello, M. (2021). Deep learning the slow modes for rare events sampling. *Proceedings of the National Academy of Sciences*, *118*(44), e2113533118.
[4] Barducci, A., Bonomi, M., & Parrinello, M. (2011). Metadynamics. Wiley Interdisciplinary Reviews: Computational Molecular Science, 1(5), 826-843.

[1] Pritzker School of Molecular Engineering, University of Chicago, Chicago, Illinois 60637, United States

[2] Department of Chemistry, University of Chicago, Chicago, Illinois 60637, United States

Graph Analysis of Interaction Networks Within Biomolecular Condensate Reveals Distinct Distributions of Topological Hubs and Cliques

Dilimulati Aierken[1,2] Danial Tan[1] Jerelle A. Joseph[1,2]

Abstract

Biomolecular interaction networks typically maintain the biomolecular condensates, and condensates formed by prion-like low complexity domains (LCDs) of proteins are one canonical example. Here, we investigate the network topologies underlying single-component LCD condensates, using a combination of coarse-grained modeling and graph network analysis. We employ a chemically specific model, and this model is then generalized to describe "hydrophobic–polar" (HP) polymers, allowing us to systematically vary sequence hydrophobicity. Our results indicate that both model systems exhibit small-world network topologies, characterized by the presence of molecular "hubs" and "cliques". Hubs, which have high network betweenness centrality, tend to localize near the centers of condensates and adopt more elongated conformations. In contrast, cliques—densely interacting molecules that form locally fully connected subgraphs—are bridged by hubs and localize near the condensate interface. In addition, the conformational properties of individual molecules and their network betweenness centrality are found to be connected by power-law relationship, which also applies to their molecular dynamics. These findings suggest that inhomogeneities in condensate network connectivity can be predicted from single-molecule properties. Furthermore, longer lifetime of cliques and spatially constrained constituent molecules suggest a potential role for these densely interacting subgraphs in shaping interface material properties.

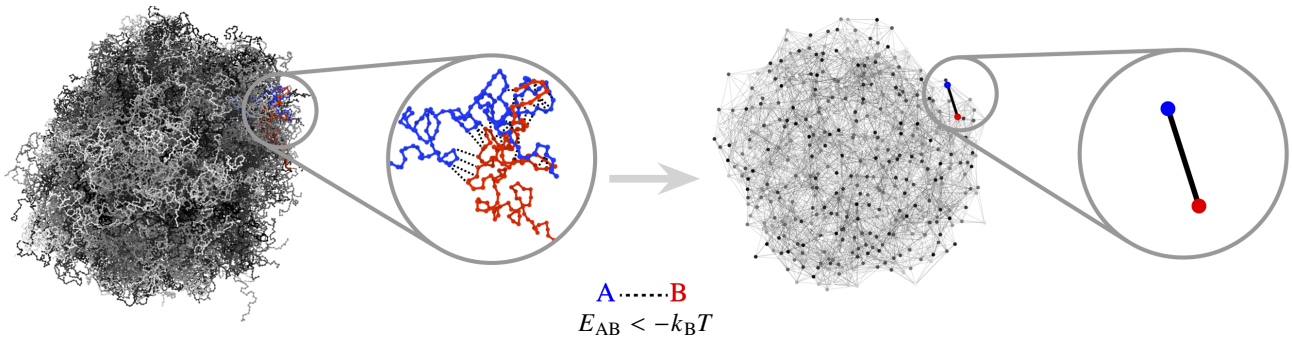

Figure 1: In the graph representation, each molecule is a node, and two nodes are connected with an unweighted, undirected edge when the sum of pairwise monomer interaction energies (E_{AB}) between them exceeds the thermal energy ($k_B T$).

References

[1] D. Tan, D. Aierken, and J.A. Joseph, Interaction networks within biomolecular condensates feature topological cliques near the interface. *bioRxiv* (2025).

[1]Department of Chemical and Bilogical Engineering, Princeton University

[2]Omenn–Darling Bioengineering Institute, Princeton University

Plasmid Loss in Spatially Constrained Microbial Populations

Amanda M. Alexander* Krešimir Josić

Abstract

Bacterial cells contain extrachromosomal DNA molecules called plasmids. In nature, plasmids often confer antibiotic resistance. Cells commonly have no mechanism for evenly partitioning plasmids during cell division, and thus there is some probability that one of two daughter cells does not inherit any plasmids. On the population scale, what factors influence the persistence of plasmid DNA over generations? Mathematical modeling is useful in answering this question, as it is difficult to experimentally resolve new plasmid loss from replication of previously plasmid-free cells over long time periods. We introduce a spatial Moran-like model of a finite cell population undergoing plasmid loss, because biologists frequently observe cell populations in spatially constrained microfluidic traps. We explore how properties of single cells impact the dynamics of the cell population in different trap geometries. This analysis reveals that the persistence of plasmid DNA in cell populations has a complex dependence on both spatial geometry and assumptions on single cell properties such as cell division age.

*University of Houston

Metabolic Modeling to Interrogate Microbiome Function

Nana Ankrah
State University of New York (SUNY) at Plattsburgh

Abstract

It is well established that changes in the composition of animal gut microbiota are correlated with health and fitness. In many animals, microbial partners contribute to host health by producing nutrients that are in short supply in the host diet. Very commonly, net nutrient production by the microbes is dictated by metabolic competition and cooperation among multiple bacterial taxa and strongly influenced by the metabolites derived from the animal host, but the mechanistic details of the multi-way metabolic interactions are poorly understood. To investigate the processes shaping animal-microbe metabolic interactions and to derive estimates of the composition and amount of nutrients exchanged between animal and microbe, we reconstructed genome scale metabolic models of the bacterial community in the Drosophila gut and used flux balance analysis to analyze the flow of metabolites through the metabolic networks of the bacterial community. We hypothesized that the composition of gut microbiota influences host health by modifying the nutritional inputs available to the host through the synthesis and consumption of host and microbial derived nutrients. Our simulations reveal that among gut microbes competitive interactions dominate and the quality and quantity of nutrients available to the host is influenced by the composition of gut microbiota which synthesize and consume host and microbe derived nutrients. Our studies elucidate the metabolic basis of animal-microbe interactions and provide the methodology to select the optimal microbial consortia for personalized microbial therapies in treating diseases associated with microbial dysbiosis.

A Topological Framework For Simultaneously Recorded Network Activity

Cagatay Ayhan*

Abstract

We introduce a topological framework for studying network responses to external stimuli, observed simultaneously over a period of time. We ask whether the activity of these responses is topologically meaningful. Roughly speaking, topological properties of a network manifest as distinct groupings or cyclic activity—corresponding to connected components, loops, and other features in an abstract space. In this talk/poster presentation, I'll define the key objects of interest—trains, neurons, and train ensembles—and walk through our pipeline step by step using schematic examples.

In a nutshell, the input to our pipeline is the network's response to a stimulus, and the output is a persistence barcode: a topological signature of population activity that is both interpretable and robust. Our results, based on a neuroscience application, suggest that the responses of such networks can indeed be topologically meaningful. While this motivating application naturally influenced our terminology, the framework itself is presented broadly and applies to a wide range of networked systems beyond neuroscience. Joint work with Tom Needham, Martin Bauer, Audrey Nash, Richard Bertram, and Roberto Vincis.

*Florida State University, Department of Mathematics

H5N1 Dynamics and Effectiveness of Intervention Strategies

Oluwatosin Babasola[12] Mohamed Makheet[12] Christina Naesborg Nielsen[12] Justin Bahl[1234]

Abstract

The highly pathogenic avian influenza (HPAI) subtype H5N1 is a severe viral disease which continues to pose a significant threat to public health and a rigorous understanding of its transmission dynamics across its major pathways is essential for developing effective control strategies. Phylogenetic analysis suggests that H5N1 spillover occurs primarily between wild and domestic birds. However, increasing contact between these species and humans increases the risk of zoonotic transmission. In this work, we develop a mathematical model to examine the transmission dynamics of H5N1 and evaluate the effectiveness of proposed control measures. The model employs a compartmental framework that includes human, domestic, and wild bird populations. We then use this model to estimate the basic reproduction number for each population group and perform a sensitivity analysis to assess the contribution of the parameters to the spread of the disease. Numerical simulations are also conducted to evaluate the impact of inter-species interactions on H5N1 infection in humans and to determine the effectiveness of different control measures. The results suggest that a vaccination strategy with high vaccine efficacy, combined with a vaccination rate above 50%, significantly reduces transmission. In addition, decreasing cross-species interactions leads to a substantial reduction in disease transmission within the human population. Moreover, an optimal control analysis indicates that a combined approach involving environmental sanitation, vaccination, and targeted culling of confirmed infected poultry is an effective strategy to control the outbreak, reducing the likelihood of spillover to humans.

[1] College of Veterinary Medicine, Department of Infectious Diseases, University of Georgia, Athens, GA

[2] Center for Ecology of Infectious Diseases, University of Georgia, Athens, GA

[3] Institute of Bioinformatics, University of Georgia, Athens, GA

[4] Department of Epidemiology and Biostatistics, University of Georgia, Athens, GA

Immunological and Epidemiological Modeling of HIV/AIDS: A Nutritional Perspective

Chirantha Piyamal Tharusha Bandara*

Abstract

HIV remains a significant global health challenge, having claimed millions of lives over the past few decades. Although numerous empirical studies highlight the importance of proper nutrition in mitigating the impact of HIV, relatively few have explored this relationship through the lens of mathematical modeling. In this talk, we introduce novel within-host (immunological) and between-host (epidemiological) models that explicitly incorporate nutritional factors into the analysis of HIV dynamics.

At the within-host level, we develop a mathematical model that captures the complex interplay between HIV, the immune system, and nutrition - specifically, protein. We establish the existence and local stability of equilibria and analyze the occurrence of backward bifurcation. In addition, we present numerical simulations demonstrating that increased viral activity leads to increased serum protein levels. We also show that the viral production rate is positively correlated with HIV viral loads, as is the virus-induced enhancement of protein levels. Furthermore, our simulations indicate a direct correlation between dietary protein intake and serum protein levels in HIV-infected individuals.

At the population level, we propose a novel between-host model that assesses the epidemiological consequences of malnutrition in the spread of HIV/AIDS. We establish the existence and global stability of both disease-free and endemic equilibria, with the latter results obtained via Lyapunov's theorem. Numerical simulations are provided to support and illustrate the analytical findings.

Keywords: HIV, nutrition, within-host model, between-host model, equilibria.

References

[1] Bandara, T., Martcheva, M. and Ngonghala, C.N., 2023. Mathematical model on HIV and nutrition. *Journal of Biological Dynamics*, 17(1), p.2287087.

*chiranth@buffalo.edu

Vanishing-spreading dichotomy in a two-species chemotaxis competition system with a free boundary

Lianzhang Bao*

Abstract

Predicting the evolution of expanding population is critical to control biological threats such as invasive species and virus explosion. In this work, we consider a two species chemotaxis system of parabolic-parabolic-elliptic type with Lotka-Volterra type competition terms and a free boundary. Such a model with a free boundary describes the spreading of new or invasive species subject to the influence of some chemical substances in an environment with a free boundary representing the spreading front. We first find conditions on the parameters which guarantee the global existence and boundedness of classical solutions with nonnegative initial functions. Next, we investigate vanishing-spreading dichotomy scenarios for positive solutions. It is shown that the vanishing-spreading dichotomy in the generalized sense always occurs; that the vanishing spreading dichotomy in the strong sense occurs when the competition between two species is weak-weak competition; and that the vanishing spreading dichotomy in the weak sense occurs when the competition between two species is weak-strong competition. Our numerical simulations verify our theoretical results and provide insights into several conjectures currently under investigation. This is a joint work with Wenxian Shen at Auburn University.

*Department of Computational Mathematics, Science and Engineering, Michigan State University, East Lansing, MI 48824, USA (baolianz@msu.edu)

Entropy as an Upper Bound for Stability in Boolean Networks*

Sai Bavisetty† Matthew Wheeler‡ Reinhard Laubenbacher§ Claus Kadelka¶

Abstract

Boolean networks, inspired by gene regulatory networks, were developed to understand the complex behaviors observed in biological systems. In this talk, we present a proof for the conjecture proposed by Willadsen, Triesch, and Wiles regarding upper bounds for the stability of basins of attraction in Boolean networks. Additionally, we extend this result from a single basin of attraction to the entire network. Specifically, we demonstrate that entropy is a tight asymptotic upper bound for the robustness of a Boolean network.

Boolean networks were first introduced by Kauffman as models for gene regulatory networks [1]. These models have gained popularity because of their simplicity and ability to capture the complex behaviors of biological systems. Currently, the repository Biodivine Boolean Models contains more than 230 Boolean network models [7].

A systematic investigation of these biological models suggests that they are incredibly robust. In particular, they are resilient to perturbations and tend to reach the same phenotype despite small disturbances. An explanation of this phenomenon was first given by Kauffman, who showed empirically that a network's connectivity determines the stability of the Boolean network [1]. This was further expanded on by Derrida, who provided a theoretical explanation for the effect of connectivity [6]. This was succeeded by many works that looked at various features of biological networks to prove empirically the relation between a network parameter and stability.

Boolean networks can also be thought of as dynamical systems on the hypercube, which allows us to apply geometric and combinatorial methods to analyze network stability and robustness. However, this alternative viewpoint raises the question of how parameters like connectivity affect the geometry of the hypercube. Willadsen, Triesch, and Wiles attempted to address this question with a systematic study of the hypercube's geometry in random Boolean networks [2]. They introduced a measure for stability called coherence and conjectured that in highly coherent networks, the basins of attraction of the phenotypes are structured as large subcubes in the hypercube.

In this article, we use combinatorial methods developed independently in graph and coding theory to confirm their conjecture [2]. In particular, we use the results in [3, 4, 5] to show that maximum coherence of a network implies that the basin is highly structured. Using techniques from analytic number theory, we then generalize their conjecture from a single basin of attraction to the entire network, showing that in highly stable networks, all basins are structured as large subcubes. Furthermore, we demonstrate that in this case, the entropy is a tight asymptotic upper bound for coherence.

References

[1] S. A. Kauffman, *Metabolic stability and epigenesis in randomly constructed genetic nets*, Journal of Theoretical Biology, 22(3):437–467, 1969.

[2] Kai Willadsen, Jochen Triesch, and Janet Wiles, *Understanding robustness in random boolean networks*, 01 2008.

[3] H. Harborth, *Codes and graphs*, in Graph Theory and Combinatorial Optimization, J. L. Ramírez Alfonsín and B. A. Reed, eds., Wiley, 1997, pp. 1-20.

[4] A. J. Bernstein, *Maximally connected arrays on the n-cube*, SIAM Journal on Applied Mathematics,15(6):1485–1489, 1967.

[5] Sergiu Hart, *A note on the edges of the n-cube*, Discrete Math., 14(2):157– 163, 1976.

[6] B. Derrida and Y. Pomeau, *Random networks of automata: A simple annealed approximation*, Europhysics Letters, 1(2):45, jan 1986.

[7] Samuel Pastva, David Safránek, Nikola Beneš, Luboš Brim, and Thomas Henzinger, *Repository of logically consistent real-world boolean network models*, bioRxiv, 2023.

[8] Richard Bellman and Harold N. Shapiro, *On a problem in additive number theory*, Annals of Mathematics, 49(2):333–340, 1948.

*The article can be accessed at `https://arxiv.org/pdf/2506.12310`

†University of Florida, Gainesville

‡University of Florida, Gainesville

§University of Florida, Gainesville

¶Iowa State University

Graph Theoretic Analyses of Tessellations of Aperiodic Polykite Unitiles

John R. Jungck* Purba Biswas†

Abstract

Aperiodic tessellations of polykite unitiles such as hats, turtles, hares, and the recently introduced red and grey squirrels have attracted significant interest due to their structural and combinatorial properties. This research takes a graph-theoretic approach to examine the adjacency and symmetry constraints of these unitiles in tessellations. We systematically classify their connectivity patterns and structural characteristics by utilizing Hamiltonian cycles of vertex degrees along the perimeters of the unitiles. This classification helps identify key binding interactions between unitiles in a tessellation, which play an important role in understanding self-assembly dynamics. In addition, we applied Blumeyer's 2x2 classification framework to investigate the influence of chirality and periodicity, while Heesch numbers and corona structures provide further insights into tiling patterns. Furthermore, if we analyze the distribution of polykite unitiles and their flipped versions (anti-polykites) with Voronoi tessellations and their Delaunay triangulations, we can detect Pitteway violations on these networks. The results of this study contribute to a better understanding of aperiodic tessellations and provide useful perspectives on self-assembling structures with potential applications in biomimetic materials, nanotechnology, and synthetic biology.

References

- Caspar, D. L. D., and Klug, A. (1962). "Physical Principles in the Construction of Regular Viruses." *Cold Spring Harbor Symposia on Quantitative Biology*, **27**, 1–24.
- Blumeyer, D. (2023). *Aperiodic Monotiles*. Retrieved from `https://douglasblumeyer.com` and `https://forum.sagittal.org/viewtopic.php?t=569`.
- Gu, Grace. (2024). "Composite Creator." *Nature*, **636**, S11.
- Jungck, J. R., Brittain, S., Plante, D., and Flynn, J. (2023). "Self-Assembly, Self-Folding, and Origami: Comparative Design Principles." *Biomimetics*, **8**(12), 1–24.
- Plante, D. K., Unzen, and Jungck, J. R. (2024). "3D Printed Self-Assembling Helical Models for Exploring Viral Capsid Structures." *Biomimetics*, **9**, Article 763.
- Smith, D., Myers, J. S., Kaplan, C. S., and Goodman-Strauss, C. (2024). "An Aperiodic Monotile." *Combinatorial Theory*, **4**(2), Article #13. `https://doi.org/10.5070/C64264241`.
- Smith, D., Myers, J. S., Kaplan, C. S., and Goodman-Strauss, C. (2024). "A Chiral Aperiodic Monotile." *Combinatorial Theory*, **4**(2), Article #13. `https://doi.org/10.5070/C64264241`.
- Todd, H. (2018). "A Class of Spherical Penrose-Like Tilings with Connections to Virus Protein Patterns and Modular Sculpture." *Mathematics and Art*.
- Twarock, R. (2004). "A Tiling Approach to Virus Capsid Assembly Explaining a Novel Role for Hexamers." *Journal of Theoretical Biology*, **226**(4), 477–482.
- Twarock, R. (2006). "The Architecture of Viral Capsids Based on Tiling Theory." *Journal of Theoretical Biology*, **240**(4), 419–432.

*Department of Biological Sciences and Department of Mathematical Sciences, University of Delaware, Newark, DE 19716, USA; jungck@udel.edu

†Department of Mathematics, Applied Mathematics and Statistics, Case Western Reserve University, Cleveland, OH 44106, USA; Department of Mathematical Sciences, University of Delaware, Newark, DE 19716, USA; purba@udel.edu, purba.biswas@case.edu

Distributed Delay Improves the Dynamics of Gene Regulation*

Yun Min Song† **Sean Campbell**‡ LieJune Shiao§ Jae Kyong Kim†
Amanda Alexander‡ Courtney White‡ William Ott‡

Abstract

Since Benzi, Sutera, and Vulpiani first introduced Stochastic Resonance (SR) in 1981 to study climate dynamics, many new types of SR effects have been found in fields ranging from quantum physics to neurobiology. We will explore how stochasticity in Gene Regulatory Networks (GRNs) – the principal decision-making apparatuses of cells – can improve cellular function through SR effects. GRNs play a critical role in a diverse array of biological processes. Some examples of what GRNs do are determining cell fate in embryonic development, inducing labor at the end of pregnancy, maintaining circadian rhythms, regulating the onset of puberty, sensing quorum in bacteria, and preventing cells from becoming cancerous. A critical feature that governs the dynamics of GRNs is the delay between the start of transcription of a gene and the formation of a functional protein. Indeed, any model of Gene Regulation must account for this delay in some way to be useful. However, the molecular mechanisms in a cell are subject to stochasticity, making this delay inherently random. Through a combination of computer simulation and explanatory modeling, we demonstrate the counterintuitive advantages arising from stochasticity in transcriptional delay. In particular, for negative feedback architectures, genetic oscillators, distributed delay increases the signal-to-noise ratio of the oscillatory signal and reduces resource utilization to maintain stable oscillations. Meanwhile, distributed delay increases mean residency times for positive feedback architectures exhibiting bistability.

References

[1] Y. M. Song, S. Campbell, L. Shiau, J. K. Kim, and W. Ott, *Noisy Delay Denoises Biochemical Oscillators*, Physical Review Letters **132**, 078402 (2024).
[2] S. Campbell, C. White, A. Alexander, W. Ott, *Noisy Delay Stabilizes Bistable Systems* (2025), [in preparation].

*The full results for oscillators can be found at `https://doi.org/10.1103/PhysRevLett.132.078402`. Results for bistable systems to appear on arXiv soon.

†Korea Advanced Institute of Science and Technology
‡University of Houston
§University of Houston, Clearlake

Geometric Methods for Constrained Molecular Structure Refinement

Xin Cao

Abstract

Molecular functions are highly related to their 3-dimensional (3D) structures. Determination of 3D structure and sampling different conformations are important for understanding immunity reactions, catalysis of enzymes, and drug design. Geometric approaches have achieved success in modeling the structures of linear chains, both analytically and in machine learning (ML) applications. In protein design, attention has focused on the loop regions because they are more flexible and play important roles in protein-protein interactions, such as antibody-antigen interactions. However constrained structures, such as protein loops and macrocycles, pose additional challenges: the two ends of a loop are geometrically constrained, and the proper internal parameters required to close the loop maintaining proper chain connectivity need to be determined. Based on the rigid rotor assumption, constrained structures can be reduced to the torsional angle space, and conversion of these torsional angles to half-tangents will result in polynomial equations with higher degrees, whose solutions form Toric varieties. As ML has shown to be successful in protein design and drug discovery, an appropriate model for constrained molecular design on toric varieties needs to be demonstrated.

In this presentation, I will describe the difficulties in constructing constrained molecular structures, and the geometric methods developed to resolve these difficulties, both analytically and in ML. For the polynomial equations constructed based on the geometry relationship of the closure constraints, the first numerically stable algorithm R6B6[1] is proposed which can deal with special cases where some axis or link lengths vanish, some joint angles are 180° in solutions or duplicate solutions of specific variables are present. The diffusion models in ML have notable successes in Euclidean space and on smooth manifolds. However, a diffusion model for algebraic varieties with singularities has not been developed. I will present how to construct such a diffusion model for constrained structures using differential geometry concepts and demonstrate its application to sample the flexibility in the loop regions to refine the quality of the predicted structures.

References:

[1] Xin Cao, Evangelos A. Coutsias, Sara Pollock (2023), *Numerically stable solution to the 6R problem of inverse kinematics,* Advances in Computational Science and Engineering, 1(2), 123.

Dynamical Motivated Analysis of Connectome Data

Carlos Joaquín Castañeda Castro

Abstract

Connectome data promises to help us understand how neural connectivity gives rise to function. One strategy is to identify overrepresented motifs in the connectome, which are directed subgraphs that occur significantly more often than chance. However, it is often difficult to interpret their meaning within the context of neuronal dynamics. Combinatorial threshold-linear networks (CTLNs) provide a simple framework that relates graph structure to neural-inspired dynamics. Through mathematically rigorous "graph rules", the structure of a directed graph becomes predictive of the network's emergent activity, which allows us to categorize motifs with similar dynamic properties and infer their behavior inside a larger network.

In this work, we first identify and classify overrepresented motifs of size $n = 4$ and $n = 5$ in the C. elegans and Drosophila ellipsoid body connectomes. We then investigate these motifs using the CTLN framework. In particular, we perform "domination reduction" by removing nodes that are guaranteed to not participate in the long-term dynamics, which enables us to arrange motifs in "dynamic equivalence classes" whose set of fixed point supports share the same structure and give rise to nearly identical attractors. Our results demonstrate that the connectome's architecture alone encodes interpretable dynamical signatures of the neural network. This work was done in collaboration with Carina Curto, Jordan Matelsky, and Erik Johnson.

References

[1] C. Curto and K. Morrison, "Graph rules for recurrent neural network dynamics". In: *Notices of the American Mathematical Society* 70.4 (2023), pp. 536-551.

[2] J. Matelsky et al. "Data-driven motifs discovery in biological neural networks". 2023. DOI: https://doi.org/10.1101/2023.10.16.562590.

Quantifying population-level robustness for distribution shift

Chen Cheng* Dmitriy Drusvyatskiy† John Duchi‡ Rohith Kuditipudi§

Abstract

We revisit the stability of optimizers in statistical estimation and stochastic optimization problems, but instead of providing guarantees on the stability of the minimizers themselves, we investigate what shifts to the underlying data-generating process perturb solutions the most. To do so, we develop some new mathematical tools for stability analyses, with guarantees beyond typical differentiable problems. We also make connections with statistical hypothesis testing and discovery, showing how these new results provide certificates of validity—or potential invalidity—of statistical estimate. We apply this framework to both simulated data and real-world datasets to evaluate the impact of distribution shifts with uncertainty quantification

The presenter (Chen Cheng) will be affiliated with University of Chicago, Department of Statistics by the time of the workshop as a postdoctoral researcher.

*Stanford University, Department of Statistics. The presenter.
†University of Washington, Department of Mathematics.
‡Stanford University, Departments of Statistics and Electrical Engineering.
§Stanford University, Department of Computer Science.

Non-Perturbative Techniques for Nonlinear Noise in Neural Networks

Shoshana Chipman * Brent Doiron †

Abstract

The dynamical systems approach to biology relies on reducing complex, nonlinear, and noisy dynamics to tractable mean-field theories. In neural systems, this often involves approximating the collective behavior of recurrently-coupled networks while treating noise as a perturbation. Here, we develop a non-perturbative framework for analyzing Langevin equations with nonlinear dependence on noise, allowing both coupling strength and noise intensity to be arbitrarily strong.

We focus on population-level models of firing rates in recurrent neural networks, in the tradition of [1], where coarse-graining introduces intrinsic noise through shared input variability. This noise appears *inside* the transfer function, which may be nonlinear. To address this nonlinear noise, we introduce a novel treatment of noise, which allows us to derive an evolution equation for the probability density of the system. In conjunction with a well-supported Ansatz that firing rates are log-normally distributed [2], we are able to compute a dynamical mean field theory of arbitrarily many moments of the firing rate distribution. We apply this framework to two neural field models: a two-population (excitatory-inhibitory) system with a piecewise-quadratic transfer function, inspired by power-law transfer functions in [5] [4], and a single-population system with a sigmoid nonlinearity in the style of [3].

The novel method captures fixed points and transient dynamics more accurately than linearized mean-field approximations and remains effective even in regimes of strong coupling and strong noise. We also discuss the limitations of the approach (namely, to smooth transfer functions), and avenues for further extension.

We consider the dynamical system

$$\begin{aligned} \tau_E \partial r_E(t) &= -r_E(t) + \phi\left(W_{EE} r_E + W_{EI} r_I + \mu_E + \sigma_E \eta_E(t)\right) \\ \tau_I \partial r_I(t) &= -r_I(t) + \phi\left(W_{IE} r_E + W_{II} r_I + \mu_I + \sigma_I \eta_I(t)\right) \\ \tau_N \eta_\alpha(t) &= -\eta_\alpha(t) + \sqrt{\tau_N} dB_\alpha(t), \quad \alpha \in \{E, I\}, \end{aligned} \tag{0.1}$$

where $\langle dB_\alpha(t) dB_\beta(t')\rangle = C_{\alpha\beta}\delta(t-t')$, allowing potential noise correlations, and ϕ is the piecewise quadratic. $W_{\alpha\beta}$ are weights. r_E, r_I are the macroscale firing rates – the ensemble average of the firing rates of individual neurons.

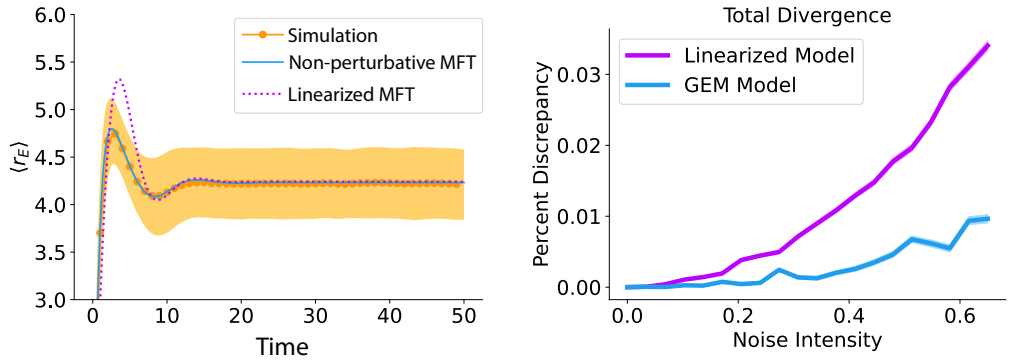

Figure 1: Left, the mean excitatory firing rate compared with the mean field theories generated by linearizing around a fixed point, and the novel non-perturbative technique. Right, the root-mean-square percent error in the fixed point of the mean field theory, when compared to the underlying simulation, in five dimensions.

*University of Chicago, Department of Physics
†University of Chicago, Heinrich Kluver Professor of Neurobiology and Statistics

References

[1] Wilson, H. R., and J. D. Cowan. 1972. "Excitatory and Inhibitory Interactions in Localized Populations of Model Neurons." *Biophysical Journal* 12 (1): 1–24. https://www.sciencedirect.com/science/article/pii/S0006349572860685.

[2] Roxin, A., N. Brunel, D. Hansel, G. Mongillo, and C. van Vreeswijk. 2011. "On the Distribution of Firing Rates in Networks of Cortical Neurons." *The Journal of Neuroscience* 31 (45): 16217–16226.

[3] Amari, S. 1977. "Dynamics of Pattern Formation in Lateral-Inhibition Type Neural Fields." *Biological Cybernetics* 27 (2): 77–87. https://doi.org/10.1007/BF00337259.

[4] Miller, K. D., and T. W. Troyer. 2002. "Neural Noise Can Explain Expansive, Power-Law Nonlinearities in Neural Response Functions." *Journal of Neurophysiology* 87 (2): 653–659. https://api.semanticscholar.org/CorpusID:1824347.

[5] Priebe, N. J., F. Mechler, M. Carandini, and D. Ferster. 2004. "The Contribution of Spike Threshold to the Dichotomy of Cortical Simple and Complex Cells." *Nature Neuroscience* 7 (10): 1113–1122. https://doi.org/10.1038/nn1310.

Modeling the Mhrt Gene Regulatory Network

Claire Christian* Colleen Mitchell* Chad Grueter†

Abstract

A key marker of heart disease is the shift in the ratio between the expression of myosin heavy chain 6 (Myh6) and myosin heavy chain 7 (Myh7). Healthy adult hearts exhibit a higher expression of Myh6, while adult hearts in heart failure exhibit a higher expression of Myh7. Studies have shown that a long noncoding RNA called Mhrt is a key factor in the regulation of both Myh6 and Myh7 ([1]). The aim of this project is to model the interaction between these three genes to gain a better understanding of the switch between Myh6 and Myh7 .

The first part of the project models the relationship between Mhrt and Myh6. These two genes share a promoter region. When RNA polymerase II (Pol II) binds to the promoter region to begin transcribing one of the genes, it blocks the initiation of transcription for the other gene. Additionally, a feedback loop shown in Figure 1a is created by a protein called brahma-related gene 1 (Brg1) and strands of Mhrt RNA. Brg1 can inhibit the production of Mhrt and Myh6 by attaching to their shared promoter region. However the Mhrt RNA can bind to Brg1, preventing the Brg1 from inhibiting transcription. The relationship between Mhrt and Myh6 gene production, Mhrt RNA, and Brg1 can be described as a coupled system of ordinary differential equations, resulting in a single stable steady state.

The second part of the project focuses on the relationship between Mhrt and Myh7. While existing on opposite strands of DNA, Mhrt and Myh7 have a region of roughly 3,000 base pairs that overlap, shown in Figure 1b. This antisense transcription is one way that Mhrt and Myh7 anti-regulate each other. If there is Pol II is transcribing RNA on both strands of DNA in opposite directions a collision can occur. A Monte Carlo simulation was used to simulate transcription of both genes. The results of the simulation were then described in a stochastic model predicting the probability of complete transcription for each gene.

Our goal is to combine the two models to create a single model describing the interaction between all three genes. We conjecture that linking the models will result in a fold bifurcation and hysteresis.

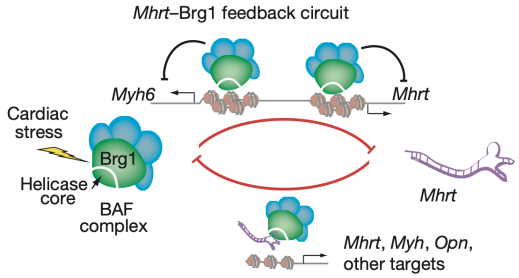

(a) The Mhrt-Brg1 feedback loop affects the production of Mhrt and Myh6.

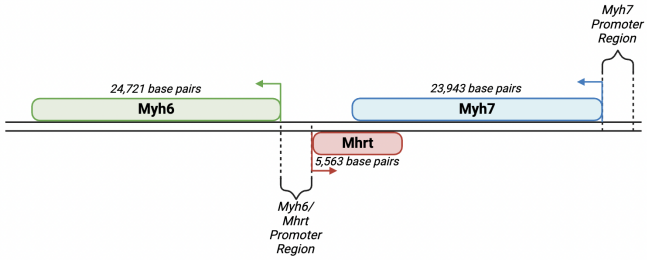

(b) The Mhrt locus on chromosome 14 shows the shared promoter region for Mhrt and Myh6 and the overlap of Mhrt and Myh7.

Figure 1

References

[1] Pei Han, Wei Li, Chiou-Hong Lin, Jin Yang, Ching Shang, Sylvia T Nurnberg, Kevin Kai Jin, Weihong Xu, Chieh-Yu Lin, Chien-Jung Lin, et al. *A long noncoding rna protects the heart from pathological hypertrophy. Nature*, 514(7520):102-106, 2014.

*Department of Mathematics, University of Iowa
†Department of Internal Medicine, University of Iowa

Engineering Predictive Biology: Model-Based Experimentation for Digital Twin Development

Stephen Cini[1] Jeremiah Zartman[1] Alexander Dowling[1]

NITMB Abstract

Digital twins are predictive, computational representations of physical systems, offering powerful tools for understanding complex biological processes. This project focuses on constructing a tissue-scale digital twin of calcium signaling dynamics in *Drosophila melanogaster*, aimed at supporting mechanistic insight into neurodegenerative diseases such as Parkinson's. We approach this by fitting systems of nonlinear differential equations to experimental calcium imaging data using multistart nonlinear regression, enabling parameter identification in high-dimensional, non-convex spaces.

One core challenge lies in the ill-posed nature of parameter estimation in biological systems, where identifiability and data informativeness are often limiting. To address this, we employ science-based design of experiments to maximize information gain per experiment. Using Pyomo.DoE, an open-source optimization package, we solve bilevel formulations where candidate experiments are evaluated and selected based on expected Fisher information. This strategy ensures that model calibration is both computationally efficient and biologically informative.

To improve convergence to global optima and assess parameter uncertainty, we perform multistart optimization with deterministic and quasi-random initializations. This framework enhances robustness against local minima and improves confidence in model predictions. The resulting digital twin facilitates hypothesis testing about biological mechanisms and allows in silico exploration of genetic perturbations. By integrating mathematical modeling, optimization, and experimental design, this work advances digital twin development as a quantitative tool for hypothesis generation and model discrimination in systems biology. Ultimately, this framework supports translational efforts by bridging quantitative analysis with experimentally grounded insights into disease progression and therapeutic response.

[1] Department of Chemical and Biomolecular Engineering, University of Notre Dame, Notre Dame, IN, 46556

Gene-Environment Interactions Partly Depend on Phenotype Scale

Manuela Costantino[1], Renée Fonseca[2], Zhengtong Liu[3], Zhenghong Huang[1], Carl Veller[4], Sriram Sankararaman[3,5,6], Iain Mathieson[7]*, Andy W. Dahl*

[1] Section of Genetic Medicine, University of Chicago, Chicago, IL, USA
[2] Department of Human Genetics, University of Chicago, Chicago, IL, USA
[3] Department of Computer Science, UCLA, Los Angeles, CA, USA
[4] Department of Ecology & Evolution, University of Chicago, Chicago, IL, USA
[5] Department of Human Genetics, David Geffen School of Medicine, UCLA, Los Angeles, CA, USA
[6] Department of Computational Medicine, David Geffen School of Medicine, UCLA, Los Angeles, CA, USA
[7] Department of Genetics, Perelman School of Medicine, University of Pennsylvania, Philadelphia, PA, USA

The tremendous sample sizes of modern genome-wide association studies has led to the discovery of large numbers of statistical interactions between genetic and environmental variables, the majority of which lack clear evidence of biological significance. We hypothesize that many published statistical interactions are artifacts of measuring phenotypes on unnatural scales, a well-known problem without established solutions. Here, we systematically study gene-environment (GxE) interactions across scales as defined by power transformations. We characterize these GxE interactions using two polygenic tests: a variance component model (GxE heritability) and a polygenic score model (PGSxE). Simulations confirm that we are able to differentiate scale-dependent and -independent interactions with high accuracy if and only if the true scale is well approximated by a power transformation. We also prove a formal condition under which GxE is present on all scales, which involves the correlation between the signs of G and E. We then broadly profiled the scale dependence GxE in UK Biobank by studying 7 environments, 45 complex traits, and ~300,000 unrelated white British individuals. We start by contrasting height, an exemplar additive trait, with testosterone, an exemplar sex-specific trait. In the case of height, we find significant GxE interactions with sex using both our tests ($p=0.00039$ for GxE heritability, $p=1.7e-35$ for PGSxE); however, we find that this interaction is entirely eliminated by the log scale ($p=0.62$ for GxE heritability, $p=0.39$ for PGSxE). In contrast, while the log scale eliminates most GxE for testosterone, the GxSex effect on testosterone cannot be eliminated on any scale. This suggests the log scale is the natural scale on which to study both height and testosterone, as it eliminates biologically meaningless GxE while preserving biologically meaningful GxE. Finally, we expand the approach to the other phenotypes, which show broadly similar results: the log scale often eliminates GxE interactions, but certain interactions persist across all scales. These are generally biologically plausible, such as the likely-heritable side effect of statins on A1c. We demonstrate that the coefficient of variation is a key measure of a trait's sensitivity to scale-dependent GxE, as expected from the classical statistical literature. These findings imply that improper choice of scale can cause pervasive false positives in GxE analyses–especially for PGSxE interactions where E has a large main effect–but also that many interactions cannot be eliminated by a power transform. Our work provides a framework for finding the scale that minimizes spurious findings and embraces principled and explicit choices of scale to maximize biological discovery.

Optimizing Viral Interventions to Mitigate Antibiotic Resistance

Zainab Dere[1] Nick Cogan[1] Bhargav Karamched[1]

Abstract

Antibiotic resistance represents a major public health challenge, complicating the treatment of bacterial infections. This study presents a mathematical model that integrates virus dynamics to explore strategies for mitigating antibiotic-resistant bacterial infections. We focus on the interaction between wild-type bacteria, antibiotic-resistant bacteria, and virus infected bacteria populations, using optimal control theory to guide virus-infected bacterial interventions. The model accounts for key biological factors, including bacterial growth rates, mutation probabilities, and viral infection dynamics. Numerical simulations demonstrate how introducing viral infection influences the stability of bacterial populations and reduces the dominance of resistant strains. Furthermore, an optimal control approach is employed to identify effective intervention strategies, with the goal of minimizing the antibiotic-resistant population while maintaining the population of wild bacteria. Our findings emphasize the importance of incorporating viral dynamics in resistance management and propose a balanced approach to control resistant infections without exacerbating the emergence of more resistant strains.

References:

[1] Uddin, T. M., Chakraborty, A. J., Khusro, A., Zidan, B. R. M., Mitra, S., Emran, T. B., Dhama, K., Ripon, M. K. H., Gajdács, M., Sahibzada, M. U. K., et al. (2021). *Antibiotic resistance in microbes: History, mechanisms, therapeutic strategies and future prospects. Journal of Infection and Public Health, 14*(12), 1750–1766.

[1] Florida State University

Emergence of Multirhythmicity in Cortical Networks with Two Types of Inhibition

Arnab Dey Sarkar, Bard Ermentrout

August 2023

1 Abstract

We study a network model composed of three interacting neuronal populations: pyramidal (Pyr) cells, parvalbumin-positive (PV) interneurons, and somatostatin-positive (SST) interneurons. Starting from a network of globally coupled quadratic integrate-and-fire (QIF) neurons with heterogeneous inputs, we reduce the full spiking network to a low-dimensional mean-field model consisting of 9 ordinary differential equations (ODEs) — three for each population.

This reduced system captures the essential dynamics of the network, allowing for tractable bifurcation and phase space analysis. We demonstrate the emergence of multistability, oscillatory switching, and coexisting rhythms (mixed beta states) across the populations. In particular, we find that the strength and directionality of inter-population interactions critically depend on SST-IN-mediated inhibition, which modulates transitions between distinct beta-band oscillatory states.

Our results reveal how multiple subtypes of inhibitory neurons coordinate to generate and regulate complex beta dynamics, with potential implications for understanding neural mechanisms underlying motor control, cognitive function, and beta-band abnormalities observed in disorders such as Parkinson's disease.

Spatiotemporal Modeling of Extracellular DNA (eDNA) Dynamics in Biofilms

Mingjie Pei[1] Alexander J. Diefes[2]

Abstract

Biofilms refer to a large class of environments in which communities of microorganisms cohabitate within a self-produced extracellular matrix, and they are heavily implicated in human disease. *Bacillus subtilis* bacteria form biofilms and can be used to study general biofilm dynamics. Using data from the Prindle lab, we observe that extracellular DNA (eDNA), a source of phosphate, is produced in growing *B. subtilis* biofilms before being degraded in a spatiotemporally coordinated pulse. To explain this phenomenon, we developed a 1D PDE model to track advection quantities of active biomass and eDNA as well as diffusion of phosphate and DNAse, an enzyme known to splice eDNA. A key assumption to this model is that we track eDNA as a collection of splicing points, which depletes as the DNAse splices the eDNA over time. Model results qualitatively match DNAse and eDNA dynamics observed experimentally over time, providing some preliminary validation for the model. In future simulations, we hope to develop a higher dimensional model to account for both vertical and radial growth of the biofilm, as the 1D model only accounts for vertical growth. We hope this model can lead to a greater mechanistic understanding of eDNA reclaiming in biofilm development, predicting new avenues for biofilm control.

[1] Northwestern University [2] Duke University

A segmentation analysis in noisy trajectories

Thuy Linh Do
Tulane University

Abstract

We introduce CPLASS, an algorithm for detecting generalized changes in velocity problems within multidimensional data, addressing fundamental challenges in probability structure and search methodology. Unlike traditional changepoint detection methods that focus on mean shifts, detecting changes in velocity requires specialized approaches due to continuity constraints and parameter dependencies. Existing algorithms, including binary segmentation and simple dynamic programming methods, struggle with these complexities. To overcome these limitations, we develop an MCMC-based approach with tailored proposal mechanisms for efficient parameter exploration. Our method is particularly suited for analyzing intracellular transport data, where molecular motor trajectories exhibit complex, multidimensional transitions. To enhance robustness in small-sample regimes, we introduce a speed penalty that improves statistical power while maintaining consistency in the large-sample limit. Additionally, we demonstrate that comparing the proportion of time spent at different speeds provides a more stable metric for trajectory characterization.

Spectral decomposition unlocks ascidian morphogenesis*

Joel Dokmegang[†] Emmanuel Faure[‡] Patrick Lemaire[§] Ed Munro[¶] Madhav Mani[‖]

Abstract

Describing morphogenesis generally consists in aggregating the multiple high resolution spatiotemporal processes involved into reproducible low dimensional morphological processes consistent across individuals of the same species or group. In order to achieve this goal, biologists often have to submit movies issued from live imaging of developing embryos either to a qualitative analysis or to basic statistical analysis. These approaches, however, present noticeable drawbacks. They can be time consuming, hence unfit for scale, and often lack standardisation and a firm foundation. In this work, we leverage the power of a continuum mechanics approach and flexibility of spectral decompositions to propose a standardised framework for automatic detection and timing of morphological processes. First, we quantify whole-embryo scale shape changes in developing ascidian embryos by statistically estimating the strain-rate tensor field of its time-evolving surface without the requirement of cellular segmentation and tracking. We then apply to these data spectral decomposition in space using spherical harmonics and in time using wavelets transforms. These transformations result in the identification of the principal dynamical modes of ascidian embryogenesis and the automatic unveiling of its blueprint in the form of scalograms that tell the story of development in ascidian embryos. Most notably, our system is able to highlight the clear distinction between the gastrulation and neurulation phases of ascidian early development, as well as efficiently time synchronous cellular divisions.

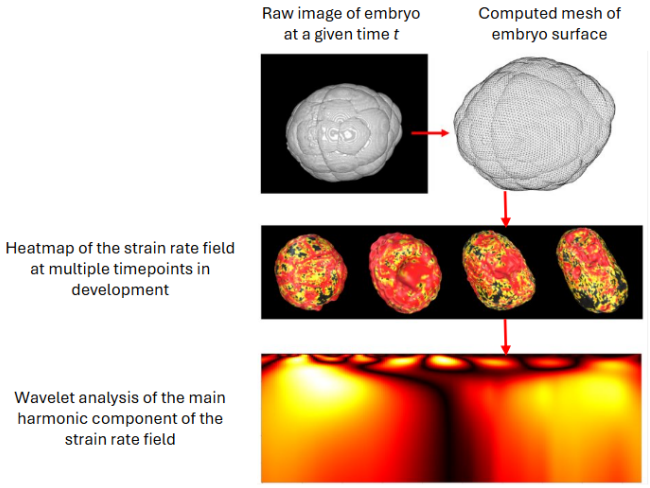

Figure 1: **Quantitative workflow of spectral decomposition of ascidian morphogenesis.**

References

[1] Dokmegang Joel, Faure Emmanuel, Lemaire Patrick, Munro Ed, Mani Madhav *Spectral decomposition unlocks ascidian morphogenesis* (2024, eLife).

---

*The full article can be accessed at `https://elifesciences.org/reviewed-preprints/94391`

[†]Northwestern University
[‡]LIRMM
[§]CRBM, CNRS
[¶]University of Chicago
[‖]Northwestern University

Nuclear size control by osmotic forces in *S. pombe*

Thomas G. Fai[1] Xuesong Bai[1] Joel Lemière[2] Fred Chang[2]

Abstract

We develop an osmotic theory based on van't Hoff's law to analyze the steady state nuclear-to-cell volume ratio.

1. Mechanism of nuclear size homeostasis

The size of the nucleus scales robustly with cell size so that the nuclear-to-cell size—the N/C ratio—is maintained during growth in many cell types (Fig. 1). To address the fundamental question of how cells maintain the size of their organelles despite the constant turnover of proteins and biomolecules, we consider a model based on osmotic force balance predicts a stable nuclear-to-cell size ratio, in good agreement with experiments on the fission yeast *Schizosaccharomyces pombe*. We model the synthesis of macromolecules during growth using chemical kinetics and demonstrate how the N/C ratio is maintained in homeostasis. We compare the variance in the N/C ratio predicted by the model to that observed experimentally.

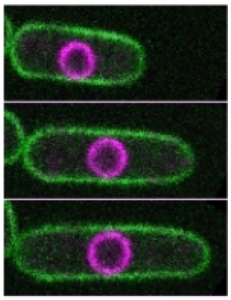

Figure 1: Cell membrane (green) and nucleus (magenta) grow proportionally during growth in *S. pombe*

References:

[1] Lemière, Joël, Paula Real-Calderon, Liam J. Holt, Thomas G. Fai, and Fred Chang, *Control of nuclear size by osmotic forces in Schizosaccharomyces pombe*, *eLife* 11 (2022).

[1] Brandeis University, Waltham, MA, USA

[2] UCSF, San Francisco, CA, USA

Modelling adhesion-based interactions in collective cell migration

Carles Falcó[*] Ruth E. Baker[*] José A. Carrillo[*] Jiwon Kim[†] Hyuntae Jeong[†]
Ian. Y. Wong[†]

Abstract

This talk presents recent advances in modelling adhesion-based phenomena in collective cell migration, with a focus on bridging theoretical models and experimental data. I will first introduce a local continuum model of cell–cell adhesion derived from a nonlocal aggregation-diffusion framework [1, 2], which simplifies previous formulations while preserving key patterning behaviours predicted by the differential adhesion hypothesis [3]. This model captures experimentally observed cell sorting and enables direct comparisons with data through its thin-film-like structure and explicit stationary solutions. Building on this framework, I will discuss collaborative work with experimental groups investigating collective cell migration. This includes a study of orbiting spheroids, where transitions from coordinated rotation to arrested motion emerge from the interplay between cell–cell adhesion, cell–matrix adhesion, and matrix curvature [4]. I will also touch on ongoing modelling efforts involving micropatterned substrates that induce cell polarisation and directional migration. Together, these projects highlight how mathematical models, rigorously developed and closely integrated with experiments, can provide mechanistic insight into collective cell behaviours and morphogenetic processes.

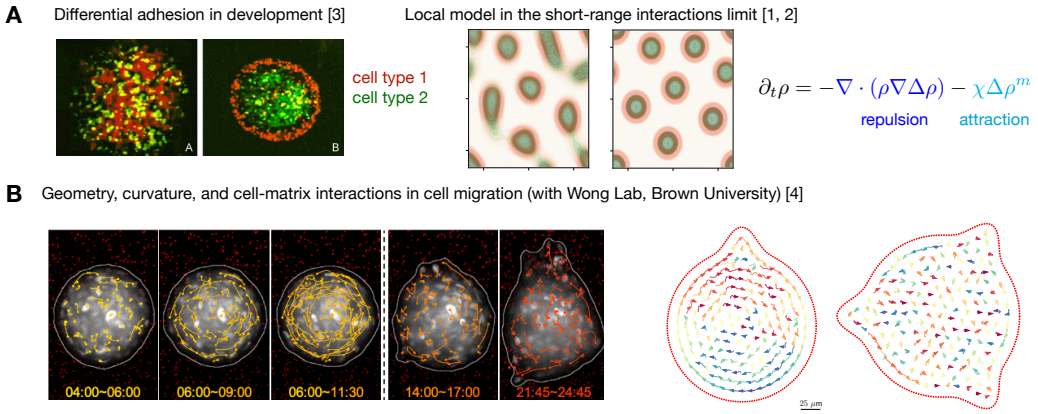

Figure 1: **Modelling collective cell behaviour driven by differential adhesion.** (A) A local continuum model of cell–cell adhesion reproduces sorting, partial engulfment, full engulfment, and mixing of two cell types over time, in agreement with the differential adhesion hypothesis. (B) Transitions from rotational to invasive behaviour in 3D spheroids emerge from the interplay between cell–cell adhesion, cell–matrix adhesion, and matrix curvature.

References

[1] C. Falcó, R. E. Baker, and J. A. Carrillo, "A local continuum model of cell-cell adhesion," *SIAM J. Appl. Math.*, vol. 84, pp. S17–S42, 2024.

[2] C. Falcó, R. E. Baker, and J. A. Carrillo, "A nonlocal-to-local approach to aggregation-diffusion equations," to appear in *SIAM Rev.*, 2025.

[3] R. A. Foty and M. S. Steinberg, "The differential adhesion hypothesis: a direct evaluation," *Dev. Biol.*, vol. 278, no. 1, pp. 255–263, 2005.

[4] J. Kim, H. Jeong, C. Falcó, A. M. Hruska, W. D. Martinson, A. Marzoratti, M. Araiza, H. Yang, C. Franck, J. A. Carrillo, M. Guo, and I. Y. Wong, "Collective transitions from orbiting to matrix invasion in 3D multicellular spheroids," *bioRxiv*, preprint, 2025. doi: 10.1101/2025.02.10.636936.

[*]Mathematical Institute, University of Oxford
[†]School of Engineering, Brown University

Time-series modeling of human temporal EEG responses to randomly alternating visual stimuli

Richard R. Foster[1,*], Connor Delaney[2], Dean Krusienski[2], Cheng Ly[1,3]

[1]*Department of Mathematics and Applied Mathematics, Virginia Commonwealth University, Richmond VA 23284*
[2]*Department of Biomedical Engineering, Virginia Commonwealth University, Richmond VA 23284*
[3]*Department of Statistics, Virginia Commonwealth University, Richmond VA 23284*

* Corresponding author: fosterrr@vcu.edu

It is well-established that visual stimuli flashing at constant temporal frequencies induce sharp peaks in the power spectrum of the electroencephalogram over the visual cortex at the driving frequency and its harmonics, known as steady-state visual evoked potentials. Visual stimuli that flash according to randomized temporal patterns can also result in predictable EEG patterns. While such EEG responses are robust and predictable, the underlying biophysical mechanisms that shape these responses are not fully understood. In pursuit of a better understanding of the relationship between the stimuli and associated EEG responses, and ultimately informing a biophysical model, we primarily examine these relationships by modeling EEG responses with a suite of statistical time-series models, starting with an autoregressive (AR) model and increasing in complexity towards a seasonal autoregressive moving average model with exogenous input (SARMAX). All models were constructed according to the Box-Jenkins methodology against an individual spatially-filtered EEG signal, in hopes that the fitted statistical models could determine key features of the visual pathway. Results indicated that model parameters, especially autoregressive-associated parameters, were strong and consistent over all model types, indicating that an emergent feedback structure exists in the EEG responses. All model types captured aspects of the EEG signal out-of-sample in the immediate time after the in-sample fit, including the distribution of EEG values (point-wise in time) and the frequency content. Our study may provide insights into the temporal dynamics of human EEG responses that could generalize to other visual stimuli.

A Delay Differential Equation Interpretation of the Leinheiser et al. Mitochondrial Fission Model

Kitrick Fynaardt* Anna Leinheiser* Colleen Mitchell*

1 Abstract

Mitochondria are the powerhouse of the cell. They perform many important functions in the cell, chief among them being the production of ATP, which cells use to power molecular functions. It is crucial for cells to keep a healthy concentration of mitochondria. This concentration can change by fusion or fission. Hyperfission, a state when mitochondria fizz too much and the cell is left with a large proportion of tiny mitochondria, has been linked to neurodegenerative disorders.

To study mitochondrial fission, Dr. Leinhesier and my advisor Dr. Mitchell designed a model of Drp1-dependent mitochondrial fission. Using the law of mass action following the diagram of fission in figure 1, they created a system of ordinary differential equations (ODEs) that model the oligomers that form on the mitochondrial surface (the C_i's) and eventually cause fission when they grow large enough by combining with each other. This model was instrumental in discovering the parameters that govern fission and pointing biologists towards the reaction rates that lead to hyperfisson.

The most unexpected property of the mitochondrial fission model is that for experimentally inspired parameter choices the solutions oscillate. It was not obvious why this behavior occurred. Furthermore, it was difficult to change the size at which fission occured without introducing more equations and numerical error hindered study of the steady states. To investigate further and solve some of these issues, I set out to create a version of the model which modeled oligomer size as a continuous variable.

Instead of having an ODE for every single oligomer size, the continuous-size model has a single partial differential equation (PDE) that describes the dynamics of all oligomer sizes. Changing the size where fission occurs is as simple as changing a parameter; the steady state calculations are easier computationally. This just left the mystery of the oscillatory behavior, which required a simplifying assumption. I changed how oligomers break apart: instead of deconstructing piece by piece (as shown in figure 1) I introduced an "ejection" parameter, which described the rate at which a size N oligomer could break down into N size 1 oligomers all at once. With this change, the PDE in the continuous-size model took on a form such that I could apply the method of characteristics.

Through the method of characteristics, I discovered the solution to the mystery. By following characteristic lines of oligomer concentrations through both size and time, I found that the concentration of oligomers that cause fission is exactly predicted by the concentration of size 1 oligomers at a previous time. This introduces a delay term into the system, transforming it into a delay differential equation (DDE). The oscillatory behavior of the system was caused by these underlying "delay dynamics" which caused many size 1 oligomers to suddenly return to the pool when fission occured, and then these many size 1 oligomers would cause a matching upsurge in fission after the delay had elapsed. These dynamics can be seen in figure 2.

*University of Iowa Mathematics Department

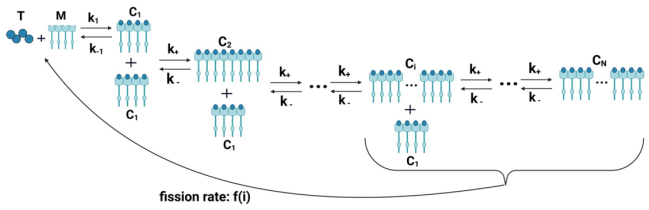

Figure 1: Reaction Schmeatic for the Drp1-dependent Fission Model

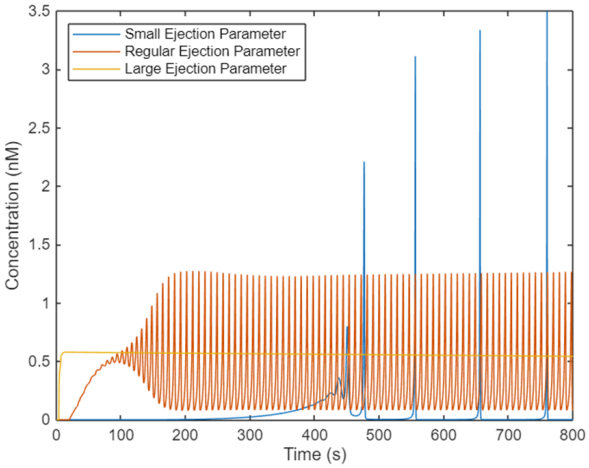

Figure 2: Three different solutions for the total fission rate of the continuous-size model. The oscillatory behavior changes if the parameter governing ejection is changed from the experimentally inspired regular value.

This continuous-size model will give further insights not only into mitochondrial fission, but any model where concentrations move between compartments. The technique of using the method of characteristics to unveil delay dynamics will be crucial for anyone studying models like these in the future.

References

[1] R. J. Youle, and A. M. van der Bliek, *Mitochondrial fission, fusion, and stress*, Science, 337 (2012), pp. 1062–1065

[2] A. K. Leinheiser et al. *A dynamical systems model for the total fission rate in Drp1-dependent mitochondrial fission*, PLoS computational biology, 20 (2024)

Evolution of aggression in consumer-resource models

Ted Galanthay[1]
Vlastimil Krivan[2]
Ross Cressman[3]
T A Revilla[4]

Abstract

Are animals in resource-poor environments more or less aggressive than animals in resource-rich environments? Dynamic game-theoretical models provide conflicting answers to this ecological question. In this work we introduce an extended consumer-resource model and explain how this model resolves this conflict.

References:

[1] Galanthay T.E., Krivan, V., Cressman, R., and Revilla T.A. (2023), *Evolution of Aggression in Consumer-Resource Models,* Dynamic Games and Applications, https://doi.org/10.1007/s13235-023-00496-w.

[1] Ithaca College, USA
[2] University of South Bohemia, Czech Republic
[3] Wilfrid Laurier University, Ontario, Canada
[4] University of South Bohemia, Czech Republic

Bioreactor Model of Methane Utilization for Product Synthesis via Engineered Biofilm

Spencer B. Gales* Thomas K. Wood † Ingmar H. Riedel-Kruse‡

Abstract

Methane is a harmful greenhouse gas that traps more heat in the atmosphere than carbon dioxide and serves as a valuable energy source for modern industry, being a primary component of natural gas. As a result, methane capture and utilization can be beneficial for economic and environmental reasons [4]. We employ a multi step reaction in microbial consortia for methane utilization and 2,3 butanediol synthesis utilizing acetate as a chemical intermediate (Figure 1). In doing so, we aim to simulate engineered Methanosarcina Acetivorans [2] for reverse methanogenenesis via anaerobic oxidation of methane (AOM) and engineered Escherichia Coli for aerobic conversion of acetate [1]. This work is carried out in collaboration with experimentalists and engineers who focus on optimizing microbial species and the reactor design with our models serving as a computational counterpart to the physical bioreactor, providing insight into design principles. We introduce and present results from our stratified biofilm model and introduce a second microbial growth model for our novel methane bioreactor. The first model is a stationary stratified biofilm model valid for time intervals during minimal microbial growth. This model affords us the ability to optimize layer thickness's of the biofilm which can serve as an initial condition to our microbial growth model. The second model we introduce, microbial growth model, is an extension to the classic [3] for a stratified biofilm. We optimize the stratified model in batch and continuous settings and in doing we are able to make recommendations to our collaborators for building an optimal reactor.

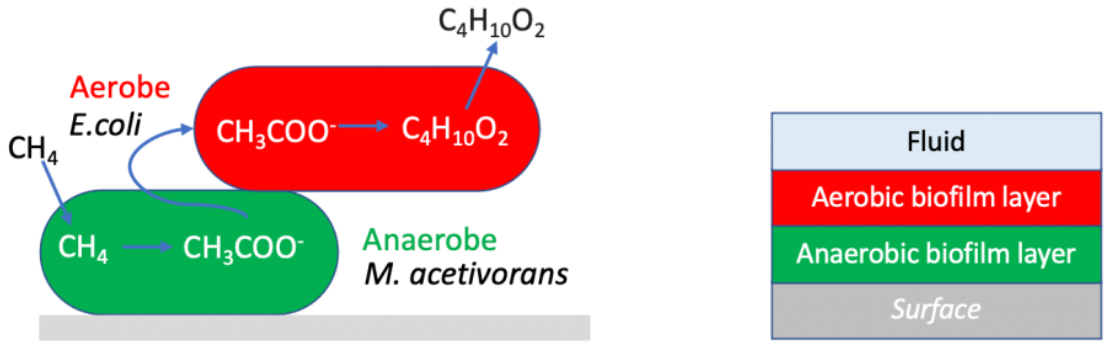

(a) (b)

Figure 1: (a) Multi step reaction from methane to butanediol via acetate. (b) The biofilm layers within the bioreactor situated above a non-permeable support surface below.

References

[1] K. Novak, R. Kutscha, and S. Pflügl. Microbial upgrading of acetate into 2, 3-butanediol and acetoin by e. coli w. *Biotechnology for biofuels*, 13:1–14, 2020.

[2] V. W. Soo, M. J. McAnulty, A. Tripathi, F. Zhu, L. Zhang, E. Hatzakis, P. B. Smith, S. Agrawal, H. Nazem-Bokaee, S. Gopalakrishnan, et al. Reversing methanogenesis to capture methane for liquid biofuel precursors. *Microbial cell factories*, 15:1–14, 2016.

[3] O. Wanner and W. Gujer. A multispecies biofilm model. *Biotechnology and bioengineering*, 28(3):314–328, 1986.

[4] T. K. Wood, I. Gurgan, E. T. Howley, and I. H. Riedel-Kruse. Converting methane into electricity and higher-value chemicals at scale via anaerobic microbial fuel cells. *Renewable and Sustainable Energy Reviews*, 188:113749, 2023.

*Program in Applied Mathemtics, University of Arizona, Tucson, Az, USA

†Department of Chemical Engineering, Pennsylvania State University, University Park, PA, USA

‡Departments of Molecular and Cellular Biology, Applied Mathematics, Biomedical Engineering, and Physics, University of Arizona, Tucson, AZ, USA.

Deep generative protein design using multimodal sequence-structure-text conditioning

Srivarshini Ganesan[1], Nikša Praljak[2], Hugh Yeh[1,3], Alexander Berlaga[4], Rama Ranganathan[1,5,6], Andrew L. Ferguson[1,4]*

The recent emergence of multimodal protein language models has initiated a transformative advancement in computational biology and molecular engineering. By integrating protein sequences and functional annotations, these models learn protein representations that enable the classification and retrieval of protein sequences from large unannotated datasets and the design of novel proteins conditioned on functional descriptions. We recently developed BioM3 as a multimodal model in which we integrated protein sequences and natural language text annotations within a shared embedding space using contrastive learning[1]. Here, we extend BioM3 by integrating protein structure as a third modality, providing spatial and conformational context that complements sequence and natural language annotations. BioM3 utilizes the Evolutionary Scale Modeling (ESM)[2] to obtain initial sequence representations (x^p) and PubMedBERT[3] to represent textual descriptions (x^t), which are then mapped to latent embeddings (z^p, z^t) by employing the InfoNCE loss. Each sequence-text embedding (z_i^p, z_i^t) is considered a positive sample drawn from the conditional distribution $p(z^p|z^t)$, and all other pairs (z_i^p, z_j^t) serve as negative samples drawn from the marginal distribution $p(z^p)$. By explicitly contrasting positive samples against multiple negative samples, InfoNCE loss encourages conditionally dependent pairs to align closely, while conditionally independent samples are pushed apart. To integrate structural information, we train a projection head that maps structural representations (x^s) derived from Foldseek[4] into latent embeddings (z^s), aligning them with the learned sequence embeddings (z^p). By explicitly integrating structure modality, our model allows the classification and annotation of protein structures and protein design based on combinations of sequence-structure-text conditioning. We are currently pursuing experimental tests of functional proteins designed using this approach in the context of SH3 Sho1 binding domains and the S1A serine protease and chorismate mutase catalytic enzymes.

References:

[1] Praljak, N. *et al.* Natural Language Prompts Guide the Design of Novel Functional Protein Sequences. Preprint at https://doi.org/10.1101/2024.11.11.622734 (2024).
[2] Rives, A. *et al.* Biological structure and function emerge from scaling unsupervised learning to 250 million protein sequences. *Proc. Natl. Acad. Sci.* 118, e2016239118 (2021).
[3] Gu, Y. *et al.* Domain-Specific Language Model Pretraining for Biomedical Natural Language Processing. (2020) doi:10.48550/ARXIV.2007.15779.
[4] Van Kempen, M. *et al.* Fast and accurate protein structure search with Foldseek. *Nat. Biotechnol.* 42, 243–246 (2024).

[1] Pritzker School of Molecular Engineering, University of Chicago, Chicago, IL 60637, USA
[2] Graduate Program in Biophysical Sciences, University of Chicago, Chicago, IL 60637, USA
[3] Medical Scientist Training Program, University of Chicago, Chicago, IL 60637, USA
[4] Department of Chemistry, University of Chicago, Chicago, IL 60637, USA
[5] Center for Physics of Evolving Systems, University of Chicago, Chicago, IL 60637, USA
[6] Department of Biochemistry and Molecular Biology, University of Chicago, Chicago, IL 60637, USA
*Corresponding Author

A Graph-theoretical Network Model for Nutrient Flow in Tissue Engineering Scaffolds

Binan Gu[1], Justyna Sokolik[2], Haniyeh Fattahpour[2], Pejman Sanaei[2]

[1]Department of Mathematical Sciences,
Worcester Polytechnic Institute, Worcester, Massachusetts

[2]Department of Mathematics and Statistics,
Georgia State University, Atlanta, Georgia

Abstract

This study introduces a network model to optimize scaffold designs in tissue engineering. Utilizing a variant of the Random Geometric Graph (RGG) method for network generation, the model simulates nutrient flow, mechanical stress distribution, and cellular migration within scaffold pores. It integrates fluid dynamics and elasticity principles to capture laminar flow and scaffold deformation. The governing equations for nutrient flow, concentration, scaffold elasticity, and cell growth are outlined, and scaling and non-dimensionalization techniques are applied to analyze the scaffold's microenvironment. The physical quantities of interest throughout the network are coupled via flux conservation at network junctions. We develop a network dynamics numerical solver based on finite-difference schemes that enforce vertex conditions arising from continuity and mass conservation. The results on the influence of vertex density and initial surface area on tissue volume growth underscore the significant impact of nutrient concentration and scaffold elasticity on tissue growth, providing actionable insights for designing scaffolds that enhance tissue regeneration.

Lower Bounds on the Sample Complexity of Species Tree Estimation when Substitution Rates Vary Across Loci*

Max Hill† Based on joint work with Sebastien Roch‡

Abstract

In this work we consider how much data is necessary to correctly infer evolutionary trees when genes are assumed to mutate at random, unknown rates.

1 Background and Problem Statement

The evolutionary history of a set of species can be represented by a leaf-labeled, edge-weighted tree, called a *species tree*. As illustrated in Figure 1, we model evolution by a stochastic process parameterized by the species tree, which in turn gives rise to *data* consisting of DNA sequences. The *phylogenetic reconstruction problem* is to recover the topology of the species tree from the DNA sequence data; that is, to "invert" the random function $\mathcal{L}$ pictured in the diagram. We are interested in this problem's *sample complexity*, which is the amount of data needed to achieve high probability of correct inference.

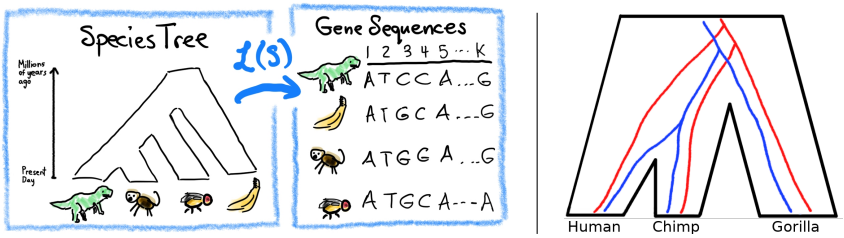

Figure 1: **Left:** A diagram showing a species tree S for four taxa, along with DNA sequences arising from a random function $\mathcal{L}$ parameterized by S. **Right:** Two gene trees (red, blue) embedded in a species tree for three species of great ape.

We assume a standard model of evolution known as the *multi-species coalescent*, which relates the overall evolutionary history of the species to the particular histories of individuals genes, called *gene trees* [3, 4]; importantly, gene trees may differ from the species tree, as shown in Figure 1 (on the right). The multi-species coalescent is then combined with a model of nucleotide mutation, known as a *substitution model* to produce sequence data [5]. We analyze the case where the mutation rates of individual genes are not known ahead of time, but are instead taken to be IID gamma-distributed random variables.

2 Results and Conclusions

Our main result is an information-theoretic lower bound which demonstrates that the amount of data required to correctly estimate the evolutionary history is substantially increased when one does not have *a priori* information about the rates of gene evolution. In particular, we reduce the problem to one of a hypothesis test for distinguishing two distinct evolutionary histories which differ in a minor way: by a short edge of length $f > 0$. By estimating the total variation distance between the sample distributions, we show that as $f \to 0$, the number of gene samples required must grow at least as fast as $1/f^2$.

We situate this result in the context of a well-studied information-theoretic tradeoff between different types of data (involving *number* vs. *quality* of gene tree estimates [2, 1]). In a departure from previous results, we show that this tradeoff collapses when mutation rates are random due to the impossibility of consistent inference with fewer than $O(f^{-2})$ samples. Our principal conclusion is that the inference problem is substantially harder without *a priori* information about mutation rates. Implications for inference and possible directions for future research will also be discussed.

---

*This abstract is based on a recent preprint of the same title, available at `https://www.biorxiv.org/content/10.1101/2025.01.28.635331v1`.

†University of Hawaii at Manoa
‡University of Wisconsin-Madison

References

[1] G. Dasarathy, E. Mossel, R. Nowak, and S. Roch, *A stochastic Farris transform for genetic data under the multispecies coalescent with applications to data requirements*, Journal of Mathematical Biology, 2022.

[2] E. Mossel and S. Roch. *Distance-Based Species Tree Estimation under the Coalescent: Information-Theoretic Trade-off Between Number of Loci and Sequence Length*, Annals of Applied Probability (2017) https://doi.org/10.1214/16-AAP1273

[3] B. Rannala, S.V. Edwards, A. Leaché, and Z. Yang, *The Multi-species Coalescent Model and Species Tree Inference*, In: Phylogenetics in the Genomic Era. (Eds: C. Scornavacca, F. Delsuc, and N. Galtier). Authors open access book (2020), Chapter 3.3. https://hal.science/hal-02535622

[4] B. Rannala and Z. Yang, *Bayes Estimation of Species Divergence Times and Ancestral Population Sizes Uinsg DNA Sequences from Mulitple Loci* Genetic (2003) 10.1093/genetics/164.4.1645.

[5] Z. Yang, *Molecular Evolution: A Statistical Approach*, Oxford University Press (2014).

Topological Insights into Viral Evolution via K-mer Topology

Yuta Hozumi*

Comparative genomics is essential for understanding evolutionary trajectories both between and within viruses. In this presentation, we introduce k-mer topology, an alignment-free sequence comparison method that utilizes the persistent Laplacian, which integrates persistent homology and spectral graph theory to analyze the positional information of k-mers. We validated our method by classifying viral families and constructing phylogenetic trees from whole genomes. Additionally, by leveraging tools from spectral graph theory, we demonstrate its promising applications in estimating antigenic distances and informing vaccine design for SARS-CoV-2.

Traditional comparative analysis relies on multiple sequence alignment (MSA), which pairwise aligns sequences to measure dissimilarity between species. However, MSA requires sufficiently similar sequences, making it unsuitable for comparing diverse virus families. Alignment-free methods overcome this limitation by extracting meaningful features without sequence alignment. A popular approach uses k-mers—substrings of length k—to construct count vectors for each sequence. These vectors can then be compared using standard distance metrics, enabling viral family classification. However, such methods overlook positional information, limiting their ability to distinguish closely related viruses.

To address this limitation, we draw on Topological Data Analysis (TDA), a powerful framework for understanding the shape of complex data. In particular, persistent homology (PH) captures invariants—such as Betti numbers—across multiple scales via a filtration process. We utilized the positions of the k-mers as a point cloud to analyze its topology, a method we call k-mer topology. These features are used to compute a genetic distance between sequences, which allows for viral classification and phylogenetic analysis. We validated our method by classifying families from the NCBI Virus database, comparing its accuracy against five other alignment-free methods. To ensure robustness to taxonomic changes—given that taxonomy is updated annually—we also tested our approach using family labels from different time points. K-mer topology consistently outperformed all baseline methods across benchmark datasets, accurately identifying both viral families and genetically similar sequences within those families. However, calculating higher-order homology and its invariants is computationally expensive, and the cost-to-performance improvement was minimal. Therefore, we focused on the 0th Betti number for the virus classification task.

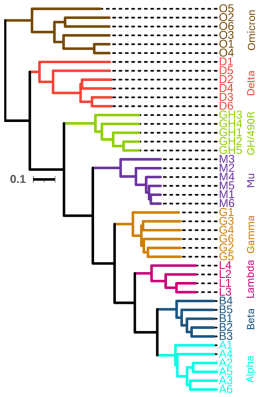

Phylogenetic analysis of SARS-CoV-2 allows for finding potential vaccine targets that covers multiple variants.

Although the viral classification task utilizing the Betti number improved accuracy, we wanted to explore the extent to which alignment-free methods using k-mer topology could be further developed. For analyzing genus, species, and variants—a task typically performed using MSA—relying solely on the 0th Betti number proved insufficient. To address this, we turned to the persistent Laplacian (PL), a method that incorporates spectral graph theory into the PH framework. PL constructs a series of graph Laplacians induced by the simplices generated through the filtration process. By computing their eigenvalues, we can extract topological and geometric information from the sequences. In particular, the multiplicity of the zero eigenvalue recovers the Betti number. Utilizing PL enabled the classification of recent dominant SARS-CoV-2 variants. Furthermore, we demonstrated a strong correlation between the antigenic distance derived from k-mer topology and the infectivity of recent variants, which we hope marks a first step toward vaccine design.

References

[1] Hozumi, Y and Wei, GW. "Revealing the Shape of Genome Space via K-mer Topology." arXiv preprint arXiv:2412.20202 (2024).
[2] Wang, R, Nguyen, DD, and Wei, GW. "Persistent spectral graph." Int J Numer Meth Bio (2020).
[3] Carlsson, G. "Topology and data." B Am Math Soc (2009).
[4] Balasubramanian, K. "Applications of combinatorics and graph theory to spectroscopy and quantum chemistry." Chem Rev (1985).
[5] Vinga, S., and Almeida, J. "Alignment-free sequence comparison—a review." Bioinformatics (2003).

*Goergia Institute of Technology

The Effect of Thresholding on Group Comparison of Graph Theory Metrics

Dominique Hughes[1] Sharon Crook[1]

Abstract

This work explores the effects of thresholding structural connectivity matrices on statistical differences found between groups for various graph measures.

In recent years, the mathematical subject of graph theory has become prevalent in neuroscience research to study the structure and function of different brain states [1]. Graphical representations of the brain can be constructed using neuroimaging data that has been parcellated into specifically defined regions, with different brain parcellations including different regions. These brain regions become the nodes of the graph, with the edges of the graph representing the connections between these brain regions. For magnetic resonance imaging (MRI), structural connections are quantified using diffusion MRI (dMRI). Structural connections are determined by white matter tracts connecting different brain regions in the parcellation [2]. Our project uses the TVB-UKBB pipeline to determine structural connectivity [2]; structural data is parcellated using the Regional Map 96 brain parcellation [3].

Once the brain graph has been constructed, it is common to further process the connectivity matrices by thresholding out certain values [4]. There is very little consensus in the literature about the correct threshold to use for structural connectivity data [4]. Our larger project focuses on using graph theory to determine the differences in aging trajectories for autistic (ASD) and neurotypical (NT) groups. We investigate the effects that thresholding has on the identification of statistical differences between ASD and NT groups for different graph measures conducted on structural connectivity matrices.

We use a sparsity threshold ranging from 0-70% with increases at 1% intervals. At 0%, the graph matrix remains unchanged from its original form. With each increasing step, that percentage of the lowest values of the matrix will be set to zero (if the matrix has more than that percentage as non-zero values), with the rest of the values remaining the same, leaving weighted undirected matrices to compute graph measures on. We then compute graph measures on the resulting thresholded graphs using the Brain Connectivity Toolbox (BCT) in MATLAB [5].

We conduct this analysis on the global graph measures: assortativity, characteristic path length, efficiency, radius, diameter, and transitivity, and the nodal graph measures: strength, betweenness centrality, eccentricity, degree, and clustering coefficient. We include 75 total subjects (35 ASD and 30 NT) aged 40+. We compare graph theory results between groups at each threshold level using a permutation test with 10,000 permutations; we use $p<0.05$ as our significance threshold.

We find that graph measures that rely on length and distance conversions (characteristic path length, efficiency, radius, diameter, eccentricity and betweenness centrality) of the connectivity matrices are relatively stable across thresholds, though the nodal measures in particular can include intermittent areas of non-significance. Additionally, strength is relatively consistent across thresholds, though it also includes intermittent areas of non-significance. Our other measures demonstrated more variability in p-values across thresholds.

References:

1. https://doi.org/10.31887/DCNS.2018.20.2/osporns
2. https://doi.org/10.3389/fninf.2022.883223
3. https://doi.org/10.1002/hbm.23506
4. https://doi.org/10.1002/jmri.27188
5. https://doi.org/10.1016/j.neuroimage.2009.10.003

[1] Arizona State University

Neural population code adaptation under changing metabolic constraints

Yi-Chun Hung* Gregory Schwartz† Emily A. Cooper‡ Emma Alexander*

Abstract

Information processing in neural populations is inherently constrained by metabolic demands and noise properties, with dynamics that are not accurately described by existing mathematical models. Recent data, for example, shows that tuning curves in mouse visual cortex undergo significant flattening in response metabolic stress, which is not predicted by previous neural coding models. We have developed a theoretical population coding framework that captures this behavior using two novel constraints: an energy budget (tied to noise levels via biophysical simulation) and an approximation of homeostasis. We analytically derive the optimal coding strategy for neurons under varying noise levels and coding goals, and show how our method generalizes existing models.

Animals' nervous systems are thought to use population-based encoding strategies that are optimized to fulfill functional roles such as representing information or discriminating between stimuli. These strategies must support successful behaviors whether an animal is well-fed or facing a reduced energy budget due to food scarcity. While such energetic constraints are a key feature determining the optimal encoding strategy, population codes are often analyzed via constrained optimization problems on neural information (often specifically on Fisher Information) with more attention typically paid to the optimization objective than to these constraints, e.g., [1, 6, 2, 5, 3]. Simple parameterizations of energetic constraints can lead to naive descriptions of neurons' adaptation to metabolic stress, which do not capture the tuning curve flattening and approximate preservation of firing rates (homeostasis) observed recently in neocortical data from food-restricted mice [4]. Using a biophysical simulation of metabolically-stressed neurons informed by [4], we address this gap by describing changes in firing rate noise and energy consumption associated with cell properties such as membrane conductance and resting potential. Fig.1a illustrates an empirical trend in tuning curves from freely fed (control) versus food restricted mice in black, our prediction in blue, and previous approaches in orange [2] and green [5]. We abstract our simulations into a standard analytical framework for Fisher Information based on tuning curve gain $g(s)$, density $d(s)$, and probability $p(s)$ of stimulus values s, under a commonly-used tiling assumption. Our framework generates novel predictions of optimal population codes (see Tab. 1), which generalize previous descriptions (see Fig. 1b) to generate the correct low-energy behavior (see Tab. 2).

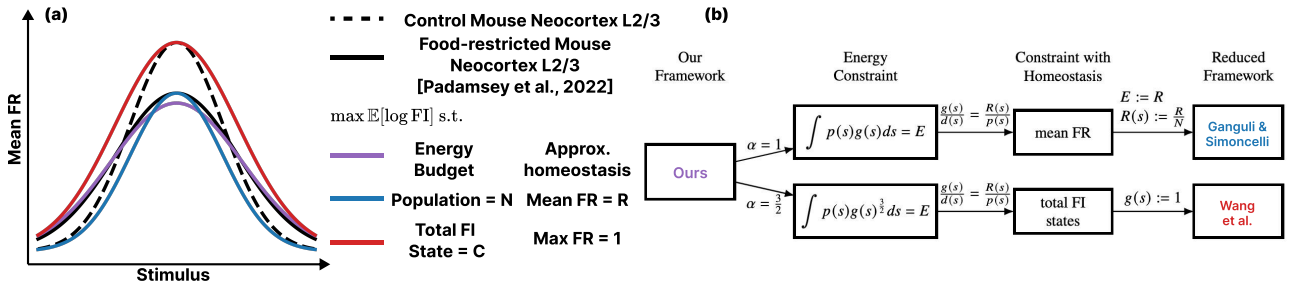

Figure 1: **Comparison of optimal tuning curves in control versus food-restricted mouse neocortex (L2/3)** (a) The figure illustrates how an example tuning curve in an optimal population adapts to a tightening of energy-related constraints. Under metabolic stress, real tuning curves flatten (dashed to solid black line, based on [4]). Our model (purple) predicts this flattening, while existing models predict either widening or shortening (red, blue). (b) Our framework generalizes previous work [2, 5], as shown by specific simplifications.

*Department of Computer Science, McCormick School of Engineering, Northwestern University
†Feinburg School of Medicine Northwestern University Evanston, USA
‡Herbert Wertheim School of Optometry and Vision Science, University of California, Berkeley, CA, 94720, USA

Table 1: **Summary of analytical solutions in our framework.**

		Infomax	**Discrimax**	**General**
Optimized function		$f(x) = \log x$	$f(x) = -x^{-1}$	$f(x) = -x^{\beta},\ \beta < \frac{\alpha}{3}$
Density (Tuning width)$^{-1}$	$d(s)$	$E^{1/\alpha} R(s)^{-1} p(s)$	$\propto E^{1/\alpha} R(s)^{\frac{-\alpha-1}{\alpha+3}} p(s)^{\frac{\alpha+1}{\alpha+3}}$	$\propto E^{1/\alpha} R(s)^{\frac{\alpha-\beta}{3\beta-\alpha}} p(s)^{\frac{\beta-\alpha}{3\beta-\alpha}}$
Modulation Gain	$g(s)$	$E^{1/\alpha}$	$\propto E^{1/\alpha} R(s)^{\frac{2}{\alpha+3}} p(s)^{\frac{-2}{\alpha+3}}$	$\propto E^{1/\alpha} R(s)^{\frac{2\beta}{3\beta-\alpha}} p(s)^{\frac{-2\beta}{3\beta-\alpha}}$
Fisher information	$J(s)$	$\propto E^{3/\alpha} R(s)^{-2} p(s)^2$	$\propto E^{3/\alpha} R(s)^{\frac{-2\alpha}{\alpha+3}} p(s)^{\frac{2\alpha}{\alpha+3}}$	$\propto E^{3/\alpha} R(s)^{\frac{2\alpha}{3\beta-\alpha}} p(s)^{\frac{-2\alpha}{3\beta-\alpha}}$
Discriminability bound	$\delta_{\min}(s)$	$\propto E^{-3/2\alpha} p(s)^{-1}$	$\propto E^{-3/2\alpha} p(s)^{\frac{-\alpha}{\alpha+3}}$	$\propto E^{-3/2\alpha} p(s)^{\frac{\alpha}{3\beta-\alpha}}$

Table 2: **Comparison of different works on neuron population codes.** Key parameters include the total number of neurons (N), mean firing rate (R), Fisher information state (C), energy budget (E).

Works	**Constraints**	**Constraints under Tiling**	**Noise**	**Low Energy**
Ganguli & Simoncelli [2]	mean FR population size	$\int p(s)g(s)\mathrm{d}s = R$ $\int d(s)\mathrm{d}s = N$	Poisson	$R\downarrow$, shortens (N fixed)
Wang et al. [5]	max FR total FI states	$g(s) = 1$ $\int \sqrt{g(s)d(s)^2}\mathrm{d}s = C$	Poisson or Gaussian	$C\downarrow$, widens
Ours	energy approx. homeostasis	$\int p(s)g(s)^{\alpha}\mathrm{d}s = E$ $\frac{g(s)}{d(s)} = \frac{R(s)}{p(s)}$	Energy-dependent Dispersed Poisson	$E\downarrow$, flattens ($R(s)$ fixed)

References

[1] Nicolas Brunel and Jean-Pierre Nadal. Mutual information, fisher information, and population coding. *Neural computation*, 10(7):1731–1757, 1998.

[2] Deep Ganguli and Eero P. Simoncelli. Implicit encoding of prior probabilities in optimal neural populations. In *Conference on Neural Information Processing Systems (NeurIPS)*, pages 658–666, 2010.

[3] Tyler S Manning, Emma Alexander, Bruce G Cumming, Gregory C DeAngelis, Xin Huang, and Emily A Cooper. Transformations of sensory information in the brain suggest changing criteria for optimality. *PLoS computational biology*, 20(1):e1011783, 2024.

[4] Zahid Padamsey, Danai Katsanevaki, Nathalie Dupuy, and Nathalie L Rochefort. Neocortex saves energy by reducing coding precision during food scarcity. *Neuron*, 110(2):280–296, 2022.

[5] Zhuo Wang, Alan A. Stocker, and Daniel D. Lee. Efficient Neural Codes That Minimize L_p Reconstruction Error. *Neural Computation*, 28(12):2656–2686, 2016.

[6] Xue-Xin Wei and Alan A Stocker. Mutual information, fisher information, and efficient coding. *Neural computation*, 28(2):305–326, 2016.

On generalizing the induced surface charge method to heterogeneous Poisson-Boltzmann models for electrostatic free energy calculation

Idowu Ijaodoro
The University of Alabama, Tuscaloosa

Abstract

The induced surface charges (ISC) method, which computes the induced charges on the molecular surface of macromolecules and uses them via Coulomb's law to calculate the polar solvation energy, was shown to be a robust and almost grid independent approach for electrostatic analysis based on the sharp-interface Poisson-Boltzmann (PB) model. Besides being physically intuitive, the ISC method avoids using the potential near the point charges, which is singular at each atom center. However, the ISC method cannot be physically generalized to heterogeneous dielectric PB models, due to the non-existence of a dielectric boundary. In this work, a novel far-field (FF) method is proposed to calculate the polar solvation free energy, which is derived through reformulating the energy functionals of nonlinear PB potential in solvent and vacuum states. Built upon a rigorous mathematical analysis, the FF method reconstructs the free energies by using far-field solutions outside the solute so that the self-energy terms generated by the singular charges are avoided, just as in the ISC method. Being valid for both sharp-interface and heterogeneous PB models, the performance of the proposed FF method has been validated by considering diffuse interface, Gaussian and super- Gaussian PB models for Kirkwood spheres and various protein systems. Comparison with grid-energy cancellation and regularization methods is also considered. The robustness of the FF method in treating a non-rigid biomolecule with different molecular structures in solvent and vacuum states has been explored, taking advantage of the fact that the far-field potential is insensitive to perturbations of singular charge locations.

Stochastic modeling of viral reproductive cycle: efficient computation of viral and cell extinction

Rahnuma Islam
The University of Pittsburgh

David Swigon
The University of Pittsburgh

Abstract

We present a stochastic model in immunology describing the evolution of diseases in the human organism. Simulation of continuous-time Markov chain versions of such stochastic models is the most accurate way of obtaining results, but it is typically time-consuming. Here, we present two simple stochastic models of viral reproduction that can be used as a basis for modeling immune response, and compute the probabilities and mean times of viral and cellular extinctions as functions of the burst size or viral production rate. Our analysis includes two types of viral production: one accounts for viral bursting, in which the release of viruses is instantaneous after cell lesion, and the other for viral budding, in which new viral particles are released from infected cells gradually. We show that in both cases, traditional diffusion approximation methods lead to serious discrepancies in extinction probabilities and mean times, and that with modified stochastic differential equations, we can achieve significant improvement in integration speed while maintaining accuracy.

Multilayer Co-Expression Networks: Mathematical Insights into Gene Expression Variability and Regulatory Interplay

Nuzla Ismail, Saiful Islam, Alber Aqil, Omer Gokcumen, Naoki Masuda (SUNY Buffalo)

Knowledge of biological processes and disease mechanisms necessitates a thorough understanding of gene regulation. Co-expression network analysis is widely employed to infer the organization of regulatory relationships and the functional roles of genes under various biological conditions. In this study, we focus on gene co-expression variability across tissues by leveraging the Genotype-Tissue Expression (GTEx) Version 10 dataset, encompassing 18,969 genes across 27 tissues modelled as a multilayer gene co-expression network, as in our previous work [1]. We classify genes into two categories. The first category includes genes (g1) that exhibit poor tissue-to-tissue co-expression for multiple tissue pairs, suggesting that polymorphism (i.e., person-to-person genetic difference) is not the primary determinant of their expression; rather, tissue-specific factors, such as hormones, may play a significant role. The second category (g2) contains genes showing high tissue-to-tissue co-expression across diverse tissue pairs, indicating that their varying expression levels are driven predominantly by genetic polymorphism.

Furthermore, if a g2 gene is highly co-expressed with a g1 gene in any given tissue, we hypothesise that g2 regulates g1. We identified 18 g1 genes and 13 g2 genes that show significant tissue-to-tissue co-expression patterns. In testis, a strong correlation was observed between several g1 and g2 genes, indicating potential regulatory relationships. (See Figure C: Co-expression matrix between g1 and g2 genes in testis.)

Figure 1. (A) 27 x 27 tissue-tissue correlation matrix of a g1 gene. (B) 27 x 27 tissue-tissue correlation matrix of a g2 gene. (C) The correlation matrix between any pair of g1 or g2 genes in a single tissue, the testis. Due to the space constraint, we omitted the tissue names in (A) and (B).

Reference

[1] A. Aqil, Y. Li, Z. Wang, S. Islam, M. Russell, T. Kunovac Kallak, M. Saitou, O. Gokcumen, N. Masuda. bioRxiv: doi:10.21203/rs.3.rs-4974188/v1. 419265

The Role of Cell Geometry in Cytoplasmic Streaming*

Olenka Jain[1,2] Brato Chakrabarti[3] Reza Farhadifar[2] Elizabeth R. Gavis[4]
Michael J. Shelley[2,5] Stanislav Y. Shvartsman[1,2,4†]

Abstract

This work probes the role of cell geometry in orienting self-organized fluid flows in the late stage *Drosophila* oocyte. Recent theoretical work has shown that a model, which relies only on hydrodynamic interactions of flexible, cortically anchored microtubules (MTs) and the mechanical loads from molecular motors moving upon them, is sufficient to generate observed flows. While the emergence of flows has been studied in spheres, oocytes change shape during streaming and it was unclear how robust these flows are to the geometry of the cell. Here we use biophysical theory and computational analysis to investigate the role of geometry and find that the axis of rotation is set by the shape of the domain and that the flow is robust to biologically relevant perturbations of the domain shape. Using live imaging and 3D flow reconstruction, we test the predictions of the theory/simulation, finding consistency between the model and live experiments, further demonstrating a geometric dependence on flow direction in late-stage *Drosophila* oocytes.

1 Biological Problem

Our work asks how the geometry of the oocyte itself determines the structure of the resulting flow field. The model of flow generation is based on the known biology of cytoplasmic streaming in the *Drosophila* oocyte. In the late-stage oocyte, stable microtubules (MTs) are cortically anchored to the cell cortex at their minus ends. These MTs serve as railroads for the plus-end directed nanoscale molecular motors, kinesins, that carry cellular cargos. By walking towards the free end of cortically anchored MTs, kinesin-cargo complexes exert a force on the cytoplasm, entraining the nearby fluid, and a compressive force on the inextensible MTs. For large compressive loads, the MTs can bend or buckle, leading to synergistic interactions between the deformations of the MTs and the flows they generate.

A previous analysis of this model established the emergence of a self-sustained intracellular cell-scale vortical flow in a spherical geometry. However, oocytes are not spheres (the late-stage oocytes are well approximated by prolate ellipsoids) and cell geometry has non-trivial consequences for the emergent flows because it is non-linearly coupled to the cytoplasmic flows. Geometry breaks the rotational symmetry in the problem and poses the question of how the interior flow is topologically organized. What sets the axis and chirality of the emergent flows?

2 Numerical Methods and Simulations

Following previous work, the joint dynamics of microtubules (MTs) coupled through a viscous fluid are described. The evolution of each microtubule $\mathbf{X}^i(s,t)$, parameterized by arc length s, time t, and in a background velocity field $\mathbf{u}$, evolves as:

$$\eta(\mathbf{X}^i_t - \bar{\mathbf{u}}_\mathbf{i}) = (\mathbf{I} + \mathbf{X}^i_s\mathbf{X}^i_s)\cdot(\mathbf{f}^i - \sigma\mathbf{X}^i_s), \tag{2.1}$$

$$\mathbf{f}^i = -E\mathbf{X}^i_{ssss} + (T^i\mathbf{X}^i_s)_s. \tag{2.2}$$

Where $\bar{u_i}$ accounts for the fact that we only consider the nonlocal contributions to the velocity field by the fibers. In other words, $\bar{u_i}$ is the velocity field induced by every other fiber that is not the ith fiber. The forces governing the dynamics of the fiber are $\mathbf{f}^i$, the elastic force per unit length from microtubule bending and σ, the coarse grained compressive force due to the movement of motor-cargo complexes. I is the identity matrix, E is the bending rigidity and T^i is the MT tension, which acts as a Lagrange multiplier to enforce the incompressibility of each fiber, and η is the drag coefficient. The drag coefficient on the slender fiber is given by $\eta = \frac{8\pi\mu}{|c|}$, where μ is the viscosity and $c = \log e\epsilon^2$ is a coefficient characterizing the slenderness of the MT (ϵ is the ratio of MT length to width).

---

*The preprint of this work can be accessed at `https://arxiv.org/abs/2409.06763`

†[1]Lewis-Sigler Institute for Integrative Genomics, Princeton University, Princeton, NJ 08544, USA; [2]Center for Computational Biology, Flatiron Institute, New York, NY 10010, USA; [3]International Center for Theoretical Sciences, Bengaluru 560089, India; [4]Department of Molecular Biology, Princeton University, Princeton, NJ 08544, USA; [5]Courant Institute, New York University, New York, NY 10012, USA.

We used large scale hydrodynamic simulations (SkellySim) to evolve fibers according to Eq. (2.1) and Eq. (2.2) in a background fluid governed by the forced incompressible Stokes equation and subject to a no-slip boundary condition at the cortex. We evolved these flows in prolate ellipsoids with aspect ratios matching those of late-stage *Drosophila* oocytes. Vortical flow emerged as the long term state of the problem. However, the axis of rigid-body rotation was independent of initial conditions and consistently close to the long axis of the ellipsoid. We call such flow "axisymmetric" flow, as it rotates around the long axis of the ellipsoid. To investigate the stability of the "axisymmetric" flow state in an ellipsoid, we performed numerical "perturbation" experiments in which we evolved flow in a sphere until steady state. We then stretched the sphere perpendicular to the axis of rotation of flow while maintaining the same surface area and MT placement. We ensured that the boundary condition of normally clamped fibers was met. We allowed the system to evolve from this vortical state, in which the axis of rotation was the short axis of the ellipsoid, and found that each simulation converged to "axisymmetric" flow. This convergence was accompanied by a minimization of elastic energy, the governing energy in this system.

3 Live Imaging and 3D Flow Reconstruction

We turned to experiments to test the predictions of the numerical analysis: (1) that cell geometry plays a role in setting the direction of the flow field in *Drosophila* oocytes, and (2) the sense of rotation of the flow should be unbiased. While experiments observing flows in *Drosophila* oocytes date back to the 1980's, there has been no characterization of their handedness or axis of rotation. We made use of fluorescently labeled inert proteins which functioned as tracer particles and developed an image analysis pipeline to extract velocity fields from thin cortical slices (as the confocal microscope cannot penetrate far into the sample).

Our experimental results showed that the average direction of the flow field was consistent with flow rotating about the long axis of the cell. With the exception of one stage 12 oocyte (of 18 in total) in which flow appeared as a vortex, the measured flow fields were consistent with axisymmetric flow. Likewise, our symmetry breaking model and simulations predicted no bias in the handedness of the flows. From experiments, it was equally likely for a flow to be clockwise as it was counterclockwise. Finally, we developed a new technique using lightsheet microscopy to obtain the first fully isotropic 3D visualization of the flows. The result was consistent with the confocal imaging: a vortical flow rotating nearly around the long axis of the cell.

4 Discussion

There is relatively little understood about how the geometry of the cell affects the processes within it. We studied this question in the important context of self organized cytoplasmic streaming in the *Drosophila* oocyte. How a system evolves from an initial configuration with many possible solutions to selecting a single solution is a challenging problem. However, prior to this work, it was unclear how geometry could contribute to the loss of solutions in this specific system. Numerically and experimentally, we argue that the domain of the container aids in reducing the number of possible flow orientations to just one: flow around the long axis. By showing that, just as simulations predict, there is a preferred direction of flow in real oocytes, we have strengthened both the evidence for the current biophysical model and our understanding of boundary driven flows in oocytes. Our updated picture of cytoplasmic streaming paves the way for future work to characterize the functional properties of the flow, namely how it transports molecules and mixes the cell's cytoplasm.

References

[1] B. Chakrabarti, M. Rachh, S. Y. Shvartsman, and M. J. Shelley, *Cytoplasmic stirring by active carpets*, Proc. Natl. Acad. Sci. USA, 121 (2024), p. e2405114121.

[2] S. Dutta, R. Farhadifar, W. Lu, et al., *Self-organized intracellular twisters*, Nat. Phys., 20 (2024), pp. 666–674.

[3] R. E. Goldstein and J.-W. van de Meent, *A physical perspective on cytoplasmic streaming*, Interface Focus, 5 (2015), p. 20150030. https://doi.org/10.1098/rsfs.2015.0030.

[4] W. Lu, M. Lakonishok, A. S. Serpinskaya, D. K. Ling, and V. I. Gelfand, *Ooplasmic flow cooperates with transport and anchorage in Drosophila oocyte posterior determination*, J. Cell Biol., 217 (2018), pp. 3497–3511.

[5] M. E. Quinlan, *Cytoplasmic streaming in the Drosophila oocyte*, Annu. Rev. Cell Dev. Biol., 32 (2016), pp. 173–195.

[6] Flatiron Institute, *SkellySim*, 2023. Available at: https://github.com/flatironinstitute/SkellySim

[7] D. B. Stein, G. De Canio, E. Lauga, M. J. Shelley, and R. E. Goldstein, *Swirling instability of the microtubule cytoskeleton*, Phys. Rev. Lett., 126 (2021), p. 028103.

[8] W. E. Theurkauf, B. M. Alberts, Y. N. Jan, and T. A. Jongens, *A central role for microtubules in the differentiation of Drosophila oocytes*, Development, 118 (1993), pp. 1169–1180.

A Nonlocal Size-Modified Poisson-Boltzmann Model for VDAC

Liam Jemison*

Abstract

Voltage-Dependent Anion Channel (VDAC) is a class of channel proteins which are abundant on the outer mitochondrial membrane, and play a major role in moving crucial ions and metabolites into and out of mitochondria. We propose a Nonlocal Size-Modified Poisson-Boltzmann ion channel (NSMPBic) model to incorporate nonlocal dielectric effects and steric ion contributions into an electrostatic description of the VDAC protein. We also present a finite element approach for solving the NSMPBic model on tetrahedral meshes of VDAC proteins based on x-ray crystallography data from the protein databank.

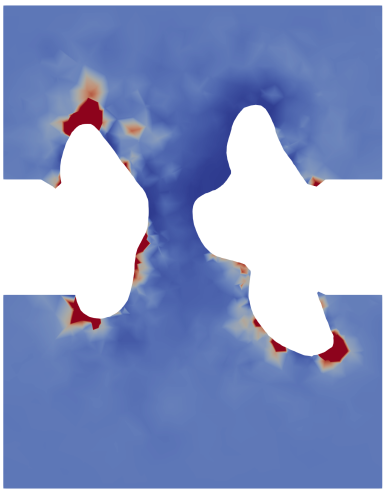

Figure 1: Simulated sodium concentration around VDAC 2JK4.

*University of Wisconsin-Milwaukee

Stochastic Modeling of Morphological Rate Evolution: Phylogenetic Regression with Approximate Bayesian Computation*

Dwueng-Chwuan Jhwueng†

Abstract

In the macroevolutionary studies, one major study of interest is understanding the evolution of traits. Several novel statistical models have been proposed to link the rate of evolution of one trait with another trait. In this framework, I expand the existing Brownian motion–type covariate (BM) to the Ornstein–Uhlenbeck (OU) process–type covariate that allows stabilizing selection to occur during evolution. In addition, the covariate type of the early burst (EB) process type covariate is also developed to consider the adaptive radiation phenomenon. Due to the lack of model likelihood, I propose the use of the approximate Bayesian computation (ABC) technique for the estimation of the model parameters. Simulations show that the models work well with posterior estimates close to the true parameters. The models are applied to analyze the 136 bird species data to reinvestigate how the rates of beak-shaped evolution in birds are influenced by brain mass.

1 Proposition 1.

THEOREM 1.1. *For* $m = 0, 1, 2, \cdots$, *the moment for the EB trait variable* x_{t,σ_0} *is expressed as following* $E\left[\left(\int_0^t \exp(r_x s) dW_s^x\right)^{2m}\right] = \frac{(2v_{r_x}(t))^m}{\sqrt{\pi}}\Gamma(m+\frac{1}{2})$, *and* $E\left[\left(\int_0^t \exp(r_x s) dW_t^x\right)^{2m+1}\right] = 0$, *where* $v_{r_x}(t) = \frac{\exp(2r_x t)-1}{2r_x}$.

Proof. Please refer to the Mathematical Appendix in the manuscript. □

References

[1] D.-C. Jhwueng, *Stochastic Modeling of Morphological Rate Evolution: Phylogenetic Regression with Approximate Bayesian Computation* . (In progress).

*The full version of the manuscript can be accessed at `https://tonyjhwueng.info/phyratereg/PhyRateCovRegOUEB.pdf`

†Department of Statistics, Feng-Chia University Taiwan

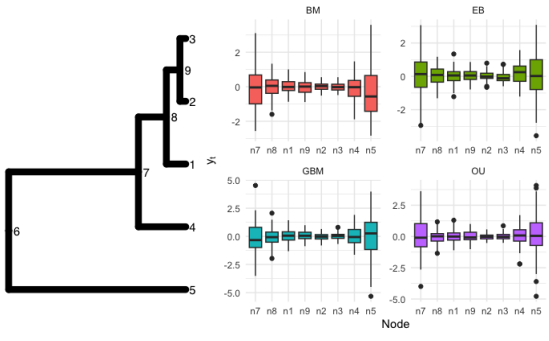

Figure 1: Left: A 5 taxa phylogenetic tree with tips numbered as n_1, n_2, n_3, n_4, n_5 and nodes numbered as n_6, n_7, n_8, n_9. Right: Boxplot for trait simulation using the SDE model $y_t = y_a + \int_0^{t_a} \sqrt{a + bx_s} dW_s^y$ under four type of covariates x_s: BM, GBM, EB, OU for a 5 taxa tree.

A multiscale model on hair follicle bulb replenishment and concentric layered differentiation

Rose Johnson-Leiva[1] Mingye Gao[1] Qixuan Wang[12]

Abstract

Hair follicles (HFs) are mini-organs in skin who undergo cyclic growth. During the anagen phase, the hair shaft is produced from the bottom part of the HF, referred to as the hair bulb. Proper regulations of the HF bulb cell fate decisions are crucial to maintain an anagen HF, therefore guaranteeing the continuous production of hair. Recent experiments have provided evidence on how HF bulb is replenished during anagen, and how cells make their fate decisions according to their positions, leading to the HF concentric layered differentiation. We develop a hybrid multiscale computational model on HF bulb, integrating an agent-based submodel of cell divisions and movement, a reaction-advection-diffusion equation submodel of diffusive signaling dynamics, and a Boolean network submodel of intra-cellular gene regulations. Using our model, we first investigate the HF bulb replenishment dynamics driven by different cell dividing strategies, showing that signaling-driven cell division may lead to efficient replenishment dynamics. Next, we use the model to test the primed cell fate decision mechanism, and explore other candidate mechanisms that may contribute to a perfect HF concentric layered differentiation.

References:

[1] M. Gao, R. Johnson-Leiva, and Q. Wang, “A multiscale model on hair follicle bulb replenishment and concentric layer differentiation.,” In preparation.

[1] Department of Mathematics, University of California, Riverside

[2] Interdisciplinary Center for Quantitative Modeling in Biology, University of California, Riverside

Accurate reconstruction of cellular time series using linear, Gaussian, and deep learning models

Taylor Kennedy[1] Orlando Arguello-Miranda[1]

Abstract

Microscopy image time series are crucial to studying molecules in single living cells, screening for new drugs and antibiotics, and investigating how cells process information over time. Beyond appropriate methods to ensure spatial and temporal resolution of image time series, the quantification of cellular processes requires accurate tools to analyze single-cell time series, which often suffer from sparsity, low signal-to-noise ratios, signal mixing, and cell tracking requirements. Without an optimized pipeline for time series processing, the information recorded from biological experiments can not be statistically interpreted and the richness of information derived from experiments is severely reduced.

This work proposes a mathematical and computational framework to maximize the information obtained from single-cell time series using Saccharomyces cerevisiae as a model organism. Our approach combines linear, Gaussian, and deep learning models at several steps of image post-processing to ensure the time series obtained from single cells are complete and accurately represent biological information. Our pipeline starts by ensuring the information in single pixels does not contain mixed signals by using a linear unmixing model that takes into consideration the physical constraints of the microscopy setup used to record the images and leverages a deep learning model for cell segmentation. Once unmixed, single-cell features are extracted using a combination of Gaussian fits and label-free deep learning segmentation algorithms to identify specific cellular features such as foci, nuclei, and cell membrane structures. Finally, we developed a single-cell tracking algorithm independent of cell movement or shape and based on generative frame interpolation.

Our results indicate that our pipeline enhances the generation of more complete and biologically meaningful time series than previous approaches. Due to the ubiquitous nature of time series analysis in biology, we expect our approach to be expanded to other data sets beyond *S. cerevisiae*, such as studying immune and cancer cells, filamentous fungal organisms, bacteria, human organoids, and potentially non-biological applications.

References:

[1] Swaraj Kaondal, Arsalan Taassob, Sara Jeon, Su Hyun Lee, Henrique L. Nuñez, Bukola A. Akindipe, Hyunsook Lee, So Young Joo, Samuel M.D. Oliveira, Orlando Argüello-Miranda. (2025). Generative frame interpolation enhances tracking of biological objects in time-lapse microscopy. bioRxiv 2025.03.23.644838; doi: https://doi.org/10.1101/2025.03.23.644838

[2] Taylor Kennedy, Berk Yalcinkaya, Shreya Ramakanth, Sandhya Neupane, Nika Tadic, Nicolas E. Buchler, Orlando Argüello-Miranda. (2024). Deep learning-driven imaging of cell division and cell growth across an entire eukaryotic life cycle, bioRxiv 2024.04.25.591211; doi: https://doi.org/10.1101/2024.04.25.591211 (Accepted awaiting Publication: ASCB MBoC)

[1] Department. of Plant and Microbial Biology, North Carolina State University

Tissue self-organization tunes the period of somite segmentation

Kemal Keseroglu[1] Ertuğrul M. Özbudak[1]

Abstract

Nonequilibrium phase transitions frequently occur in both living and non-living matters. However, the mechanism governing dynamics of biological phase transitions, such as mesenchymal to epithelial transition (MET), remains unclear. A well-known MET is the segmentation of somites, the embryonic precursors of the vertebral column [1,2]. Although somite segmentation is instructed by a molecular segmentation clock, the period of segmentation differs from that of the clock, yet the reason for this discrepancy remains unknown. By combining live imaging of clock dynamics with time-controlled perturbation experiments, we uncover here that the timing of segmentation is regulated by a somite-size-dependent mechanism modulated by cytoskeletal activities (Fig. 1). We further show that activities of myosin-II, Arp2/3, Rho-kinase, integrin-linked kinase and N-cadherin tune the timing of somite segmentation, independent of the segmentation clock (Fig. 1). This size-dependent timing of MET of somites is akin to size-dependent pacing of phase transitions in living and non-living matters. We anticipate future studies will investigate size-dependent control of patterning in other developing tissues and engineer methods to control timing in organoid systems.

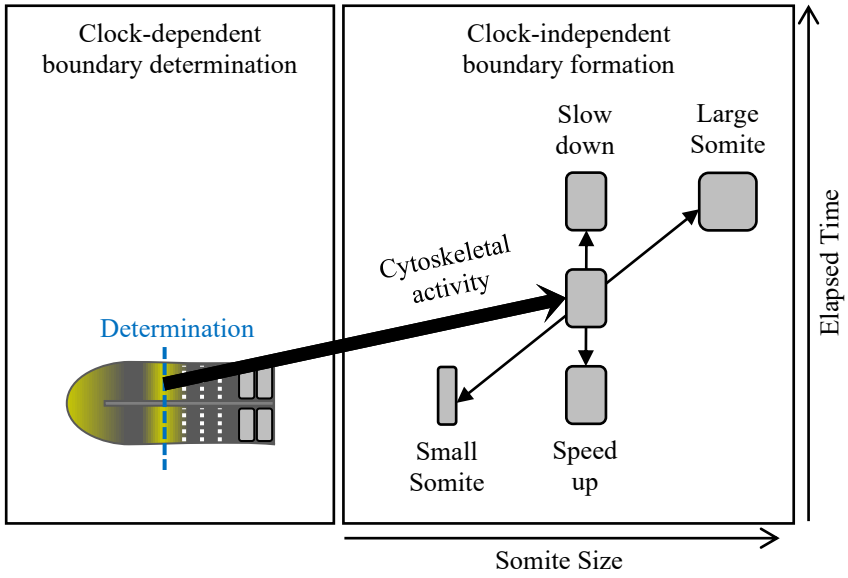

Figure 1: The time elapses between boundary determination and formation is independent of the clock period but dependent on the somite length and cytoskeletal activity.

References:

[1] Miao, Y. & Pourquie, O. Cellular and molecular control of vertebrate somitogenesis. *Nat Rev Mol Cell Biol* **25**, 517-533 (2024).
[2] McDaniel, C., Simsek, M. F., Chandel, A. S. & Ozbudak, E. M. Spatiotemporal control of pattern formation during somitogenesis. *Sci Adv* **10**, eadk8937 (2024).

[1] Department of Cell and Developmental Biology, Northwestern University Feinberg School of Medicine, Chicago, IL 60611, USA

Topological Data Analysis of Zebrafish Skin Patterns: A Sweeping Filtration Approach

Nour Khoudari* John Nardini† Alexandria Volkening*

Abstract

We are interested in investigating skin pattern formation in zebrafish, which exhibit distinctive black and gold pigment patterns arising from interactions between different cell types. We employ a topological data analysis (TDA) approach based on sweeping filtration of binary images of zebrafish skin patterns. Sweeping filtration is a technique in persistent homology that, unlike Vietoris-rips, is rarely applied to biological systems but is extremely useful to explore emergent behaviors and provide new insights into multi-agent biological systems. In some cases, zebrafish skin patterns are disrupted. To analyze and quantify these variations, we use the TDA framework described above, which allows us to extract meaningful biological measurements of stripe and break widths, in addition to the statistics of different types of broken/unbroken patterns.

Background

Wild-type zebrafish are known for their alternating black stripes and golden interstripes skin patterns that develop over months through the interaction of different pigment cells [3]. Figure 1 shows an example of a zebrafish skin pattern and the quantities of interest that could be measured and studied using *topological data analysis*. TDA is a field of computational mathematics that consists of algorithmic methodologies to identify structures in noisy high-dimensional datasets [1, 2]. Examples of TDA approaches are Vietoris-rips (commonly used in biological applications) and sweeping filtrations (less commonly used). Sweeping filtration consists of sliding a line across an image in a fixed direction, where only the data to the left of the line are included in each step, and the number of connected components and loops is measured.

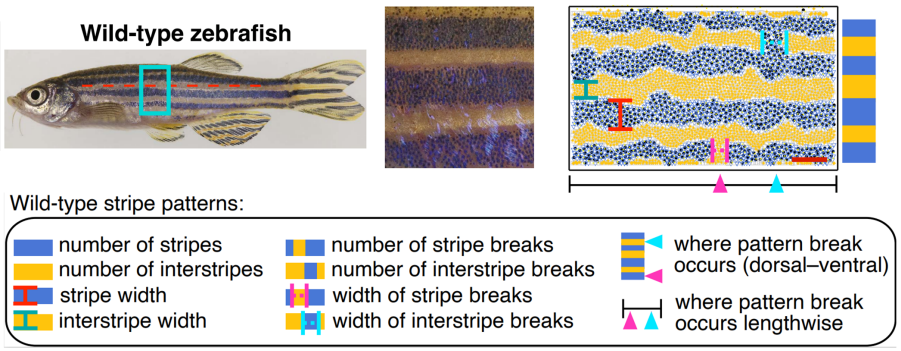

Figure 1: [From left to right] Picture of a wild-type zebrafish with a corresponding zoom into its striped skin pattern and a corresponding point cloud data showing the quantities of interest to be measured.

References

[1] Topaz CM, Ziegelmeier L, Halverson T. *Topological Data Analysis of Biological Aggregation Models*. PLoS ONE 10(5), 2015.

[2] Nardini J et al. *Topological data analysis distinguishes parameter regimes in the Anderson-Chaplain model of angiogenesis*. PLoS Computational Biology 17(6), 2021.

[3] Volkening A, Sandstede B. *Modelling stripe formation in zebrafish: an agent-based approach*. J R Soc Interface, 12(112), 2015.

*Purdue University

†The College of New Jersey

Quantifying the Limits of Electrophysiological Single-Cell Recordings for Estimating Photoreceptor Kinetics in Visual Transduction by Bayesian Inference

Colin Klaus[1], Giovanni Caruso[2], Clint Makino[3], Vsevolod Gurevich[4], Heidi Hamm[5]

Abstract

Far less is generally known about cone photoreceptors' biochemistry kinetics than rod photoreceptors' due to experimental challenges in purifying cone proteins. Single-cell electrophysiology is a critical tool for overcoming this gap, yet as increasingly realistic transduction networks are used to model the vision cascade, scientists become increasingly ambitious in what they hope to learn from electrophysiology. Here we use Bayesian inference, Hamiltonian MCMC, and parallel tempering to quantify the limits of what is learnable from single-cell recordings.

1. Background

Rod and cone photoreceptors are the sensory cells responsible for converting light stimulus into the eventual membrane hyperpolarization and change in neurotransmitter release that the brain interprets as vision information. Rod photoreceptors are specialized for dark adapted conditions while cone photoreceptors are specialized for bright light conditions. Historically, proteins present in rod photoreceptors have been significantly easier to isolate and purify than their cone counterparts. As a consequence, it remains generally true that far less is known from protein purification concerning the biochemistry kinetics of cone proteins compared to rod. Electrophysiological suction electrode recordings of light-induced single-cell responses have therefore been an essential tool in analyzing cone photoreceptors as well as an important tool for analyzing the rod. The signaling networks that underlie visual transduction, while still continually refined, have been reasonably understood for several decades; however, reliably estimating kinetics parameters for realistic signaling networks (~40+ parameters) from electrophysiology recordings is a substantial challenge. The uncertainty in cone parameters is vast, spanning orders of magnitude in some cases, high-dimensional, and plausibly suffers from a lack of parameter identifiability. Notwithstanding, single-cell electrophysiology recordings remain crucial for vision scientists to interrogate the systems biology of photoreceptor cells.

2. Novelty

In this work, we quantify the limits of what may be learned from suction electrode recordings of photoreceptors using a Bayesian inference approach. For the model likelihood we use a Gaussian process whose mean is the solution predicted by the reaction network conditioned on model parameters, while model priors are suggested by the vision literature. We combine Hamiltonian Markov chain Monte Carlo with parallel tempering (*ie* replica exchange) to robustly sample this nonconvex and potentially multimodal posterior energy landscape over parameter space. To the authors' knowledge, this is the first time such an analysis has been performed for visual transduction. We find that parameter identifiability, as reported by their 1d marginal posteriors, falls on a spectrum. Some parameters, such as arrestin binding rates, are tightly constrained by the electrophysiology data while other parameters, such as concentrations of G-protein and effector phosphodiesterase, are hardly constrained at all. Such findings also indicate which parameters should take priority for future experimental measurements. Additionally, we report synthetic, *in silico* trials that quantify parameter identifiability as a function of the number of simultaneous electrophysiology recordings used to estimate parameters. These findings indicate a strong

[1] University of Chicago

[2] Italian National Research Council

[3] Boston University

[4] Vanderbilt University

[5] Vanderbilt University

information gain in using five recordings as opposed to one, but a lesser gain in information using ten recordings compared to five. This trend suggests that what is learnable from single-cell recordings may saturate beyond a certain number of responses.

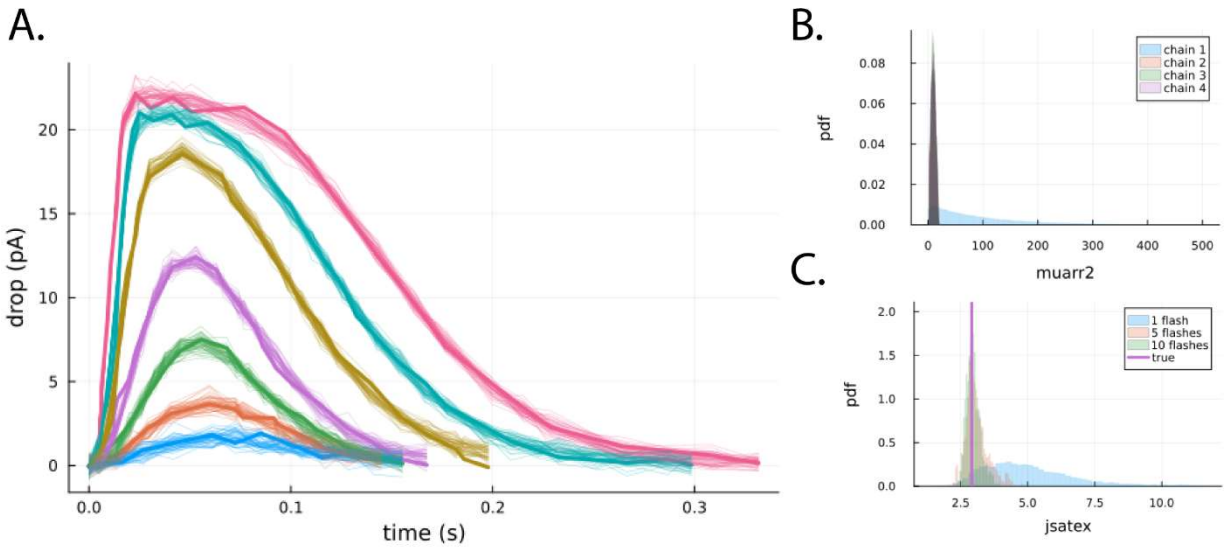

Figure 1: Retrodicted experimental single-cell recordings (flash responses) with selected MCMC posteriors. A. Bayesian posteriors were conditioned on the flash responses of (1). Experimental data is shown as thicker solid lines, while 50 randomly selected posterior predictions are shown as thin traces. Note: the model uses one biochemistry parameter set to generate all seven responses across their different light intensities. B. Posterior distributions (chains 2-4) for an arrestin binding rate compared to its prior distribution (chain 1). C. Synthetic trials where the model with a known parameter set generated 1, 5, and 10 single-cell recordings. Bayesian inference was then run on the sets of recordings and posterior distributions were compared as a function of the number of responses (*ie* flashes) used to estimate them.

References:

1. Chen NS, Ingram NT, Frederiksen R, Sampath AP, Chen J, Fain GL. Diminished Cone Sensitivity in cpfl3 Mice Is Caused by Defective Transducin Signaling. Invest Ophthalmol Vis Sci. 2020;61(4):26.

An Efficient Multilayer Spiking Network as a Model of Ascending Pathways

Veronika Koren[1], Alan J. Emanuel[2], Stefano Panzeri[1]

1 Institute for Neural Information Processing, University Medical Center Hamburg-Eppendorf (UKE), 20251 Hamburg, Germany **2** Department of Cell Biology, Emory University School of Medicine, Atlanta, GA, 30322, USA

Abstract A large part of mammalian brains is dedicated to sensory processing. Sensory receptors extract distinct but partly correlated features of the environment that vary at different timescales [1], and transmit them through a succession of recurrently connected subcortical and cortical areas. A general theory on how sensory pathways efficiently encode, propagate, and transform sensory information across sensory pathways is still missing. To understand how biophysically realistic neural networks might support these fundamental brain functions, we developed an analytical framework based on the principle of efficient coding [2]-[4]. Each brain area was conceptualized as a neural processing layer (hereafter, layer), and we assumed that the objective of each layer is to efficiently encode and transform multiple time-dependent stimulus features by optimally trading off the objectives of accurate information encoding and minimizing metabolic cost [5]. Further, we assumed that the feedforward input to the next layer is a linear combination of multiple population-level readouts from the previous layer. From these assumptions, we analytically derived a mechanistic model of neural dynamics. Our optimal solution was a set of spiking networks with generalized leaky integrate-and-fire (LIF) neurons endowed with spike-triggered adaptation. Feedforward and recurrent synaptic connections were structured with like-to-like connectivity patterns. Recurrent connections realized efficient coding through lateral inhibition, while the feedforward connectivity supported reliable transmission of population signals across layers. The model accurately implements mixing of sensory signals with positive (aligning) or negative (contrasting) interaction across stimulus features. Our framework is the first extension of efficient coding to multiple layers and provides groundwork for understanding neural computations for hierarchical sensory processing in biological brains.

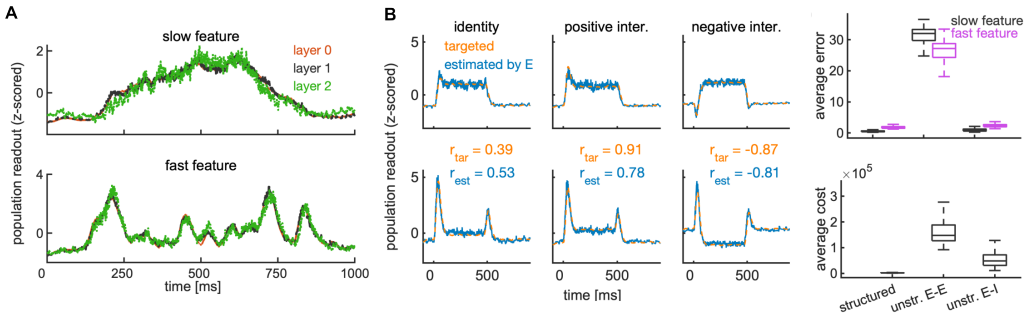

Figure 1. **A)** Z-scored population readout across layers in response to an Ornstein-Uhlenbeck stimulus in a single trial, showing the representation of the slow (top) and fast stimulus feature (bottom) in a network propagating identical signals. The model precisely encodes and transmits fluctuations of the slow and fast feature across layers. **B)** Targeted (orange) and readout (blue) population signals in the final layer in response to a step stimulus. We show the realization of three different computations on stimulus features, i.e., identity (left), aligning computation (middle), and contrast computation (right). r_{tar} (r_{est}) mark the Pearson correlation coefficient across the two targets and the two readouts, respectively. **C)** Trial- and time-averaged encoding error (top) and metabolic cost (bottom) in the final layer ($n = 2$), in networks with efficiently structured (left) or partially unstructured (middle and right) feedforward connectivity. Distributions are across 200 trials. Unstructured feedforward connectivity decreases model efficiency by increasing the metabolic cost and/or the encoding error.

Sensory neurons. We built our model on the example of the ascending somatosensory pathway in mammals, in which multiple types of sensory receptors in the non-hairy skin respond to different features ($s_m^{(0)}$) of the tactile stimulus [1]. We posed that the activity of each sensory neuron i of type m in layer ($n = 0$) minimizes an efficiency objective that evaluates the instantaneous encoding error and the metabolic cost of neural activity:

$$\mathrm{E}_{mi}^{(0)}(t) = \left(x_m^{(0)}(t) - \hat{x}_{mi}^{(0)}(t)\right)^2 + \beta_m^{(0)} \left(r_{mi}^{(0)}(t)\right)^2, \qquad m = 1, \ldots, M,\ M \geq 2 \tag{1}$$

with a dynamical readout $\hat{x}_{mi}^{(0)} = \omega_{mi}^{(0)} z_{mi}^{(0)},\ \omega_{mi}^{(0)} > 0$. Variables $z_{mi}^{(0)}$ and $r_{mi}^{(0)}$ are low-pass filtered spike trains of neuron i with time constants $\tau_m^{(0)}$ and $\tau_r^{(0)}$, respectively, and $\beta_m^{(0)} \geq 0$ is the weighting between the encoding error and the metabolic cost. By assuming that the neuron fires a spike only if doing so momentarily decreases its loss function and adding noise for biological plausibility, we analytically derived a network of generalized LIF neurons with leak current, feedforward current, spike-triggered adaptation and noise:

$$\frac{d}{dt}V_{mi}^{(0)} = -\frac{1}{\tau_m^{(0)}}V_{mi}^{(0)} + \frac{1}{C_m}\left(I_{mi}^{\mathrm{FF},(0)}(t) + I_{mi}^{\mathrm{ad},(0)}(t)\right) + \sigma_m^{(0)}\eta_{mi}^{(0)}(t), \qquad \tau_r^{(0)} > \tau_m^{(0)}. \tag{2}$$

with C_m the capacitance of the neural membrane and with fire-and-reset rule: $V_{mi}^{(0)}(t^-) \geq \vartheta_{mi}^{(0)}(t^-) \rightarrow V_{mi}^{(0)}(t^+) = V_{mi}^{\mathrm{reset}}$.

Recurrent layers. In the subsequent processing stages, the signals generated by different types of sensory neurons converge onto the same neurons [1],[6]. To account for convergence of sensory signals, we attributed to each neuron i in layers $n > 1$ a vector of M decoding weights, $\boldsymbol{\omega}_{yi}^{(n)} \in \mathbb{R}^{Mx1}$, with $y \in \{E, I\}$ the index for E and I neuron type. We defined the population readout as $\hat{\boldsymbol{x}}_y^{(n)}(t) = \Omega_y^{(n)} \boldsymbol{z}_y^{(n)}(t)$, with $\boldsymbol{z}_y^{(n)} = [z_{yi}^{(n)}]_{i=1,\ldots,N_y^{(n)}}$ a vector of synaptic (low-pass) filters of spike trains and $\Omega_y^{(n)} \in \mathbb{R}^{MxN_y^{(n)}}$ a matrix composed of decoding vectors of $N_y^{(n)}$ neurons. We posed that the objective of the population $y \in \{E, I\}$ is to minimize the following loss function:

$$\mathrm{E}_y^{(n)}(t) = \left\|\boldsymbol{x}^{(n)}(t) - \hat{\boldsymbol{x}}_y^{(n)}(t)\right\|^2 + \beta_y^{(n)} \sum_{i=1}^{N_y^{(n)}} (r_{yi}^{(n)}(t))^2, \qquad y \in \{E, I\},\ \beta_y^{(n)} > 0, \tag{3}$$

with $r_{yi}^{(n)}$ a low-pass filter of the spike train of neuron i of type y. To account for possible mixing of sensory features, we assumed that the target signal $\boldsymbol{x}^{(n)}(t)$ depends on a linear transformation of the population readout from the previous (presynaptic) layer $(n-1)$:

$$\frac{d}{dt}\boldsymbol{x}^{(n)}(t) = -\frac{1}{\tau_x^{(n)}}\boldsymbol{x}^{(n)}(t) + A^{(n)}\hat{\boldsymbol{x}}_E^{(n-1)}(t), \tag{4}$$

with $A^{(n)}$ an M-by-M matrix that determines the type of transformation. Assuming the same condition for emitting a spike as in sensory neurons, we analytically derived a recurrently connected E-I spiking network with generalized LIF neurons. The dynamics of the membrane potential in neuron i of type $y \in \{E, I\}$ depend on a leak current, feedforward and recurrent synaptic currents, spike-triggered adaptation and additive noise:

$$\frac{d}{dt}V_{yi}^{(n)} = -\frac{1}{\tau_y^{(n)}}V_{yi}^{(n)} + \frac{1}{C_m}\left(I_{yi}^{\mathrm{FF},(n)}(t) + I_{yi}^{\mathrm{REC},(n)}(t) + I_{yi}^{\mathrm{ad},(n)}(t)\right) + \sigma_y^{(n)}\eta_{yi}^{(n)}(t), \tag{5}$$

with a fire-and-reset rule as in eq.2. We tested the model on a minimal example with layers $n = 0, 1, 2$ and with $M = 2$ sensory neuron types that capture a signal proportional to the stimulus (slow feature) and to the absolute change in the stimulus (fast feature). Free parameters were constrained by simulating the model and searching for a parameter configuration that minimized the average loss in each layer (eqs. 1 and 3). The model efficiently encoded, transmitted (Fig. 1A), and transformed (Fig. 1B) a pair of correlated fast and slow stimulus features and required structured feedforward connectivity (Fig. 1C). Compared to the most similar previous work [7], our contribution innovates by modeling sensory receptor neurons, extending the model to multiple layers, formulating mechanistic feedforward currents, and introducing realistic timescales for all synapses.

References [1] Abraira, VE and Ginty DD (2013), *Neuron* 79(4), pp. 618-639 [2] Barlow, HB (1961), *Sensory Communication* 1, pp. 217-233 [3] Olshausen, BA and Field, DJ (1997), *Vision Research* 37(23), pp. 3311-3325 [4] Boerlin, M, Machens, CK and Denève, S (2013), *PLOS Comp. Bio.* 9(11) [5] Niven, JE (2016), *Curr. Opinin. Neurobiol.* 41, pp. 129–135 [6] Chirila AM, Rankin G, Tseng SY, Emanuel AJ, Chavez-Martinez CL, Zhang D, Harvey CD, Ginty DD. (2022), *Cell* 185(24), pp. 4541-59 [7] Koren, V and Panzeri, S (2022), *NeurIPS* 35, pp. 20607-20620

A mathematical model of viral rebound after treatment interruption in HIV infected individuals

Jasmine A. F. Kreig, Ruian Ke, Ruy M. Riberio[1]

Abstract

Given current antiretroviral therapies (ARTs), Human Immunodeficiency Virus (HIV) infections can very effectively be controlled, and the virus kept below detectable levels [1]. However, treatment must be life-long because of the existence of the HIV reservoir: a population of cells latently infected by HIV. In most individuals, stopping ART will cause viral rebound [1]. Interestingly, the time to viral rebound is variable from weeks (in most individuals) to years. Currently, the factors that determine time to viral rebound after treatment interruption is not understood by medical and scientific communities. A previous study showed that one such factor is the size of the reservoir [2]; however, recent clinical data suggest the time of ART initiation [3], the composition of the reservoir (i.e. the viral genotypes), and the level of host immune response also play important roles [4,5]. We have developed a simplified model that simulates the seeding of the latent reservoir at the time of infection, the use of ART to control the viral load, and viral rebound that occurs after treatment interruption. Using this model, we explore different factors - such as time of ART initiation, viral fitness, and immune response – that could be associated with extending the time to viral rebound and aid towards the goal of stopping viral rebound in individuals living with HIV.

References:

[1] Conway JM, Perelson AS, Li JZ *PLoS Comput Biol* **15**: e1007229, 2019.
[2] Hill AL, et al *Proc Natl acad Sci USA* **111**: 13475, 2014.
[3] Gunst JD, et al *Nature Medicine* **28**: 2424, 2022.
[4] Colby DJ, et al *Nature Medicine* **24**: 923, 2018.
[5] Cody JW, et al *PLoS Comput Biol* **17**: e1009204, 2021.

[1] T6 Theoretical Biology & Biophysics, Los Alamos National Laboratory, USA

Beyond Convex Codes: Neural Rings in Boolean Matrix Factorization

Juliann Geraci* Alexander B. Kunin† Alexandra Seceleanu*

Identifying the latent building blocks of complex systems is a challenging problem in biology. For example, given a feed-forward neural network with a hidden layer, we may try to try to infer its structure from measurements of input-output pairs. Given a measure of which output neurons activate when each input neuron i is stimulated, we want to determine the number of hidden neurons and their connections. Thus we arrive the Boolean Matrix Factorization problem: Given an $m \times n$ binary matrix A, find $m \times r$ and $r \times n$ binary matrices V, H such that $A = VH$ under Boolean arithmetic (i.e. where $1+1=1$). In our example, A represents the observed input-output pairs, and V, H are adjacency matrices of bipartite graphs that share a part (the hidden layer of r neurons); $A_{ij} = 1$ iff there is at least one feed-forward path from node i in V to node j in H. The boolean rank of A is the minimum r for which such a factorization exists. We present a novel algebraic formulation of this problem, some partial progress, and some related results that may be of independent interest.

Given a matrix A, consider the set of its rows as an affine variety over $\mathbb{F}_2$; we call this a *combinatorial code*. The coordinate ring of this variety, R_A, is the *neural ring* [1] of A. This ring was originally introduced to study the intrinsic properties of neural codes (taking cues from hippocampal place cells and how they encode relationships among their place fields), ultimately leading to the study of convex codes (as in [2]). Our present motivation is twofold: first, we aim to answer the practical problem of computing boolean matrix factorizations. Second, we aim to further develop the algebraic and combinatorial theory of these codes and rings in their own right.

We first show that the boolean rank of A is the minimum number of monomial generators of R_A. This follows from the observation that, under certain assumptions, the coordinates of points in V are products of coordinates of points in A. Maps of this sort define the morphisms in a category of codes introduced in [3]. Further, they induce a graded partial order on (equivalence classes of) codes [4], where the rank function is always at least the cardinality of the code. We introduce the *defect* of a code, its rank minus its cardinality, and show that when A is a cone (i.e. it consists of all possible products of H with row vectors in $\{0,1\}^r$), then V must be defect-free in any factorization $A = VH$. We next show that morphisms of codes and Boolean matrix multiplication are adjoints in a Galois connection between $\{0,1\}^n$ and $\{0,1\}^r$. Using this connection, we overcome one of the difficulties of BMF, the fact that is is generally non-unique, using the closure operator of the connection to define a canonical choice of V for a given H.

Finally, we consider the generators of the vanishing ideal $I_A \subseteq \mathbb{F}_2[x_1, \ldots, x_n]$, the set of polynomials which vanish on all rows of A. When A is a cone, each generator can be written in the form $\prod_{i\in\sigma} x_i \prod_{j\in\tau}(1-x_j)$ for some subsets $\sigma, \tau \subseteq [n]$ with $|\sigma| \leq 1$. For an arbitrary code, the ideal may have some generators of this form and some not. Building on recent results [5] we are able to show that given any code, by simply discarding the generators not of this form, we recover the vanishing ideal of the cone of that code. In our context, we speculate this may provide an avenue towards new and efficient algorithms for approximate Boolean matrix factorization, but this result should be of general interest to anyone who studies or uses pseudomonomial ideals [6].

References

[1] Curto, C., Itskov, V., Veliz-Cuba, A. & Youngs, N. The neural ring: an algebraic tool for analyzing the intrinsic structure of neural codes. *Bull. Math. Biol.*. **75**, 1571-1611 (2013)

[2] Curto, C., Gross, E., Jeffries, J., Morrison, K., Omar, M., Rosen, Z., Shiu, A. & Youngs, N. What makes a neural code convex?. *SIAM J. Appl. Algebra Geom.*. **1**, 222-238 (2017)

[3] Jeffs, R. A. Morphisms of Neural Codes. *SIAM Journal On Applied Algebra And Geometry*. **4**, 99-122 (2020)

[4] Jeffs, R. Sunflowers of convex open sets. *Advances In Applied Mathematics*. **111** pp. 101935 (2019)

[5] Geller, H. & R.G., R. Canonical Forms of Neural Ideals. *La Matematica*. **3**, 721-752 (2024)

[6] Macauley, M., Robeva, R., Algebraic models, inverse problems, and pseudomonomials from biology. *Letters in Biomathematics*, **7**(1), 81-104 (2020)

*University of Nebraska – Lincoln, Lincoln, NE, USA

†Creighton University, Omaha, NE, USA

A mathematical and digital approach to assess real-world dynamics of circadian rhythms, sleep, and psychiatric disorder risks from wearables

Minki P. Lee

Department of Mathematics, University of Michigan, Ann Arbor, Michigan, United States

ABSTRACT

The circadian clock is an intrinsic timekeeping system that orchestrates daily physiological and behavioral rhythms, including the sleep-wake cycle. Disruptions in the alignment between circadian rhythms and sleep have been increasingly recognized as key contributors to the development of psychiatric disorders such as depression, making this interaction a particularly interesting target for investigation. Accurate tracking of both circadian phase and sleep is therefore critical for understanding their complex dynamics and translational relevance, especially in real-world settings. Wearable devices offer a promising, non-invasive means of monitoring physiological signals modulated by the circadian-sleep system. Yet, the high dimensionality and nonlinear nature of wearable data have posed significant challenges for traditional analytical frameworks. In this presentation, I will introduce a novel computational approach based on the level set Kalman filter, a state-space estimation technique that integrates wearable-derived physiological data with a Bayesian inference algorithm designed for scalability and efficiency, to efficiently analyze the real-world dynamics of the circadian-sleep system. We applied this framework to over 200,000 days of longitudinal data from more than 3,000 individuals, achieving significantly enhanced circadian phase estimation compared to existing state-of-the-art methods. Moreover, the inferred circadian and sleep metrics are used to derive digital biomarkers with the potential to predict individual psychiatric risk, including mood disorders, depression, anxiety, and suicidal ideation. Together, these efforts establish a powerful platform for decoding the real-world dynamics of circadian rhythms and sleep—and for leveraging this information in the pursuit of preventive psychiatry.

A dynamical systems model for the total fission rate in Drp1-dependent mitochondrial fission*

Anna K. Leinheiser[†,§] Colleen C. Mitchell[†] Ethan Rooke[†] Stefan Strack[‡]
Chad E. Grueter[§]

Abstract

Mitochondrial hyperfission in response to cellular insult is associated with reduced energy production and programmed cell death. Thus, there is a critical need to understand the molecular mechanisms coordinating and regulating the complex process of mitochondrial fission. We develop a nonlinear dynamical systems model of dynamin related protein one (Drp1)-dependent mitochondrial fission and use it to identify parameters which can regulate the total fission rate (TFR) as a function of time. The TFR defined from a nondimensionalization of the model undergoes a Hopf bifurcation with bifurcation parameter $\mu = \frac{k_+ \mathcal{M}}{k_-}$ where $\mathcal{M}$ is the total concentration of mitochondrial fission factor (Mff) and k_+ and k_- are the association and dissociation rate constants between oligomers on the outer mitochondrial membrane. The variable μ can be thought of as the maximum build rate over the disassembling rate of oligomers. Though the nondimensionalization of the system results in four dimensionless parameters, we found the TFR and the cumulative total fission (TF) depend strongly on only one, μ. Interestingly, the cumulative TF does not monotonically increase as μ increases. Instead it increases with μ to a certain point and then begins to decrease as μ continues to increase. This non-monotone dependence on μ suggests interventions targeting k_+, k_-, or $\mathcal{M}$ may have a non-intuitive impact on the fission mechanism. Thus understanding the impact of regulatory parameters, such as μ, may assist future therapeutic target selection.

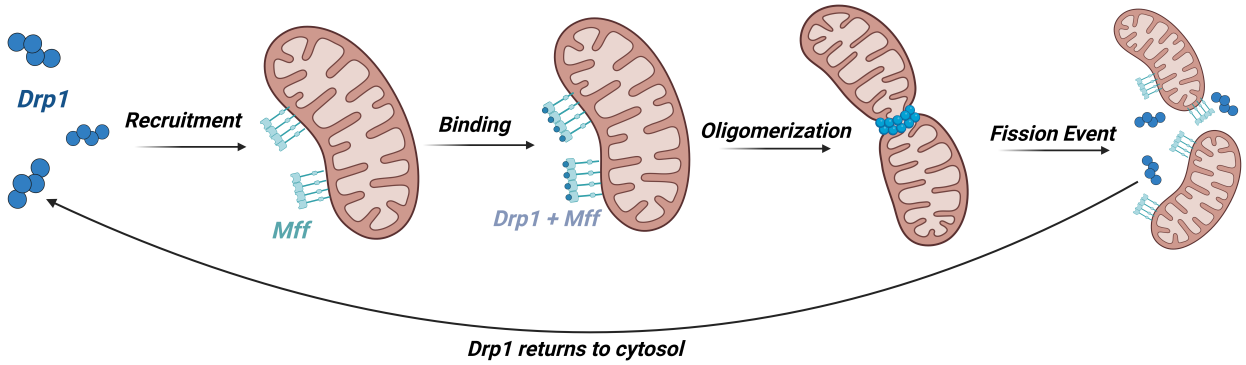

Figure 1: The mechanism our model approximates begins with the recruitment of Drp1 tetramers from the cytosol to the outer mitochondrial membrane where they bind to Mff. These Drp1-Mff complexes build oligomers which constrict around the outer membrane and lead to a fission event. After a fission event, Drp1 tetramers and Mff proteins return to their respective unbound pools in the cytosol and on the outer mitochondrial membrane. Created with BioRender.com

*The full version of the paper can be accessed at https://journals.plos.org/ploscompbiol/article?id=10.1371/journal.pcbi.1012596

[†]Department of Mathematics, University of Iowa, Iowa City, Iowa, USA
[‡]Department of Neuroscience and Pharmacology, University of Iowa, Iowa City, Iowa, USA
[§]Department of Internal Medicine, Division of Cardiovascular Medicine, Francois M. Abboud Cardiovascular Research Center, Fraternal Order of Eagles Diabetes Research Center, University of Iowa, Iowa City, Iowa, USA

Attractor Degeneracy in Threshold-Linear Networks

Zelong Li*

Abstract

Degenerate mechanisms – different underlying cellular and molecular properties or neural circuit configurations may generate highly similar functional behaviors – has been observed and studied in the pyloric network within the stomatogastric nervous system (STNS) of crustaceans ([1], [2], [3] and etc.). Despite substantial variability in the biophysical properties of individual neurons and synaptic connections, the rhythmic oscillatory dynamics generated by the network exhibit remarkable stability. Threshold-Linear Networks (TLNs) provide a mathematical framework for understanding the suprising degeneracy phenomena emerged among their dynamical attractors. In this presentation, we will introduce the well-established TLN model repertorie ([4], [5], [6] and etc.) and describe a simple parameter domain within which our desired robust dynamics occurs. Furthermore, we will also demonstrate how this domain can be effectively expanded using the training of recurrent neural network, highlighting the potential for machine learning approaches to explore degeneracy in neural circuit. This is a joint work with Juliana Londoño Álvarez† and Carina Curto‡.

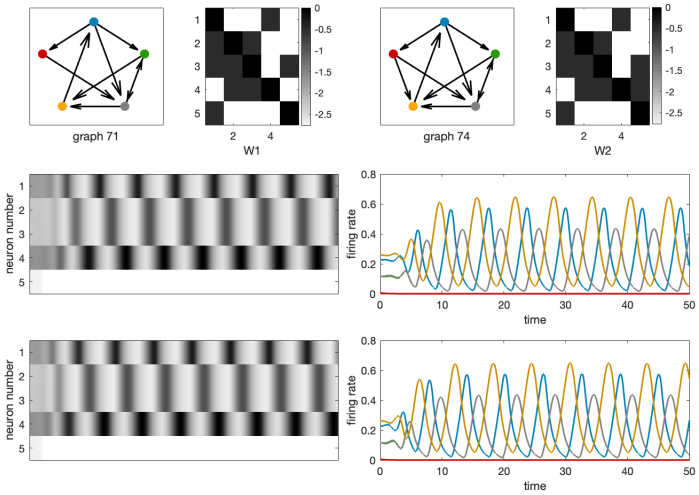

Figure 1: Two (combinatorial) TLNs exhibit the same attractors

References

[1] Prinz, A. A., Bucher, D., & Marder, E. (2004). Similar network activity from disparate circuit parameters. Nature Neuroscience, 7(12), 1345–1352.

[2] Marder, E., & Taylor, A. L. (2011). Multiple models to capture the variability in biological neurons and networks. Nature Neuroscience, 14(2), 133–138.

[3] Ratliff, J., Franci, A., Marder, E., & O'Leary, T. (2021). Neuronal oscillator robustness to multiple global perturbations. Biophysical Journal, 120(8), 1454–1468.

[4] Parmelee, C., Moore, S., Morrison, K., & Curto, C. (2022). Core motifs predict dynamic attractors in combinatorial threshold-linear networks. PLoS ONE, 17(2), e0264456.

[5] Curto, C., & Morrison, K. (2023). Graph rules for recurrent neural network dynamics. Notices of the American Mathematical Society, 70(2), 182–192. Extended version: arXiv:2301.12638.

[6] Morrison, K., Degeratu, A., Itskov, V., & Curto, C. (2024). Diversity of emergent dynamics in competitive threshold-linear networks. SIAM Journal on Applied Dynamical Systems, 23(1), 69–101.

*Department of Mathematics, Penn State University
†Department of Applied Mathematics, Brown University
‡Department of Applied Mathematics and Carney Institute of Brain Science, Brown University

Bayesian parameter inference of complex pattern formation in agent-based models using topological data analysis

Yue Liu* Alexandria Volkening†

Abstract

Collective behaviour of individual agents is present across a variety of biological systems, such as in the case of migrating cells during development, the formation of animal skin patterns, and bird flocking. Agent-based models, which describe the microscopic interactions between individual, autonomous parts of a system, provide a natural and flexible framework for capturing such phenomena. In order to ensure that the mechanistic insights and predictions offered by these models are biologically sound, it is important to be able to infer the values of model parameters from data, and to assess whether the parameters are practically identifiable. In this talk, we study a complex agent-based model for pigmentation patterns on zebrafish skin arising from cell–cell interactions.

Such quantitative study of agent-based models poses two significant challenges. First, the complexity and stochastic nature of these models, as well as the computational cost of simulating them, mean that many well-known methods of inference are computationally infeasible. Second, it is difficult to mathematically formulate a metric between patterns that respects the qualitative features relevant to biology.

By developing an analysis pipeline that combines approximate approximate Bayesian computation (AABC) and topological data analysis (TDA), we are able to address both challenges in a computationally efficient manner. The pipeline provides accurate estimates of the parameter values, and allows for the determination of parameter identifiability through the construction of an approximate posterior distribution. We also discuss how parameter identifiability depends on various choices within the pipeline, such as methods for summarising and weighting topological information, and the selection and combination of features from multiple sources. This approach can be readily adapted to analyse a wide range of agent-based models for spatio-temporal phenomena.

*Purdue University, West Lafayette, Indiana (presenting author)

†Purdue University, West Lafayette, Indiana

TFSage: Compendium-Powered Search Engine for Transcription Factor Binding and Gene Regulatory Network Inference

Brandon Lukas[1] Yang Dai[1,2]

Abstract

Background: Accurate identification of transcription factor (TF) binding is a foundational step in gene regulatory network (GRN) inference. However, most existing GRN inference methods rely on motif scanning, which suffers from major limitations, including high false positive rates, incomplete or inaccurate motif libraries, and an inability to detect non-canonical binding events such as indirect binding through protein complexes [1]. In contrast, TF ChIP-seq experiments provide experimental evidence of TF binding and are considered one of the most reliable sources of binding information [2]. Large-scale public databases such as the ENCODE project [3] and ChIP-Atlas [4] offer compendia of thousands of TF ChIP-seq, ATAC-seq, and H3K27ac ChIP-seq experiments across diverse cell types and conditions. However, these resources are underutilized for context-specific TF binding prediction due to challenges in querying them effectively.

Methods: We present TFSage, a compendium-powered, data-driven search engine for predicting TF binding profiles and constructing GRNs from epigenomic datasets. TFSage enables automated search of contextually relevant TF ChIP-seq experiments and generation of context-specific TF binding profiles (Figure 1). First, our method represents each experiment as a regulatory potential (RP) vector that summarizes presence of called peaks near transcription start sites. These RP vectors are then embedded into a shared low-dimensional space using principal component analysis (PCA) followed by fast mutual nearest neighbor (MNN) correction. This embedding allows a query experiment – such as ATAC-seq or H3K27ac ChIP-seq– to rank the most contextually relevant TF ChIP-seq experiments from the compendium without using explicit labels. For any TF, TFSage subsequently aggregates the top ranked TF ChIP-seq experiments and computes interpretable binding scores across the entire genome that reflect the balance of support for TF binding versus non-binding at each locus. These scores can be thresholded to call putative TF binding peaks, which a RP model can use to assemble a context-specific, RP-weighted GRN.

Results: We evaluated the search and generation capabilities of TFSage using the ENCODE project. Assessing the quality of 1,353 ranked lists using mean reciprocal rank (MRR), mean average precision (MAP), and normalized discounted cumulative gain (NDCG), we determined the optimal default settings for TFSage to sort TF ChIP-seq experiments based on expected relevance to the query ATAC-seq or H3K27ac ChIP-seq experiment. We then generated 7,134 TF binding prediction profiles with TFSage and evaluated the predictions against held-out, ground-truth TF ChIP-seq called peaks using auROC, auPRC, and precision at various recalls. Additionally, we benchmarked TFSage-based TF binding predictions against four motif scanning methods (CisBP v.2, HOCOMOCO v.11, JASPAR2020, and gimmemotifs v.5) and found that TFSage consistently and significantly outperforms all (Figure 2).

Conclusion: TFSage offers a powerful new paradigm for predicting global TF binding sites and subsequent GRN inference from a single ATAC-seq or H3K27ac ChIP-seq experiment by unlocking the value of public epigenomic compendia.

References

[1] Y. Yang and D. Pe’er, "REUNION: transcription factor binding prediction and regulatory association inference from single-cell multi-omics data," *Bioinformatics,* vol. 40, *(Supplement_1),* pp. i567–i575, 2024.
[2] R. Mundade *et al*, "Role of ChIP-seq in the discovery of transcription factor binding sites, differential gene regulation mechanism, epigenetic marks and beyond," *Cell Cycle,* vol. 13, *(18),* pp. 2847–2852, 2014.
[3] N. de Souza, "The ENCODE project," *Nature Methods,* vol. 9, *(11),* pp. 1046, 2012.
[4] S. Oki *et al*, "Ch IP-Atlas: a data-mining suite powered by full integration of public Ch IP-seq data," *EMBO Rep.,* vol. 19, *(12),* pp. e46255, 2018.

[1] Department of Biomedical Engineering
University of Illinois Chicago

[2] Center of Bioinformatics and Quantitative Biology
University of Illinois Chicago

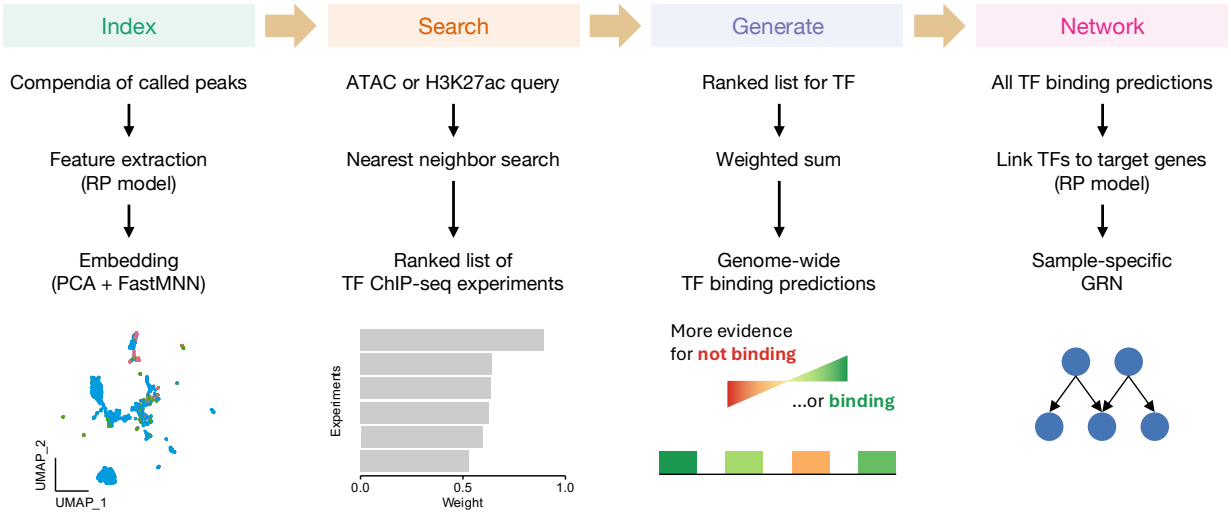

Figure 1. TFSage consists of four main steps: (1) indexing an epigenomic compendium, (2) searching for relevant experiments, (3) generating TF binding predictions, and (4) inferring GRNs.

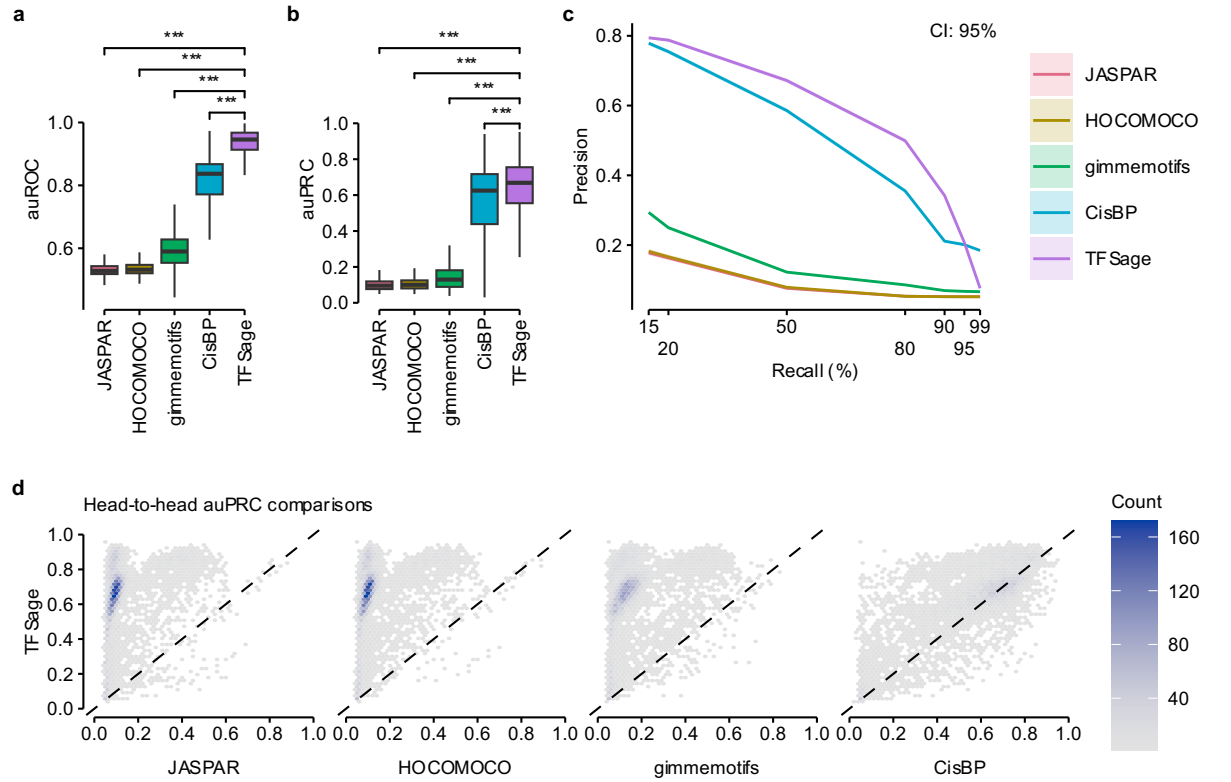

Figure 2. TFSage outperforms traditional motif scanning methods in predicting genome-wide TF binding from ATAC-seq or H3K27ac ChIP-seq called peaks. Performance assessed by **(a)** area under the receiver operator characteristic curve (auROC), **(b)** area under the precision-recall curve (auPRC), and **(c)** precision evaluated under various recall levels. **(d)** Density plots comparing auPRC values of TFSage against multiple motif scanning methods.

Probabilistic Modeling of Antibody Kinetics Post Infection and Vaccination

Rayanne A. Luke*‡ Prajakta Bedekar†‡ Anthony J. Kearsley‡

Abstract

Modeling the deterioration of antibody levels is essential to understanding the time-dependent response to infections or vaccinations. Important questions remain despite significant experimental studies. The influence of the order of events and time elapsed between infection and vaccination on the kinetics of "hybrid immunity" is not well understood. Moreover, disease or vaccination prevalence in the population and time-dependence on a personal scale simultaneously influence the immune response.

A rigorous mathematical characterization may inform public health decision making. Thus, we design a time-inhomogeneous Markov chain model for event-to-event transitions coupled with a probabilistic framework for post-event antibody kinetics. This approach is ideal to model sequences of infections and vaccinations, or personal trajectories in a population, and predict missed events. Further, this framework extends beyond the capability of a susceptible-infected-recovered (SIR) characterization, which models disease transmission but cannot track the distribution of antibody response of a population across time. In contrast, we provide such probabilistic information.

We present ideas from our recent work [1] and a promising extension that allows multiple immune events. To illustrate, we apply our mathematical machinery to longitudinal severe acute respiratory syndrome coronavirus 2 (SARS-CoV-2) data from individuals reporting infection and vaccination events. Our work is an important step towards a comprehensive understanding of antibody kinetics that could lead to an effective way to analyze the protective power of natural immunity or vaccination and provide booster timing recommendations.

References

[1] P. Bedekar, R. A. Luke, A. J. Kearsley, *Prevalence estimation methods for time-dependent antibody kinetics of infected and vaccinated individuals: a Markov chain approach*. Bull Math Biol 87(26), 2025.

*Department of Mathematical Sciences, George Mason University, USA, rluke@gmu.edu

†Department of Applied Mathematics and Statistics, Johns Hopkins University, USA

‡Applied and Computational Mathematics Division, National Institute of Standards and Technology, USA

Modeling Drug Perfusion in Complex Soft Matter Systems

Hailey Lynch[1], Golnaz Asaadi Tehrani[2], Meenal Datta[2], Jonathan K. Whitmer[1]

Abstract

Tuberculosis granulomas and solid tumors exhibit similar transport limitations which often pose barriers to treatment efficacy. This work describes mathematical modeling of drug transport for the development of improved treatment approaches.

The underlying mechanisms in the tumor microenvironment influence behaviors that foster cancer progression through processes such as metastasis. Metastasis accounts for 90% of cancer-related deaths due to the difficulties in treating cancers that spread throughout the body [1]. As shown in Fig. 1, tuberculosis granulomas are morphologically and structurally similar to solid tumors [2]. Due to the remodeling processes that occur during disease progression, the resulting altered microenvironment exhibits abnormal physiological barriers which pose transport limitations that are similar in both tuberculosis granulomas and solid tumors [3]. These transport limitations often result in poor efficacy of treatment strategies such as chemotherapy agents and may lead to chemoresistance [4, 5]. Here we propose to use computational mechanistic modeling approaches to determine the reaction uptakes of various therapeutic agents for drug transport in experimental studies using a reaction-diffusion equation. This will in turn provide a better understanding of the influence of the parametric dependence of material properties within the system for facilitated drug delivery. The modification of this computational model requires the implementation of multiphysics principles to model the drug distribution which will be essential for modeling drug delivery in other systems composed of soft matter such as cancer spheroids in breast tissue.

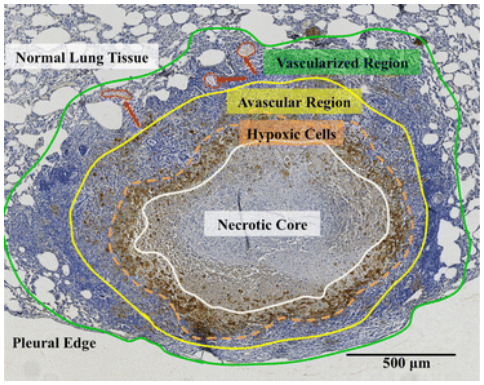

Figure 1: Defined regions in tuberculosis granulomas for modeling objectives [2].

References:

[1] Dillekås, H., Rogers, M. S., & Straume, O. (2019). Are 90% of deaths from cancer caused by metastases?. *Cancer Medicine*, *8*(12), 5574-5576.

[2] Datta, M., Via, L. E., Chen, W., Baish, J. W., Xu, L., Barry, C. E., & Jain, R. K. (2016). Mathematical model of oxygen transport in tuberculosis granulomas. *Annals of Biomedical Engineering*, *44*, 863-872.

[3] Datta, M., Kennedy, M., Siri, S., Via, L. E., Baish, J. W., Xu, L., ... & Jain, R. K. (2024). Mathematical model of oxygen, nutrient, and drug transport in tuberculosis granulomas. *PLoS Computational Biology*, *20*(2), e1011847.

[4] Nikolaou, M., Pavlopoulou, A., Georgakilas, A. G., & Kyrodimos, E. (2018). The challenge of drug resistance in cancer treatment: a current overview. *Clinical & Experimental Metastasis*, *35*, 309-318.

[5] Jain, R. K. (2014). Antiangiogenesis strategies revisited: from starving tumors to alleviating hypoxia. *Cancer Cell*, *26*(5), 605-622.

[1]Department of Chemical and Biomolecular Engineering, University of Notre Dame, Notre Dame IN, 46556
[2]Department of Aerospace and Mechanical Engineering, University of Notre Dame, Notre Dame IN, 46556

Gene regulation of toxicity and iron acquisition in *Vibrio vulnificus*

Kathryn Lynch[1] James P. Keener[1]

Abstract

Vibrio vulnificus is an opportunistic halophilic bacteria with a high mortality rate when compared with other foodborne pathogens. Despite this, the virulence factors of *V. vulnificus* are not yet fully understood. One possible mechanism for virulence is the utilization of heme as a source of iron; as iron is a growth limiting factor, the ability to find a consistent source of iron when inside a human host is essential. Like many other Gram-negative bacteria, *V. vulnificus* can use heme as a source of iron. Key aspects of its heme acquisition system include heme receptor HupA and hemolysin VvhA. Working in tandem, this allows the bacteria to use heme as a consistent source of iron when inside a human host. The ability of this system to respond to environmental pressure is important and offers some insight as to the rapid establishment of infection seen in many clinical cases. As establishment of infection depends on *Vibrio vulnificus*'s ability to rapidly change from a marine to human environment, the ability to switch on the heme-intake system is an important part of establishment of initial infection.

HupA is the heme receptor portion of a TonB heme transporter; its regulation is primarily controlled by divergently transcribed transcription factor HupR. The dynamics of this regulation result in a genetic switch, allowing the bacteria to differentiate between high iron or high heme environments, depending on which source should be used. Bifurcation analysis of this network uncovers a saddle-node bifurcation, which encodes this switch-like behavior into the regulation of the heme transport system and allows different levels of expression for HupA depending on external concentrations of heme and iron. The influences of other parameters in this system are also explored; in particular, promoter leakage is required to enable this bistability, indicating the importance of imperfect regulation in a cell's ability to respond to the environment.

Of course, the vast majority of heme inside a human is stored inside erythrocytes and not readily available for bacterial consumption. To combat this, *V. vu*lnificus excretes a toxin VvhA to lyse erythrocytes, thereby releasing heme into the extracellular environment where the bacteria can use it as a source of iron via the HupA transporter. This toxin is regulated by a complex set of factors including nutrient availability and quorum sensing. Exploring this gene regulatory network via bifurcation analysis reveals a complex bifurcation structure. In particular, the bistability in the system indicates how a bacterium can turn on expression of VvhA in response to iron starvation. The interdependence between toxin production, nutrient availability, and colony growth result in interplay between the bacteria and their environment, allowing for insights into the overall course of infection.

The regulation of both genes allows an individual bacterium to integrate a variety of environmental signals and use this to inform cellular level decisions. This then contributes to establishment and survival of a colony within the host, starting off the rapid course of infection. Individual bacterium make decisions at a genetic level as a result of various types of gene regulation; this process plays out on a population level to inform colony growth. Bistability in the VvhA system also points to the likelihood of a heterogenous bacterial colony, where many bacteria benefit from a smaller number of hemolysin producers, perhaps contributing to rapid colony growth. This offers physiological mechanism for population heterogeneity and some level of feedback between population level growth and individual cell decisions. The interdependence between toxin production, nutrient availability, and colony growth result in interplay between the bacteria and their environment, allowing for insights into the overall course of infection.

[1] University of Utah

An Ensemble Learning Method for Generic Track Annotation in Live Cell Imaging

Woody March-Steinman[1] Elizabeth Jose[2] Chance Parkinson[2] Andrew Paek[1,2,3]

Abstract

Automated tracking of cells can reduce bias and increase throughput from single cell experiments. We develop a method of inferring time of apoptosis using common cell trajectory data, while also determining lineage to understand the impact of cell and circadian cycle on heterogeneous cellular response to stress. We use single time-point features as input into a classifier to predict biological fate classification on a per-frame basis. We show that useful statistics of this classifier are stationary and can be used as input into a Hidden Markov Model for time series correction and subsequent time of event prediction for single cells. We show results on several biological datasets and describe the use of the method across cell types. This method makes use of limited features from live cell tracking time series to be able to efficiently annotate existing datasets without reprocessing whole movies or applying convolutional classification approaches except in narrow temporal and spatial windows to validate or correct time of death predictions for cells. We discuss a minimal feature set to enable the use of this method across a variety of experimental designs (different nuclear markers and cell types) and imaging setups. We provide a software package to facilitate external use.

[1] Program in Applied Mathematics, The University of Arizona

[2] Department of Molecular and Cellular Biology, The University of Arizona

[3] University of Arizona Cancer Center

Spatial analysis provides robust, precise, and agnostic quantification of zebrafish patterns

W. Duncan Martinson,[*] Markus Schmidtchen,[†] Alexandria Volkening,[‡] Chandrasekhar Venkataraman,[§] Joshua A. Bull,[¶] José A. Carrillo[‖]

Abstract

Understanding the mechanisms underlying pattern formation represents a key intersection of mathematical and biological research. Quantitative comparison of experimental patterns with those obtained from *in silico* models remains challenging, however, due to inherent variability that can arise between experimental and computational replicates. Here, we propose that tools from spatial point cloud analysis that can investigate structures at arbitrary length scales, specifically pairwise correlation functions and point cloud geometry metrics, enable precise, accurate, and robust quantification of spatial patterning. We demonstrate these qualities by developing a pipeline to extract the above statistics from experimental images of *in vivo* stripe formation in zebrafish (*Danio rerio*) in addition to results from an agent-based model (ABM) and a partial differential equation (PDE) similarly proposed for this process. We show that our analysis pipeline yields consistent statistics across multiple experimental and synthetic replicates, even when the *in silico* data have been generated from initial conditions perturbed from a spatially uniform state. We perform unsupervised clustering of patterns based on pseudometrics obtained from the feature vectors, and demonstrate that the resulting clusters identify interpretable groups. Additionally, we perform supervised learning to determine the combination of statistics required to accurately label new patterns with high accuracy. We envision that this spatial analysis pipeline, which is agnostic to data source, will streamline connection of theoretical models of spatially heterogeneous phenomena to experimental data.

[*]The Francis Crick Institute, UK
[†]TU Dresden, Germany
[‡]Purdue University, IN, USA
[§]University of Sussex, UK
[¶]University of Oxford, UK
[‖] University of Oxford, UK

Model Homogenization Reveals Insights into the Spread of Chronic Wasting Disease at Large Scales

Jen McClure*

Abstract

Environmental transmission thresholds can dramatically influence disease dynamics in wildlife populations. While their effects are well-understood in spatially homogeneous systems, much less is known about their impact across highly heterogeneous landscapes—where behavior, movement, and infection risk can vary significantly over short distances. In this talk, I present a strategic, multiscale model for chronic wasting disease (CWD), a fatal prion-mediated illness affecting cervids. The disease spreads both directly between individuals and indirectly via environmental reservoirs, the latter pathway exhibiting threshold behavior analogous to a strong Allee effect. Beginning with a fine-scale partial differential equation model of transmission over hours and tens of meters, I apply mathematical homogenization techniques to derive a coarse-scale, asymptotically accurate model that operates over years and kilometers. This homogenized model captures the aggregate impact of threshold-driven transmission in heterogeneous environments—a novel result in the study of environmentally persistent diseases. Analyzing the homogenized model suggests insights that are hard to extract from the original model with all its complexity. For example, direct transmission leads to pulled fronts of infection, while environmental transmission produces pushed fronts that enable disease spread even when the basic reproduction number is below one. Which kinds of fronts are possible depends in part on the composition of the landscape. To demonstrate this, I introduce a stylized habitat model with alternating landscape types. The homogenized equations accurately predict how landscape composition shapes disease propagation, offering practical insight into habitat-informed mitigation strategies.

*Department of Mathematics and Statistics, Utah State University

Topological Model Selection: A case-study in tumour-induced angiogenesis

Robert A McDonald[*] Helen M Byrne[†] Heather A Harrington[‡] Thomas Thorne[§]
Bernadette J Stolz[¶]

Abstract

Mathematical models provide powerful analytical approaches for unravelling mechanisms underlying complex biological systems. While numerous approaches exist to describe the spatial and temporal dynamics of a biological system, significant challenges persist in objectively evaluating and comparing their outputs. In particular, spatio-temporal models often lack tractable likelihood functions, which significantly hinders both parameter inference for individual models and model selection across multiple candidate approaches. In this work, we showcase a combination of Topological Data Analysis (TDA) and Approximate Bayesian Computation (ABC) for parameter inference and model selection in mathematical models of tumor-induced angiogenesis. Building on recent advances in ABC and TDA, we develop a flexible three-step pipeline for parameter inference and model selection in spatio-temporal models where likelihood functions are computationally intractable. Our approach leverages techniques from topological parameter inference [1] and extensions to traditional ABC algorithms [2, 3]. In summary, our pipeline makes the following contributions:

1. A method for identifying a small subset of informative summary statistics that capture the parameter-dependent characteristics of simulated data.
2. A distance function based on these summary statistics, implemented within an Approximate Bayesian Computation Sequential Monte Carlo (ABC-SMC) framework for robust parameter inference.
3. A comprehensive model selection approach that not only identifies the best-fit model but also provides posterior probability estimates and generates data approximations for unobserved scenarios.

We demonstrate our three-step pipeline by applying it to three established models of tumor-induced angiogenesis. Through a comprehensive analysis, we compare how spatially-averaged and topological statistics capture the effect of four parameters in each model. Using synthetic test cases, we successfully approximate both the parameter posterior distributions for individual models and the overall model posterior probabilities.

References

[1] T. Thorne, P. D. W. Kirk, and H. A. Harrington, "Topological approximate Bayesian computation for parameter inference of an angiogenesis model," *Bioinformatics*, vol. 38, pp. 2529–2535, 02 2022.

[2] L. Raynal, J.-M. Marin, P. Pudlo, M. Ribatet, C. P. Robert, and A. Estoup, "ABC random forests for Bayesian parameter inference," *Bioinformatics*, vol. 35, pp. 1720–1728, 10 2018.

[3] P. Pudlo, J.-M. Marin, A. Estoup, J.-M. Cornuet, M. Gautier, and C. P. Robert, "Reliable ABC model choice via random forests," *Bioinformatics*, vol. 32, pp. 859–866, 11 2015.

[*]Mathematical Institute, University of Oxford, Radcliffe Observatory Quarter, Woodstock Road, Oxford, OX2 6GG, United Kingdom

[†]Mathematical Institute, University of Oxford, Radcliffe Observatory Quarter, Woodstock Road, Oxford, OX2 6GG, United Kingdom; Ludwig Institute for Cancer Research, Nuffield Department of Medicine, Old Road Campus Research Building, Oxford OX3 7DQ, United Kingdom

[‡]Mathematical Institute, University of Oxford, Radcliffe Observatory Quarter, Woodstock Road, Oxford, OX2 6GG, United Kingdom; Faculty of Mathematics, Technische Universität Dresden, 01062 Dresden, Germany; Centre for Systems Biology Dresden (CSBD), Pfotenhauerstrasse 108, 01062 Dresden, Germany; Max Planck Institute of Molecular Cell Biology and Genetics (MPI-CBG), 01307 Dresden, Germany

[§]Computer Science Research Centre, University of Surrey, GU2 7XH, United Kingdom. Corresponding author: tom.thorne@surrey.ac.uk

[¶]Department of Machine Learning and Systems Biology, Max Planck Institute of Biochemistry, Am Klopferspitz 18, 82152 Martinsried, Germany. Corresponding author: stolz@biochem.mpg.de

Revealing the Design Principles of Physical Networks through Surface Optimisation

Xiangyi Meng,[1,2] Benjamin Piazza,[2] Csaba Both,[2] Baruch Barzel,[2] and Albert-László Barabási[2]

[1] *Department of Physics, Applied Physics, and Astronomy, Rensselaer Polytechnic Institute, Troy, New York 12180, USA*

[2] *Network Science Institute, Northeastern University, Boston, Massachusetts 02115, USA*

From tree branches to the connectome, physical networks combine both a graph structure, describing their topological connectivity patterns, and a physical structure, capturing the geometry of all nodes and links. While the former is abstract, the latter requires material resources for constructing the physical nodes/links and is therefore, intrinsically costly. In one-dimensional systems, this cost is directly proportional to the lengths of all links, leading to the classic wiring economy that seeks to connect all nodes via finite paths while minimizing overall link length.

Such wiring minimization lies at the heart of the Steiner graph optimization problem [Fig. 1(a–b)]: We begin with a set of spatially distributed terminals that we wish to link via finite pathways. As links are drawn from a specific terminal they may, at any given location, branch into several daughter links, creating branching points that effectively add intermediate nodes to the network. This results in a graph $\mathcal{G}$ of $L_{\mathcal{G}}$ physical links. Optimizing the total length of links predicts that all nodes in $\mathcal{G}$ are of degree three, i.e., bifurcations, and that at each bifurcation, links form a planar structure at equal angles. To examine this, we analyze empirical physical networks, from connectomes [Fig. 1(c)] to corals, finding, quite consistently that these predictions are frequently violated. Real physical networks, we observe, feature degrees higher than three (e.g., trifurcations), non-planar branching motifs and a distribution of branching angles [Fig. 1(d–f)]. How then do we reconcile this seemingly *wasteful* network structures with the natural tendency for a parsimonious wiring economy?

To address this observation, we employ a *string-theoretical* approach and generalize the classic Steiner graph to higher dimensions (Fig. 2). Indeed, physical networks are never one-dimensional objects, and hence their cost is not simply governed by the *length* of all links. In two dimensions, for example, the wiring economy is determined by the overall network surface area, and in three-dimension it is governed by volume. As we advance to higher dimensions, the network is best represented by a manifold, whose total surface area/volume captures the actual network construction cost. Under these higher dimensional constructions, we show, cost optimization, leads to potentially richer structural motifs, as indeed we observe in our empirical networks. Hence, advancing beyond the classic one-dimensional length minimization offers a crucial window into the design principles of real-world physical networked systems (Fig. 3).

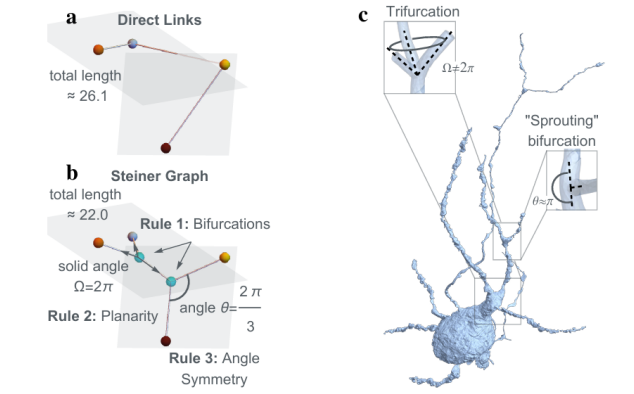

d

Steiner Rule 1: Bifurcations ($k = 3$)

Physical Network	Number of Nodes with Degree k: 3 (bifurcation)	4 (trifurcation)	5	6	...
Human neuron	1499 (79%)	266 (14%)	78	65	...
Fruit fly neuron	4660 (92%)	329 (6.5%)	61	13	...
Blood vessel	1570 (91%)	144 (8.3%)	17	3	...
Tropical tree	1512 (77%)	348 (18%)	83	20	...
Coral	1803 (89%)	177 (8.7%)	42	9	...
Arabidopsis	791 (94%)	39 (4.6%)	12	1	...

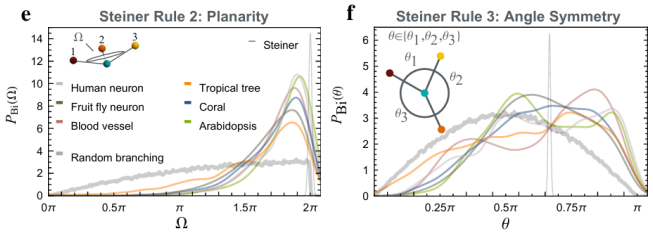

FIG. 1: **Real physical networks versus Steiner predictions**. **(a)** Physical networks aim to connect spatially distributed nodes (coloured) with physical links in three dimensions. **(b)** The Steiner graph minimises the wire length by permitting intermediate nodes (green). The Steiner graph offers three predictions: Rule 1. All branching instances are bifurcations with degree $k = 3$. Rule 2. Bifurcations are all planar, having a solid angle of $\Omega = 2\pi$. Rule 3. The angles between adjacent links are $\theta = 2\pi/3$. **(c)** A neuron of the human connectome, demonstrating the violations of the Steiner rules. In the top inset, we highlight a trifurcation ($k = 4$) violating Rule 1. We also highlight a non-symmetric branching angle, in which links sprout out perpendicularly (right inset), breaking Rule 3. **(d)** The percentage of $k = 4$ nodes across our six empirical physical networks. **(e)** The probability density $P_{\rm Bi}(\Omega)$ vs. Ω as obtained from all bifurcations in our empirical network ensemble (coloured solid lines). **(f)** The probability density $P_{\rm Bi}(\theta)$ vs. θ as obtained from our set of empirical networks (coloured solid lines).

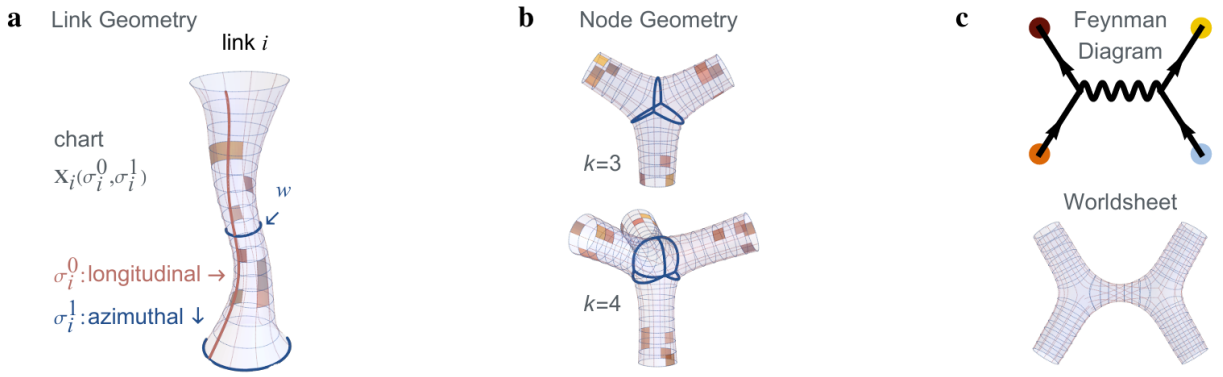

FIG. 2: **Physical network manifold**. **(a)** In a physical network the links are represented by charts, with a manifold morphology $\mathbf{X}_i(\boldsymbol{\sigma}_i)$. Each chart i is described by its local coordinate system $\boldsymbol{\sigma}_i$. The natural parametrisation of a surface is provided by the longitudinal (σ_i^0, red) and azimuthal (σ_i^1, blue) coordinates. The minimum circumference around a link is denoted by w. **(b)** The intersections between the links define the geometry around the nodes. The local charts must be stretched and expanded to ensure a smooth and continuous patching at their boundaries (blue lines), guaranteeing that $\boldsymbol{\sigma}_i = (\sigma_i^0, \sigma_i^1)$ match perfectly with $\boldsymbol{\sigma}_j = (\sigma_j^0, \sigma_j^1)$ at the i, j intersection. When charts intersect at an angle, their surface must stretch to enable smooth and continuous patching. **(c)** A Feynman diagram (top) describes the interactions between two elementary particles in field theory. In string theory, Feynman diagrams are smooth and continuous manifolds in higher dimensions (bottom) known as a worldsheet, that translate the discrete diagram on the top into the integrable object at the bottom. An exact mapping of the surface minimisation problem to these higher dimensional worldsheets allow us to map an abstract topology into a structurally consistent physical network.

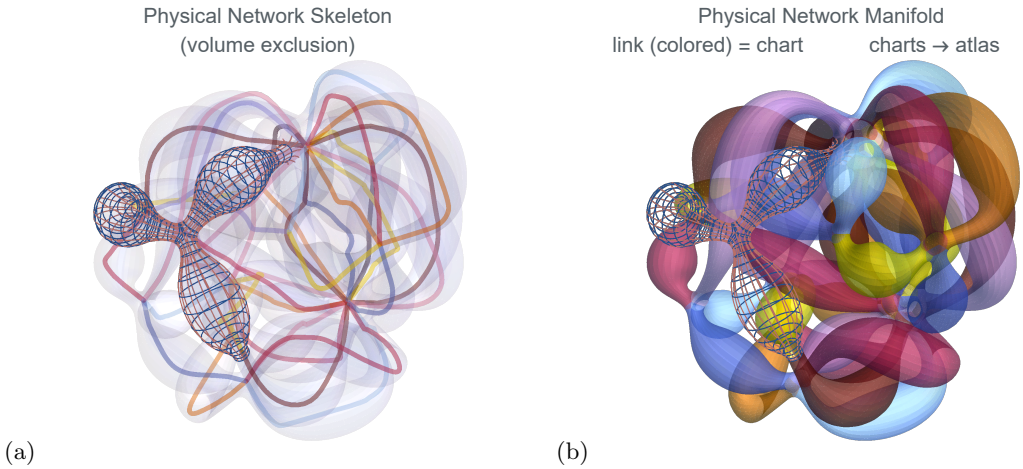

FIG. 3: **Complex physical network manifold**. **((a))** The underlying skeleton graph, featuring curved links and loops. Volume exclusion is implemented to prevent link intersections. **((b))** The resulting two-dimensional manifold, 'dressed' around the skeleton, demonstrating variable link thicknesses. Each link corresponds to a chart. When all links are patched together continuously we obtain the network manifold $\mathcal{M}(\mathcal{G})$, describing the physical network morphology. All local charts $\boldsymbol{\sigma}_i$, $i = 1, 2, \ldots$ can now be consolidated into a single global coordinate system $\boldsymbol{\sigma}$, called atlas.

Metabolic Kinetic Flux Profiling *

Breanna Guppy, Colleen Mitchell† and Eric Taylor

Abstract

Kinetic flux profiling (KFP) uses isotope tracing data to estimate the rates of metabolic reactions. In this talk, we will develop a general method for converting the reaction diagram of a metabolic pathway into a hybrid system of ordinary differential equations and algebraic constraints. In the tracing experiments, the isotope-labeled nutrient is metabolized through the pathway and integrated into the downstream metabolite pools. Using measurements of the proportion labeled of each metabolite in the pathway taken at multiple time points, we use Bayesian parameter estimation to fit the parameters in the model. Estimation of the flux parameters for the reaction rates allows us to identify changes in the fluxes, shedding light on the pathophysiology of diseases with metabolic causes and consequences. We investigate flux parameter identifiability given data collected only at the steady state of the differential equation. Next, we give criteria for valid parameter estimations in the case of a large separation of timescales with fast-slow analysis. These analyses provide constraints that serve as guidelines for the design of KFP experiments to estimate metabolic fluxes

1 An Illustrative Example

For clarity, let us begin with a simple example with three metabolites. In this example, we assume that the reactions are in metabolic steady state with constant metabolite concentrations and constant reaction rates. The only thing changing is the proportion of each metabolite that is labeled with the isotopically labeled input. The three metabolites are named X_1, X_2, and X_3 and ten reactions with constant fluxes $f_1, f_2, \ldots f_{10}$. We can write a system of differential equations in terms of the concentrations of unlabeled metabolites $x_i^{\mathcal{U}}$, $i = 1, 2, 3$. For example,

$$\dot{x}_1^{\mathcal{U}} = \frac{x_3^{\mathcal{U}}}{x_3^{\mathcal{T}}} f_{10} - \frac{x_1^{\mathcal{U}}}{x_1^{\mathcal{T}}} f_4 - \frac{x_1^{\mathcal{U}}}{x_1^{\mathcal{T}}} f_3 + f_2.$$

Our goal is to estimate the flux parameters $f_1, f_2, \ldots f_{10}$ subject to the algebraic constraints for the balance of inputs and outputs for each metabolite. For example the inputs into X_1 will balance the outputs giving

$$f_1 + f_2 + f_{10} = f_4 + f_3.$$

2 Parameter Identifiability

Kinetic Flux Profiling experiments are designed to provide data that can be used to estimate flux parameters in an ODE system. While the setup of the system of ODEs from a directed weighted graph is not unique to this system, KFP models have several idiomatic characteristics that give the equations additional structure. These include the fluxes of both labeled and unlabeled substrates into the pathway, the mixed fluxes out of the pathway, and the algebraic constraints on the flux parameters. Our goal in this talk will be to understand how the structure of the pathway and the design of the experiment impact both the accuracy and the reliability of the estimated fluxes from incomplete and often noisy data. Finally, we will show a specific example using our KFP protocol to measure changes in the fate of Pyruvate following its transport into mitochondria.

*The full version of the manuscript can be accessed at `https://link.springer.com/article/10.1007/s11538-024-01386-x`

†Speaker

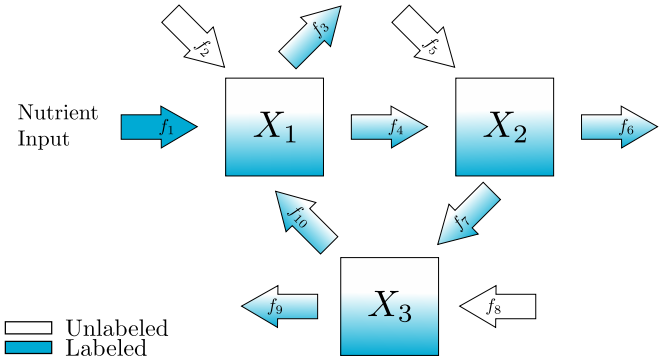

Figure 1: An example reaction network diagram with three metabolites connected in a cycle. The influx f_1 is made up entirely of a labeled substrate. Each metabolite also has an unlabeled influx. All outflux are partially labeled proportional to their metabolite pool of origin.

Mechanisms Controlling the Assembly Dynamics of Cytoskeletal Structures in a Shared Pool

Md Sorique Aziz Momin[1] Lishibanya Mohapatra[1]

Abstract

Cytoskeletal dynamics play a vital role in regulating various aspects of cellular behavior, including morphology, motility, and intracellular organization. To carry out these functions, cytoskeletal monomeric proteins—such as actin monomers and tubulin dimers—polymerize into higher-order structures like filaments and bundles (Fig. 1) [1-2]. For example, microvilli are uniformly sized actin bundles—typically a few microns long—that line the small intestine, where they enhance cell adhesion and nutrient uptake. Stereocilia, composed of actin filaments ranging from 1 to 120 microns, form a staircase-like architecture crucial for signal transduction in the inner ear. Cilia, by contrast, are microtubule-based bundles found across many cell types, supporting both motility and sensory functions. The size of these assemblies is critical for their proper function, and deviations can lead to cellular dysfunction. For instance, defects in microvilli are associated with celiac disease, while impaired stereocilia can cause hearing and balance disorders. Similarly, ciliary dysfunction results in ciliopathies, including primary ciliary dyskinesia and polycystic kidney disease. A fundamental question in cell biology is how these structures maintain defined sizes while assembling from a shared pool of subunits [3-4]. Experimental evidence suggests that mechanisms promoting their disassembly and replenishing the subunit pool may play a key role. Here we compare the role of two modes of disassembly – monomer loss, and loss of fragments (severing) - in the assembly of bare filaments and bundles, which are modelled as a collection of linear filaments. Through a combination of theoretical analysis and simulations, we demonstrate that severing can accelerate the assembly kinetics of both types of structures and ensure their precise size control while assembling simultaneously in a shared pool. We also analyze length fluctuations of the structures and find that the decay of the autocorrelation function is faster in the presence of severing. Specifically, our study identifies key parameters that can influence both the assembly kinetics and the decay of autocorrelations in length fluctuations, while suggesting several quantitative signatures for severing-based size control mechanisms. Overall, these findings provide a framework for designing experiments to differentiate between size control mechanisms in cytoskeletal structures.

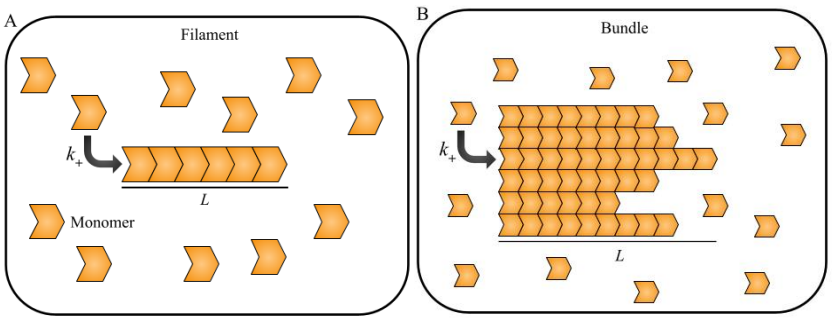

Figure 1: Schematics showing the growth of (A) a bare filament and (B) a bundled structure assembled from monomeric subunits.

References:

[1] Desai A, Mitchison TJ. Microtubule polymerization dynamics. Annu Rev Cell Dev Biol. 1997;13:83-117.
[2] Mooseker MS, Tilney LG. Organization of an actin filament-membrane complex. Filament polarity and membrane attachment in the microvilli of intestinal epithelial cells. J Cell Biol. 1975 Dec;67(3):725-43.
[3] Mohapatra L, Lagny TJ, Harbage D, Jelenkovic PR, Kondev J. The Limiting-Pool Mechanism Fails to Control the Size of Multiple Organelles. Cell Syst. 2017 May 24;4(5):559-567.e14.
[4] Mohapatra L, Goode BL, Jelenkovic P, Phillips R, Kondev J. Design Principles of Length Control of Cytoskeletal Structures. Annu Rev Biophys. 2016 Jul 5;45:85-116.

[1] School of Physics and Astronomy, College of Science,
Rochester Institute of Technology, Rochester, NY 14623, USA

Modelling plant-aphid interactions with Holling type-II functional response and adaptive ant-plant cooperative relationships

Priyanka Mondal*, B.S.R.V. Prasad†

Department of Mathematics, School of Advanced Sciences, Vellore Institute of Technology, Vellore, India.

Abstract

The efficacy of agricultural biological control measures depends on the interactions between plants and their aphid predators. Pests can be portrayed as plants and predators as aphids in prey-predator systems. Plants are known to use numerous defensive strategies against predators to escape from predation pressure. One such technique is baiting a non-prey species with resources, which directly benefits both the plant and the non-prey species by interacting with predators. Many plant-aphid-ant systems mutually interact to get benefits from each other. Numerous studies have shown that ants adapt to foraging and choose which food to eat, whether it is provided by plants or humans. This adaptive foraging habit can compromise the protection supplied by ants to the plant. We employed a variant of the Rosenzweig-MacArthur prey-predator model to investigate how the ant's mutualistic interactions with adaptive foraging behaviour influence plant-aphid dynamics. The system analysis reveals intriguing and complex dynamics, including the existence of stable limit cycles, global stability conditions, and various bifurcations. This technique is particularly helpful in agricultural contexts where plants can alter predator foraging efficiency by influencing ant protective behaviour.

References

[1] Tomás A. Revilla, Vlastimil Krivan, Applied Mathematics and Computation 433(4):127368 (2022), https://doi.org/10.1016/j.amc.2022.127368.

*priyanka.mondal2021@vitstudent.ac.in
†srvprasad.bh@vit.ac.in

[2] M. L. Rosenzweig and R. H. MacArthur, "Graphical Representation and Stability Conditions of Predator-Prey Interactions", The American Naturalist, vol. 895, pp. 209-223, 1963.

[3] P.A. Abrams, R. Cressman, V. Krivan, ˇ Role of behavioral dynamics in determining the patch distributions of interacting species, Am. Nat. 169 (4) (2007) 505–518, doi:10.1086/511963.

[4] C. Nagy, J.V. Cross, V. Markó, Sugar feeding of the common black ant, Lasius niger (L.), as a possible indirect method for reducing aphid populations on apple by disturbing ant-aphid mutualism, Biol. Control 65 (1) (2013) 24–36, doi:10.1016/j.biocontrol.2013.01.005.

[5] D.J.W. Simpsona, J.D. Meissb, Aspects of Bifurcation Theory for Piecewise-Smooth, Continuous Systems, arXiv:1006.4123v1 [nlin.CD] 21 Jun 2010.

Decoding Oral Temperature from Gustatory Cortex Activity in Freely Licking Mice

Audrey N. Nash* Cagatay Ayhan* Tom Needham* Martin Bauer* Cecilia G. Bouaichi†
Katherine B. Odegaard† Richard Bertram‡ Roberto Vincis§

Abstract

The gustatory cortex (GC) is traditionally studied for its role in taste perception, but emerging evidence suggests it may also contribute to encoding other oral sensory modalities. In this work, we investigate how GC neurons represent thermal information, using simultaneous recordings from over 400 neurons across multiple sessions in mice freely licking water droplets delivered at non-nociceptive temperatures. This approach allowed us to examine both single-neuron responses and population-level representations of oral thermal stimuli.

To quantify how well neural activity distinguished between thermal conditions, we developed a Bayesian classification framework that integrates spike rate and lick-phase timing. Our analysis shows that GC neurons can reliably differentiate between thermal stimuli, particularly when temperature differences are large, but also—though to a lesser extent—when contrasts are subtle. Comparing decoding performance between the gustatory and somatosensory cortices further revealed that, while the somatosensory cortex exhibited higher classification accuracy, the GC nonetheless carried substantial thermosensory information.

These findings underscore the gustatory cortex's broader role in processing oral stimuli, suggesting that temperature should be considered a key variable in future studies of taste coding. Our analysis pipeline also explores population-level structure using advanced computational techniques, offering a complementary perspective on how neural ensembles encode sensory information.

References

[1] Audrey Nash, Morgan Shakeshaft, Cecilia G. Bouaichi, Katherine B. Odegaard, Tom Needham, Martin Bauer, Richard Bertram, Roberto Vincis, *Cortical Coding of Gustatory and Thermal Signals in Active Licking Mice*, J. Physiol., 603 (2025), pp. 909–928.

*Department of Mathematics, Florida State University
†Department of Biological Science and Program in Neuroscience, Florida State University
‡Department of Mathematics and Programs in Neuroscience and Molecular Biophysics, Florida State University
§Department of Biological Science, Programs in Neuroscience, Molecular Biophysics, and Cell and Molecular Biology, Florida State University

A calculus for transcription

Joseph Nasser[1], Kee-Myoung Nam[2], Jesse Engreitz[3], Jeremy Gunawardena[2]
1. Brandeis University
2. Harvard Medical School
3. Stanford University

What language should we use to describe biological systems: words, pictures, math, computer programs, something else? I will highlight recent insights gained by using mathematics to describe transcription.

Transcription is the process by which RNA is synthesized from a DNA template. The regulation of transcription is critical to all of known life. Decades of research in molecular biology and biochemistry have identified many of the molecules and chemical reactions involved in transcription. Yet our quantitative and conceptual understanding of transcriptional regulation is limited.

A "calculus for transcription" refers to a mathematical framework which can be used to formally reason about transcription. Our initial efforts are based on a graph theoretic interpretation of Markov processes known as the 'linear framework' (Gunawardena, PLoS 2012). This framework is capable of translating assumptions about transcriptional mechanisms into a formal mathematical language and computing the logical consequences of those assumptions.

We have recently used this framework to provide a mathematical formalization of a previously introduced informal model of metazoan transcription (Nasser, Nam, Gunawardena, eLife 2025; Fulco, Nasser et al Nature Genetics 2019). Our formalization clarifies the assumptions of the informal model and leads to many potential new insights. Along the way, we have attempted to provide a formal mathematical definition for what it means for two regulatory systems to operate on transcription "independently". Despite the word 'independence' being broadly used in the transcription community, providing a mathematical definition of this concept is surprisingly difficult. Simply the act of trying to formally define independence within the context of transcription has led to many useful insights and new interpretations of experimental data.

Our research has also produced mathematical questions which may be of interest beyond their application to biology. These include defining equivalence classes on semi-infinite graphs and more generally deepens the connections between Markov processes, linear algebra and graph theory.

The take-home message will be that perhaps there is a role for mathematics in biology beyond just analyzing experimental data - formal mathematical reasoning may be useful in its own right.

Correlation of tree structures in population genetics

Maximillian Newman

April 15, 2025

Abstract

In population genetics, one is concerned with how one may infer demographic history, population admixture, disease etiology and other critical phenomena from genetic data. One of the strongest tools to do this is by means of coalescent theory, where a sample at a single genetic locus from n individuals is assumed to form a coalescent tree. The correlation of the structure of these trees, even at unlinked loci, is poorly understood. Initiated by the work of [1], empirical works such as [5, 6] and theoretical works such as [4, 2, 3] have made efforts to understand how shared parental histories affect the correlation of genetic trees at unlinked loci in well-mixed populations of a constant size. However, there is much work that needs to be done to make robust theoretical insights to be applicable to human populations, including accounting for the explosion in human population sizes, population structure, and classical assumptions about the scales of sample sizes failing. In this talk I would like to express some of the mathematical techniques at play here, including interacting particle systems, duality, and random measures, as well as some future directions where new mathematical tools are needed.

References

[1] Ball, R Martin Jr et al. "GENE GENEALOGIES WITHIN THE ORGANISMAL PEDIGREES OF RANDOM-MATING POPULATIONS." Evolution; international journal of organic evolution vol. 44,2 (1990): 360-370. doi:10.1111/j.1558-5646.1990.tb05205.x

[2] Diamantidis, Dimitrios et al. "Bursts of coalescence within population pedigrees whenever big families occur." Genetics vol. 227,1 (2024): iyae030. doi:10.1093/genetics/iyae030

[3] Newman, Maximillian, John Wakeley, and Wai-Tong Louis Fan. "Conditional Gene Genealogies Given the Population Pedigree for a Diploid Moran Model with Selfing." arXiv, 2024, arxiv.org/abs/2411.13048.

[4] Tyukin, Andrey. Quenched Limits of Coalescents in Fixed Pedigrees. Master's thesis, Johannes-Gutenberg-Universität Mainz, 2015, https://www.glk.uni-mainz.de/files/2018/08/andrey_tyukin_msc.pdf.

[5] Wakeley, John et al. "Gene genealogies within a fixed pedigree, and the robustness of Kingman's coalescent." Genetics vol. 190,4 (2012): 1433-45. doi:10.1534/genetics.111.135574

[6] Wilton, Peter R et al. "Population structure and coalescence in pedigrees: Comparisons to the structured coalescent and a framework for inference." Theoretical population biology vol. 115 (2017): 1-12. doi:10.1016/j.tpb.2017.01.004

Auditory encoding modeling using neural networks

Jonathan Gonzalez Martinez (1), Quynh-Anh Nguyen (1), (2)

(1) Department of Mathematical Sciences, University of Indianapolis, Indianapolis, Indiana, United States
(2) Center for Data Science, University of Indianapolis, Indianapolis, Indiana, United States

As you walk down a busy street with noise from various sources, you can distinguish sounds coming from cars, bicycles, trucks, people talking/running, and so on. As you enjoy an orchestra performance, you can pick out music from the violine, the flute, the piano, and so on. These tasks seem simple and effortless because the auditory system can perform them instantly and even simultaneously. In the primary auditory cortex (A1), the inputs are integrated with information from other sensory systems, and thus A1 plays an important role in information processing and the formation of auditory objects. Nevertheless, little is understood in A1 neuronal encoding/decoding problems and how the neuronal responses in A1 give rise to perceptual and cognitive functions (Nelken, 2008). Many studies of A1 use spectrotemporal receptive field to investigate the relationship between the stimulus and the neural responses. This method, however, assumes linearity of auditory responses while different experimental and computational studies have indicated that neuronal response in the auditory system is not merely linear (Atencio et al., 2009; Sahani and Linden, 2002). In this study, we use neural networks to investigate auditory cortical responses. Neural networks have gained tractions recently due to their speed, availability of open datasets, and efficiency of training algorithms. For instances, recurrent neural network framework has been used to studied cognitive and perceptual functions, and convolution neural network has been utilized to understand visual as well as auditory cortical responses (Lindsay, 2021; Pennington and David, 2023). Here, we construct neural network models to explain auditory responses from external stimuli (i.e. auditory encoding problem) and analyze the networks' structures together with stimulus features to investigate the relationship between the response patterns and the stimulus. This will enable us to propose a potential mechanism of information processing in the auditory cortex.

Acknowledgement: This study was supported by the Faculty Scholarship Grant, University of Indianapolis (Grant Number: 995049)

References

Atencio, C.A., Sharpee, T.O., & Schreiner, C.E. (2009). Hierarchical computation in the canonical auditory cortical circuit, *Proceedings of the National Academy of Sciences, 106*(51), 21894-21899.

Lindsay G.W. (2021). Convolution neural networks as a model of the visual system: past, present, and future. *Journal of Cognitive Neuroscience, 33*(10), 2017-2031.

Nelken, I. (2008). Processing of complex sounds in the auditory system. *Current Opinion in Neurobiology, 18*(4), 413-417.

Pennington, J.R. & David, S.V. (2023). A convolution neural network provides a generalizable model of natural sound coding by neural populations in auditory cortex. *PLoS Computational Biology, 19*(5), e1011110.

Sahani, M. & Linden, J.F. (2002). How linear are auditory cortical responses? *Proceedings of the 15th International Conference on Neural Information Processing Systems*, 125-132.

A control strategy for the Sterile Insect Technique using exponentially decreasing releases to avoid the hair-trigger effect

Nga Nguyen*

Abstract

In this talk, I focus on mathematical modeling of the propagation and biological control of *Aedes* mosquitoes, vectors of various diseases such as dengue, zika, chikungunya, and yellow fever. I will present a stage-structured compartmental model using a partially degenerate reaction-diffusion system to describe the dynamics of the mosquito population under biological control of the *Sterile Insect Technique* (SIT) [1]. This technique aims to suppress or even eliminate the entire population of a particular insect species by mass releases of sterilized male individuals that mate with indigenous females yet produce no fertile offspring. One standout advantage of the SIT is that it relies on the natural ability of males to locate and mate with females, even in areas that cannot be reached with conventional control techniques (i.e., insecticides). However, due to the enormous reproducibility of *Aedes* mosquitoes, the target population can recover and reinvade the territory after the controls terminate.

This reinvasion can be explained in our model by the so-called *hair-trigger effect*. We show that even with only a few individuals at the beginning, there is a traveling wave of the mosquito population across the space. A *"rolling carpet"* strategy should be applied where a large number of sterile insects are released near the front of the invasion, and as soon as this area is free from wild mosquitoes, we move the releases forward but keep a small amount of sterile individuals in the treated area to avoid reinvasion. To model this strategy, we design an exponentially decreasing release function in a 'forced' moving interval in the opposite direction to the natural mosquito propagation. We prove that for a sufficiently large number of sterile males released, the population was pushed backward at the same speed as the release. The proofs rely on constructing generalized sub- and super-solutions for the corresponding traveling wave system by gluing elementary functions suitably. Our work [2] provides a proof of concept for the *"rolling carpet"* strategy, and proposes that reaction-diffusion models and traveling wave analysis could be a useful supplementary tool to study the propagation of insects in a vast region where field experiments are costly and infeasible.

References

[1] V. A. Dyck, J. Hendrichs, and A. S. Robinson. *Sterile Insect Technique: Principles and Practice in Area-Wide Integrated Pest Management.* 2nd ed. Boca Raton: CRC Press, Jan. (2021).

[2] A. Leculier and N. Nguyen. *A control strategy for the Sterile Insect Technique using exponentially decreasing releases to avoid the hair-trigger effect.* en. In: Mathematical Modelling of Natural Phenomena 18 (2023).

*École Normale Supérieure, 75005, Paris, France

Towards Computational Foundations for Medicine

Stephen Wolfram, Willem Nielsen[†]

Abstract

We present a general-purpose computational metamodel of medicine, in contrast to traditional system-specific mathematical models. This approach uses simple computational rules (e.g. a one-dimensional cellular automaton) to simulate an idealized "model organism". Diseases are represented as perturbations to the organism's state, and treatments as secondary perturbations introduced to counteract disease effects and restore normal behavior. Despite its simplicity, we find that the model reproduces many phenomena of health and disease, highlighting their abstract computational underpinnings. This is an excerpt from our article[1], where we introduce our model of disease and treatment:

Some perturbations (like the one in the second panel here) quickly disappear; in essence the system quickly "heals itself". But in most cases even single-cell perturbations like the ones here have a long-term effect. Sometimes they can "increase the lifetime" of the organism; often they will decrease it. And sometimes—like in the last case shown here—they will lead to essentially unbounded "tumor-like" growth.

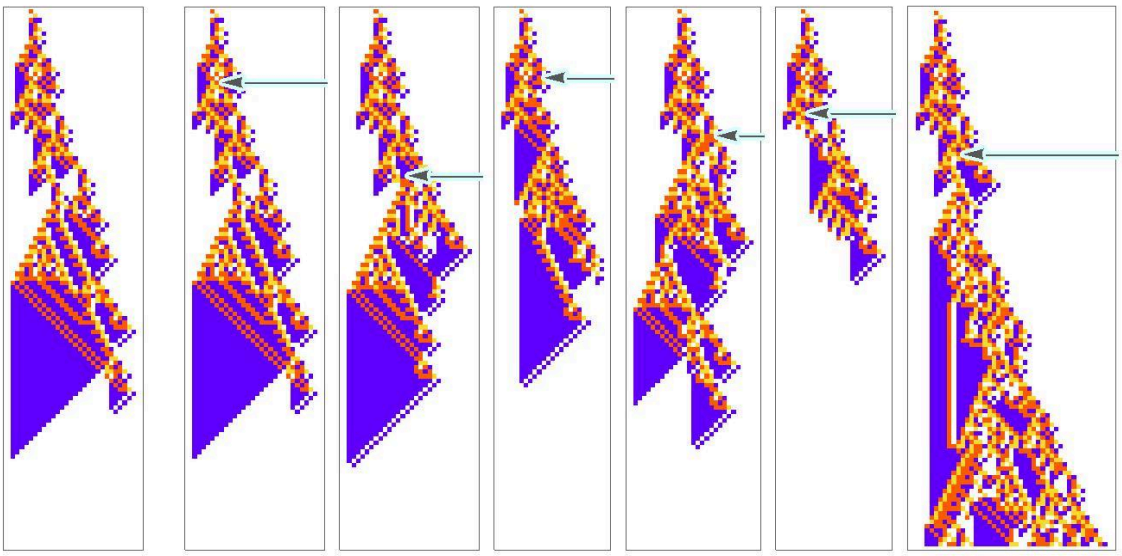

Figure 3. In the first panel from the left, we show an unperturbed cellular automaton, our model for a "healthy organism". In the subsequent panels, we show the resulting automata if we change one cell in the pattern, indicated by the light-blue arrow.

But now we can formulate what we can think of as the "fundamental problem of medicine": given that perturbations have had a deleterious effect on an organism, can we find subsequent perturbations to apply that will serve as a "treatment" to overcome the deleterious effect? The first panel here shows a particular perturbation that makes our idealized organism die after 47 steps. The subsequent panels then show various "treatments" (i.e. additional perturbations) that serve at least to "keep the organism alive":

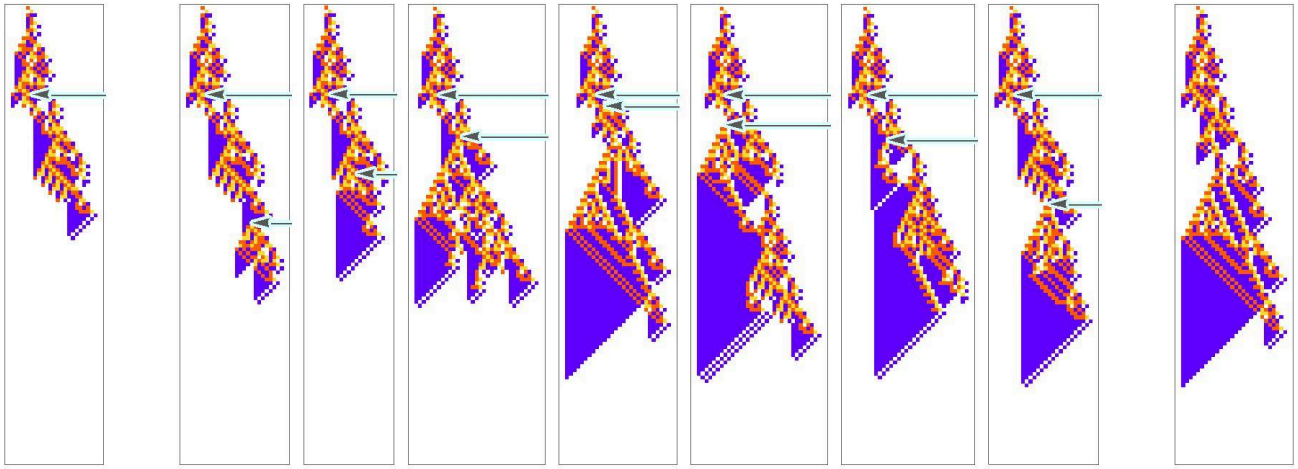

Figure 4. In the first panel from the left, we show a perturbed cellular automaton, our model for a "diseased organism". In the subsequent panels, we show the resulting automata if we make a second perturbation after the initial perturbation, in an attempt to recover the original automaton, which is shown first from the right.

In the later panels here the "life history" of the organism gets closer to the "healthy" unperturbed form shown in the final panel. And if our criterion is restoring overall lifetime, we can reasonably say that the "treatment has been successful". But it's notable that the detailed "life history" of the organism will essentially never be the same as before: as we'll see in more detail later, it's almost inevitably the case that there'll be at least some (and often many) long-term effects of the perturbation+treatment even if they're not considered deleterious.

References

[1] Stephen Wolfram Writings. 2025. Towards a Computational Formalization for Foundations of Medicine. https://writings.stephenwolfram.com/2025/02/towards-a-computational-formalization-for-foundations-of-medicine/

---

†Wolfram Institute for Computational Foundations of Science

Computational Model of Eversion of Drosophila Wing

Ethan Nowaski[1], Benjamin Speybroeck[2], Weitao Chen[1], Zhiliang Xu[3], Navaira Sherwani[1], Jeremiah Zartman[2], Mark Alber[1]

1 Department of Mathematics and Interdisciplinary Center for Quantitative Modeling in Biology, University of California, Riverside, CA
2 Department of Chemical and Biomolecular Engineering, University of Notre Dame, Notre Dame, IN
3 Department of Applied and Computational Mathematics and Statistics, University of Notre Dame, Notre Dame, IN

One of the most important open questions in developmental biology is determining how organs and tissues form and maintain their shape. The robust formation of organs during development depends on the careful regulation of cellular processes such as cell adhesion, mechanical stiffness of the cell membrane, and internal pressure to create the tissue-scale architecture. A sophisticated communication system coordinates these developmental processes. This project utilizes the fruit fly wing imaginal disc, a powerful biological model system, to study how downstream effectors of ecdysone signaling contribute to regulating cell mechanical properties that influence cell shapes and overall tissue structures during wing disc eversion. Eversion is one of the final parts of development involving decline of cell proliferation and folding of the wing driven by cell rearrangements and morphological changes driven by actomyosin dynamics. The project workflow includes iteration between quantitative experiments and biologically calibrated computational model simulations. In this poster presentation, a novel extension of the two dimensional subcellular element computational model of the developing Drosophila wing [1] will be described and model simulations will be used to demonstrate potential mechanisms of wing folding during eversion.

1. Nilay Kumar, Jennifer Rangel Ambriz, Kevin Tsai, Mayesha Sahir Mim, Marycruz Flores-Flores, Weitao Chen, Jeremiah J. Zartman and Mark Alber [2024], Balancing competing effects of tissue growth and cytoskeletal regulation during Drosophila wing disc development. *Nat Commun* 15, 2477 (2024).

A Repurposed Nonstationary Time Series Heuristic Captures Domain Architecture in Synthetic Hi-C Matrices

Adam O'Regan* Maalavika Pillai† Luís A. Nunes Amaral ‡

April 15, 2025

Abstract

Chromatin conformation capture (3C) techniques have revolutionized the study of three-dimensional genome organization. Hi-C, a variation of 3C, provides a high-resolution view of all DNA-DNA interactions within a biological sample vis-á-vis massively parallel sequencing. This approach has been instrumental to characterizing topologically associated domains (TADs), or contiguous regions of chromatin that display enhanced probability of interaction [1]. Visually, TADs present as blocks along the symmetric contact matrix diagonal and delimit the locations of off-diagonal features. Previous research demonstrates their association with genetic regulation. [2] These properties render TADs an excellent focal point of Hi-C analysis. The present study investigates a computational algorithm for TAD detection generalized from the Fukuda et al. heuristic for segmenting nonstationary time series data [3]. The method leverages iterative statistical testing to identify domain boundaries within the symmetric contact matrix. Specifically, the algorithm scans the matrix diagonal and, using a two-sided t-test, identifies the position where the difference between on-diagonal and off-diagonal sample clusters is maximal. There, the matrix is divided, and the process continues recursively until no further statistically significant divisions remain. Since decision-making occurs individually in distinct iterations, we refer to this approach as greedy. Building on previous observations of chromatin architecture, we validate the algorithm by modeling Hi-C as a block diagonal matrix spanning the parameters of domain size, domain magnitude, matrix order, and the coefficient of variation. Extracting parameters from empirical Hi-C data is still unfolding. Results from these simulations indicate that the methodology detects TAD boundaries with high sensitivity, as measured by its ability to measure one hundred percent of synthetic domain boundaries across a wide range of input parameters. Matrices with high noise recapitulate this sensitivity. Smaller matrices have an elevated probability of returning a spurious boundary, or false discovery; this likelihood approaches the alpha level with increasing matrix order. Current endeavors consider a bootstrapping technique to increase the confidence of boundary calls. Comparative analysis with existing methods like the Arrowhead Method position our repurposed approach as a possible advancement in Hi-C analysis with implications for unresolved questions in chromatin topology and genetic regulation.

References

(1) Belton, J.-M.; McCord, R. P.; Gibcus, J.; Naumova, N.; Zhan, Y.; Dekker, J. *Methods (San Diego, Calif.)* **2012**, *58*, 10.1016/j.ymeth.2012.05.001.

(2) Rao, S. S. P.; Huntley, M. H.; Durand, N. C.; Stamenova, E. K.; Bochkov, I. D.; Robinson, J. T.; Sanborn, A. L.; Machol, I.; Omer, A. D.; Lander, E. S.; Aiden, E. L. *Cell* **2014**, *159*, Publisher: Elsevier, 1665–1680.

(3) Fukuda, K.; Stanley, H. E.; Amaral, L. A. N. *Physical Review E* **2004**, *69*, DOI: 10.1103/PhysRevE.69.021108.

*Quantitative and Systems Biology Master's Program, Northwestern University

†Interdisciplinary Biological Sciences Graduate Program, Northwestern University

‡Erastus Otis Haven Professor of Engineering Sciences and Applied Mathematics, Northwestern University

Stochastic Agent-Based Modeling of *Salmonella* Infections

Katalin Anna Olasz[1]

[1]Semmelweis University, Faculty of General Medicine

Introduction

Modeling host-pathogen interactions contributes to a deeper understanding of infectious processes. In our study, we examined macrophages infected with *Salmonella* using advanced image processing techniques, deep learning algorithms, and agent-based modeling.

Objective

Our goal was to measure bacterial incubation time, maximum bacterial load, the number of bacteria released during lysis, the division time of cells, and to quantify infection, death, and replication rates. Based on our experimental data, we developed a stochastic agent-based model to describe these processes. This model allows us to extrapolate features of the macrophage-bacteria system that are difficult to assess experimentally. Parameter optimization was performed using `pygad`, a genetic algorithm-based optimization library.

In addition to optimizing infection parameters, we also used `pygad` to estimate the maximum bacterial load that macrophages can tolerate before undergoing lysis. The simulation was implemented in `NetLogo`, allowing for easy and repeatable runs under various conditions.

Methods

We infected RAW 264.7 mouse-derived macrophage cell lines with *Salmonella Typhimurium* at low (MOI 10) and high (MOI 50) multiplicities of infection. The cell cultures were maintained in DMEM medium supplemented with 10% FBS. Macrophages were labeled with Cy5 and bacteria with TRITC fluorescent dyes. Data were acquired using a Nikon Eclipse Ti-E microscope in wells 8–21 of a 96-well plate, capturing 60 time points over 20 hours at 21 positions per well. These biological experiments were conducted during the Summer Undergraduate Research Program 2024 at NITMB, Northwestern University, in the Lane Lab under the guidance of PhD student Anika Marand and lab director Keara Lane.

Image processing was performed using the Cellpose segmentation algorithm. Using known infection, death, and division rates, along with lysis parameters, we constructed a delayed Gillespie-based stochastic agent model. Parameter fitting and bacterial load threshold estimation were achieved through `pygad` optimization. The mathematical modeling and simulation work was carried out at the University of Szeged, Hungary.

The delayed stochastic simulation algorithm (dSSA) modifies the traditional Gillespie formulation to account for reactions with a deterministic delay τ. The master equation is represented as:

$$\frac{dP(\vec{X},t)}{dt} = \sum_{j=1}^{M} \left[a_j(\vec{X} - \vec{\nu}_j) P(\vec{X} - \vec{\nu}_j, t - \tau_j) - a_j(\vec{X}) P(\vec{X}, t) \right], \tag{1}$$

where $\vec{X}$ is the state vector, $\vec{\nu}_j$ is the state change vector for reaction j, a_j is the propensity function, and τ_j is the delay associated with reaction j.

Results

At MOI 10, infected cells appeared after approximately 420 minutes, while at MOI 50, infection was detectable by 200 minutes. Incubation time ranged between 240–540 minutes and was significantly influenced by cell size. Lysis occurred 200–300 minutes post-infection, once infected cells reached approximately 40% infection-to-cytoplasm pixel ratio.

The released bacteria occupied an average area of 45 pixels, corresponding to the release of around 40–50 bacteria into the extracellular space. Based on literature (Gog et al., 2012; Shi et al., 2016; Vlazaki et al., 2020; Ciupe and Heffernan, 2017; Cesar et al., 2022; Wang et al., 2023; Wrande et al., 2020), we set the cell death rate to 1.2×10^{-3} s^{-1}, the division rate to 2.5×10^{-4} s^{-1}, and the infection rate to 2.5–12.5×10^{-5} s^{-1}.

Conclusion

Our results provide detailed insights into the behavior of macrophages infected with *Salmonella*. With the extracted parameters, we were able to construct a realistic stochastic infection model. The simulation was developed in `NetLogo`, enabling flexible and repeated experimentation. Our validated agent-based model may also serve as a simulation tool for infections in human-derived macrophages.

Acknowledgments

The author gratefully acknowledges the Lane Lab at Northwestern University for hosting the biological part of this project as part of the NITMB Summer Undergraduate Research Program 2024, under the mentorship of PhD student Anika Marand and lab director Keara Lane. The mathematical modeling component was carried out at the University of Szeged, Hungary, under the supervision of Peter Boldog, PhD.

References

- Gog, J. R., Murcia, P. R., & Ostler, T. (2012). Influenza: modelling disease dynamics. *Nature Reviews Microbiology*, **10**(8), 522–532. https://doi.org/10.1038/nrmicro2807
- Shi, Z., Chapes, S. K., Ben-Arieh, D., & Wu, C.-H. (2016). An Agent-Based Model of a Hepatic Inflammatory Response to Salmonella. *PLOS ONE*, **11**(8), e0161131. https://doi.org/10.1371/journal.pone.0161131
- Vlazaki, M., Huber, J., & Restif, O. (2019). Integrating mathematical models with experimental data to investigate the within-host dynamics of bacterial infections. *Pathogens and Disease*, **77**, ftaa001. https://doi.org/10.1093/femspd/ftaa001
- Ciupe, S. M., & Heffernan, J. M. (2017). In-host modeling. *Infectious Disease Modelling*, **2**(2), 188–202. https://doi.org/10.1016/j.idm.2017.04.002
- Wrande, M., Vestö, K., et al. (2020). Replication of Salmonella enterica serovar Typhimurium in RAW264.7 Phagocytes Correlates With Hypoxia and Lack of iNOS Expression. *Frontiers in Cellular and Infection Microbiology*, **10**, 537782. https://doi.org/10.3389/fcimb.2020.537782

Non-Unique Rational Behavior during an Epidemic with Pathogen Reservoir

Connor Olson

Human behavior is central to the unfolding of an epidemic. The COVID epidemic response in democratic nations demonstrated that while institutions can successfully coordinate policy, they have limited ability to influence human behavior and can lose credibility the more draconian their enforcement efforts become. The classic theory of mathematical epidemiology does not parameterize human behavior and correcting this oversight has been a major research effort over the last quarter century. The approach we adopt to study the question of individual human behavior during an epidemic is a differential population game, where we model the individual in an economic fashion and use optimization theory to calculate behaviors.

In this talk, we extend social distancing games (SDGs) to present new results for novel Environmental Distancing Games (EDGs) where an environmental disease reservoir contributes to infection risk. As opposed to SDGs, which are proven to have unique Nash strategies in the SI case, the EDGs are revealed to possess multiple subgame perfect equilibrium strategies even in the simplest cases. By exploiting Filippov representations, Riccati conditions, and special cases of integrability, we can characterize the game solution structure in terms of model parameters. Our results reveal how multiple Nash strategies manifest in this modeling framework and suggest a second approach to studying the solution structure. These approaches show promise for addressing further open problems in the field. We conclude by discussing why our results are indicative of complicated solution structures in behavior models coupled with more complex epidemic models.

Theoretical Advances in Population Models with Free Boundaries: Existence Results

Kayode Oluwasegun* David Ambrose* Douglas Wright*

Abstract

With the introduction of mathematics into biological research, patterns arising from biological problems can be effectively studied. The complex interactions involving biological systems and invading pathogens can be described using mathematical frameworks of partial differential equations (PDEs). More specifically, the spread of new or invasive species can be set up as a population model with a freely moving boundary. Proving the existence of solutions to this model helps us scientists to have a solid understanding of how the population works and predict how it changes in the future.

1 The Free Boundary Problem

We seek to propose a different approach to understanding the spread of species. Our approach is based on the following diffusive logistic problem:

$$\begin{cases} u_t - du_{xx} = u(a - bu), & t > 0,\ 0 < x < h(t), \\ u_x(t,0) = 0, \quad u(t,h(t)) = 0, & t > 0, \\ h'(t) = -\mu u_x(t,h(t)), & t > 0, \\ h(0) = 1, \quad u(0,x) = u_0(x), & 0 \le x \le 1, \end{cases} \tag{1.1}$$

where $x = h(t)$ is the moving boundary to be determined, μ, d, a, and b are given positive constants, and the initial function $u_0(x)$ satisfies

$$u_0 \in C^2([0,1]), \quad u_0'(0) = u_0(1) = 0, \quad \text{and} \quad u_0 > 0 \text{ in } [0,1). \tag{1.2}$$

We attempt to use (1.1) to model the spreading of a new or invasive species with population density $u(t,x)$ over a one dimensional habitat. The free boundary $x = h(t)$ represents the spreading front, while the homogeneous Neumann boundary condition at $x = 0$ indicates that the left boundary is fixed, with the population confined to its right. The coefficient a represents the intrinsic growth rate of the species, b measures its intraspecific competition, and d is the dispersal rate.

Theorem 1.1. *For any given u_0 satisfying* (1.2)*, there is a $T > 0$ such that problem* (1.1) *admits a solution.*

Proof. An outline of the proof.

i) Straighten the free boundary by applying relevant transformations.
ii) Redefine an approximate problem by introducing a regularizing operator called **mollifier**.
iii) Define relevant energy functions associated with the approximate problem, that capture the biological properties of the system.
iv) Select appropriate function spaces to work in.
v) Estimate the growth of the approximate solutions by restricting the growth of the energy functions.
vi) Exploit compactness which guarantees that from an infinite sequence of functions, we can extract a uniformly convergent subsequence (Arzela-Ascoli).
vii) Prove existence of solution to the original problem by passing to a limit, the solution of the approximate problem as needed.
□

References

[1] Y. Du & Z. Lin, *Spreading-vanishing dichotomy in the diffusive logistic model with a free boundary,* SIAM Journal on Mathematical Analysis, vol. 42, no. 1, pp. 377-405, (2010).

[2] A. Majda & A. Bertozzi, *Vorticity and Incompressible Flow* (Cambridge Texts in Applied Mathematics). Cambridge University Press, (2001).

*Department of Mathematics, Drexel University, 3141 Chestnut St, PA 19104, Philadelphia, Pennsylvania, USA

Forecasting West Nile Virus in Maricopa County using climate factors

Kayode Oshinubi[1]

Abstract

Mosquito-borne diseases present a significant public health challenge, with effective prevention requiring accurate forecasting of mosquito populations and associated disease prevalence. West Nile Virus (WNV) spread rapidly across the United States, primarily due to its transmission through highly mobile, migratory birds. Climate change is expected to alter the large-scale distribution of mosquito populations and disease patterns, making predictive modeling increasingly essential due to its complexity. According to data from the Centers for Disease Control and Prevention (CDC), Maricopa County, Arizona, is among the top U.S. counties with a high WNV disease burden. Using a 10-year time series (2014–2024) of weekly mosquito abundance and WNV prevalence data collected in Maricopa County, we investigated how local climate variations influence mosquito population dynamics and disease transmission. We developed a mechanistic model of WNV dynamics driven by daily temperature and 30-day accumulated precipitation to predict mosquito populations and WNV prevalence. Our statistical forecasting framework leveraged climate factors to improve predictive accuracy by integrating adaptive modeling techniques and Bayesian methods to infer precise model parameters. A key enhancement addressed limitations observed in prior models, particularly the inability to capture spring season dynamics in mosquito populations. To achieve this, we applied the Ensemble Kalman Filter (EnKF) method to estimate both time-varying parameters (baseline population growth rate and mosquito bite rate) and static parameters. Using generalized additive models (GAMs), we forecasted these time-varying parameters on a two-week basis, incorporating precipitation and temperature as covariates. These forecasts were used as inputs for a mechanistic ordinary differential equation (ODE) model, which predicted mosquito abundance and WNV prevalence while capturing associated uncertainties. Our iterative framework was applied over a 52-week period, successfully capturing seasonal variations in mosquito populations and WNV prevalence throughout the decade-long dataset. Compared to traditional Markov Chain Monte Carlo (MCMC) approaches, the EnKF demonstrated superior performance in fitting mosquito abundance and WNV prevalence data. Despite changes in environmental conditions, data quality, and underlying dynamics over the 10-year period, our method consistently captured key trends and variations, highlighting its robustness and adaptability. This enhanced methodology provides actionable insights for public health decision-makers, supporting resource allocation and improving mosquito-borne disease prevention outcomes. Our findings underscore the importance of integrating climate data with adaptive filtering techniques to address forecasting challenges and enable effective responses to emerging or re-emerging mosquito-borne pathogens, which, driven by human behavior and environmental changes, may potentially escalate to pandemic levels. Figure 1 provides an overview of the research approach used in this study.

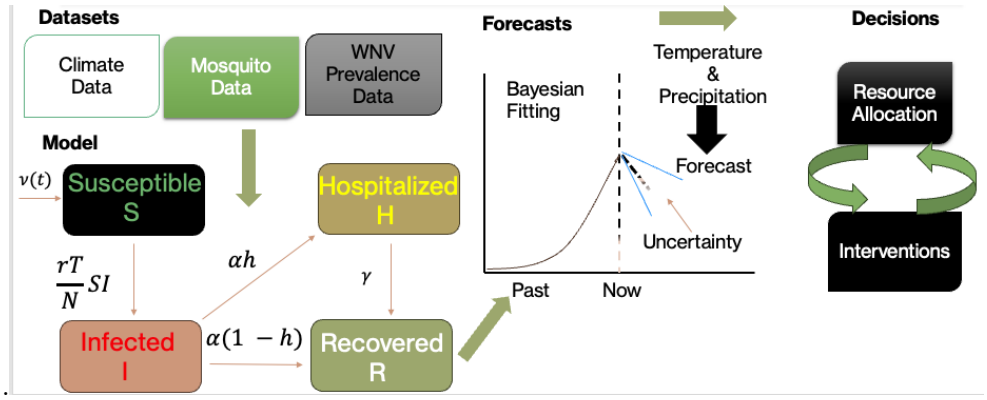

Figure 1: Approach overview

[1] Northern Arizona University

References:

[1] Center for Disease Control (CDC) WNV, 2024. https://www.cdc.gov/west-nile-virus/index.html (accessed on October 24, 2024).
[2] Hepp C, Cocking JH, Valentine M, Young S, Damian D, Samuels-Crow K, et al. Phylogenetic analysis of West Nile Virus in Maricopa County, Arizona: Evidence for dynamic behavior of strains in two major lineages in the American Southwest. PLoS One 2018; 13: e0205801.
[3] Waku J, Oshinubi K, Adam UM, Demongeot J. Forecasting the Endemic/Epidemic Transition in COVID-19 in Some Countries: Influence of the Vaccination. Diseases. 2023; 11(4):135.

Information and Optimization in Markov Decision Process Models of Drug Protocols

Jonathan Asher Pachter[*,1,2], Peng Chen[1,2], Michael Hinczewski[1], Jacob G. Scott[1,2,3]

[1]*Department of Physics, Case Western Reserve University, OH*
[2]*Translational Hematology & Oncology Research, Lerner Research Institute, Cleveland Clinic, OH*
[3]*School of Medicine, Case Western Reserve University, OH*
[*]jonathan.pachter@case.edu

Abstract

When a population of disease cells - such as a bacterial infection or a cancerous tumor - is exposed to a drug, the very treatment seeking to eradicate the disease can actually induce the emergence of a mutant strain that thrives in the presence of the drug [1, 2]. But sometimes the mutated population can now be particularly susceptible to a second drug - a phenomenon known as "collateral sensitivity" [3]. This suggests that cycling between different drugs in a specific sequence can be more effective than a single drug. But how does one decide which drug to administer, and when?

A Markov Decision Process (MDP) is a framework for modeling a system evolving stochastically under the influence of some control mechanism: at each time step, some action is taken which determines the transition probabilities for the evolution of the stochastic system in that time step [4]. Different actions are selected with different probabilities depending on the state of the stochastic system at that time - these probabilities are known as the protocol.

MDPs are a natural framework for modeling drug protocols in disease treatment: there is a choice at each time step of which drug to administer, and the genetic makeup of the population of disease cells then evolves stochastically in the presence of the drug. Given perfect knowledge of the genetic state of the disease as it evolves, as well as perfect knowledge of how every genotype responds to every drug, an optimal protocol can be found which is most likely to most effectively treat the disease (quantified by minimizing the expected fitness of the population).

Previous work from our research group [5] introduced some examples of drug protocols employing limited information and compared their performance to the most optimal protocol. Combining numerical simulations with analytical theoretical efforts, we are building on the previous paper to explore general properties of a tradeoff between information and optimality in MDP models of drug protocols. Besides uncovering new fundamental properties of constrained MDPs, this work could someday inform real clinical decisions regarding when to obtain genetic sequencing of a disease in the course of treating it, by quantifying the benefit of that increased information.

References

[1] Darby et al. "Molecular mechanisms of antibiotic resistance revisited" *Nature Reviews Microbiology* **2023**
[2] Vasan et al. "A view on drug resistance in cancer" *Nature* **2019**
[3] Roemhild et al. "Mechanisms and therapeutic potential of collateral sensitivity to antibiotics" *PLOS Pathogens* **2021**
[4] Zhao "Mathematical Foundations of Reinforcement Learning" *Springer Nature Press and Tsinghua University Press* **2025**
[5] Weaver et al. "Reinforcement learning informs optimal treatment strategies to limit antibiotic resistance" *Proceedings of the National Academy of Sciences* **2023**

Catastrophic changes in coral reef dynamics under macroalgal toxicity, elevated sea surface temperature (SST), overfishing and invasion of predators

Samares Pal
Department of Mathematics, University of Kalyani, Kalyani, India
samaresp@yahoo.co.in

Coral reef ecosystems are most vulnerable to changes in sea surface temperature (SST), a key environmental factor critical to reef-building growth. Elevated SST reduces the ability of corals to produce their calcium carbonate skeletons. Prolonged high SST results in coral bleaching owing to the uncoupling of symbiosis among corals and microalgae. Corals have narrow temperature tolerances. The skeletal growth rate of corals falls sharply to zero even at a slight increase of SST above its temperature tolerance level. Corals are also vulnerable to macroalgal toxicity. Several benthic macroalgae species are known to bring about allelopathic chemical compounds that are very harmful to corals. The toxic-macroalgae produce allelochemicals for which the survivability and settlement of coral larvae are highly affected. Toxic macroalgae species damage coral tissues when in contact by transferring hydrophobic allelochemicals present on macroalgal surfaces, leading to a reduction of corals and even coral mortality. The abundance of toxic macroalgae changes the community structure towards a macroalgae-dominated reef ecosystem.

Introduction:
Coral reefs are the most striking and different marine ecosystems in our globe. Productive and complex, coral reefs host hundreds of thousands of species, but few are described by science. Coral reefs are very well known for their biological diversity, beauty and high productivity [1]. Coral Reefs tend to exist in alternate coral or algae-dominated states [2, 3]. Faster-growing macroalgae always dominate coral reefs by making less available space for the successful settlement of coral larvae. Corals may die due to bleaching, and it takes decades to recover partially or completely. Most of the bleaching events occur when the temperature is at least one degree more than the temperature threshold.

In the present work, the main emphasis will be placed on the dynamic behaviour of coral reefs ecosystem due to increasing sea surface temperature. In our model, we have considered the effect of SST on the growth of corals. So, we take the recruitment of adult corals as a temperature-dependent function. We study how the changes in SST can lead to a change in the regime in coral reefs.

References:

[1] Hoegh-Guldberg Ove (1999) Climate change, coral bleaching and the future of the world's coral reefs. Marine and Freshwater Research 50, 839-866.

[2] Bruno JF, Sweatman H, Precht WF, Selig ER, Schutte VG. Assessing evidence of phase shifts from coral to macroalgal dominance on coral reefs. Ecology. 2009 Jun; 90(6):1478-84.

[3] Albins MA, Hixon MA. Invasive Indo-Pacific lionfish Pterois volitans reduce recruitment of Atlantic coral-reef fishes. Marine Ecology Progress Series. 2008 Sep 11;367:233-8.

Analyzing human behavior data and modeling the impact of human behavior on SARS-CoV-2 transmission dynamics

Binod Pant*

Abstract

The COVID-19 pandemic not only has profoundly impacted global health and socioeconomic systems, but has also significantly impacted human behavior toward adherence (or lack thereof) to public health intervention and mitigation measures implemented in communities around the world. However, a relatively small number of epidemiological models have attempted to assess the impact of human behavior on the dynamics of SARS-CoV-2 transmission. In addition, detailed characterizations of how population-level behaviors change over time during multiple disease outbreaks and spatial resolutions are not yet widely available. In this talk, a behavior-epidemiology model that incorporates multiple mechanisms of behavior change is presented. Although epidemiological models with differential susceptibility can exhibit backward bifurcation, we show that for a special case of the behavior-epidemiology model, the disease-free equilibrium is globally asymptotically stable when the associated reproduction number is less than one. In addition, data from 431,211 survey responses collected in the United States, between April 2020 and June 2022, are used to provide a description of how human behavior fluctuated during the first two years of the COVID-19 pandemic. Then, we explicitly incorporate survey-collected human behavior data into the epidemiological model—a feat that, to our knowledge, has not yet been accomplished in the case of COVID-19. We show that models that do not incorporate behavior tend to underestimate the basic reproduction number, thereby underestimating the disease's contagiousness in the early phase of an outbreak.

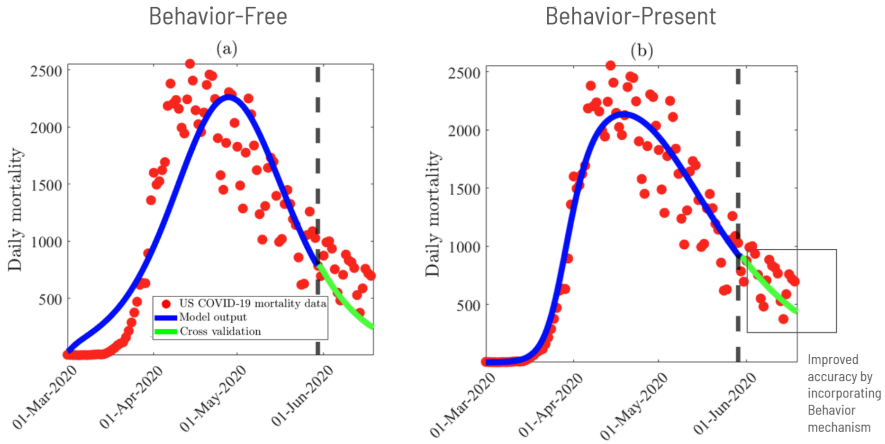

References

[1] Binod Pant, Salman Safdar, Mauricio Santillana, and Abba B. Gumel. "Mathematical Assessment of the Role of Human Behavior Changes on SARS-CoV-2 Transmission Dynamics in the United States." Bulletin of Mathematical Biology 86, no. 8 (2024): 92.

[2] Tamanna Urmi, Binod Pant, George Dewey, Alexi Quintana-Mathé, Iris Lang, James N. Druckman, Katherine Ognyanova, Matthew Baum, Roy H. Perlis, Christoph Riedl, David Lazer, Mauricio Santillana. "Characterizing Population-level Changes in Human Behavior during the COVID-19 Pandemic in the United States." medRxiv (2024): 2024-12.

*Network Science Institute, Northeastern University, Boston, Massachusetts, 02115, USA

A SIMPL Model of Phage-Bacteria Interactions Accounting for Mutation and Competition

Carli Peterson, Darsh Gandhi, Austin Carlson, Emma Richardson, Aaron Lubkemann, John E. Serralta, Michael S. Allen, Souvik Roy, Christopher M. Kribs, Hristo V. Kojouharov

Abstract

Pseudomonas aeruginosa is an opportunistically pathogenic bacteria that causes fatal infections and outbreaks in hospital environments. Due to the increasing prevalence of antibiotic-resistant strains of *P. aeruginosa*, the need for alternative therapies is critical. Bacteriophage therapy is emerging as a promising approach; however, it remains unapproved for clinical use and is hindered by limited understanding of the complex interactions between bacterial cells and phage virions. Mathematical models provide insight into these interactions. Through a system of ordinary differential equations, we successfully capture the dynamics observed between susceptible, infected, and mutated bacterial cells and bacteriophage virions in a microwell setting. Data fitting based on this model produced a set of parameter estimates unique to our experimental observations of a specific phage and *P. aeruginosa* strain. In translating observed optical density readings into bacterial concentrations, we also found that bacterial debris has a significant impact on optical density, with a lysed bacterium contributing roughly 31% as much to optical density readings as a living cell.

References

[1] C Peterson, *et al*. A SIMPL Model of Phage-Bacteria Interactions Accounting for Mutation and Competition. *Submitted Aug 2024, resubmitted Apr 2025*.

On Gaussian process methods for inferring genotype-phenotype maps

Sam Petti * Carlos Martí-Gómez [†] Justin B. Kinney[†] Juannan Zhou[‡]
David M. McCandlish[†]

Abstract

One of the main goals of genetics is understanding how biological sequences, such as DNA or proteins, determine observable phenotypes. Recent advancements in high-throughput phenotyping technologies, such as deep mutational scanning, have enabled the generation of vast datasets that map sequence variants to biological functions, allowing us to study genotype-phenotype maps at an unprecedented scale. However, standard regression models used for analyzing these datasets, such as additive and pairwise interaction models, often make unrealistic assumptions about the generalizability of mutational effects, limiting our understanding of the inferred genotype-phenotype map. Gaussian process regression models naturally circumvent these limitations by setting a prior distribution on the set of possible genotype-phenotype maps. We (1) introduce a tractable and expressive family of priors, (2) establish the relationship between Gaussian process regression, regularized regression, and gauge-fixing, and (3) describe a kernel trick for efficiently computing statistics of genotype-phenotype maps. Overall, our framework unifies and extends our ability to infer and interpret genotype-phenotype maps. **Oral talk preferred.**

1 Expressive priors for modeling genotype-phenotype maps with Gaussian process regression

We developed new Gaussian process priors with interpretable site-, allele- and mutation-specific hyperparameters that control the extent to which each possible mutation decreases the predictability of the effects of other mutations. Leveraging GPU-based methods, we overcome traditional scalability limitations, infer our interpretable hyperparameters through evidence maximization, and make phenotypic predictions in datasets containing hundreds of thousands of measurements. We demonstrate the power and versatility of these methods across diverse datasets, including nearly complete data of short protein and regulatory sequences, as well as sparser data from longer proteins and SNPs across the yeast genome.

2 Relationship between regularized regression, gauge-fixing, and Gaussian process regression

One way to interpret a genotype-phenotype map is to decompose the map in a way that elucidates the contributions of individual subsequences. Because any genotype-phenotype map can be written as a weighted sum over subsequences in multiple ways, meaningfully interpreting these weights requires "gauge-fixing," i.e., defining a unique representation for each map. Recent work has established that most gauge-fixed representations arise as the unique solutions to L_2-regularized regression in an overparameterized "weight space" where the choice of regularizer defines the gauge [1]. We establish the relationship between regularized regression in overparameterized weight space and Gaussian processes that operate in "function space," i.e. the space of all real-valued functions on a finite set of sequences. We disentangle how weight space regularizers both impose an implicit prior on the learned function and restrict the optimal weights to a particular gauge. We also show how to construct regularizers that correspond to arbitrary explicit Gaussian process priors combined with a wide variety of gauges and characterize the implicit function space priors associated with common weight space regularizers.

3 A kernel trick for computing statistics of genotype-phenotype maps

We establish a kernel trick for efficiently computing the posterior distribution (under function space Gaussian process) of a large class of statistics of genotype-phenotype maps without having to compute the full map. This class includes gauge-fixed weights and epistastic coefficients, providing efficient estimates and uncertainty bounds for these often interpreted quantities.

References

[1] Posfai A, Zhou J, McCandlish DM, Kinney JB. *Gauge fixing for sequence-function relationships.*, PLoS Comput Biol., 21 (2025)

*Department of Mathematics and Department of Computer Science, Tufts University, Medford, MA, 02155
†Simons Center for Quantitative Biology, Cold Spring Harbor Laboratory, Cold Spring Harbor, NY, 11724
‡Department of Biology, University of Florida, Gainesville, FL, 32611

Uncovering the hierarchical organization of human multilayer gene regulatory networks

Maalavika Pillai[1], Karla Medina[1], Liebe Cho[2], Vadim Backman[3,4], Luís A.N. Amaral[5,6,7,8]

Gene expression is tightly controlled by several small-scale networks of gene interactions that coalesce to form larger global gene regulatory networks (GRNs). The architecture and topology of these networks determine the expression levels and dynamics of its gene components, thereby regulating the phenotype of a cell. [1,2] While previous research has uncovered how certain network structures give rise to specific phenotypes [3], most studies assume that these networks are static, i.e., there are no changes in the structure of the regulatory network over time. They also often fail to account for the nano-scale interactions between transcription factors (TFs), DNA, histone proteins and RNA Polymerase that control transcription. In this work, we model gene expression using a dynamic multi-layered network, where each layer represents a distinct mode of transcriptional regulation captured using high throughput sequencing, such as, variations in chromatin accessibility (ATAC-seq) or the spatial distribution of histone modifications (ChIP-seq). Using a stochastic block model framework [4], we identify groups of genes in the network corresponding to specific transcriptional states, i.e., genes with similar accessibility profiles and histone modification distributions. Lastly, we use our model to identify changes in transcriptional states when genome connectivity is disrupted and validate our findings against changes in the spatial distribution of TFs, RNA Polymerase II, and histone modifications measured using super-resolution microscopy. Overall, we create a framework that combines super-resolution microscopy and multi-layered network-based analysis of high throughput sequencing data to quantify the association between transcription and changes in chromatin organization.

References

[1] R. Guimera and L. A. Nunes Amaral, "Functional cartography of complex metabolic networks," Nature (2005).
[2] R. Guimera and L. A. N. Amaral, "Cartography of complex networks: modules and universal roles," Journal of Statistical Mechanics: Theory and Experiment (2005).
[3] A. Boyle, C. Araya, C. Brdlik et al. "Comparative analysis of regulatory information and circuits across distant species," Nature (2014).
[4] T. P. Peixoto, "Hierarchical block structures and high-resolution model selection in large networks," Phys. Rev. X (2014).

[1] Interdisciplinary Biological Sciences, Northwestern University
[2] Quantitative and Systems Biology, Northwestern University
[3] Center for Physical Genomics and Engineering, Northwestern University
[4]Department of Biomedical Engineering, Northwestern University
[5] Department of Engineering Sciences and Applied Mathematics, Northwestern University
[6] Department of Molecular Biosciences, Northwestern University
[7] Northwestern Institute on Complex Systems, Northwestern University
[8] NSF-Simons National Institute for Theory and Mathematics in Biology, Northwestern University

Was lockdown the optimal strategy? Insights for devising intervention and control frameworks using Compartmental Modeling: A case study of COVID-19 transmission in Illinois

Suraj Powar* Dashun Xu*

*Department of Mathematical and Statistical Sciences, Southern Illinois University, Carbondale, IL, USA - 62901

Abstract

The year 2020 witnessed a global outbreak of an infectious disease—COVID-19—that severely impacted not only public health but also the world economy. The prolonged spread of the disease led to a pandemic and countries around the world had to exercise lockdown. It had become a pressing need for robust mathematical modeling that can handle this pandemic. To understand the dynamics of such outbreaks, epidemiological models are essential tools for analyzing disease behavior based on real-world data. There are a plethora of studies conducted by other researchers to study disease transmission in many countries. The USA has a peculiar geography where some areas of the country are densely populated and some are sparsely. This diversity is related to population and topographic dynamics, which is why USA become a good case study for our work. We chose to study Illinois state because the diversity that we have in the USA can be expressed as the diversity of Illinois state. We propose an approach for policymakers that will employ disease transmission and dynamics of the population to create optimal intervention measures that can be adopted in the future if we are hit by another disease.

We used compartmental model for our analysis based on SEIR model. Our modeling approach is divided into two phases corresponding to the initial and later stages of the COVID-19 outbreak. The process was deliberately broken into two phases from the beginning of the disease spreading till 21st March 2020, and the second phase ended on 5th May 2020, which was advised by the governor of Illinois state. We analyzed data from all 102 counties in Illinois, and used a parameter estimation technique to fit the model and derive contact rates for each phase. The method we used to fit the model was the Nelder-Mead technique. The estimated basic beta (transmission rate) values were used to assess the spread of the disease across the state. We define basic beta as $\beta = \beta_{\text{disease}} \cdot \beta_{\text{population}}$. The β_{disease} is a disease-related transmission rate which can be different for different epidemic diseases, but $\beta_{\text{population}}$ is the contact rate in terms of movement which is county-specific as it depends on population density or lifestyle of the population, which is not likely to change over a relatively long period. We derived the $\beta_{\text{population}}$ based on a geometric approach for understanding the contact rate and movement among the population in a given county. Later, we disintegrated the total population in terms of the impact of disease spread. To achieve this, we used a machine learning technique, Gaussian Mixture Model clustering, to classify the counties based on their transmission rate.

According to our investigation, our analysis shows varied rates of disease transmission, ranging from nearly 6 to 0. We classified the regions based on this disease transmission rate, by separating Cook County as it showed the highest transmission value (nearly 6) see (Figure 1). We treated Cook county as a high impact zone. We then divided the remaining counties due to higher heterogeneity at rates of 2, 1, and 0.5 into blue, mid-blue, and white. This means that the blue ones are infectious relative to 2 and 0.5, so they can be treated as a medium impact zone. The transmission rate with value 0 does not need immediate action because the control measures were treated as a low impact zone. The idea is that we do not need to generalize the lockdown state-wise. If we can focus our attention on county-wise lockdown, the disease's spread can be controlled efficiently. We can see in (figure 2) the contour of beta values where we used gaussian interpolation for smooth contouring of the beta values based on GIS data to get insight into the transmission between two counties as shown in (Figure 3). Furthermore, we used this beta rate for Gaussian Mixture Model clustering and observed that we have one cluster with Cook, Sangammon, St.

Clair and Champaign counties as we can see in (Figure 4). We also observed that the contour surface map reveals the cities associated with these counties have a higher rate of transmission due to interpolation of counties based on Geographic Information Systems data. In the end, we studied the difference in time-delay between county cases when the covid outbreak hit Illinois. Found the variation of case growth in terms of heterogeneity of the population.

It is our modest attempt to suggest governors to use different control strategies when a new disease hits for control and interventions so that they can use our study to classify the counties in different zones and impose restrictions on them as opposed to state-level lockdown. This work may provide some insights for policymakers to devise strategies for controlling outbreaks if we were to be hit by any epidemic in the future.

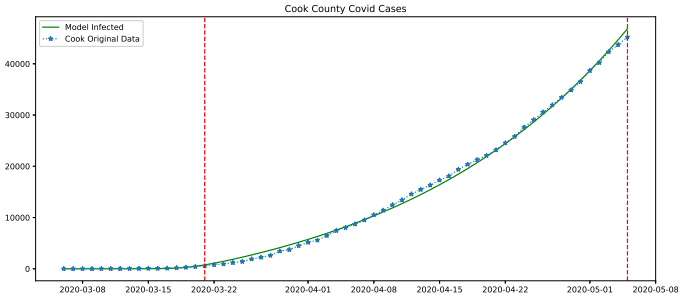

Figure 1: Cook County Model Fitting

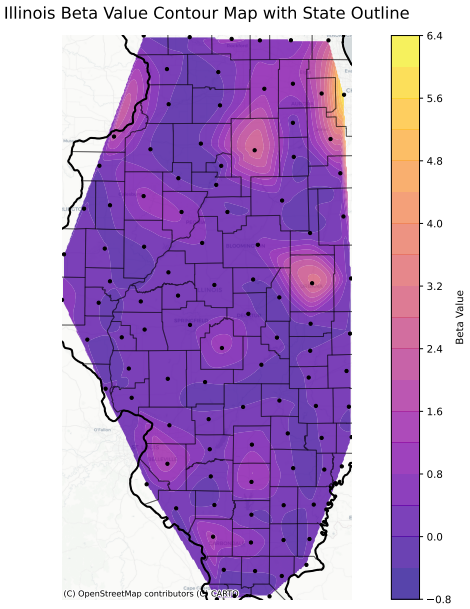

Figure 2: Contour Map using β

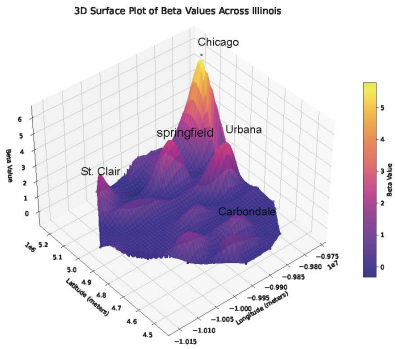

Figure 3: 3-d Surface Plot

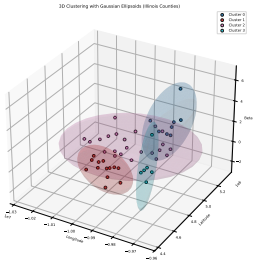

Figure 4: Gaussian Mixture Model clustering

Advancing Treatments of Tourette Syndrome via Thalamo-Cortical Modelling

Angelica Pozzi[1], Stephen Coombes[1], Reuben O'Dea[1], Stephen Jackson[2]

Tourette Syndrome (TS) is a common neurological disorder characterised by motor and vocal tics, affecting approximately 1 in 100 children. Although it is more prevalent among children, many adults continue to experience significant symptoms. Tourette's is associated with thalamo-cortical circuit dysfunction, but a precise mechanistic explanation is lacking. Recent studies have shown that non-invasive median nerve stimulation (MNS) can help reduce tics, highlighting the need for a deeper exploration of the brain circuits involved to improve the design of healthcare treatments utilising wearable devices.

Here, we develop a mathematical model of the thalamo-cortical loop in the context of TS. We couple a neural mass model of the cortex, capturing the interplay between excitatory and inhibitory populations, with a mean-field model of the thalamus, incorporating interactions between reticular and thalamo-cortical cells (expressing so-called rebound currents). We first analyse these subsystems independently using bifurcation theory before coupling them. Neuroimaging data (MEG/EEG) inform model parameters to replicate power spectrograms observed in both healthy individuals and TS patients undergoing MNS. To gain a deeper understanding of such responses, we determine the Arnol'd tongue structure of the network model in response to periodic forcing via a numerical calculation of the largest Lyapunov exponent. This is complemented with an analytical study of the tongue borders using tools from coupled oscillators and Floquet theory. Our findings provide a foundation for in-silico testing of neurostimulation protocols to optimise treatment strategies for TS.

[1] School of Mathematical Sciences, University of Nottingham, Nottingham, UK
[2] School of Psychology, University of Nottingham, Nottingham, UK

Modeling Microtubule-Associated-Proteins (MAPs) driven Phase Separation

Sayandeepa Raha[1], Kelsey Gasior[2], Holly V. Goodson[1]

1. Department of Chemistry and Biochemistry, University of Notre Dame
2. Department of Applied and Computational Mathematics and Statistics, University of Notre Dame

Microtubules (MTs) are energy-utilizing cytoskeletal polymers that play critical roles in cellular organization and intracellular transport. Many of these functions rely on regulation of microtubule dynamics by microtubule associated proteins (MAPs). MT plus-end tracking proteins (+TIPs) are a structurally and functionally diverse group of MAPs that localize dynamically to growing MT plus ends. +TIPs bind to each other in a complex network of intra- and inter-molecular interactions that create regulatory pathways and also help localize proteins to their site of action. However, these interactions also enable the +TIP network to undergo liquid-liquid-phase-separation (LLPS). LLPS has been clearly observed in vitro or when overexpressed in cells – our lab has proposed that these structures are biomolecular condensates that act as polymerization chaperones, increasing the rate of polymerization by zipping up lateral bonds between protofilaments that constitute the microtubule lattice. To biophysically characterize these condensates, we have developed a mathematical model that incorporates the Cahn-Hilliard diffuse interface phase field model, the Flory-Huggins free energy scheme, and mass-action kinetics to study how MAP-microtubule interactions can drive LLPS. This model examines the dynamics of two different MAP species that diffuse and interact on the microtubule lattice to form a complex that can drive phase separation when bound to the MT. While the two MAPs are governed by standard reaction-diffusion dynamics, it is their complex (C_1) that produces the observed condensates. Using this system, we demonstrate how interactions between MAPs and the microtubule lattice give rise to a diverse range of behaviors—including droplet dynamics and intradroplet patterning—and how condensate formation is modulated by biophysical parameters such as protein diffusivity and reversible reaction kinetics. **This modeling framework enables us to explore key biological questions, including:** *What biophysical conditions drive MAPs to form phase-separated condensates on the microtubule lattice? How do variations in protein diffusivity and reaction kinetics influence condensate size, number, and internal organization? How does MAP binding to and release from the MT lattice control the spatial patterning of condensates?* We are currently extending the model to incorporate **periodic boundary conditions** to better represent the cylindrical geometry of microtubule allowing for more realistic simulation of condensate spreading and patterning along the circumferential surface of the microtubule lattice. Together, this modeling framework offers a powerful tool for probing the physical principles underlying MAP-driven condensate formation while revealing its role in spatial and temporal regulation of MT dynamics.

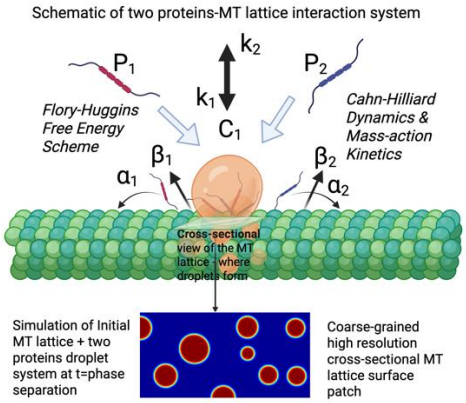

Refernces:
1. Wu YFO, Bryant AT, Nelson NT, Madey AG, Fernandes GF, et al. (2021), Overexpression of the microtubule-binding protein CLIP-170 induces a +TIP network superstructure consistent with a biomolecular condensate. *PLOS ONE*, 16(12): e0260401.
2. Gasior, K., Zhao, J., McLaughlin, G., Forest, M. G., Gladfelter, A. S., and Newby, J. (2020). Partial demixing of RNA-protein complexes leads to intradroplet patterning in phase-separated biological condensates. *Physical Review E*, 101(1), 012411.

Understanding Nonequilibrium Steady State(s) in Dynamical Systems of Microtubules

Sayandeepa Raha[1], Alexander Simmons[1], Alan Lindsay[2], Holly V. Goodson[1]
1. Department of Chemistry and Biochemistry, University of Notre Dame
2. Department of Applied and Computational Mathematics and Statistics, University of Notre Dame

Microtubules (MTs) are energy-utilizing cytoskeletal polymers found in all characterized eukaryotic organisms. MTs display an energy-driven behavior called 'Dynamic Instability' (DI). DI is characterized by stochastic switching between phases of growth and shortening, separated by abrupt transitions called catastrophe and rescue, and is central to the functionality of MTs. MTs are steady-state (non-equilibrium) polymers, requiring a constant input of GTP to maintain a particular level of polymerization. A predictive understanding of MT dynamics and other steady-state polymers requires studying them across multiple scales and determining the relationships between these scales. Here, we aim to quantitatively profile the distinct steady states in a dynamical system of MTs and predict the relationship between the time to reach these steady states and parameters like tubulin concentration. We employ a previously established agent-based model, where MT subunits (tubulin dimers) act as agents governed by rules based on experimentally tuned kinetic parameters, and macro-level behaviors (e.g., MT DI, polymer mass) are emergent properties of the simulation. In this project, we have found that there exist at least three different steady states that a system of microtubules can achieve: GTP-cap-steady-state, polymer-growth-rate-steady-state (of which polymer-mass-steady-state is a special case), and length-distribution-steady-state. We have identified a set of equations that can be used to estimate the time to reach these steady states and show that they work for both plus and minus ends. In this poster, we focus on the polymer mass steady state**,** and show that both the shapes of the (a) poly mass vs. time curve and the (b) steady-state dynamics display an intriguing 'statistical equivalence' at different tubulin concentrations. This behavior is called 'affine invariance' and enables us to predict both the time to reach the steady state (e.g., T_{50}, T_{95}) and the steady-state polymer mass ($PolMass_{NESS}$) for *any* concentration of free tubulin below the critical concentration for net assembly (CC_{NA}), given T_{50} and $PolMass_{NESS}$ at as few as two other concentrations. The modeling framework and results we provide here aid experimental design and interpretation while providing a deeper multiscale understanding of steady-state polymers.

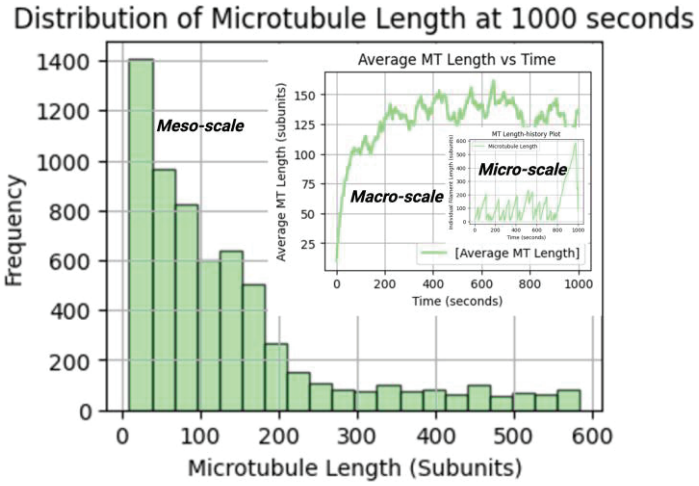

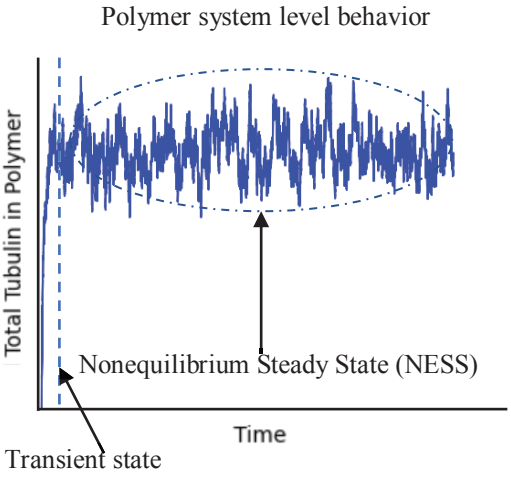

References:

1. Goodson HV, Jonasson EM. Microtubules and Microtubule-Associated Proteins. Cold Spring Harb Perspect Biol. 2018.
2. Jonasson…Goodson Behaviors of individual microtubules and microtubule populations relative to critical concentrations: dynamic instability occurs when critical concentrations are driven apart by nucleotide hydrolysis, MBoC 2021.
3. Margolin et al…Goodson The mechanisms of microtubule catastrophe and rescue: implications from analysis of a dimer-scale computational model, MBoC 2012.
4. Margolin et al…Alber Analysis of a mesoscopic stochastic model of microtubule dynamic instability Physical Review E, 2006
5. Xue-Juan Zhang…Min Qian, Stochastic theory of nonequilibrium steady states and its applications. Part I, Physics Reports, Volume 510, Issue s 1-2, January 2012.
6. Hao Ge… Hong Qian, Stochastic theory of nonequilibrium steady states. Part II: Applications in chemical biophysics, Physics Reports, Volume 510, Issue 3,2012.
7. Da-Quan Jiang…Min-Ping Qian, Mathematical Theory of Nonequilibrium Steady State, Springer 2006.

Tug-of-war in axonal transport: a model of large vesicle transport driven by kinesins and dynein

Nizhum Rahman
University of Michigan and
School of Mathematics and Physics, University of Queensland

Dietmar Oelz
School of Mathematics and Physics, University of Queensland

Abstract

We develop a mathematical model to investigate the axonal transport of large cargo vesicles, focusing on their mechanical interaction with the axon's membrane-associated periodic cytoskeletal structure (MPS), which consists of regularly spaced actin rings arranged transversely to the axonal axis.

To capture the coupling between vesicle motion and the MPS, we construct a system of force-balance equations that incorporate viscoelastic Kelvin-Voigt elements. By applying a homogenization technique, we reformulate the system as a free boundary problem and derive a nonlinear force-velocity relationship in the quasi-steady-state regime. The model reveals that transport velocity decreases with increasing cargo size.

We extend the analysis through numerical simulations that incorporate the forces generated by molecular motors and those exerted by contractile transverse actomyosin rings. The results reproduce experimentally observed phenomena, including bidirectional transport interspersed with pauses. Furthermore, our simulations suggest that the prolonged anterograde phases observed under blebbistatin treatment during retrograde-biased transport can be attributed to stretch-induced mechanotransductive recruitment of myosin motors into actin rings. These findings shed light on the dynamic mechanical regulation of axonal transport and offer testable hypotheses for future experimental work.

Information-theoretic Emergence in Biological Complex Systems

Hardik Rajpal* Fernando Rosas† Omar El Oakley‡ Pedro Mediano* Katie Bentley‡
Malcolm Logan§ Henrik Jeldtoft Jensen*

Abstract

The study of *Emergence* has been central to understanding various complex systems. It is the property of a system with many components exhibiting non-trivial collective behaviour that cannot be attributed to the individual components. Furthermore, in many cases, the emergent collective behaviour can guide the future evolution of the components of the system by constraining their dynamics. In biological systems, the spontaneous emergence of order from interacting proteins, cells and organisms is observed throughout the tree of life. Therefore, understanding the mechanisms that drive biological emergence is crucial to answering questions about evolution, morphogenesis and consciousness.

Recent advances in information theory have enabled the quantification of emergence in complex systems [1, 2, 3]. Here, we use the framework of causal emergence proposed by Rosas et. al. [2] to quantify statistical dependencies across different scales of a system. The computationally efficient estimators of causal emergence and downward causation proposed in the original work can be used to identify the presence of emergence in a system and the mechanisms that drive it. We apply these methods to study emergence in three distinct biological systems: (1) higher-order cooperation among species in ecological evolution, (2) coordinated motion of fibroblast cells in muscle tissue and (3) synchronised oscillations in a network of interacting neurons. In each case, we show that the emergence of collective behaviour can be quantified by quantifying the information processing between the macro behaviour and the micro components of the system. Beyond the quantification of emergence, we also explore how these measures can be used to identify the underlying mechanisms crucial for the collective behaviour observed in these systems.

We use computational agent-based models that capture the essential dynamics of the biological systems mentioned above. These models can reproduce the emergent behaviour and be modified to study the effect of different mechanisms on the collective behaviour. Furthermore, the large number of simulations generated by these models allows us to estimate the marginal and joint probability distributions necessary for the estimation of information-theoretic measures.

First, we use the Tangled Nature model to study the emergence of groups of interacting species that maximise their joint persistence, using the framework of *Information Individuality* [4]. Next, we study the collective organisation of the extracellular matrix (ECM) using an agent-based model of fibroblast cells. We show that the ECM is causally emergent from the coordinated motion of fibroblast cells. However, when the model is used to simulate fibroblast activity observed in Radial Dysplasia, the emergence of the ECM is disrupted. Finally, we study the emergence of synchronised oscillations in a network of interacting neurons in A Pyramidial Inter-nuron Gamma (PING) model. We show that the synchronised oscillations are emergent and have a downward causal influence on the future activity of individual neurons. We also validate our findings on spiking data obtained using Neuropixel probes from the mouse visual cortex.

The framework of causal emergence provides a powerful tool to quantify and probe the emergence of collective behaviour in biological systems. It allows the identification of the mechanism implicated in diseased states and the development of interventions to restore the healthy emergent behaviour.

References

[1] Erik P Hoel, Larissa Albantakis, and Giulio Tononi. Quantifying causal emergence shows that macro can beat micro. *Proceedings of the National Academy of Sciences*, 110(49):19790–19795, 2013.

[2] Fernando E Rosas, Pedro AM Mediano, Henrik J Jensen, Anil K Seth, Adam B Barrett, Robin L Carhart-Harris, and Daniel Bor. Reconciling emergences: An information-theoretic approach to identify causal emergence in multivariate data. *PLoS computational biology*, 16(12):e1008289, 2020.

[3] Lionel Barnett and Anil K Seth. Dynamical independence: discovering emergent macroscopic processes in complex dynamical systems. *Physical Review E*, 108(1):014304, 2023.

[4] Hardik Rajpal, Clem von Stengel, Pedro AM Mediano, Fernando E Rosas, Eduardo Viegas, Pablo A Marquet, and Henrik J Jensen. Quantifying hierarchical selection. *arXiv preprint arXiv:2310.20386*, 2023.

*Imperial College London
†University of Sussex
‡Francis Crick Institute
§King's College London

The role of apical junctional protein NMII in regulating epithelial morphology in Mouse villus

Dominik Robak[1], **Soumyadipta Ray**[2], Dipjyoti Das[3], Lishibanya Mahapatra[2], Seham Ebrahim[1]

Abstract

Robust tissue structure and functioning is essential in various physiological processes, such as morphogenesis, tissue homeostasis, and tissue remodelling, and an alteration may indicate a pathological situation [1]. While physical properties of the cellular environment, including cellular forces, and cell-cell interaction may largely affect the tissue-scale properties and organisation. It is still not well understood that how the cell level physical properties control the tissue-scale morphology. Here, we focus on an epithelial junctional protein NMII (Nonmuscle myosin II) within mouse villi epithelia, specifically one of its isoforms, NMIIC, which is responsible for mediating junctional forces and tissue homeostasis [2].

The NMIIC proteins are organised in a periodic puncta-like manner along the cell-cell junctional line and help maintain a regular epithelial morphology (Fig 1A). Experiments reveal that in the absence of NMIIC, these cells recruit another isoform NMIIA puncta along cell periphery which significantly alters the tissue organisation. We observe distortions in cell shapes and cell edges (Fig 1B), which suggests a substantial change in junctional forces.

In order to understand what roles the junctional proteins play tissue morphology, we developed a two-dimensional active force-based model of tissue monolayers, where each cell is a soft deformable object made of beads and springs (Fig 1C). The beads serve a coarse-grained representation of the NMII puncta across the cell periphery. Our model reveals that the increasing bead number and its heterogeneity across cells results in irregular tissue morphology (Fig 1(D-E)) with long tailed shape index distribution and curved cell edges as seen in experiments - Finally, our model makes other predictions that can be tested in experiments, such as increasing bead number will lead to a decrease in the overall tissue tension. Thus, our results and simulation framework offer potential mechanistic insights that may open up new avenues in developmental biology and physiology.

[1] MPBP, University of Virginia, VA, USA

[2] Dept. of Physics, RIT, Rochester, NY, USA

[3] Dept. of Biol. Sc., IISER Kolkata, India

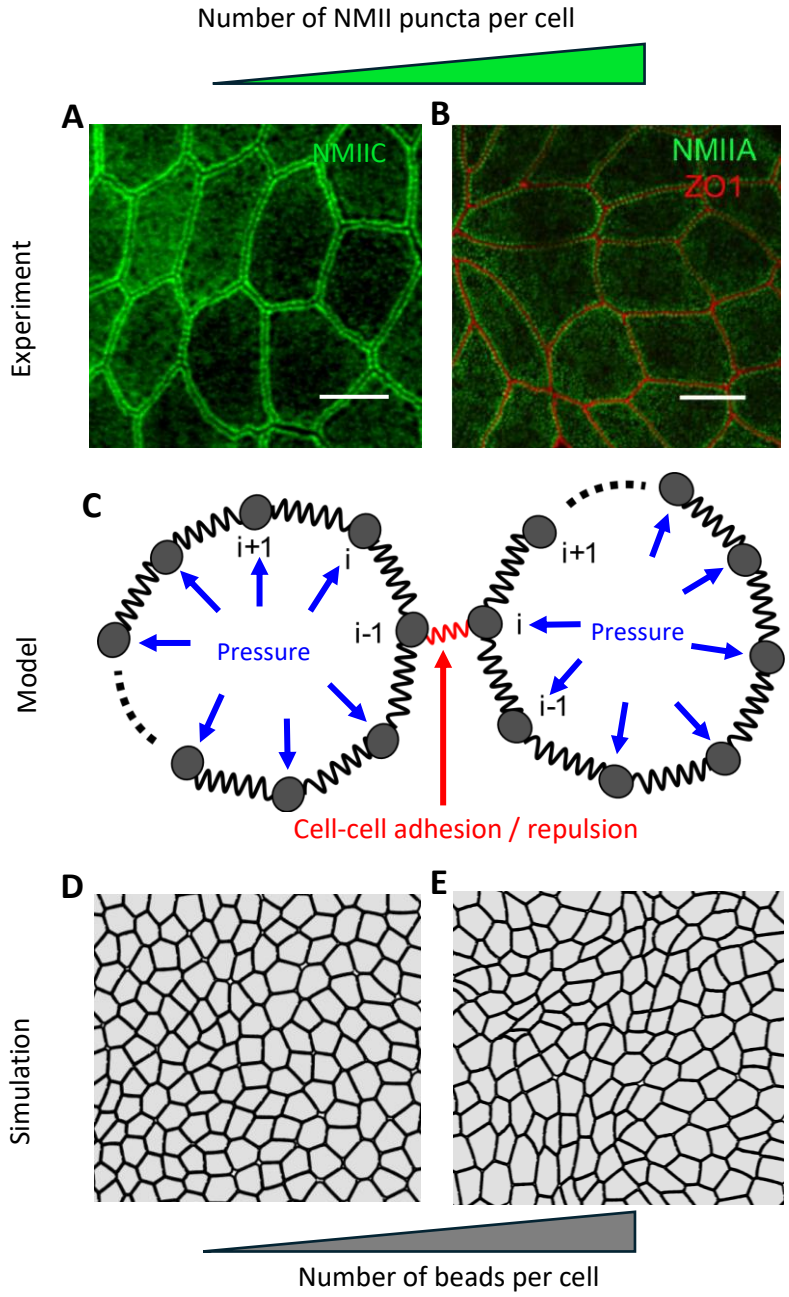

Fig 1. (**A-B**) Tissue morphology in mouse villi epithelia. (A) Regular polygonal cell shapes in WT cells (with NMIIC), while the tissue geometry gets distorted when NMIIC is knocked out (B). Notably, the number of NMII puncta per cell increases upon NMIIC knocked out. ZO1 is a junctional protein that acts as a junction marker. (**C**) Schematic of our 2D bead-spring model of cells. Each cell comprises of beads and springs, having internal outward pressure. Two cells interact via spring-like adhesion or repulsion. (**D-E**) Simulation snapshots of tissue with lower bead number (D), that resembles panel A, and with higher bead number and heterogeneity (E), accompanying panel B. Scale bar 10 μm.

References:

[1] C. Guillot and T. Lecuit, Mechanics of Epithelial Tissue Homeostasis and Morphogenesis, Science **340**, 1185 (2013).

[2] S. Ebrahim et al., NMII Forms a Contractile Transcellular Sarcomeric Network to Regulate Apical Cell Junctions and Tissue Geometry, Current Biology **23**, 731 (2013).

Rayleigh-friction driven models of collective dynamics: Flocking, Consensus, and Synchronization

David Nicholas Reynolds (Universidad de Granada)

August 2025

Abstract

We will discuss three closely related models that govern the collective dynamics of agents. All three models, have an external Rayleigh-friction and self-propulsion type forcing that drives each individual agent. Agents are further coupled pushing them towards an agreement whether that be velocity alignment (flocks o f b irds), c onsensus (opinion dynamics), or phase-locking (synchronization). The first c ontext i s a biologically-inspired flocking a nd a lignment m odel, w here t he f amous Cucker-Smale model (2007) has been appended with the friction and self-propulsion force, driving each agent to a common velocity. The result is achieved via a grassmannian reduction method that reduces the problem to an essentially two dimensional system, where we can take advantage of the dissipative structure. Reducing to a first-order s ystem t he m odel c an be seen as a nonlinear consensus model for opinion dynamics, where the friction force functions as a stubbornness term. This model is related to the Taylor model (1968) of opinion dynamics, however, the nonlinear force in our model captures more rich asymptotic behavior, including stable disagreement fixed p oints. F inally, a llowing for complex-valued stubbornness parameters results in the coupled Stuart-Landau model of synchronization, which is closely related to the Kuramoto model (1975). The Stuart-Landau system has been used extensively within the neuroscience community to model mesoscopic brain activity, however rigorous mathematical justification of t he model h ave p roved e lusive. We will investigate convergence to the various asymptotic states of this model focusing on the effects of allowing heterogeneous amplitude parameters.

Keywords: emergence, flocking and alignment, Cucker-Smale model, Consensus, Nash Equilibrium, Synchronization, Amplitude Death, Stuart-Landau oscillators

A Novel Mathematical Model of Oropouche Virus

Austin Carlson[1], Amira Claxton[1] , Darsh Gandhi[1] , Carli Peterson[1] , Elizabeth Rubio[1] , Emma Slack[1] , Christopher M. Kribs[1]

Abstract

Oropouche virus (OROV) is a vector-borne arbovirus that has caused more than 500,000 infections across South America, Central America, and the Caribbean. Its primary vector, *Culicoides paraensis*, acquires the virus from wild reservoir species and transmits it to humans during blood feeding. As outbreaks within the Amazon basin continue to occur and confirmed cases steadily increase, a proper understanding of the interplay between climatic variables, vector behavior, and OROV transmission is crucial to develop effective public health interventions. In this paper, we develop a novel mathematical model of Oropouche virus spread in Amazonas, Brazil using non-autonomous ordinary differential equations (ODEs). We present qualitative and quantitative analyses, emphasizing how seasonality influences midge biting rates and population trends and, in turn, disease prevalence. Our results offer insights into the conditions necessary for the persistence of OROV and demonstrate the critical role of seasonality in shaping transmission dynamics.

[1] The University of Texas at Arlington

Dynamic Homeostasis in Relaxation and Bursting Oscillations

Christopher J. Ryzowicz * Richard Bertram* Bhargav R. Karamched*

April 12th, 2025

Abstract

Many physiological systems, from gene networks to whole organisms, exhibit homeostasis to keep certain variables within a given range despite fluctuations in their environment. Previous studies on modeling homeostasis rely on the physiological regulation taking the form of control to a static equilibrium [1, 2]. However many physiological processes are inherently oscillatory (e.g. body temperature, insulin secretion, and gene expression), prompting the need for a more dynamic framework. In this study, we explore *dynamic homeostasis* [3], a reemerging concept that extends the classical regulation of static equilibria to oscillatory systems by considering the time-average of a species. Using the FitzHugh-Nagumo model [4, 5], a canonical system for excitable neurons, we show the time-average of the slow variable is invariant across a range of input stimuli. The range of the homeostatic plateau can be tuned by changing the parameter that controls the strength of the feedback. We also investigate the minimal Chay-Keizer model [6], a 3-variable model that captures bursting patterns in pancreatic β-cells. We show the time-average for the calcium concentration (the slow variable) is invariant with respect to the calcium pump rate parameter. In addition, we incorporate stochasicity into both models and show dynamic homeostasis is preserved and in some cases extended over a larger parameter range compared to the deterministic counterpart. These findings suggest that relaxation and bursting oscillations can serve as a general framework for modeling dynamic homeostasis.

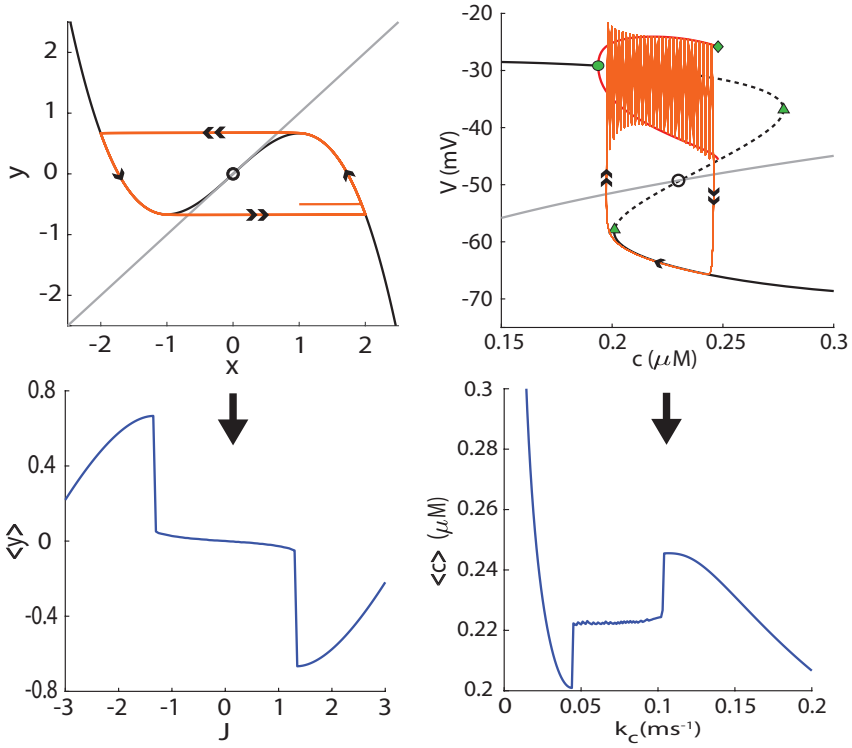

Figure 1: Dynamic homeostasis in slow variable time-average in FitzHugh-Nagumo model (left column) and the minimal Chay-Keizer model (right column). Phase space with sample trajectory (top) and homeostatic chair curve (bottom).

*Department of Mathematics, Florida State University, Tallahassee, Florida, 32306, USA

References

[1] M. Reed, J. Best, M. Golubitsky, I. Stewart, H. Frederik Nijhout, *Analysis of Homeostatic Mechanisms in Biochemical Networks*. Bulletin of Mathematical Biology. 2017.

[2] H. Frederik Nijhout, J. Best, M. Reed, *Escape from homeostasis*. Mathematical Biosciences. 2014.

[3] L. Xiong, A. Garfinkel, *Are physiological oscillations physiological?* The Journal of Physiology. 2023.

[4] R. FitzHugh, *Impulses and physiological states in theoretical models of nerve membrane* Biophysical Journal. 1961.

[5] J Nagumo, S. Arimoto, S. Yoshizawa, *An active pulse transmission line simulating nerve axon*. Proceedings of the IRE. 1962.

[6] T.R. Chay, J Keizer, *Minimal model for membrane oscillations in the pancreatic beta-cell*. Biophysical Journal. 1983.

Modeling bias in decision-making attractor networks

Safaan Sadiq* Carina Curto †

Abstract

In attractor network models for decision-making circuits, basins of attraction can be used as a model for bias. For decisions represented by attractors, the relative volumes of their basins of attraction encode the relative bias towards each of them. The same parameters of an attractor network encode both the set of attractors and the basins of attraction, but it is established that the framing of a decision can affect preferences. Given this, to what extent can the basins be encoded separately from the attractors? In other words, can bias be encoded separately from decisions? We investigate this question in the context of threshold linear networks (TLNs), a common type of firing rate model with recurrent network dynamics. We consider three ways that basins may encode biases which assume high dimensional, low dimensional, and path-following dynamics respectively. We show that, in the case of a competitive model of two neurons, we can analytically calculate basins of attraction and demonstrate how parameters can be used to reshape them while preserving the set of attractors. Lifting the problem into larger networks, we consider TLNs which correspond to directed graph structures which are known to fix their attractor set. We show how, under assumptions of lower dimensional dynamics, the combinatorial properties of the underlying directed graph can be associated with the encoded decision-making biases even if analytic solutions for the basins of attraction are challenging to obtain.

1 Background

An attractor neural network model for a cortical decision-making circuit treats it as dynamical system, often in the state space of neural firing rates, with the various attractors corresponding to the decisions.[2] As the initial condition determines the attractor to which the trajectory converges, the sets of initial conditions associated with each attractor, the basins of attraction, are encoding the preferences towards each of the choices.

We study basins of attraction in threshold linear networks, a recurrect network model governed by the system of differential equations:

$$\frac{dx_i}{dt} = -x_i + \left[\sum_{j=1}^{n} W_{ij}x_j + \theta_i\right]_+, \; i \in \{1, \ldots, n\}.$$

where $[x]_+ = \max(0, x)$ is the rectified linear activation function (ReLU). In particular, we are interested in competitive TLNs where $W \leq 0$ and $W_{ii} = 0$. The piecewise linearity of TLN differential equations makes them fairly tractable.

The weight matrix W can also be derived from a graph according to the rules described in [1] and when done so from a directed acyclic graph (DAG), it has been shown that the attractors are supported on the neurons corresponding to the sinks of the graph.[1] Since the rest of the network is inactive in the attractor states, its only role is in shaping the basins of attraction. By comparing TLNs derived from different DAGs with the same sinks, we can compare how network structure shapes different basins for the same set of attractors (Fig 1). We will discuss how we can draw information from the combinatorial structure of the DAG to understand how the basins encode the biases.

*Department of Mathematics, Penn State University
†Department of Applied Mathematics, Brown University

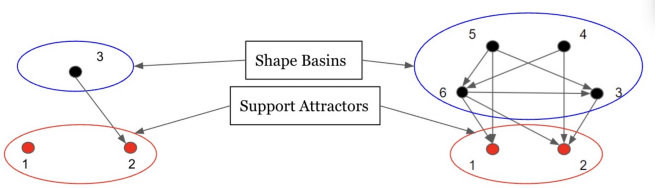

Figure 1: TLNs derived from DAGs

References

[1] C. Curto K. Morrison. Predicting neural network dynamics via graphical analysis. https://arxiv.org/pdf/1804.01487.pdf.

[2] X.J. Wang. Neural dynamics and circuit mechanisms of decision-making. *Current Opinion in Neurobiology*, 22(6), 2012.

A mathematical model of hopping with stopping controlled by muscle damping instantaneous change: biological implications and limitations *

Alessandro Maria Selvitella † Kathleen Lois Foster ‡

Introduction. Animal life is strictly linked to the capability of animals to move, which is necessary for survival. To understand gait patterns, researchers develop mathematical models, ranging from high dimensional, which prefer accuracy, to low dimensional, which focus on biological interpretability [1,2]. Reductionist models concentrate on the essential dynamics, most often of the center of mass, and describe motion through a system of ordinary differential equations (ODEs). This reduction is not trivial because it is hard to encompass the key biological features in a handful of variables and because these reductions must include latent variables, which do not have direct biological correspondence [3]. This is the case when hopping, jumping, and running are represented by a spring-mass damped oscillator during stance (and ballistic motion during flight), since there, the stiffness and muscle damping constants are quantities summarizing heterogeneous contributions. Nevertheless, these reductionist models succeed in describing and give approximate representations of important biological parameters and tend to fit kinematics and kinetic data accurately. However, often these models aim at describing only the periodic motion of a perpetual gait and neglect the starting and stopping phases. This is also the case for 1-dimensional models describing hopping on the spot. The goal of this abstract is to start filling this gap and introduce a new model of hopping with stopping controlled by an instantaneous change in the damping of the muscle.

Methods. We consider a point mass m (kg) that moves straight in the vertical direction. The motion is driven by a (hybrid) linear second order ODE, linking the mass acceleration $\ddot{y}$ (m/s^2) with the velocity $\dot{y}$ (m/s) and the height y (m) of the mass. The elastic force, with spring constant k (N/m) and compression given by $l - y$ (l equals both the leg length and the height at touch down and take off), and the muscle damping force, proportional to the velocity of the mass with damping constant b (kg/s), act only during contact phases, while the force of gravity with constant g (m/s^2) acts during both the flight and the stance phases. The stopping stance is triggered by an instantaneous increase in the muscle damping constant at the beginning of the stance phase.

Results & Discussion. Our model treats the stopping phase as happening at a different time scale T b, where m/b^2 is infinitesimal. Due to this, the dynamics in the stopping phase is essentially described by a first order ODE. Although parameters such as b vary discontinuously, the height, velocity, and acceleration of the mass remain continuous, as observed in human or animal hopping. As depicted in Fig. 1, the stopping phase relaxes the body mass to a height that is lower than the leg length. This limitation is present in the current version of the model, but can be easily overcome by introducing a recovery phase, in which damping decreases again or where the stiffness compensates for the increased damping. Solutions of this model can be written explicitly, even if the system is hybrid (continuous plus discrete) because all the phases are described by linear ODEs. Analyzing this model qualitatively, one finds that stopping is only possible when the squared pendulum velocity g/l is smaller than the squared spring velocity k/m. The current model has not been validated using animal data yet (e.g. human or kangaroo) and this will be done in future work.

Significance. If not the first, our model is one of the few that accounts for stopping, as it introduces a terminal stride that concludes the periodic motion with relaxation towards an equilibrium position. This model is interesting beyond hopping because the idea of introducing a stopping phase can be extended to walking, running, and multipedal motions and might be part of a controller for jumping or running robots. Successful stopping is part of rehabilitation following knee or ankle surgery and so extensions of this model can be implemented to verify progress in muscle recovery.

Acknowledgments. AMS and KLF are supported by the collaborative NSF Awards # 2152789 and # 2152792 on RUI: Collaborative Research: DMS/NIGMS 1: The mathematical laws of morphology and biomechanics through ontogeny.

References. [1] Selvitella and Foster. (2022), *Integr. Comp. Biol.*, **62** (5). [2] Selvitella and Foster. (2024), *J. Theor. Biol.*, **595**. [3] Selvitella and Foster. (2023), *R. Soc. Open. Sci.*, **10**.

*The full version of the boook can be accessed at `https://farside.ph.utexas.edu/Books/Euclid/Elements.pdf`

†Department of Mathematical Sciences, Purdue University Fort Wayne | eScience Institute, University of Washington.

‡Department of Biology, Ball State University.

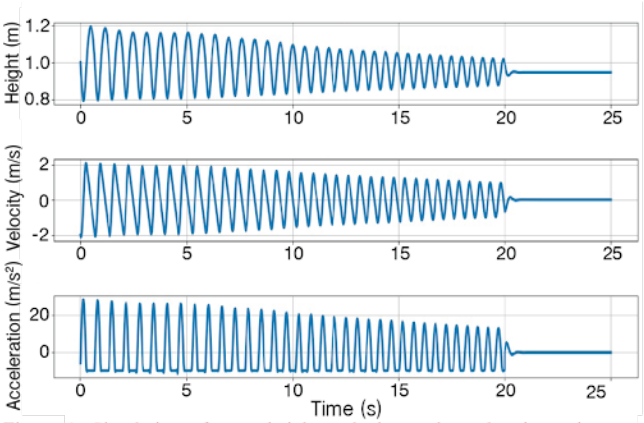

Figure 1: Simulation of mass height, velocity, and acceleration using our hopping with stopping model. Here m=80 kg, l=1 m, k=15,000 N/m and b=10 kg/s (stance) or b=1000 kg/s (stopping). The movement starts at a height of 1 m, with initial velocity of -2 m/s.

Artificial intelligence and machine learning approaches to investigate metabolomics data for precision medicine

Metabolomics is the large-scale study of metabolites– essential molecules involved in biochemical pathways that produce, store, or transfer energy. Due to metabolomic data's high-dimensional and non-linear nature, it is traditionally analyzed using bioinformatic and statistical approaches which reveal insights into disease diagnostics and progression. However, these tools often lack the sensitivity and accuracy that artificial intelligence (AI) and machine learning (ML) techniques provide; the recent integration of AI/ML into metabolomics has allowed for improved biomarker identification, disease prediction, and classification of metabolic patterns. This metastudy examines the scientific goals, methodologies, datasets, and sources of AI/ML approaches applied to metabolomic data and assesses their implications in precision medicine. Recent advancements (2019–2024) in AI/ML applications to metabolomics were systematically reviewed, with a focus on peer-reviewed research indexed in PubMed. A total of 24 studies were analyzed covering diseases such as cancer, cardiovascular conditions, and diabetes. Results indicate that the most commonly used AI/ML techniques were Support Vector Machines (SVM), Random Forest (RF), Gradient Boosting, and Logistic Regression, highlighting their effectiveness in processing complex metabolomic data. Ultimately, this study's findings underscore the transformative potential of AI/ML in metabolomics and its critical role in advancing precision medicine, enabling the earlier diagnosis of diseases.

Authors:
Sahana Senthilkumar [1]*, Antony Shenouda [1]*, Youssef Mourad [1]*, Joy Xie [1]*, Elizabeth Peker [1]*, Zeeshan Ahmed [1][2]

*Equally contributing first authors

Affiliations:
1) Rutgers Institute for Health, Health Care Policy, and Aging Research, Rutgers, The State University of New Jersey, 112 Paterson St, New Brunswick, 08901, NJ, USA.
2) Department of Medicine, Division of Cardiovascular Diseases and Hypertension, Robert Wood Johnson Medical School, Rutgers Health, 125 Paterson St, New Brunswick, NJ, 08901, USA

Citation:
Shenouda, A., Senthilkumar, S., Xie, J., Mourad, Y., Peker, E., and Ahmed, Z. (2025). Artificial intelligence and machine learning approaches to investigate metabolomics data for precision medicine. *Briefings in Bioinformatics (Oxford)*. In peer review.

Infinite-Dimensional Dynamics, Spatiotemporal Gamma Oscillations, and Balance of Excitation and Inhibition in Cortical Networks

Farshad Shirani*

Abstract

In this talk I present our analytical and computational results on global spatiotemporal cortical dynamics as well as local dynamics of excitation and inhibition, obtained based on biophysically reasonable mean-field models of cortical activity. The model we used for our global dynamics analyzes is composed of a system of coupled ordinary and partial differential equations that capture electrocortical activity at a mesoscopic scale, as observed in EEG recordings. It has been used in the literature for studying rhythmic activity in the cortex, cortical phase transition and burst suppression during general anesthesia, the effect of anesthetic drugs on the EEG, epileptic seizures, and sleep.

The coupled ODE-PDE nature of this model makes the analysis of the regularity of the solutions and global dynamics of this model subtle. Our rigorous mathematical results [1] prove wellposedness of the model in both weak and strong typologies. In the biophysically plausible phase space that we establish for the model, we show that the semigroups of weak and strong solution operators possess bounded absorbing sets; provided certain conditions are satisfied on the parameters of the model. We verify that these conditions are indeed satisfied for the entire range of biophysically reasonable values of the parameters. The conditions also identify critical parameters of cortical networks, which in pathological cases may lead to instabilities in the cortical dynamics. Our proof of existence of bounded absorbing sets involves establishing Lyapunov functionals, which indeed have physical meaning as energy functionals and can hence be used as rough estimates of the energy stored in intracortical and cortico-cortical activities in the brain.

Our analysis importantly reveals the presence of very high-dimensional (infinite-dimensional in theory) and spatially localized dynamics in the cortex—a property that is likely essential for cortical processing, learning, and memory. The presence of such a high-dimensional dynamics is in contrast with the conclusions of some analytical and computational studies, which often overlook the spatial aspects of cortical activity and conclude low-dimensional dynamics (or low-dimensional attractor) based on local ODE models or neuronal recordings. We obtained our results by proving that, for some sets of biophysical parameter values, the equilibrium set of the model is not compact. This means that the model has an infinite-dimensional global attracting set, which is bounded and closed but is not compact.

In addition to our analytical results, I also presents numerical bifurcation analysis results along with numerically computed solutions of the model (using the finite-element software COMSOL Multiphysics®), which demonstrate a plausible mechanism of the emergence of transient gamma-band (30-80 Hz) oscillations in cortical networks [2]. This mechanism relies on coordinated modulations of inhibitory and excitatory neurons, that first disturb the balance of excitation and inhibition resulting in the emergence of gamma oscillations, and then restore the balance causing the termination of the oscillations. Further, I show that our results identify an important source of misinterpretation in understanding the underlying dynamics of EEG activity; Such misinterpretations originate from patterns of EEG activity which are artifacts of the low spatial resolution of EEG electrodes.

Finally, I briefly present my key findings of an extensive bifurcation-analysis-based study of a more biophysically detailed (but only local) mean-field (neural mass) model—also verified by simulating an equivalent spiking network model—aimed to identify how variations in each of the structural and physiological parameters of cortical networks affect the balance of excitation and inhibition in cortical networks [3]. The results reveal the functional optimality and criticality of the key parameters included in the study. In particular, the results predict that cortical network dynamics will transition to a high-amplitude slow oscillatory (1-4 Hz) regime when a critical level of imbalance (over-excitation) is created in the network. Such oscillatory activities are known to be strongly correlated with states of diminished consciousness.

References

[1] F. Shirani, W. M. Haddad, and R. de la Llave, *On the global dynamics of an electroencephalographic mean field model of the neocortex*, SIAM Journal on Applied Dynamical Systems, 16 (2017), pp. 1969–2029.

[2] F. Shirani, *Transient neocortical gamma oscillations induced by neuronal response modulation*, Journal of Computational Neuroscience, 48 (2020), pp. 103–122.

[3] F. Shirani and H. Choi, *On the physiological and structural contributors to the overall balance of excitation and inhibition in local cortical networks*, Journal of Computational Neuroscience, 52 (2024), pp. 73–107.

*Emory University, Atlanta, GA

Characterization of Microtubule Dynamic Instability Using Artificial Intelligence

Alexander W. Simmons[1,2], Walter J. Scheirer[3], Holly V. Goodson[1,2]

1. University of Notre Dame, Biophysics PhD. Program, Notre Dame, IN 46556, USA, 2. University of Notre Dame, Department of Chemistry and Biochemistry, Notre Dame, IN 46556, USA, 3. University of Notre Dame, Department of Computer Science and Engineering, Notre Dame, IN 46556

Microtubules (MTs) are noncovalent biological polymers formed from 13 protofilaments arranged in a hollow tube. MTs serve a key role in intracellular transportation, where they function as the "train tracks" of the cell; they also self-organize into the "mitotic spindle" that separates the chromosomes during cell division. MTs exhibit a surprising behavior where they switch randomly between periods of persistent growth and periods of intermittent collapse, referred to as dynamic instability (DI). The transition from growth to shortening is known as "catastrophe," while the reverse transition is called "rescue." Dysregulation of MT DI can lead to diseases ranging from neurodegeneration to heart failure, and while drugs that target MT DI are important therapies for diseases as diverse as cancer and gout, the mechanism of DI remains mysterious, inhibiting attempts to design new drugs targeting this process. The classical explanation for DI is that as GTP-Tubulin polymerizes, delayed GTP to GDP hydrolysis results in a GTP-cap. This GTP-cap promotes polymerization. When this GTP-cap is lost, GDP-Tubulin is exposed at the MT end, resulting in catastrophe. However, there are issues with this classical description of DI. First, it is unclear as to what the exact mechanisms behind catastrophe and rescue are (i.e., how the GTP-cap is lost or reformed respectively). Moreover, multiple groups have reported evidence that additional DI phases (e.g., pauses and stutters) exist. This information implies that the current GTP-cap model is not sufficiently complex to fully describe the DI behavior of a MT. Multiple groups have proposed and provided evidence that the mechanisms of catastrophe and rescue depend on various aspects of the MT's tip structure (e.g., the degree of tip taper). The goal of this project is to elucidate the dimer-scale mechanisms behind DI by using artificial intelligence (AI) to analyze the results of a previously validated dimer-scale computer simulation of microtubule dynamic instability.

Here, we report the development of Artificial Neural Networks (ANNs) capable of predicting the DI behavior of a simulated MT at a moment in time based only on the configuration of its tip structure at that time. These ANNs were trained and evaluated using datasets where tip structures were labeled as exhibiting one of three different DI behavior classes specifically growth, shortening, or stutter (Fig.1). These models could achieve greater than 80% accuracy when predicting the DI behavior of tip structures that had not been previously seen, with ~66% accuracy achieved for examples of stutter. This performance is meaningful as it is greater than what would be expected for random guessing or confusion between two classes. These results suggest that ANNs were able to identify features present in the MT tip structure that correlate with DI behavior and reinforce previous evidence that MTs exhibited at least one additional phase, stutter, distinct from growth and shortening. Clustering analysis is applied to these features grouping MT tips with similar structure-behavior relationships. In the future, we plan to test examples of structures from these subgroups by simulating their behavior using our dimer-scale model to see if specific sub-behaviors are being identified. We will then use these data to test the hypothesis that stutter correlates with tip taper and/or the presence of GDP tubulin at protofilament tips. This work will provide foundational knowledge for research into MT-based treatments for heart disease, neurodegenerative disease, and cancer.

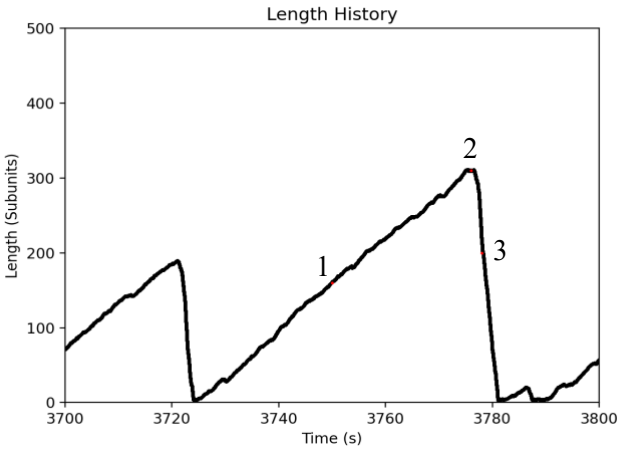

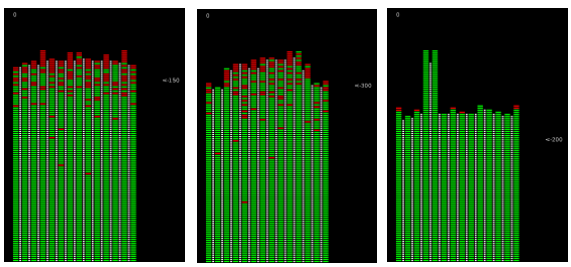

1. Growth 2. Stutter 3. Shortening

Figure 1. Example of a microtubule's length history plot and the tip structures and corresponding phases the microtubule progresses through.

Dissecting mechanisms of marginal zone B cell ontogenesis and homeostasis

Apoorva Singh[1] Melissa Verheijen[2], Benedict Seddon[2], Sanket Rane[1]

[1]Columbia University, Irving Institute for Cancer Dynamics, New York, USA; [2]University College London, Institute of Immunity and Transplantation, London, UK.

Marginal zone (MZ) B cells, located at the junction of the red and white pulp in the spleen, are essential for our defense against blood-borne pathogens. Owing to their innate-like features, MZ B cells generate rapid, early antibody responses and also help kickstart the T cell-dependent high-affinity responses. Indeed, their dysregulation is linked with an increased risk of sepsis, infections from encapsulated bacteria, and autoimmune pathologies. Despite their significance, quantitative aspects of MZ B cell biology—development, maintenance, longevity, and population structure—are still poorly understood. Conventionally, MZ B cells are considered long-lived, self-renewing populations that develop from late-stage transitional B cells. However, recent studies indicate that their immediate precursors constitute a heterogeneous subset of cells representing the full spectrum of transitional stages, potentially encompassing fully differentiated follicular (Fo) B cells. To resolve this, we studied their numbers, replacement dynamics, and extent of division using a well-established bone marrow chimera system, which tracks the infiltration of new donor-derived cells in intact host lymphocyte compartments. We combined these data with an array of mechanistic mathematical models that explored different pathways of MZ B cell development and quantified the contributions of precursor influx, division, and loss to their maintenance. Contrary to the prevailing view, our analyses reveal that MZ B cells are a short-lived, homogeneous population that are largely maintained by a continuous flux from both early and late-stage transitional B cells. Further validating our models using data from young (day 10 onwards) animals revealed inefficient generation of MZ B cells in early life. Our findings provide a continuous picture of age-dependent dynamic regulation of MZ B cell development and homeostasis from the neonatal period to adulthood.

How Rainfall Variability Impacts Vegetation Pattern Formation in Drylands

Arjun Sohur (U.Chicago), Punit Gandhi (Virginia Commonwealth University), Matthew Oline (University of Chicago), and Mary Silber (University of Chicago).

Drylands are water-controlled ecosystems that are sustained by infrequent, discrete, and largely unpredictable resources [1]; the essential water inputs take the form of 'pulses', which refresh the soil moisture content, and are the result of rare rainstorms in these semi-arid environments. Vegetation in drylands is often spatially patchy due to the deficit in essential water. Remarkably, in certain drylands, the vegetation patches form regularly spaced bands, on a kilometer scale, and can be readily monitored by remote sensing satellites, see Figure 1 for an example from Google. The bands of vegetation, which alternate with bare soil, are typically oriented perpendicular to gentle hillslopes, and exploit a run-on-run-off feedback mechanism that concentrates the limited water where it is needed in the bands. We investigate the relationship between rainfall characteristics and vegetation pattern characteristics using the kick-flow mathematical modeling framework for dryland ecosystems that was developed by Gandhi et al. [2]. The flow portion of the model evolves biomass and soil moisture together, between storms, using a reaction-diffusion PDE. The kick portion of the model captures positive feedback between biomass and water infiltration; it adds soil moisture preferentially in the vegetated zones. The kick timing and strength depends on a statistical precipitation model and captures rainfall variability. We explore how different rainfall distributions lead to different patterns via an analysis of pattern-forming instabilities of a spatially-uniformly vegetated state. Interestingly, the resulting linear stability problem leads to linear, discrete-time maps with random elements. Predictions obtained from this linear stochastic dynamical system are tested against simulations of the fully nonlinear kick-flow model.

Figure: Google maps example of banded vegetation in Somalia (9.83N, 48.95E).

[1] I. Noy-Meir, Desert ecosystems: environment and producers. Annual Review of Ecology, Evolution, and Systemics 4 (1973).

[2] P. Gandhi, M. Oline, and M. Silber, "A flow-kick model of dryland vegetation patterns: the impact of rainfall variability on resilience", arXiv:2501.01569 (2025).

Instability of Uniform Oscillations in the Spatially Extended May-Leonard System

I.Sorin[1], *A.Nepomnyashchy*[1], *V.Volpert*[2], *A.Bayliss*[2]
(1) Technion-Israel Institute of Technology, Mathematics, Haifa, Israel, idansorin@campus.technion.ac.il.
(2) Northwestern University, Engineering Sciences and Applied Mathematics, Evanston, IL, USA.

It is known that small-amplitude spatially uniform nonlinear oscillations can be subject to a modulational instability. The spatial instabilities of strongly nonlinear oscillations are still less explored. In [1], spatial instabilities of oscillations close to a homoclinic orbit have been studied.

We investigate the stability of uniform oscillations in the spatially extended May-Leonard system with non-equal diffusion coefficients for different species. For critical values of parameters, the system has a family of time-periodic solutions that spreads from small-amplitude oscillations to strongly nonlinear oscillations close to a heteroclinic cycle. In the case of a model symmetric to a cyclic permutation of variables, the oscillatory solutions can be found analytically. By means of a special kind of perturbation theory, we show analytically that the oscillations are never unstable with respect to longwave spatial modulations. However, in a definite region of the values of diffusion coefficients, oscillatory solutions sufficiently close to the heteroclinic cycle can be unstable with respect to a period-doubling instability with a finite wavenumber (see Fig. 1). The generalization of the obtained results to the case of an asymmetric model is discussed.

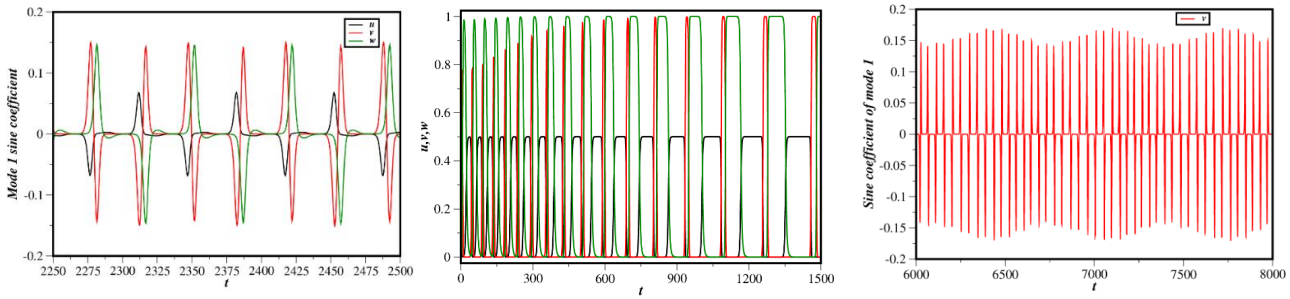

(a) (b) (c)

Figure 1: Solutions of the system in its nonlinear regime. (a) Oscillations of the first spatial Fourier mode above the threshold of the finite-wavenumber period-doubling bifurcation; (b) Solution approaching the heteroclinic cycle; (c) Quasiperiodic solution with two apparently incommensurate frequencies.

References

[1] M. Argentina, P. Coullet, E. Risler, *Self-parametric instability in spatially extended systems*, Phys. Rev. Lett. 86 (2001) 807-809.

Advances in Interface-Fitted Tetrahedral Mesh Generation for Ion Channel Models: Preserving Pore Topology and Enhancing Computational Efficiency with ICMPv3

Matthew Stahl*

Abstract

Generating interface-fitted, irregular tetrahedral meshes for domains that include ion channels, membranes, and solvent regions is a critical yet challenging step in solving finite element models of dielectric continuum ion channels (such as PB/PNP ion channel models).

I will discuss the protein surface representation, outline the workflow for generating tetrahedral meshes, and highlight the challenges involved in accurately capturing the complex geometries of protein, membrane, and solvent regions while maintaining numerical stability in computational methods. Additionally, I will introduce a novel scheme for generating surface meshes of single ion channels that preserves the topological hole defining the protein's pore, with minimal impact on the surrounding protein structure.

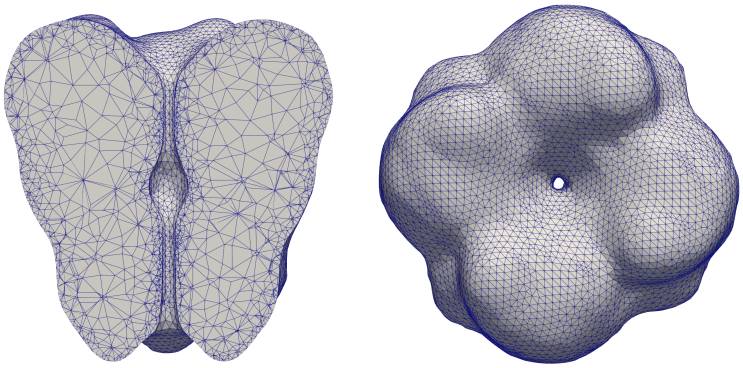

Figure 1: Resulting mesh for a single-ion potassium channel (KCSA) with PDBID 1bl8

*University of Wisconsin Milwaukee

Quantifying and perturbing immune activity in the solid tumor microenvironment

Anne Talkington[1]

Abstract
We present an *in silico* and *in vitro* system to elucidate immune regulation and dysregulation in the presence of antigen stimulus.

1. Immune regulation and perturbation

Immune cells are regulated by a series of receptors that behave as "on" or "off" switches for immune function, known as immune checkpoints [1]. An immune response is thus up- or downregulated as a result of the signals received in the cells' local environment. We investigate activation and exhaustion behaviors in the solid tumor microenvironment, which is traditionally understood as a dysregulated system. Through a combined dynamical systems and agent-based modeling approach [2], we demonstrate the role of immune checkpoint blockade as a perturbation of immune activity both at the system level and individual cell level (Fig. 1). We present preliminary data on immune activity and exhaustion over time, measured from an in-house system, and integrated into a simulated 3D solid tumor model. Finally, we present conclusions on the sensitivity of the tumor-immune system to checkpoint blockade efficiency. These results, and the implementation of our *in silico-in vitro* system as a whole, provide valuable insight into fundamental immunological processes and immune control. Such findings hold valuable implications for future biomedical interventions.

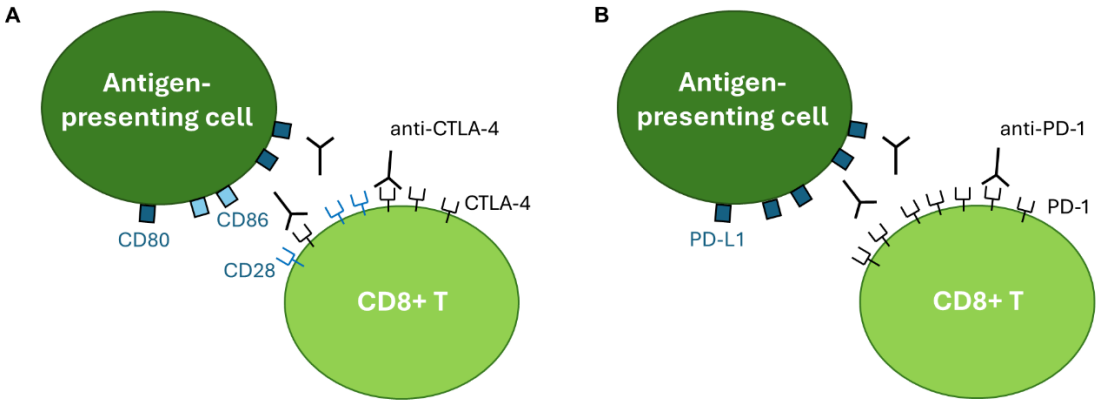

Figure 1: Schematic illustrating the process of perturbation by immune checkpoint blockade via (A) anti-CTLA-4 and (B) anti-PD-1. The goal of immune checkpoint blockade is to inhibit the T cell's "off" switches (PD-1 and CTLA-4), while leaving the "on" switches (CD28) available.

References:

[1] Pardoll, D. M. (2012). The blockade of immune checkpoints in cancer immunotherapy. *Nat. Rev. Cancer*, *12*(4), 252–264. https://doi.org/10.1038/nrc3239
[2] Talkington, A., & Kearsley, A. (n.d.). Optimization of immune checkpoint blockade via a multiscale model system. *Under Review*.

[1] Division of Pharmacokinetics, Pharmacodynamics, and Systems Pharmacology, Department of Pharmaceutical Sciences, University at Buffalo, SUNY, Buffalo, NY 14214

Decomposing Spiking Neural Networks with Graphical Neural Activity Threads

Bradley H. Theilman[1]

The flexibility of natural behavior is thought to emerge in part through the unique computational capacities of biological spiking neural networks. To understand information processing in these networks, we require appropriate mathematical abstractions for neural activity. Ideally, these abstractions should be naturally adapted to the spiking and synaptic dynamics of natural brains. Typically, neural activity is artificially partitioned into time bins to define neural population state vectors. Sequences of state vectors define a trajectory in a high-dimensional space that corresponds, in some way, to the computation. However, these time bins are defined relative to the external experimenter's clock and have no immediate relevance for the brain itself. These approaches necessarily smear out individual spikes and may obscure computationally relevant relations within neural dynamics.

In this work, we introduce an alternative decomposition of spiking neural network activity by constructing a directed acyclic graph (DAG) directly from the synaptic interactions between neurons in simulated spiking networks. Interestingly, this graph naturally splits into disjoint connected components we term "Graphical Neural Activity Threads" (GNATs), which we identify as putative individual computations. We provide an efficient algorithm for identifying quasi-isomorphic subthreads in large spiking datasets and show that the GNATs exhibit compositionality by demonstrating that similar GNATs recur and recombine over the course of the network's dynamics. Thus, GNATs provide a mathematical abstraction distinct from the population state vector and are more naturally adapted to the spatiotemporally distributed dynamics of spiking neural networks.

Mathematically, the graph underlying GNATs defines a finite topology on the set the spikes, with continuous maps for this topology corresponding to order-preserving maps between spike trains. This connection suggests new questions and opens new mathematical tools for interpreting spiking neural network activity. We will discuss some of the implications and outline open problems for further research.

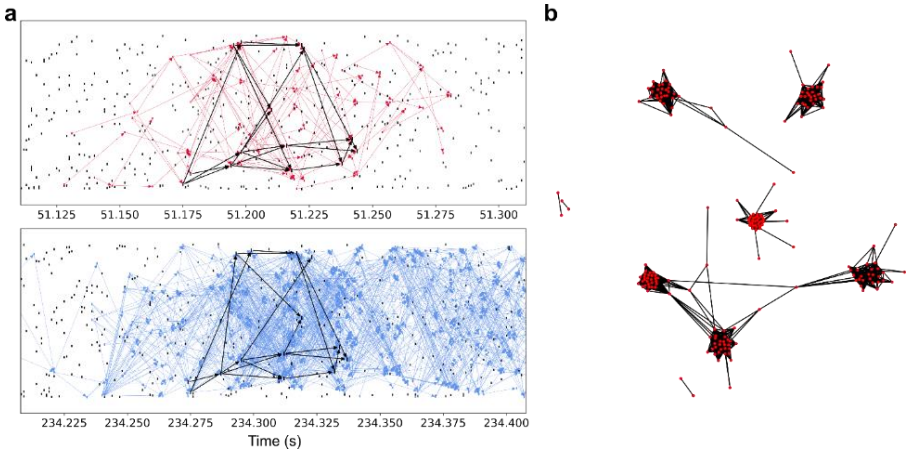

Figure 1: Graphical Neural Activity Threads. a) Depiction of quasi-isomorphic subthreads separate in time in a spike dataset. b) Reappearing isomorphic threads cluster into computational classes with compositional structure. Edges indicate shared subthreads as in a.

References:

[1] Theilman, B.H., Wang, F., Rothganger, F., and Aimone, J.B. (2023), *Decomposing spiking neural networks with Graphical Neural Activity Threads.* https://arxiv.org/abs/2306.16684

[1] Sandia National Laboratories, Albuquerque, NM, USA **SAND2025-04593A**

Covering Relations in the Poset of Combinatorial Neural Codes

R. Amzi Jeffs* Trong-Thuc Trang†

Abstract

A combinatorial neural code C is a subset of $2^{[n]}$ for some $n \in \mathbb{N}$ where $[n] = \{1, \ldots, n\}$. Each $i \in [n]$ represents a place cell, and each element $\sigma \in C$ represents a codeword which records the co-firing event of some place cells. Consider a space $X \subseteq \mathbb{R}^d$, simulating an animal's environment, and a collection $\mathcal{U} = \{U_1, \ldots, U_n\}$ of open subsets of X. Each $U_i \subseteq X$ simulates a place field which is a specific region where a place cell i is active. Then, the code of $\mathcal{U}$ in X is defined as $\text{code}(\mathcal{U}, X) = \left\{\sigma \subseteq [n] \middle| \bigcap_{i\in\sigma} U_i \setminus \bigcup_{j\notin\sigma} U_j \neq \varnothing\right\}$. If a neural code $C = \text{code}(\mathcal{U}, X)$ for some X and $\mathcal{U}$, we say C has a realization of open subsets of some space X. Although every neural code always has such realization, determining whether it admits a realization by some open convex subsets remains unsolved. Many studies attempted to tackle this decision problem, but only partial results were achieved. In fact, a previous study showed that the decision problem of convex neural codes is NP-hard. Furthermore, the authors of this study conjectured that every convex neural code can be realized as a minor of a neural code arising from a representable oriented matroid, which can lead to an equivalence between convex and polytope convex neural codes. Even though this conjecture has been confirmed in dimension two, its validity in higher dimensions is still unknown. To advance the investigation of this conjecture, we provide a complete characterization of the covering relations within the poset $\mathbf{P}_{\mathbf{Code}}$ of neural codes and an enumeration algorithm that can exhaust all distinct isomorphism classes of covering codes of a given neural code.

References

[1] C. Curto, *What can topology tell us about the neural code?*, Bulletin of the American Mathematical Society, 54, pp. 63–78, 2017.

[2] J. Cruz, C. Giusti, V. Itskov, and B. Kronholm, *On open and closed convex codes*, Discrete & Computational Geometry, 61(2), pp. 247–270, 2019.

[3] R. A. Jeffs, *Morphisms of Neural Codes*, SIAM Journal on Applied Algebra and Geometry, 4(1), pp. 99–122, 2020.

[4] A. Kunin, C. Lienkaemper, and Z. Rosen, *Oriented Matroids and Combinatorial Neural Codes*, Combinatorial Theory, 3(1), pp. 427–458, 2020.

[5] B. Bukh and R. A. Jeffs, *Planar Convex Codes are Decidable*, SIAM Journal on Discrete Mathematics, 37(2), pp. 951–963, 2023.

*Pacific Northwest National Laboratory

†Florida Atlantic University

Missed an antibiotic dose - what to do?

Hwai-Ray Tung*

Abstract

Despite the prevalence of missed antibiotic doses, there is little or vague guidance on what to do when a dose is forgotten. In this talk, we consider the effects of different patient responses to missing a dose using a mathematical model that links antibiotic concentration with bacterial population dynamics. In some parameter regimes, we find that (a) missing just a few doses can cause treatment failure, and (b) this failure can be remedied by simply taking a double dose after a missed dose. We then develop an analytically tractable random walk model that yields simple conditions for comparing taking one or two doses after a missed dose. This work was done with Sean Lawley and is published in *Bulletin of Mathematical Biology* [1].

References

[1] Tung, HR., Lawley, S.D. How Missed Doses of Antibiotics Affect Bacteria Growth Dynamics. *Bull Math Biol* 87, 58 (2025). https://doi.org/10.1007/s11538-025-01430-4

*University of Utah, Department of Mathematics

Immune Control of the Gut Microbiota

Obinna A. Ukogu[1] Armita Nourmohammad[234]

The gut microbiota is a dynamic, complex ecosystem that can provide metabolic benefits to the host and/or harm the host if microbes breach the epithelium barrier. This microbial ecology interacts with the host immune system, which toggles between inflammation or tolerance of microbes. However, immune "control" is limited by the specificity of immune cells for microbes. How can the immune system monitor the gut ecology to promote beneficial function while avoiding harm? Recent experimental studies have explored this question by profiling the immune response to pre-defined microbial consortia [1]. These early results suggest that there is a low-dimensional mapping between groups of distinct microbes and immune receptors that bind to them. Using a generalized niche-competition model and a coarse-grained model for the immune repertoire, we investigate how the specificity of the immune response shapes the composition of commensal microbes in the gut. Our model demonstrates that the composition of the microbiota can constrain immune control. We also explore the proposition that the immune repertoire encodes information about the composition-to-function mapping of microbes in the gut. For instance, the balance of inflammatory and tolerogenic cells specific to groups of microbes may indicate their role in the gut: beneficial, harmful, or commensal. Understanding the rules of this emergent mapping has the potential to guide the rational design of targeted therapies in the gut.

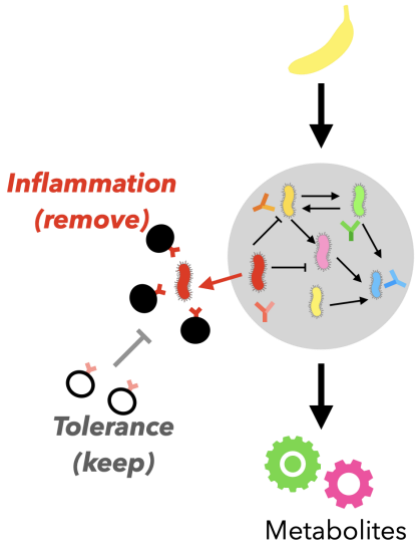

Figure 1: Schematic of gut-immune interactions.

References:

[1] K. Nagashima, A. Zhao, K. Atabakhsh, M. Bae, J. E. Blum, A. Weakley, S. Jain, X. Meng, A. G. Cheng, M. Wang, S. Higginbottom, A. Dimas, P. Murugkar, E. S. Sattely, J. J. Moon, E. P. Balskus, M. A. Fischbach, Mapping the T cell repertoire to a complex gut bacterial community. Nature, doi: 10.1038/s41586-023-06431-8 (2023).

[1] Department of Applied Mathematics, University of Washington, USA
[2] Department of Applied Mathematics, University of Washington, USA
[3]Department of Physics and Astronomy, University of Washington, USA
[4] Fred Hutchinson Cancer Center, USA

Preservation of functional memory CD8 T cells with early treatment initiation underlies sustained post-treatment control of HIV infection

Bharadwaj Vemparala[1], Caroline Passaes[2,3], Delphine Desjardins[4], Anaïs Chapel[2,3], Valérie Monceaux[2,3], Julien Lemaitre[4], Adeline Mélard[5], Federico Perdomo-Celis[3], Cyril Planchais[6], Maël Gourvès[2], Nastasia Dimant[4], Annie David[3], Nathalie Dereuddre-Bosquet[4], Aurélie Barrail-Tran[4,7], Hélène Gouget[4], Céline Guillaume[4], Francis Relouzat[4], Olivier Lambotte[4,8], Michaela Müller-Trutwin[3], Hugo Mouquet[6], Christine Rouzioux[9], Véronique Avettand-Fenoël[5,10], Roger Le Grand[4], Asier Sáez-Cirión[2,3], Narendra M Dixit[1,11,*], Jérémie Guedj[12,*]

The current standard-of-care for HIV infections involves combination antiretroviral therapy (ART). While ART is potent enough to suppress viral replication, it is not curative, and treatment interruption typically results in viral rebound. Thus, with ~40 million people living with HIV (PLWH), therapeutic interventions that cure or elicit sustained long-term remission are needed. Efforts to develop such interventions are motivated by the rare PLWH phenotypes termed post-treatment controllers: PLWH experiencing progressive disease elicit robust viral control after ART interruption. Multiple studies have shown that early ART initiation is associated with a higher chance of post-treatment control, owing to superior post-treatment CD8 T cell responses. However, the mechanisms underpinning the superiority of CD8 T cell responses with early ART initiation are unclear. We hypothesized that the cumulative level of exposure to antigen of the CD8 T cell pool pre-treatment, which regulates the development of their memory functionality, underlies the strength of their responses post-treatment. Early ART initiation limits the exposure to antigen enough to generate memory responses that trigger remission post-treatment, while late ART initiation irreversibly blunts the memory potential of the CD8 T cell pool, triggering progressive disease. We developed a within-host mathematical model to test our hypothesis. Our model predicted bistability: one state corresponding to high viral load and weak memory responses, and the other to low viral load and strong memory responses. Early treatment made the latter state more accessible post-treatment. We then performed model inference using data from experiments on SIV infection in macaques, analogous to HIV in humans. The experimental study comprised 11 macaques each in the early and late treatment groups, with data collected from pre-ART, ART, and post-ART phases, in addition to 16 untreated macaques in control group. We employed nonlinear mixed effects approach to simultaneously fit the model to the complete dataset. Our model recapitulated the data well, explaining the effect of the timing of treatment initiation, offering strong support to our hypothesis. Using the estimated parameter distributions, we quantified the maximum delay affordable in treatment initiation and the minimum size of the associated memory pool required for post-treatment control. The framework could be employed in formulating quantifiable targets for therapies aimed at eliciting long-term remission in PLWH.

[1]Department of Chemical Engineering, Indian Institute of Science, Bengaluru, India, [2]Institut Pasteur, Université Paris Cité, Viral Reservoirs and Immune Control Unit, Paris, France, [3]Institut Pasteur, Université Paris Cité, HIV Inflammation and Persistence Unit, Paris, France, [4]Université Paris-Saclay, CEA, INSERM, UMR1184, Immunology of Viral, Auto-immune, Hematological and Bacterial diseases (IMVA-HB/IDMIT Department), Fontenay-aux-Roses/Le Kremlin-Bicêtre, France, [5]Université Paris Cité; INSERM, U1016; CNRS, UMR8104 Paris, France, [6]Institut Pasteur, Université Paris Cité, INSERM U1222, Humoral Immunology Unit, Paris, France, [7]Université Paris-Saclay, AP-HP, Hôpital Bicêtre, Service de Pharmacie, Le Kremlin Bicêtre, France, [8]Université Paris-Saclay, AP-HP. Hôpital Bicêtre, Clinical Immunology Department, 94270 Le Kremlin Bicêtre, France, [9]Université Paris Cité/APHP Hôpital Necker - Enfants Malades, Paris, France, [10]APHP Hôpital Cochin, Service de Virologie, Paris, France, [11]Department of Bioengineering, Indian Institute of Science, Bengaluru, India, [12]Université Paris Cité, IAME, INSERM, F-75018 Paris, France. *Equal contribution

Vyriad: a Deep Learning Framework to Catalyze Viral Discovery and Identification from Metagenomic Datasets

Skylar Sargent Walters
Brown University

Abstract

As infectious diseases increase in prevalence, developing advanced methods to identify novel or emerging viruses from metagenomic data is critical. However, current kmer- and protein-based approaches struggle to identify genetically divergent sequences due to their dependence on viral reference sequences and rapid viral mutation rates.

We present Vyriad, a deep learning framework for viral taxonomic classification from metagenomic data, introducing three advancements over existing frameworks: (1) introduction of a variable-length-mer encoding (VME) preprocessing pipeline, improving on fixed-length k-mer-based preprocessing, (2) a hybrid MLP-CNN architecture modeling short- and long-range nucleotide dependencies, and (3) a dataset balanced via strategic subsampling, where underrepresented viral families were supplemented with partial nucleotide sequences to mitigate taxonomic bias. With these advances, Vyriad achieved 97.05% accuracy in classifying testing reads into viral families, outperforming or matching the state-of-the-art deep learning methods for viral taxonomic classification. To evaluate novel virus identification, we hold out 12 viral species across 6 families during training, then assess the model's performance on the held-out species. Additionally, we conduct perturbation testing to analyze the model's robustness to mutations. Latent-space analysis of VME-derived motifs uncovered conserved genomic regions linking model decisions to biologically-interpretable features.

By expanding our ability to detect diverse viral genomes, Vyriad aims to address limitations in outbreak settings where conventional diagnostics fail to identify genetically diverse pathogens, enabling early virome characterization, diagnostic pipeline specificity, and viral detection.

Stochastic Modeling of Morphological Rate Evolution: Phylogenetic Regression with Approximate Bayesian Computation*

Dwueng-Chwuan Jhwueng†

Abstract

In the macroevolutionary studies, one major study of interest is understanding the evolution of traits. Several novel statistical models have been proposed to link the rate of evolution of one trait with another trait. In this framework, I expand the existing Brownian motion–type covariate (BM) to the Ornstein–Uhlenbeck (OU) process–type covariate that allows stabilizing selection to occur during evolution. In addition, the covariate type of the early burst (EB) process type covariate is also developed to consider the adaptive radiation phenomenon. Due to the lack of model likelihood, I propose the use of the approximate Bayesian computation (ABC) technique for the estimation of the model parameters. Simulations show that the models work well with posterior estimates close to the true parameters. The models are applied to analyze the 136 bird species data to reinvestigate how the rates of beak-shaped evolution in birds are influenced by brain mass.

1 Proposition 1.

THEOREM 1.1. *For* $m = 0, 1, 2, \cdots$, *the moment for the EB trait variable* x_{t,σ_0} *is expressed as following* $E\left[\left(\int_0^t \exp(r_x s) dW_s^x\right)^{2m}\right] = \frac{(2v_{r_x}(t))^m}{\sqrt{\pi}}\Gamma(m+\frac{1}{2})$, *and* $E\left[\left(\int_0^t \exp(r_x s) dW_t^x\right)^{2m+1}\right] = 0$, *where* $v_{r_x}(t) = \frac{\exp(2r_x t)-1}{2r_x}$.

Proof. Please refer to the Mathematical Appendix in the manuscript. □

References

[1] D.-C. Jhwueng, *Stochastic Modeling of Morphological Rate Evolution: Phylogenetic Regression with Approximate Bayesian Computation* . (In progress).

*The full version of the manuscript can be accessed at `https://tonyjhwueng.info/phyratereg/PhyRateCovRegOUEB.pdf`

†Department of Statistics, Feng-Chia University Taiwan

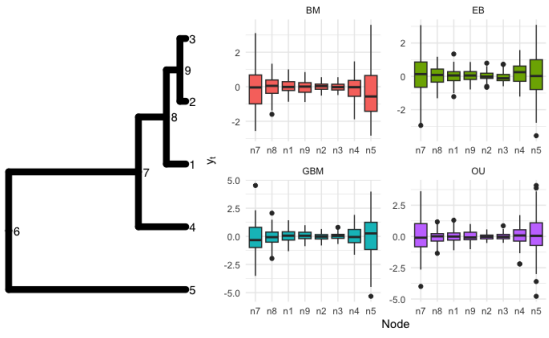

Figure 1: Left: A 5 taxa phylogenetic tree with tips numbered as n_1, n_2, n_3, n_4, n_5 and nodes numbered as n_6, n_7, n_8, n_9. Right: Boxplot for trait simulation using the SDE model $y_t = y_a + \int_0^{t_a} \sqrt{a + bx_s} dW_s^y$ under four type of covariates x_s: BM, GBM, EB, OU for a 5 taxa tree.

An unusually low-energy cofactor facilitates efficient energy transduction in the Nfn-1 redox enzyme

Emily Y. Wang[1], Andrew J. Smith[1], Kelsey A. Parker[1], David N. Beratan[1,2,3]

Abstract

Electron bifurcation (EB) is an elegant energy transduction mechanism evolved in some natural redox enzymes to efficiently produce higher energy products from lower energy reactants. To accomplish this task, the EB enzyme splits two electrons received from a donor substrate, sending one electron to a low energy acceptor substrate to drive sending the other to a high energy acceptor substrate. The enzyme NADH-dependent ferredoxin-$NADP^+$ oxidoreductase I (Nfn-1) contains an unusually low-energy iron-sulfur cluster cofactor (H1) in its low energy electron transport branch, causing Nfn-1 to deviate from the theoretical EB scheme prediction. The significance of this cofactor for efficient EB is not well-understood. We apply master equation kinetics to simulate EB in Nfn-1's bumpy versus the theoretical EB scheme's ramp-like energetic landscape. Our theoretical study reveals the low-energy H1's essential role for facilitating efficient EB by maximally reducing energy wasting electron short-circuiting with minimal cost to bifurcation turnover rate. This effect is achieved by forming an electron blockade against short-circuiting pathways. Our findings explain the chemical logic underpinning nature's bumpy, non-linear EB energy landscapes and could inform the design of efficient synthetic bifurcators.

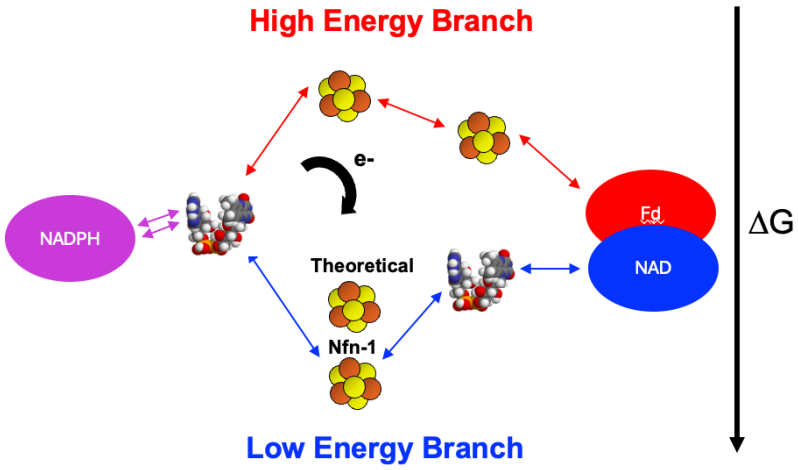

Figure 1: Schematic of the Nfn-1 energy landscape and short-circuit pathway.

[1] Department of Chemistry, Duke University
[2] Department of Biochemistry, Duke University
[3] Department of Physics, Duke University

Self-Supervised Learning for Discovery of Complex Patterns in Neural Time Series

Recent advances in neuroscience recording technologies have made it possible to collect massive volumes of complex data in behavioral and physiological contexts once thought inaccessible. In experimental settings that exceed the scope of predefined hypotheses—for example, freely moving animals versus binary decision tasks—data-driven discovery becomes essential. While these datasets offer transformative potential, conventional analysis methods—designed for hypothesis testing—often fail. To address this gap, we present a novel computational framework that integrates advanced signal processing, topological data analysis, and modern machine learning. Its core innovation lies in a biologically grounded adaptation of self-supervised learning—a machine learning approach that extracts salient content from the data itself, enabling systematic identification of informative features, separation of signal from noise, and detection of structures such as clusters or temporal dependencies—all without external labels [1]. When combined with biological insight, this unified framework enables automatic discovery of meaningful patterns in complex biological signals, advancing our understanding of neural dynamics and behavior.

Traditional methods often rely on simplifying assumptions rooted in known hypotheses, which constrain their ability to discover structure in high-dimensional, nonlinear data. We illustrate this challenge with two representative datasets: (i) multi-channel kinematic recordings of mouse reach-to-grasp behavior that capture detailed limb coordination [2], and (ii) high-frequency voltage traces from retinal ganglion cells [3]. Together, these datasets underscore the need for analytical tools that can autonomously uncover structure without relying on ground-truth labels. In the first dataset, motor behavior analysis has historically depended on linear models or discrete-state approximations such as Hidden Markov Models or autoregressive models. Yet, the dynamics of freely moving animals are inherently continuous and nonlinear. Similarly, the second dataset—high-resolution neural voltage traces—exhibits both long-range dependencies (e.g., bursts) and transient spikes. These temporal features, critical for identifying cell types, span frequency scales that exceed the limits of conventional decomposition methods.

To tackle these challenges, we integrate wavelet analysis, persistent homology, and self-supervised learning. At the global level, wavelet analysis first disentangles overlapping oscillatory components by localizing them in frequency. Persistent homology then identifies stable, recurring patterns such as synchronized oscillations across behavioral channels. By applying self-supervised learning to these persistent features, the framework uncovers coordination motifs between limbs, revealing how motor control unfolds during natural behavior—without the need for trial labels or task segmentation. At the local scale, the framework uses an adaptive, minimally redundant representation, guided by the Heisenberg uncertainty principle, to explore fine-scale temporal dynamics. This enables fine-grained tracking of how oscillatory components at different time scales interact within local sequences. Applied to retinal recordings, this method reveals how fast spiking events and slower rhythms combine to form unique electrophysiological signatures that distinguish cell types. This analysis provides new insight into how neurons integrate information across time, clarifying key mechanisms in neural communication and encoding. Crucially, our approach integrates global and local analyses into a coherent, multilevel self-supervised learning framework. This approach yields a comprehensive view of biological signals that neither scale could provide alone. By unifying innovative mathematical tools with deep biological relevance, it is also a generalizable framework for discovering neurobiological structure in complex time series.

References:

[1] Wang et al., https://arxiv.org/abs/2305.11953
[2] De Laittre & Maclean https://www.biorxiv.org/content/10.1101/2024.12.20.629771v1
[3] Goetz et al., Cell Reports 2022

Analysis of Colon Motor Patterns in the Proximal Colon

Cameron Watt* Bard Ermentrout*

Abstract

Colonic motor patterns in the proximal colon are not explained by current models which are based on studies in the distal region. The motor patterns in the proximal colon consist of ripples and colon motor complexes (CMCs). Ripples are slow waves of electrical activity produced by interstitial cells of cajal (ICCs) that influence the smooth muscle through gap junctions. CMCs are clusters of contractions that result from feedback between the smooth muscle and the enteric nervous system. In this talk, we look at a model to understand the motor patterns in the proximal colon. Our model incorporates interactions of the ICCs, the enteric nervous system, and the smooth muscle. We examine the factors that influence the onset and the duration of CMCs in order to design a reduced model. We will also study the coupling of oscillators in a chain. In particular, we observe that unidirectional coupling in one direction has a much stronger effect than coupling in the other direction. We examine the implications of this observation on the coupling for a chain of oscillators.

*University of Pittsburgh

Topologically informed model selection of agent-based models for collective cell motion

Alyssa R. Wenzel[1]
Patrick M. Haughey[1]
Kyle C. Nguyen[2,5]
John T. Nardini[3]
Jason M. Haugh[4]
Kevin B. Flores[1,5]

Abstract

Fibroblasts in a confluent monolayer are known to adopt morphologies that differ from those of isolated cells. Moreover, confluent fibroblasts, though completely surrounded by neighboring cells, are known to be motile. Previous studies involving time lapse microscopy showed that confluent fibroblast cells spontaneously arrange themselves into a nematic order. We previously collected and analyzed new time lapse microscopy data to show that the movement of neighboring cells in confluent monolayers are oriented parallel to each other and often moving in opposite directions in a collective motion phenomenon we refer to as "fluidization" of the cell population. Here, we performed an *in-silico* model selection study to show that topological data analysis could be used to distinguish between biophysical mechanisms that generate distinct fluidization patterns in an agent-based model of cell motility. We have added a new mechanism to represent cell alignment to the existing D'Orsogna model. We have compared this model to the D'Orsogna model using Bayesian Information Criteria.

[1] Department of Mathematics, North Carolina State University
[2] Sandia National Laboratories
[3] Department of Mathematics and Statistics, The College of New Jersey
[4] Department of Chemical and Biomolecular Engineering, North Carolina State University
[5] Center for Research in Scientific Computation, North Carolina State University

Mathematical Models of Ovulation: A Parameter Sensitivity Analysis

Savannah Williams*

Abstract

The ovulatory cycle can be disrupted through a variety of factors, including stress and associated physiological responses. Although the mechanisms are complex, these effects can be examined through mathematical modeling. This work analyzes previous mathematical models of ovulation as preliminary steps towards modeling the effects of stress on ovulation. We perform a parameter sensitivity analysis and identify a metric to quantify model outputs and important parameters that help to distinguish ovulatory phenotypes. We also discuss implications of this work for stress-related mechanisms that influence ovulatory function.

*Bryn Mawr College

Emerald Win **NITMB MathBio Convergence Conference**

Poster Title: Modeling Chemical Signaling Network to Regulate Cellular Cytoskeletal Components in the Cross Section of the Drosophila Wing Disc

Poster Abstract: The Drosophila wing disc, which eventually becomes the adult wing of a fruit fly, has primarily been used to study the underlying mechanisms for the development of growing epithelium. The relative simplicity and accessibility of the wing disc, combined with the wealth of genetic tools available, have combined to make it a premier system for identifying genes and deciphering systems that play crucial roles in animal development. In this study, we consider a tissue-level morphogen Dpp which is responsible for the regulation of cell growth and division through a downstream regulation on cytoskeletons. Via combining the receptor Tkv, downstreams of Dpp-Tkv complex regulate two critical intracellular signals, Rho1 and Cdc42, which polarize at different cellular compartments and are responsible for regulating distributions of actomyosin. We develop a comprehensive chemical signaling model that incorporates the fundamental mechanisms that regulate the spatiotemporal dynamics of Dpp, Rho1, Cdc42 and Integrin. Bayesian optimization, a machine learning technique, is applied to calibrate the model with experimental measurements. We apply the model to systematically test mechanisms of the coupled regulation of chemical signals and cytoskeletal regulators that guide the morphogenesis of multilayered tissues.

Robust Extraction of Pneumonia-Associated Clinical States from Electronic Health Records

Feihong Xu* Félix L. Morales† Luís A. Nunes Amaral‡

Abstract

Mining of electronic health records (EHR) promises to automate the identification of comprehensive disease phenotypes. However, the realization of this promise is hindered by the unavailability of generalizable ground-truth information, data incompleteness and heterogeneity, and the lack of generalization to multiple cohorts. We present here a data-driven approach to identify clinical states that we implement for 585 critical care patients with suspected pneumonia recruited by the SCRIPT study, which we compare to and integrate with 9,918 pneumonia patients from the MIMIC-IV dataset. We extract and curate from their structured EHRs a primary set of clinical features (53 and 59 features for SCRIPT and MIMIC-IV, respectively), including disease severity scores, vital signs, and so on, at various degrees of completeness. We aggregate irregular time series into daily frequency, resulting in 12,495 and 94,684 patient-day pairs for SCRIPT and MIMIC, respectively. We define a "common-sense" ground truth that we then use in a semi-supervised pipeline to optimize choices for data pre-processing, and reduce the feature space to four principal components. We describe and validate an ensemble-based clustering method that enables us to robustly identify five clinical states, and use a Gaussian mixture model to quantify uncertainty in cluster assignment. Demonstrating the clinical relevance of the identified states, we find that three states are strongly associated with disease outcomes (dying vs. recovering), while the other two reflect disease etiology. The outcome associated clinical states provide significantly increased discrimination of mortality rates over standard approaches. For more details, see [1].

References

[1] Feihong Xu, Félix L. Morales, and Luís A. Nunes Amaral. "Robust extraction of pneumonia-associated clinical states from electronic health records." *Proceedings of the National Academy of Sciences*, 121(45): e2417688121, 2024. doi:10.1073/pnas.2417688121.

*Department of Engineering Sciences and Applied Mathematics, Northwestern University, Evanston, IL 60208, USA; Interdisciplinary Biological Sciences Program, Northwestern University, Evanston, IL 60208, USA;

†Department of Engineering Sciences and Applied Mathematics, Northwestern University, Evanston, IL 60208, USA;

‡Department of Engineering Sciences and Applied Mathematics, Northwestern University, Evanston, IL 60208, USA; Department of Medicine, Division of Pulmonary and Critical Care Medicine, Northwestern University Feinberg School of Medicine, Chicago, IL 60611, USA; Department of Molecular Biosciences, Northwestern University, Evanston, IL 60208, USA; Department of Physics and Astronomy, Northwestern University, Evanston, IL 60208, USA; Northwestern Institute on Complex Systems, Northwestern University, Evanston, IL 60208, USA; NSF-Simons National Institute on the Theory and Mathematics in Biology, Northwestern University, Chicago, IL 60611, USA;

Impact of spatial cell wall elastic moduli on modeling of tip growth and morphogenesis

Rholee Xu[1], Luis Vidali[1,2], Min Wu[1,3]

[1]*Department of Bioinformatics and Computational Biology, Worcester Polytechnic Institute, Worcester, MA 01605, USA*
[2]*Department of Biology and Biotechnology, Worcester Polytechnic Institute, Worcester, MA 01605, USA*
[3]*Department of Mathematical Sciences, Worcester Polytechnic Institute, Worcester, MA 01605, USA*

Keywords: cell wall mechanics, tip growth, morphogenesis, elasticity

Plant cell morphology and growth are essential for plant development and adaptation. Some key cell types, such as pollen tubes and root hairs, develop by tip growth. Cell wall material deposition and cell wall rearrangement are major contributing factors to tip cell growth and morphogenesis. As the wall is extended due to turgor pressure, we must understand its mechanical response. Studies into this mechanical process include theoretical models, which are mostly based on the classical Lockhart theory, where the wall extends irreversibly in response to turgor pressure. These models predict that the shape of growing cells is dependent on a dramatic increasing gradient of mechanical properties from the tip to the shank region. This assumption was not validated until recently, when the wall elastic gradient in hyphae was measured to be within an order of magnitude. We found that the previously described methods did not work well given certain morphologies, and the level of measurement was not detailed enough at the tip transition region. Instead, we have developed and tested our own novel method to measure the spatial distribution of cell wall elastic moduli using our moss model organism, *Physcomitrium patens*. This method relies on a triangulation that quantifies wall deformation from fluorescent bead tracking. Using the method, we were able to measure a more explicit bulk modulus gradient in two types of *P. patens* tip cells and verified that the gradient was not as steep as predicted. Furthermore, we found that by applying our experimental results into our growth model, normal tip cell growth and morphogenesis could be achieved.

Spatial Pattern Formation in Eco-Evolutionary Games with Environment-Driven Motion

Tianyong Yao[1,2,*] and Daniel B. Cooney[2,3,*]

[1]Department of Mathematics, University of Michigan, Ann Arbor, MI, USA
[2]Department of Mathematics, University of Illinois Urbana-Champaign, Urbana, IL, USA
[3]Carl R. Woese Institute for Genomic Biology, University of Illinois Urbana-Champaign, Urbana, IL, USA
[*]Correspondence to yuzutyao@umich.edu and dbcoone2@illinois.edu

Abstract

The sustainable management of common resources often leads to a social dilemma known as the tragedy of the commons: individuals benefit from rapid extraction of resources, while communities as a whole benefit from more sustainable extraction strategies. In this talk, we explore a PDE model of evolutionary game theory with environmental feedback, describing how the spatial distribution of resource extraction strategies and environmental resources evolve due to reaction terms describing eco-evolutionary game-theoretic dynamics and spatial terms describing diffusion of environmental resources and directed motion of resource harvesters towards regions of greater environmental quality. Through linear stability, we show that this biased motion towards higher-quality environments can lead to spatial patterns in the distribution of extraction strategies, creating local regions with improved environmental quality and increase payoff for resource extractors. However, by measuring the average payoff and environmental quality across the spatial domain, we see that this pattern-forming mechanism can actually decrease the overall success of the population relative to the equilibrium outcome in the absence of spatial motion. This suggests that environmental-driven motion can produce a spatial social dilemma, in which biased motion towards more beneficial regions can produce emergent patterns featuring a worse overall environment for the population.

References

[1] Tianyong Yao & Daniel B. Cooney (2025). Spatial Pattern Formation in Eco-Evolutionary Games with Environment-Driven Motion. *arXiv preprint arXiv:2502.0672.*

Investigation of pattern formation in urban crime models with law enforcement

Madi Yerlanov
University of Colorado

Abstract

Mathematical ecology and biology have been rapidly developing fields. Influenced by their growth and potential effectiveness, other fields have started employing similar mathematical tools. Social sciences are a set of disciplines that complement their natural counterparts in the global effort to understand human nature. An example of how mathematics has been actively utilized in social sciences is crime modeling. We consider one of such models, a nonlinear system of partial differential equations, initially developed by a team in UCLA in 2008. In a short period, it has attracted a lot of attention from the mathematical community, partially due to the nontrivial dynamics of the system solution. One of these solution behaviors is constant in time but varying in space steady states. These spatially heterogeneous yet persistent solutions are called hotspots in criminology. In this work, we obtain the amplitude equations that describe the hotspot pattern formation in the model using weakly nonlinear analysis techniques. We find the existence of super- and sub-critical pitchfork bifurcations. Moreover, we propose different real-world suppression strategies and investigate numerically how the suggested approaches effectively eradicate the two types of hotspots. We highlight the challenges in weakly nonlinear analysis and the limitations of the proposed suppression mechanisms, emphasizing the need for further theoretical and practical work on this urban crime model with law enforcement. If time permits, we supplement our discussion with formal theorems on the existence and stability of the bifurcating branches emerging from constant steady-state solutions. This work should be viewed as an example of how mathematics can be helpful as a part of a collaborative effort to tackle critical social phenomena, which is a part of an effort to quantify human behavior.

Identifying Drug Targets with a Reduced Model for Competitive Inhibitor Stimulation

Garrett Young* Colleen Mitchell* Mitchell Riley† Michael Welsh†

Abstract

Studies on Terazosin (TZ) have demonstrated that it may be neuroprotective, possibly due to increasing the production of adenosine triphosphate (ATP) through its interaction with the enzyme phosphoglycerate kinase 1 (PGK1) despite behaving as a competitive inhibitor by binding in the same pocket as adenosine diphosphate (ADP). A mathematical model developed purely through mass action was able to replicate experimental results; however, the model lacks an analytical solution due to its nonlinearity. Understanding the mechanism of competitive inhibitor stimulation could provide better understanding of how to slow neurodegenerative disease progression or even benefit drug development by offering insight into determining when this stimulation will occur. Thus, there is a desire to reduce this model into a form that can be analyzed and allow for a clearer picture of when and why inhibitors could lead to increased product production.

1 Introduction

Parkinson's disease is a neurodegenerative disease, and studies have demonstrated that moderate doses of Terazosin (TZ) may be neuroprotective. It is hypothesized that TZ may increase the production of adenosine triphosphate (ATP) through interaction with the enzyme phosphoglycerate kinase 1 (PGK1) in glycolysis. The crystal structure of TZ implies that it binds to PGK1 in the same manner and location as the substrate adenosine diphosphate (ADP)—lending credence to the idea that TZ behaves as a competitive inhibitor. Since TZ has been observed increasing ATP, this seems counterintuitive and justified study through a mass action model.

In the mass action model, introducing many different dosages of TZ reveals qualitatively similar results as seen experimentally. Small doses have very little positive impact, moderate doses lead to increased ATP production, and larger doses lead to very little positive impact and even detrimental effects by causing the reaction to come to a standstill. The model qualitatively matching the experimental results suggests a deeper understanding of the biochemical mechanism in question. It seems to hinge on the relationship of rate parameters dictating direction of flow for the chemical reactions. However, the model lacks an analytical solution due to its nonlinear nature.

2 Results

The reduced model maintains hallmarks from the original model such as the non-monotone biphasic dose response. The rescaling of all the variables and time along led to the identification of ε_1 and ε_2. ε_1 is proportional to the amount of substrate while ε_2 is proportional to the rate of the phosphotransfer. Because the substrates exist in excess, their rate of change is very slow, meaning ε_1 corresponds to the slowest time scale. The phosphotransfer is a quicker reaction, so ε_2 corresponds to the fastest time scale. Therefore, these values delineate the system into three distinct time scales. The original model focuses on a result one minute into the reaction; thus, the intermediate time scale is of primary interest. In this slow time scale, the super slow reactions have not realized any significant change while many of the fast reactions can be approximated using quasi-steady-state and equilibrium approximations. In this regime, proper grouping of the variables reduces the large system to a system of only two linear differential equations that have a conserved quantity, thereby effectively only requiring one differential equation which can be solved analytically. Upon solving this system, the non-monotone biphasic property of the production of ATP continues to be observed. In the reduced model, the reaction rate exhibits Michaelis-Menten kinetics as a function of either substrate. In contrast the reaction rate is a novel higher order rational function of TZ dose that retains the non-monotone dose dependence. In addition to this behavior, the reduced model allows further study into the interplay and impact of rate parameters, initial concentrations of substrates and products, and drug dosage.

References

*Applied Mathematics and Computational Sciences Program, University of Iowa
†Department of Internal Medicine, University of Iowa

[1] M. Riley, C. Mitchell, S. Ernst, E. Taylor, and M. Welsh, *A model for stimulation of enzyme activity by a competitive inhibitor based on the interaction of terazosin and phosphoglycerate kinase 1.* PNAS, 121.9 (2024)

Causality in Replay: Detecting Effective Connectivity from Spike Trains

Marium Yousuf* Laurent Pagnier* Michael Chertkov* Jean-Marc Fellous†

Abstract

Hippocampal replay is characterized by the re-activation of population-wide neural sequences during non-exploratory states, such as sleep and rest. The reactivated neural activity closely resembles the patterns observed during prior active state. Replay is often correlated with firing sequences observed during preceding spatial navigation tasks during which an agent, such as a rat, investigates novel environments or performs a learning task. The generation of replay is crucial for memory consolidation and retention and is key to retrieving formed memories.

Replay episodes contain information about the causality structure within a network of neurons, which helps to experimentally track how the memories are formed during learning. We investigate the relationship between replay and effective connectivity by simulating the activity of a network of CA3 place cells, as observed in rats during spatial navigation. We use the NEURON simulation environment to implement a single-compartment, multi-current pyramidal cell network. The network is connected using realistic AMPA and NMDA synapses to simulate biologically relevant synaptic transmission. It is also equipped with realistic in vivo-like excitatory and inhibitory uncorrelated background noise.

Synaptic conductance is scaled by a connectivity matrix, which we manipulate to introduce controlled causal influences among the subgroups of neurons. We compare the results from three approaches/algorithms designed to identify these subgroups of neurons and the order in which they fire. The first approach uses spike counts within a chosen fixed synchrony window; the second approach leverages cross-correlation to determine similarity between spike trains; and the third approach extracts a directed acyclic graph that best describes the cause-effect relationships between neurons by capturing the underlying causal structure.

All three methods are tested against the ground-truth connectivity matrix to assess robustness and degradation profiles by varying the size of the network, sparsity of the network, synaptic strengths, and sample sizes. We discuss how extracting the neurons involved in replay, along with the replay order in which the episodes propagate, highlights the role of place cells in spatial navigation and provides insights into learning and decision-making in complex environments. In future work, these algorithms will assess effective connectivity in datasets with key graphical properties that characterize complex navigation environments.

*University of Arizona

†University of California San Diego

How the dynamic interplay of cortico-basal ganglia-thalamic pathways shapes the time course of deliberation and commitment

Zhuojun Yu
Carnegie Mellon University

Abstract

Although the cortico-basal ganglia-thalamic (CBGT) network is identified as a central circuit for decision-making, the dynamic interplay of multiple control pathways within this network in shaping decision trajectories remains poorly understood. Here we develop and apply a novel computational framework — CLAW (Circuit Logic Assessed via Walks) — for tracing the instantaneous flow of neural activity as it progresses through CBGT networks engaged in a virtual decision-making task. Our CLAW analysis reveals that the complex dynamics of network activity is functionally dissectible into two critical phases: deliberation and commitment. These two phases are governed by distinct contributions of underlying CBGT pathways, with indirect and pallidostriatal pathways influencing deliberation, while the direct pathway drives action commitment. We translate CBGT dynamics into the evolution of decision-related policies, based on three previously identified control ensembles (responsiveness, pliancy, and choice) that encapsulate the relationship between CBGT activity and the evidence accumulation process. Our results demonstrate two contrasting strategies for decision-making. Fast decisions, with direct pathway dominance, feature an early response in both boundary height and drift rate, leading to a rapid collapse of decision boundaries and a clear directional bias. In contrast, slow decisions, driven by indirect and pallidostriatal pathway dominance, involve delayed changes in both decision policy parameters, allowing for an extended period of deliberation before commitment to an action. These analyses provide important insights into how the CBGT circuitry can be tuned to adopt various decision strategies and how the decision-making process unfolds within each regime.

Variational Inference of Transcription Factors

Mehrdad Zandigohar[1] Jalees Rehman[1,2] Yang Dai[1]

Abstract

scRegulate is a novel deep generative model integrating regulatory priors into a variational autoencoder to dynamically infer interpretable transcription factor activities from single-cell RNA-seq data.

1. Single-Cell Regulatory-Embedded Variational Inference of Transcription Factor Activity from Gene Expression

Transcription factors (TFs) orchestrate gene expression programs fundamental to cellular identity, differentiation, and disease. Experimental methods (e.g., ChIP-seq, CRISPR interference) directly quantify TF binding or perturbation effects but are impractical for high-throughput, single-cell analysis. Thus, computational approaches are essential, yet most rely on static regulatory assumptions [1,2], failing to capture dynamic, cell-specific regulatory interactions. To address these limitations, we developed scRegulate, a deep generative model embedding gene regulatory network directly into a variational autoencoder framework shown in Fig. 1. scRegulate dynamically refines gene regulatory network interactions through training, balancing prior-driven constraints with data-driven learning. This ensures biological coherence, interpretability, and the inference of nuanced, cell-type-specific regulatory mechanisms.

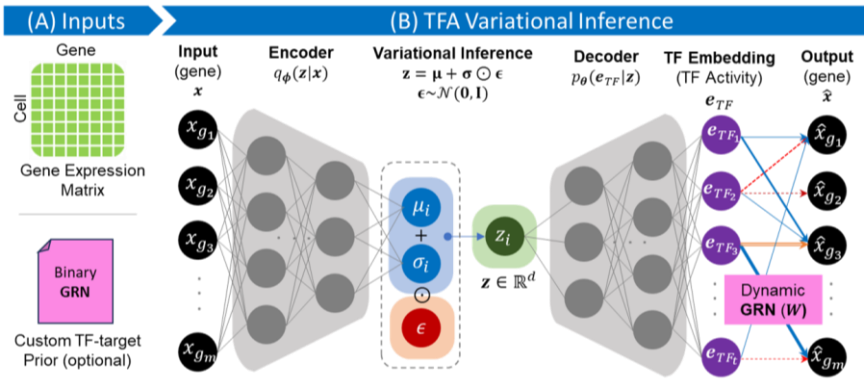

Figure 1. A schematic representation of scRegulate's approach to inferring TF activity and regulatory networks from single-cell gene expression data. (A) Inputs include a gene expression matrix and a TF-target gene prior. (B) TF activity is inferred through a variational autoencoder framework, where the encoder maps input data into a latent space (z), followed by a TF embedding layer to predict gene ex-pression and capture TF activities, informed by the dynamic GRN.

Benchmarking on synthetic datasets (PBMC, tumor, Dahlin; Fig. 2A)[3] shows scRegulate consistently outperforming existing computational methods [1,2,5] in gene regulatory network reconstruction. Validation using experimental Perturb-seq data confirms accurate recovery of expected TF perturbation effects (Figure 2B). Furthermore, applying scRegulate to peripheral blood mononuclear cells (PBMCs) uncovered biologically meaningful regulatory networks and key lineage-defining TFs aligned with established immune pathways. Overall, scRegulate offers a powerful, scalable solution to reveal dynamic regulatory processes at single-cell granularity, significantly advancing computational inference of transcriptional regulation.

[1] Department of Biomedical Engineering, University of Illinois Chicago

[2] Department of Biochemistry and Molecular Genetics, University of Illinois Chicago

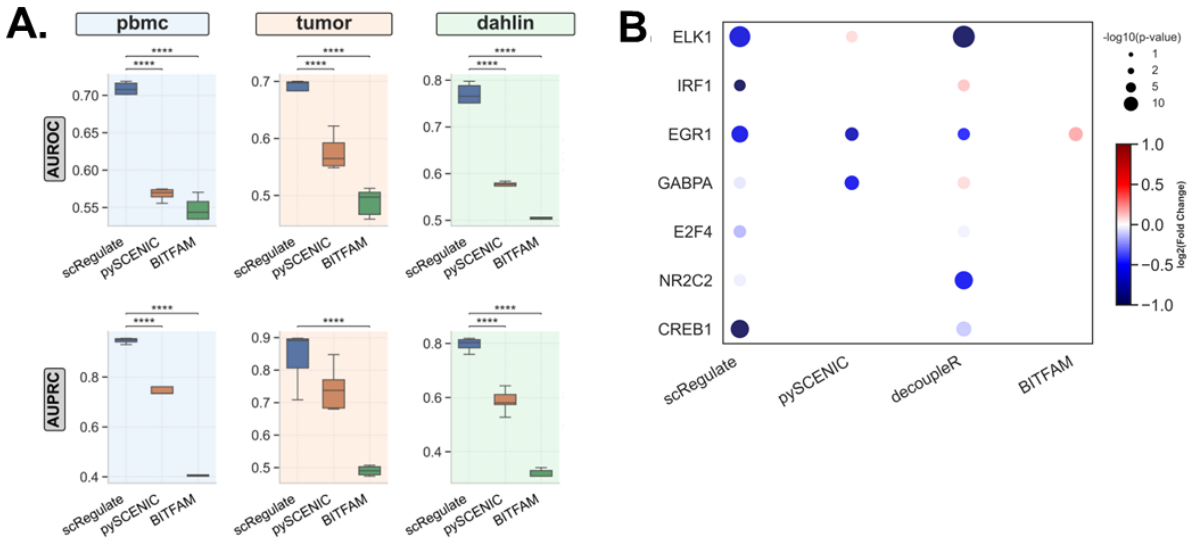

Figure 2. Benchmarking of scRegulate in (A) gene regulatory network inference of 3 synthetic gold standard data of PBMC, tumor and Dahlin, and (B) TF activity inference using real perturb-seq dataset with double knockout effect, compared to other state-of-the-art methods.

References:

[1] Aibar, S. et al. (2017). *SCENIC: Single-cell regulatory network inference and clustering.* Nature Methods, 14, 1083–1086.

[2] Gao, S. et al. (2021). *A Bayesian inference transcription factor activity model for single-cell transcriptomes.* Genome Research, 31, 1296–1311.

[3] Zinati, Y. et al. (2024*). GRouNdGAN: GRN-guided simulation of single-cell RNA-seq data using causal generative adversarial networks.* Nature Communications, 15, 4055.

[4] Dixit, A. et al. (2016). *Perturb-Seq: Dissecting molecular circuits with scalable single-cell RNA profiling of pooled genetic screens.* Cell, 167, 1853–1866.e17.

[5] Badia-i-Mompel P, et al. (2022). *decoupleR: ensemble of computational methods to infer biological activities from omics data.* Bioinformatics Advances, 2(1):vbac016.

The Flywheel Effect in the Pdu Metabolic Pathway

Yifan Zhang

Abstract

Pdu pathway is a 1,2-propanediol utilization metabolic pathway that produces the toxic intermediate propionaldehyde. Based on experimental data [1], we observe that this toxic intermediate is rapidly converted to 1-propanol to mitigate toxicity on a short timescale, and gradually reconverted back to propionaldehyde for further reactions on a longer timescale. We refer to this temporary storage behavior as the "flywheel effect." In this presentation, we explore the evolutionary pressures driving the emergence of the flywheel effect and map out the parameter regime of reaction kinetics under which this effect can occur.

References

[1] Kennedy NW, Mills CE, Abrahamson CH, Archer AG, Shirman S, Jewett MC,Mangan NM, Tullman-Ercek D,2022. Linking the Salmonella enterica 1,2-Propanediol Utilization Bacterial Microcompartment Shell to the Enzymatic Core via the Shell Protein PduB. J Bacteriol204:e00576-21.https://doi.org/10.1128/jb.00576-21

[2] C.E. Mills, C. Waltmann, A.G. Archer, et al. Vertex protein pdun tunes encapsulated pathway performance by dictating bacterial metabolosome morphology. Nat commun, 13(3746), 2022

[3] Jakobson, C. M., Tullman-Ercek, D., Slininger, M. F. & Mangan, N. M. A systems-level model reveals that 1,2-Propanediol utilization microcompartments enhance pathway flux through intermediate sequestration. PLOS Comput. Biol. 13, e1005525 (2017).

Persistent Directed Flag Laplacian (PDFL)-Based Machine Learning for Protein–Ligand Binding Affinity Prediction

Mushal Zia[1†], Benjamin Jones[1], Hongsong Feng[1], and Guo-Wei Wei[1,2,3]
1 Department of Mathematics,
1 Michigan State University, East Lansing, MI 48824, USA.
2 Department of Electrical and Computer Engineering, Michigan State University, East Lansing, MI 48824, USA.
3 Department of Biochemistry and Molecular Biology, Michigan State University, East Lansing, MI 48824, USA.
† Address correspondences to Mushal Zia. E-mail: ziamusha@msu.edu

Abstract:
Directionality in molecular and biomolecular networks plays a significant role in the accurate representation of the complex, dynamic, and asymmetrical nature of interactions present in protein-ligand binding, signal transduction, and biological pathways. Most traditional techniques of topological data analysis (TDA), such as persistent homology (PH) and persistent Laplacian (PL), overlook this aspect in their standard form. To address this, we present the persistent directed flag Laplacian (PDFL), which incorporates directed flag complexes to account for edges with directionality originated from polarization, gene regulation, heterogeneous interactions, etc. This study marks the first application of the PDFL, providing an in-depth analysis of spectral graph theory combined with machine learning. Besides its superior accuracy and reliability, the PDFL model offers simplicity by requiring only raw inputs without complex data processing. We validated our multi-kernel PDFL model for its scoring power against other state-of-art methods on three popular benchmarks, namely PDBbind v2007, v2013, and v2016. Computational results indicate that the proposed PDFL model outperforms competitors in protein-ligand binding affinity predictions, indicating that PDFL is a promising tool for protein engineering, drug discovery, and general applications in science and engineering.

Keywords : Topological data analysis, Persistent homology, Persistent topological Laplacians, Directed flag complex, Directed flag Laplacians, Clique complex.

DOI: 10.1021/acs.jctc.5c00074

Author Index